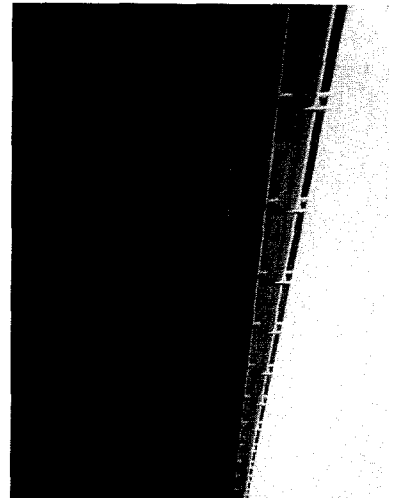
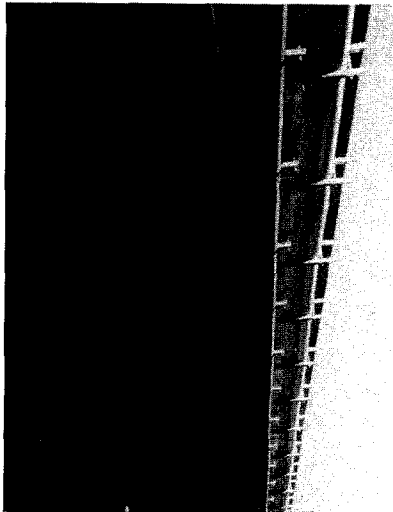


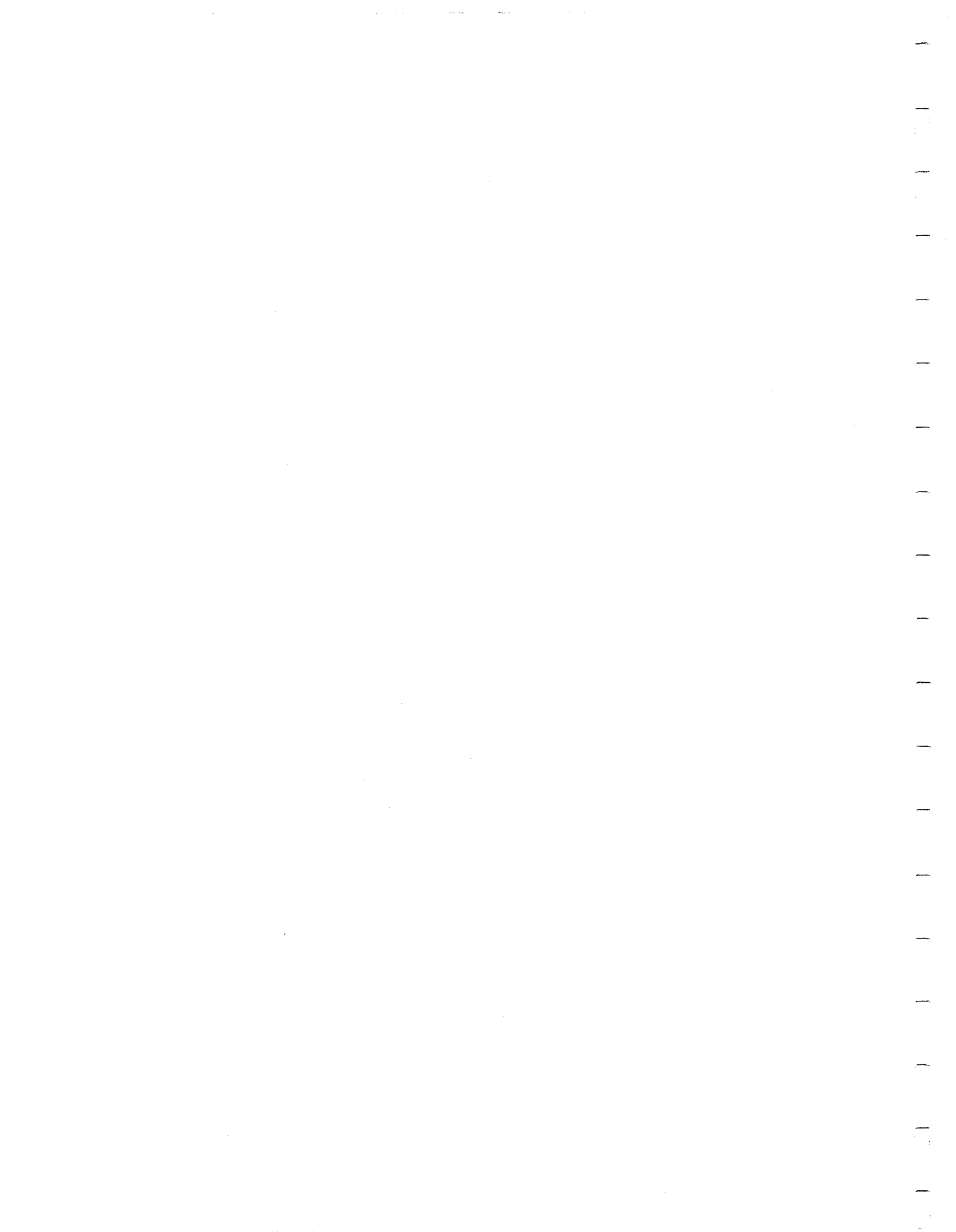


U.S. Department
of Transportation
**Federal Highway
Administration**

Heat-Straightening Repairs of Damaged Steel Bridges

A Technical Guide and Manual of Practice







U.S. Department
of Transportation
**Federal Highway
Administration**

Heat-Straightening Repairs of Damaged Steel Bridges

A Technical Guide and Manual of Practice

Report No. FHWA-IF-99-004

Prepared by

Structural Damage Control, Inc.
13524 Mary Edith Place
Baton Rouge, LA 70809

Prepared for

Bridge Office
Office of Infrastructure
Federal Highway Administration
400-7th St. N.W.
Washington, DC 20590

October 1998

1. Report No. FHWA-IF-99-004	2. Government Accession No.	3. Recipient's Catalog No.	
4. Title and Subtitle Heat-straightening Repairs of Damaged Steel Bridges A Manual of Practice and Technical Guide		5. Report Date October 1998	
		6. Performing Organization Code	
7. Author(s) R. Richard Avent, David Mukai		8. Performing Organization Report No.	
9. Performing Organization Name and Address Structural Damage Control 13524 Mary Edith Place Baton Rouge, LA 70809		10. Work Unit No. (TR AIS)	
		11. Contract or Grant No. DTFH61-96-X-00040	
12. Sponsoring Agency Name and Address Bridge Office Office of Infrastructure Federal Highway Administration 400-7th St. N.W. Washington, DC 20590		13. Type of Report and Period Covered Final Report Jan 1997-Dec 1998	
		14. Sponsoring Agency Code	
15. Supplementary Notes Krishna Verma, Welding Engineer, Agreement Officer's Technical Manager Bridge Office, Office of Infrastructure, Federal Highway Administration			
16. Abstract <p>The purpose of this manual is to provide comprehensive guidelines on heat straightening repair techniques for damaged steel bridge members. The manual is designed to be used in conjunction with a multimedia instructional computer program and video produced as part of this project.</p> <p>The manual is divided into three parts. Part I provides a background and overview of the heat-straightening process. The introductory chapter defines the fundamental types of damage amenable to heat-straightening repair. Chapter 2 describes the basics of heat straightening including: Why heat straightening works, types of heats, basic damage and heating patterns, equipment and its use and practical considerations. Chapter 3 describes methods of assessing, planning and conducting successful repairs along with common mistakes to avoid.</p> <p>Part II is a technical guide to heat straightening directed primarily to engineers. Chapters 4-6 provide details on affects of heating on material properties of steel, behavior of flat plates and response of rolled shapes subjected to heat straightening.</p> <p>Chapter 7 provides technical information on damaged composite beams and proper methods to repair them. Chapter 8 addresses axially loaded members and Chapter 9 discusses local damage. For all cases the proper heating patterns are used and the response is measured. Results are illustrated graphically and methods are given for predicting behavior.</p> <p>Part III contains guides, specifications and reference material. A comprehensive literature review is given in Chapter 10. A concise engineering guide to heat straightening is given in Chapter 11. A set of recommended specifications is given in Chapter 12 for selecting a heat straightening contractor as well as technical specifications which can be incorporated into a contract. Finally, a bibliography, glossary and list of nomenclature are given in Chapters 13-15.</p>			
17. Key Words Bridges, steel, heat straightening, damage repair		18. Distribution Statement Unrestricted. This document is available through the National Technical Information Service, Springfield, VA 21161	
19. Security Classif. (of this report) Unclassified	20. Security Classif. (of this page) Unclassified	21. No. of Pages 268	22. Price

Foreword

This manual represents the results of a comprehensive investigation of the use of heat straightening to repair steel bridge members and elements. For the practitioner, it is a manual demonstrating safe and economical procedures for implementing heat-straightening repairs. For the supervisor, it is a guide for ensuring proper conduct of repairs. For the bridge engineer, it provides engineering guidelines as well as information on developing plans and specifications for heat-straightening repair.

The manual is divided into three parts. Part I provides a background and overview of the heat-straightening process. It is intended for an audience ranging from practitioner to contractor to supervisor to bridge engineer. Part II is a technical guide intended primarily for engineers. This section provides detailed technical information on most aspects of heat straightening. Part III contains guides, specifications and reference material.

Sufficient copies of the manual are being distributed by FHWA Bulletin to provide a minimum of two copies to each FHWA regional and division office and five copies to each State highway agency. Additional copies are being made available to other interested parties including consultants and practitioners.

David Densmore
Bridge Office
Office of Infrastructure

Notice

This document is disseminated under the sponsorship of the Department of Transportation in the interest of information exchange. The United States Government assumes no liability for its contents or use thereof.

The contents of this report reflect the views of the contractor who is responsible for the accuracy of the data presented herein. The contents do not necessarily reflect the official policy of the Department of Transportation.

This report does not constitute a standard, specification, or regulation.

The United States Government does not endorse products or manufacturers. Trade or manufacturers' names appear herein only because they are considered essential to the object of this document.

Preface

Damage caused by overload, vehicle impact, mishandling, earthquake, or fire is a perennial problem associated with steel bridges. For almost half a century, heat-straightening techniques have been applied to bends and distortions in order to restore the original shape of steel elements. A few craftsmen, who have years of experience with heat straightening, perform the technique in the field with varying degrees of success. However, the scientific principles of heat straightening have not been well understood or documented for the profession. In order to address these issues, the Federal Highway Administration has sponsored a project to develop a set of comprehensive training materials on methods of conducting heat-straightening repairs. This manual is one part of this project and serves as a reference manual on heat straightening. Additional materials include a video illustrating heat-straightening repair techniques and an interactive computer program designed to be used as an educational tool for heat straightening. This package of materials is available through the Federal Highway Administration.

Acknowledgements

The following project review committee provided invaluable review and comments on the manual during its preparation.

Krishna K. Verma
Welding and Structural Engineer
Bridge Office
Office of Infrastructure
Federal Highway Administration
400-7th St., S.W. Room 3203
Washington, DC 20590

Jeffrey W. Post
J.W. Post and Associates, Inc.
19834 Sundance Dr.
Humble, TX 77346

Dean C. Krouse
Senior Metallurgical Engineer
Bethlehem Steel Corp.
1170 Eighth Ave.
Bethlehem, PA 18016

David L. McQuaid
D & L, Inc.
Four Gateway Center, 12th Floor
Pittsburgh, PA 15222

Jon J. Edwards, Chief
Shop Plans and Fabrication Unit
Bureau of Bridges and Structures
Illinois Department of Transportation
2300 South Dirksen Parkway
Springfield, IL 62764

Fred Beckman
167 Hawthorne St.
Chicago, IL 60411

Jerry Hill
G. Hill and Associates
3843 Sandhill Rd.
Lansing, MI 48911

This project was a subcontract with Southern University as a part of their contract with FHWA. The principal investigators were:

Dr. I. K. Dabipi, Chairman
Department of Electrical Engineering
Southern University
Baton Rouge, LA 70813

Dr. Judy Perkins
Department of Civil Engineering
University of New Orleans
New Orleans, LA 70148

The American Society of Civil Engineers is gratefully acknowledged for granting permission to reprint material.

The following organizations are acknowledged for the support of the research upon which most of this manual is based.

Department of Civil and Environmental
Engineering
Louisiana State University
Baton Rouge, LA 70803

Louisiana Transportation Research Center
Louisiana Department of Transportation and
Development
Baton Rouge, LA 70803

METRIC (SI*) CONVERSION FACTORS				
APPROXIMATE CONVERSIONS TO SI UNITS				
Symbol	When You Know	Multiply By	To Find	Symbol
LENGTH				
in	inches	25.4	millimetres	mm
ft	feet	0.3048	metres	m
yd	yards	0.914	metres	m
mi	miles	1.61	kilometres	km
AREA				
in ²	square inches	645.2	millimetres squared	mm ²
ft ²	square feet	0.0929	metres squared	m ²
yd ²	square yards	0.836	metres squared	m ²
mi ²	square miles	2.59	kilometres squared	km ²
ac	acres	0.395	hectares	ha
MASS (weight)				
oz	ounces	28.35	grams	g
lb	pounds	0.454	kilograms	kg
T	short tons (2000 lb)	0.907	megagrams	Mg
VOLUME				
fl oz	fluid ounces	29.57	millilitres	mL
gal	gallons	3.785	litres	L
ft ³	cubic feet	0.0328	metres cubed	m ³
yd ³	cubic yards	0.0765	metres cubed	m ³
NOTE: Volumes greater than 1000 L shall be shown in m ³ .				
TEMPERATURE (exact)				
°F	Fahrenheit temperature	5/9 (after subtracting 32)	Celsius temperature	°C

APPROXIMATE CONVERSIONS TO SI UNITS				
Symbol	When You Know	Multiply By	To Find	Symbol
LENGTH				
mm	millimetres	0.039	inches	in
m	metres	3.28	feet	ft
m	metres	1.09	yards	yd
km	kilometres	0.621	miles	mi
AREA				
mm ²	millimetres squared	0.0016	square inches	in ²
m ²	metres squared	10.764	square feet	ft ²
km ²	kilometres squared	0.39	square miles	mi ²
ha	hectares (10 000 m ²)	2.53	acres	ac
MASS (weight)				
g	grams	0.0353	ounces	oz
kg	kilograms	2.205	pounds	lb
Mg	megagrams (1 000 kg)	1.103	short tons	T
VOLUME				
mL	millilitres	0.034	fluid ounces	fl oz
L	litres	0.264	gallons	gal
m ³	metres cubed	35.315	cubic feet	ft ³
m ³	metres cubed	1.308	cubic yards	yd ³
TEMPERATURE (exact)				
°C	Celsius temperature	9/5 (then add 32)	Fahrenheit temperature	°F

These factors conform to the requirement of FHWA Order 5190.1A.

* SI is the symbol for the International System of Measurements

Table of Contents

	Page
Part I. Overview	1
Chapter 1. Introduction	3
Purpose of This Manual.....	3
History of Heat Straightening.....	3
Typical Types of Damage.....	5
1. Category S.....	5
2. Category W.....	5
3. Category T.....	6
4. Category L.....	8
Objectives of This Manual.....	8
How to Use This Manual.....	8
Chapter 2. Heat Straightening Basics	11
What is Heat Straightening.....	11
Why Heat Straightening Works.....	12
Fundamental Heating Patterns.....	13
Vee Heat.....	13
Edge Heats.....	14
Line Heats.....	14
Spot Heats.....	16
Strip Heats.....	17
Defining Basic Damage Patterns and Zones.....	17
Basic Heating Patterns.....	20
Flat Plate Bent About Major Axis (Category S).....	20
Structural Members Bent About Their Strong (Major) Axis (Category S).....	20
Structural Members Bent About Their Weak (Minor) Axes (Category W).....	21
Structural Members Subject to Twisting Damage (Category T).....	21
Flanges and Webs with Local Buckles (Category L).....	25
Angles.....	25
Equipment and Its Use.....	25
Safety Considerations.....	25
Temperature Control.....	26
Restraining Forces.....	27
Practical Considerations.....	30
Torch Tip Size and Intensity.....	30
Material Configuration.....	30
Judging the Temperature.....	30
Jacking Forces.....	31
Heating Patterns.....	31
Sequencing of Heats.....	32
Lack of Movement.....	32
Cooling the Steel.....	32
Key Points to Remember.....	33

Chapter 3. Assessing, Planning and Conducting Successful Repairs 35

Role of Engineer, Inspector and Contractor 35

Keys to a Successful Repair 36

Steps in the Assessment Process. 37

 1. Initial Inspection and Evaluation for Safety and Stability. 37

 2. Detailed Inspection for Specific Defects. 38

 Signs of Fracture. 38

 Degree of Damage. 38

 Material Degradation. 40

 Geometry of the Structure. 40

Steps in the Planning and Design Process. 41

 1. Analysis of Damage and Determination of the Maximum Strain Due to Damage 41

 Example 3.1. 43

 2. Conduct a Structural Analysis of the System. 44

 Change in Cross Section Shape. 44

 P- Δ Effects. 45

 Residual Forces. 47

 3. Select Regions Where Heat Straightening is Applicable. 48

 4. Select Heating Patterns and Parameters. 50

 Vee Depth. 50

 Vee Angle. 51

 Number of Simultaneous Vee Heats. 51

 5. Develop a Constraint Plan. 51

 Example 3.2. 53

 6. Estimate the Heats Required to Straighten the Members. 53

 7. Repair Plans and Specifications. 54

 Example 3.3. 54

Supervisor's Responsibilities. 56

 Monitoring the Heating Temperature. 61

 Controlling Restraining Forces. 56

 Approving Heating Patterns. 59

 Checking Tolerances. 59

Common Mistakes to Avoid. 59

 Mistake No. 1. Heating the Steel Until it is Cherry Red. 59

 Mistake No. 2. Jacking the Girder Straight While it is Hot. 59

 Mistake No. 3. Heating Too Large an Area. 59

 Mistake No. 4. Heating Outside the Yield Zones. 59

 Mistake No. 5. Using Inefficient or Improper Heating Patterns. 60

Checking Procedures for Supervisors. 60

Key Points to Remember. 60

Part II. Technical Guide for Heat-Straightening Repairs. 63

Chapter 4. Effects of Heating on the Material Properties of Steel. 65

Introduction. 65

Residual Stresses in Heat-Straightened Plates. 66

Residual Stresses in Rolled Shapes 71

Basic Material Properties From Laboratory Tests. 79

 Thermal Expansion 79

 Modulus of Elasticity. 80

 Yield Stress. 80

 Ductility After Heat Straightening. 81

Notch Toughness	81
Rockwell Hardness.....	82
Mechanical Properties of Heat-Straightened Plates.....	82
Yield Stress and Tensile Strength.....	82
Modulus of Elasticity.....	84
Ductility.....	84
Mechanical Properties of Heat-Straightened Wide Flange Beams.....	86
Yield Stress.....	86
Modulus of Elasticity.....	86
Ductility.....	86
Mechanical Properties From Heat Straightened Girders.....	90
Member Shortening.....	90
Redistribution of Material.....	92
Impact of Heat Straightening on Mechanical Properties of Steel.....	93
Key Points to Remember.....	95
Chapter 5. Heat Straightening of Flat Plates.....	97
Introduction.....	97
Experimental Program.....	100
Evaluation of Results of Experimental Program.....	100
Vee Angle.....	101
Depth of Vee.....	101
Plate Thickness and Geometry.....	102
Temperature.....	107
Restraining Forces.....	108
Analytical Development.....	112
Example 5.1.....	117
Significance of Plate Response to Heat Straightening.....	117
Key Points to Remember.....	118
Chapter 6. Heat Straightening Rolled Shapes.....	121
Introduction.....	121
Behavior of Channels with Strong Axis Damage (Category S).....	123
Behavior of Channels with Weak Axis Damage (Category W).....	126
Behavior of Wide Flange Beams with Weak Axis (Category W)	
Damage.....	130
Repetitive Damage and Straightening for Category W Wide	
Flange Beams.....	130
Behavior of Wide Flange Beams with Strong Axis (Category S)	
Damage.....	134
Angles.....	136
Out-of-Plane Movement.....	138
Example 6.1.....	140
Summary.....	141
Key Points to Remember.....	141
Chapter 7. Heat-Straightening Repair for Composite Deck-Girder Bridges .	143
Experimental Procedures.....	144
Heat Straightening Repair of a W 10x39 Composite Beam.....	144
Heat Straightening Repair of a W 24x76 Composite Beam.....	151
Evaluation of Factors Affecting Heat-Straightening Behavior of	
Composite Girders.....	154

Heat Patterns	154
Residual Moments	155
Restraining Forces.	156
Stiffening Effect of Web	158
Hot Mechanical Straightening	158
Cracking	158
Theoretical Model for Heat-Straightening Response	159
Modeling of Simple Span Composite Girders.	159
Modeling Statically Indeterminate Spans Due to Intermediate Diaphragms	163
Example 7.1	165
Summary	165
Keys to Remember	166

Chapter 8. Heat straightening Trusses and Other Axially Loaded Members 167

Introduction.	167
Response of Columns to Heat Straightening.	167
Heat Straightening Response of Columns With Category W Damage.	168
Response of Columns to Heat Straightening For Category S Damage.	172
Summary	173
Key Points to Remember	173

Chapter 9. Heat-Straightening Repair of Localized Damage 175

Category L/U Damage of Unstiffened Elements	178
Damage Assessment of Category L/U Damage	178
1. Span/Deflection Ratio.	179
2. Flange Edge Elongation.	179
Experimental Results for Category L/U repairs	179
Phase I.- Initial Heating and Jacking Patterns.	184
1. Restraining Forces.	184
2. Vee Heats.	185
3. Line Heats.	185
4. Web Line Heat.	185
Phase II.-Heating/Jacking Pattern if $\theta_n = 0$	185
Phase III- Heating Pattern if $\theta_f = \theta_w$	186
Flange Damage in Opposite Direction.	186
Computation of Restraining Forces.	186
Experimental Results of Active Heat Straightening.	188
Mechanical Properties of Test Specimens.	189
Category L/S Damage for Stiffened Elements	189
Experimental Results	191
1. Ring Line Heats.	191
2. Radial Line Heats.	191
3. Star Vee Heats.	191
Recommended Methodology	193
1. Selection of Jacking Force.	193
2. Estimation of the Number of Heats Required And Modification of Jacking Force.	194
3. Initial Heating Pattern.	194
4. Final Heating Pattern.	194
Summary	195
Key Points to Remember.	195

Chapter 10. Heat Straightening of Steel: Fact or Fable.	197
Introduction.	197
Summary and Conclusions.	213
Part III. Specifications, Guides, and References	215
Chapter 11. Engineering Guide.	217
Section 1. General.	217
Section 2. Damage Assessment.	217
Section 3. Material Assessment.	220
Section 4. Design of Repair Sequence.	222
Section 5. Field Supervision of Repair.	225
Chapter 12. Specifications for the Selection of Contractors and the Conduct of Heat-Straightening Repairs.	227
Selection of Contractor (or the Field Supervisor).	227
Tolerances.	228
Technical Specifications for the Conduct of Heat Straightening Repairs. . .	228
Chapter 13. Glossary.	233
Chapter 14. Nomenclature.	239
Chapter 15. Bibliography.	243

List of Tables

		Page
2.1	Recommended Torch Tips for Various Material Thicknesses.	29
4.1	Heating Parameters for Undamaged Plates.	69
4.2	Heating Conditions and Degree of Damage for Deformed Plates.	69
4.3	Heating Conditions for Undamaged Wide Flange Beams.	73
4.4	Material properties of damaged plates.	83
4.5	T-test confidence levels for material properties of heat-straightened plates.	85
4.6.	Comparison of material properties in heat straightened steel plates with unheated specimens and ASTM standard values.	85
4.7	Mechanical properties of damaged and heat straightened W 6 x 9 Category W wide flange beams (Vee angle=45°, jacking ratio=50% and depth ratio=75%) ^{1,2}	87
4.8	Comparison of material properties in heat-straightened steel beams with unheated specimens and ASTM minimum standard values ¹	89
4.9	Material properties taken from an improperly heat straightened girder of an Iowa bridge removed from service.	90
5.1	Plastic rotations for Example 5.1.	116
6.1	Summary of damaged beam data for W 6x9 beams with Category W damage.	132
6.2	Increasing yield zone after each damage/repair cycle for W 6x9 with Category W damage.	133
6.3	Plastic rotations for Category S damage to wide flange beams (heating temperature = 1200°F)	135
6.4	Damaged angle specimens with the heating pattern shown in Fig. 6.17b ¹	139
6.5	Comparison of out-of-plane plastic rotations to plastic rotations in the in-plane direction of movement for initially straight L 4x4x¼ angles (in-plane movement shown in Fig.6.18)	139
7.1	Summary of plastic rotations for a damaged composite W10 x 39 beam after heat straightening with various heating patterns.	148
7.2	Summary of plastic rotations for a damaged W24 x 76 beams after heat straightening with various patterns.	152
8.1	Plastic rotations for category W damaged HP 12x53 beam with compression axial loads (45° vee heats and 1200°F (650°C) temperature).	171
8.2	Plastic rotations for Category S damaged W10X39 columns (30° vee angle and 1200°F or 650°C heating temperature).	173
9.1	Configuration of Flange Damage for Category L/U Repairs in W8x13 Beams (1 in. = 25.4 mm).	180
9.2	Results of tensile tests on dent specimens.	190
9.3	Relationship between r/l_c and Shell Stress Factor.	191
10.1	Summary of Experimental Results on Base Properties of Heat-Straightened Steel by Other Researchers	200
12.1	Recommended Tolerances for Heat Straightening Repair.	229
12.2	Recommended torch tips for various material thicknesses	229

List of Figures

	Page
1.1 Graphic Illustration of Category S Damage.....	5
1.2 Examples of Category W Damage.....	6
1.3 Examples of Category T Damage.....	7
1.4 Category L Damage Showing Flange Buckles on Wind Bracing on Mississippi River Bridge in Greenville, MS.....	8
2.1 Conceptual Example of Shortening a Steel Bar.....	13
2.2 Stages of Movement During Vee Heat.....	14
2.3 Schematic Diagram of Edge Heats Used to Heat-Curve a Beam.....	14
2.4 Line Heat in Progress on the Web of a Wide Flange Beam.....	15
2.5 Schematic of Line Heat Mechanism.....	15
2.6 Strip Heat in Progress With a Completed Strip Heat in the Foreground.....	16
2.7 Schematic of Strip Heat on the Top Flange of a Wide Flange Beam.....	17
2.8 Yield Zones for Basic Damage Patterns.....	18
2.9 Yield Zone and Vee/Strip Heat Layout for a Category S I Shaped Beam.....	20
2.10 Plate Vee Heat Pattern Over Yield Zone.....	21
2.11 Heating Patterns for Wide Flanges and Channels Bent About Their Major Axes (Category S).....	21
2.12 Heating Patterns for Wide Flanges and Channels Bent About Their Minor Axes (Category W).....	22
2.13 Wide Flanges and Channels With Twisting Damage (Category T).....	22
2.14 Typical Heating Patterns for Local Damage.....	22
2.15 Heating Patterns for Angles.....	22
2.16 Oxyacetylene Fuel System.....	23
2.17 Fuel Mixing Nozzle.....	23
2.18 Single Orifice Tip.....	24
2.19 Rosebud Tip.....	24
2.20 Technician Preparing to Heat Straighten in a Fabrication Shop.....	26
2.21 Characteristics of Plastic Flow and Restraint During Heat Straightening.....	29
3.1 Brittle Fracture During Heat Straightening.....	37
3.2 Offset Measurements to Calculate Degree of Damage and Radius of Curvature.....	39
3.3 Relationship of Degree of Damage to Radius of Curvature and Cord Length.....	39
3.4 Radius of Curvature for a Damaged Beam of Curvature and Cord Length.....	41
3.5 Strain Ratio vs. Normalized Radius of Curvature (μ vs. κ / γ_{\max}).....	42
3.6 Offset Measurements for Example 3.1 (1 in. = 25.4 mm and 1 ft. = 0.305 m).....	43
3.7 Reduction in Effective Section Modulus for a W 24x76 Beam Subjected to Varying Degrees Of Idealized Damage (Note: 1 in. = 25.4 mm).....	45
3.8 Reduction in Effective Section Modulus for a W 10x39 Beam Subjected to Varying Degrees Of Idealized Damage (Note: 1 in. = 25.4 mm).....	45
3.9 Reduction in the Square of the Effective Minimum Radius of Gyration for a W 24x76 Beam Subjected to Varying Degrees of Idealized Damage (Note: 1 in. = 25.4 mm).....	46

3.10	Reduction in the Square of the Effective Minimum Radius of Gyration for a W 10x39 Beam Subjected to Varying Degrees of Idealized Damage (Note: 1 in. = 25.4 mm)	46
3.11	Effect of Amplification Factor for Lateral Deflections on Compression Members.	46
3.12	Plastic Analysis for Residual Moments in a Laterally Impacted Girder.	48
3.13	Diaphragm Damage Due to Vehicle Impact on Girder.	49
3.14	Heating Pattern and Sequence for Bending Combination About Both the Strong and Weak Axis.	49
3.15	Heating Pattern and Sequence for Combination Weak Axis Bending and Local Flange Bulge.	49
3.16	Heating Pattern and Sequence for Combination of Weak Axis Bending of Lower Flange and Twisting.	51
3.17	Heating Pattern for Reverse Curvature Bending.	51
3.18	Jacking arrangements for Global and Local Damage on a Composite Girder Bridge.	52
3.19	Schematic Diagrams for Example 3.3 (Note: 1 ft. = 0.305 mm and 1 ft.-kip = 1.36 kN-m)	55
3.20	Temperature Sensing Crayons.	57
3.21	Contact Pyrometer for Measuring Heating Temperature.	57
3.22	Heating in Progress Illustrating Silver Color Around Torch tip.	58
3.23	Jacks in Place on a Wisconsin Bridge.	58
4.1	Iron-Carbon Equilibrium Diagram.	66
4.2	Experimental Strain and Theoretical Residual Stress Distribution for 2/3 Depth, 45°F vee heated plate subjected to 1000°F temperature (Roeder, 1985)	67
4.3	Measured Residual Stresses in a Vee Heated Plate Prior to Heating.	68
4.4	Average Residual Stress Values for Vee Heated Plates Which were Originally Undamaged.	68
4.5	Regions Utilized in Residual Stress Measurements of Damaged and Heat Straightened Plates (Note: 1 in. = 25.4 mm)	70
4.6	Residual Stress Distribution for Damaged and Vee Heated Plates in Region B (Assumed Modulus = 29,000 ksi or 200,000 MPa).	71
4.7	Residual Stress Distribution for Damaged and Vee Heated Plates in Region A and C (Assumed Modulus = 29,000 ksi or 200,000 MPa)	71
4.8	Stresses in Angle VI-1 (20° vee, apex at toe, $M_j/M_p = 0.00$, depth Ratio = 1.00)	72
4.9	Stresses in Angle VI-4 (45° vee, apex at toe, $M_j/M_p = 0.00$, depth Ratio = 1.00)	72
4.10	Stresses in Angle L4x4 (45° vee, apex at heel, $M_j/M_p = 0.50$, depth Ratio = 1.00)	72
4.11	Stresses in Angle L6x4x5/16 (45° vee, apex at heel, $M_j/M_p = 0.33$, depth Ratio = 1.00)	72
4.12	Stresses in channel IX-6 (45° vee, $M_j/M_p = 0.50$, depth Ratio = 1.00)	73
4.13	Residual Stress Strip Locations (Category S Heat)	73
4.14	Residual Stress Strip Locations (Category W Heat)	p. 73
4.15	Residual Stresses in Unheated Wide Flange Beam "UH"	74
4.16	Stresses in beam B-1 (20° vee, $M_j/M_p = 0.00$, depth ratio = 1.00)	75
4.17	Stresses in beam B-2 (30° vee, $M_j/M_p = 0.00$,	

	depth ratio = 1.00)	75
4.18	Stresses in beam B-3 (45° vee, $M_j/M_p = 0.00$, depth ratio = 1.00)	76
4.19	Stresses in beam B-4 (45° vee, $M_j/M_p = 0.25$, depth ratio = 1.00)	76
4.20	Stresses in beam B-5 (45° vee, $M_j/M_p = 0.50$, depth ratio = 1.00)	76
4.21	Stresses in beam B-6 (20° vee, $M_j/M_p = 0.00$, depth ratio = 1.00)	76
4.22	Stresses in Beam B-7 (20° vee, $M_j/M_p = 0.50$, depth ratio = 1.00)	77
4.23	Stresses in beam B-8 (45° vee, $M_j/M_p = 0.00$, depth ratio = 1.00)	77
4.24	Residual stress distribution damaged, Category W side flange beams (assumed $E = 29,000$ ksi or $200,000$ MPa)	78
4.25	Residual Stresses in Category S damaged wide flange beam (45° vee, $M_j/M_p = 0.50$, depth ratio = 1.00)	79
4.26	Variation of coefficient of Thermal expansion versus Temperature (Roeder, 1985)	79
4.27	Normalized yield stress and modulus of elasticity versus Temperature (Roeder, 1985)	80
4.28	Yield stress versus number of damage/repair cycles.	88
4.29	Tensile stress versus number of damage/repair cycles.	88
4.30	Percent elongation versus number of damage/repair cycles.	89
4.31	Shortening of a Beam or plate after Heat Straightening.	91
4.32	Shortening versus Degree of Damage for Plate Elements.	92
5.1	Illustration of vee heat geometry.	99
5.2	Influence of vee depth on plastic rotations of originally straight plates for various vee angles and jacking ratios (heating temperature = 1200°F or 650°C)	103
5.3	Vee angle versus average plastic rotation for damaged plates having different depth ratios (Jacking ratio = 0.5 and Temperature = 1200°F or 650°C)	103
5.4	Influence of plate thickness on plastic rotation (average of 3 heats with depth ratio = 1, jacking ratio = 0, temperature = 1200°F or 650°C).	104
5.5	Influence of plate thickness on plastic rotations, Roeder, 1985 (single heats with $\theta = 60^\circ$, depth ratio = 0.67, heating temperature = 1025-1260°F or 552-682°C)	105
5.6	Comparison of plastic rotations for 5.9 in. (150 mm) (average of 2 heats) and 7.9 in. (200 mm) (single heat) plate widths, Roeder, 1985 ($\theta = 60^\circ$, depth ratio = 0.67, and heating temperature was approximately 1200°F or 650°C)	106
5.7	Comparison of average plastic rotation (for three 20° vee heats) for plates of three widths (jacking ratio = 0, depth ratio = 0.75, and heating temperature = 1200°F or 650°C)	107
5.8	Influence of heating temperature on plastic rotation for 3/4 depth vee heats and a jacking ratio of 0.16.	108
5.9	Influence of jacking ratio on average plastic rotation for 3/4 depth vee heats and 1200°F (650°C) heating temperatures (lines represent a least squares curve fit)	110
5.10	Influence of jacking ratio on average plastic rotation for full depth vee heats and 1200°F (650°C) heating temperature (lines represent a least squares curve fit)	111
5.11	Average plastic rotation versus jacking ratio for 60° vee heated plates from Roeder, 1985 (depth ratio = 2/3 and heating temperature	

	= 1200°F or 650°C)	111
5.12	Jacking ratio versus vee angle for straightening damaged Plates (Temperature = 1200°F or 650°C and depth ratio = 1).	111
5.13.	Influence of axial jacking force on plastic rotation of vee heated plates (Temperature = 1200°F or 650°C and depth ratio = 1)	112
5.14	Geometric changes resulting from a vee heat on a plate.	113
5.15	Plastic rotation versus vee angle for vee heated plates having a heating temperature of 1200°F (650°C)	116
6.1	Primary and Secondary plate elements for a channel bent about its major axis (Category S damage)	122
6.2	Typical yield zone patterns in the plate elements of the channel shown in Fig. 6.1.	122
6.3	Weak axis bending resulting in a yield line in the plate element.	123
6.4	Heating patterns for channels bent about their strong axis (Category S)	124
6.5	Experimental and theoretical plastic rotations for a C 6x8 channel with Category S damage.	125
6.6	Unfolded flange for a Category S channel.	126
6.7	Heating patterns for channels bent about the weak axis (Direction of moment producing damage indicated by M_p)	127
6.8	Experimental and theoretical plastic rotations for Category W damage of a C 6x8.2 with the open end of vees at flange- web-juncture as shown in Fig. 6.7a.	127
6.9	Geometric effects on heat straightening a channel with negative curvature damage.	129
6.10	Heating patterns for weak axis damage to a wide flange beam (Category W)	130
6.11	Vee angle versus plastic rotation for wide flange beams using the Category W heating pattern, Horton (1973)	131
6.12	Plastic rotation versus vee angle for W 6x9 using the Category W heating pattern (Temperature = 1,200°F or 650°C)	131
6.13	Spreading of yield zone in subsequent cycles of damage and repair for W 6x9 wide flange beam specimens.	132
6.14	Yield zone and heating pattern for Category S damage to wide flange beams.	135
6.15	Influence of vee angle and jacking ratio on plastic rotation for W 6x9 (Category S damage pattern)	136
6.16	Geometric relationship between Category S wide flanges and plates.	136
6.17	Yield zone and heating patterns for flexural damage of a typical angle	137
6.18	Influence of vee angle and jacking ratio on plastic rotation for L 4x4x1/4 angles with the heating pattern of Fig. 6.17a.	137
7.1	Typical deformed shape and yield zones in damaged composite girders.	145
7.2	View from underside looking up at damaged beam SB-1.	145
7.3	Heating patterns for composite girder.	147
7.4	Comparison of average plastic rotation for various patterns and jacking ratios.	148
7.5	Line heat in progress on a composite girder.	150
7.6	Heat straightening progression for a damaged W 10x39 beam using heating sequence No. 6 (1 in. = 25.4 mm)	152
7.7	Crack in web of beam after heating sequence 12.	154
7.8	Crack in bottom flange of beam after heating sequence 13.	155

7.9	Apparent jacking ratio versus plastic rotation for composite girders.	157
7.10	Actual load ratio versus plastic rotation for composite girders.	162
7.11	Web stiffness reduction factor versus d/t_w ratio.	162
7.12	Lower flange of composite girder modeled as a continuous beam.	164
7.13	Deflected shape and structural analysis of damaged beam.	165
8.1	Dead load conditions on a simply supported beam.	168
8.2	$P\Delta$ effect on an axially loaded column.	168
8.3	Jacking force applied to axially loaded column in test frame (Tension rods are visible on right side of column)	170
8.4	Stress distribution in axially loaded column (A = cross section area and S = section modulus)	170
8.5	Deformations of one flange over 10 heating cycles for compression member No. 1 (45° vee heats, 1200°F (650°C) temperature, and modified jacking ratio of 50%).	172
8.6	Plastic rotation versus jacking ratio for axially loaded Category W columns ($f_a/F_a = 0.35$ except as noted, vee angles = 45° and heating temperature = 1200°F or 650°C)	172
8.7	Plastic rotation versus jacking ratio for Category S columns (30° vee angle and 1200°F or 650°C heating temperature)	173
9.1	Typical localized damage classified as Category L.	176
9.2	Category L/U flange bulge damage on Mississippi River Bridge at Greenville, MS.	177
9.3	Typical Category L/U damage.	177
9.4	Heat straightening local flange damage (Category L/U)	178
9.5	Inducement of damage to produce a flange bulge in the flange of a W 8x13.	180
9.6	Flange movements for various heating patterns for Beam No. 1 with Category L/U damage (N and B refer to near and both sides of the flange, respectively and 1 in. = 25.4 mm)	182
9.7	Flange Movements for Various Heating Patterns for Beam No. 2 with Category L/U Damage (N and B refer to near and both sides of the flange, respectively and 1 in. = 25.4 mm)	182
9.8	Flange Movements for Various Heating Patterns on Beam No. 3 with Category L/U Damage (N and B refer to near and both sides of the flange, respectively and 1 in. = 25.4 mm)	183
9.9	Flange Movements for Various Heating Patterns for Beam No. 4 with Category L/U Damage (N and B refer to near and both sides of the flange, respectively and 1 in. = 25.4 mm)	183
9.10	Average Flange Deflection per Heating Cycle for the Most Effective Patterns (3 cycles minimum) for Category L/U Damage (N and B Refer to Near and Both Sides of the Flange, Respectively and 1 in. = 25.4 mm)	184
9.11	Arrangement of Restraining Forces During Various Stages of Repair.	185
9.12	Arrangement of Vee and Line Heats.	186
9.13	Jacking Sequence if Damage is Reversed from that Shown in Figure 9.11.	187
9.14	Yield-Line Analysis for Idealized Flange Bulge Geometry.	188
9.15	Bulge Cross Section Geometry (1 in. = 25.4 mm)	190
9.16	Star Vee Heat Pattern.	191
9.17	Decrease in Deflections of Stiffened Web for Beam 6 (W 16x26) with Category L/S Damage (1 in. = 25.4 mm)	192
9.18	Decrease in Deflection of Stiffened Web for Beam 7 (W 16x26) with Category L/S Damage (1 in. = 25.4 mm)	192
9.19	Curvature and Line Heating Patterns for Category L/S Damage.	195
10.1	Variation of Steel Yield Stress with Temperature.	198

PART I. OVERVIEW

Chapter 1. Introduction

Purpose of This Manual

Damage caused by overload, vehicle impact, mishandling, earthquake, or fire is a perennial problem associated with steel structures. For almost half a century, heat-straightening techniques have been applied to bends and distortions in order to restore the original shape of steel elements. A few craftsmen, who have years of experience with heat straightening, perform the technique in the field with varying degrees of success. Some of these experts have mastered heat straightening, but the process is still considered more of an art than a science.

The ability to repair damaged structural steel members in place, often without the need for temporary shoring, has generated interest in heat straightening from the engineering profession. However, engineers have had to rely primarily on their own judgment and the advice of experienced technicians in applying heat-straightening techniques. Two key questions have often been raised: Do heat-straightening procedures exist which do not compromise the structural integrity of the steel? And if so, how can such repairs be engineered to ensure adequate safety of the repaired structure, both during and after repair? The primary goal of this manual is to answer these two questions.

This manual is divided into three parts. Part I provides a background and overview of the heat-straightening process. It is intended for a general audience ranging

from heat-straightening practitioner, to contractor, to inspector, and to bridge engineer.

Part II is a technical guide to heat straightening. Intended primarily for engineers, this section provides detailed technical information on most aspects of heat straightening. These chapters provide the experimental, analytical and theoretical basis for the heat-straightening process.

Part III contains guides, specifications and reference material. An engineering guide serves as a standard for the practice of heat straightening. Portions are intended for the practitioner, contractor, inspector and bridge engineer. A set of standards or specifications for heat straightening repair are included along with a glossary and references. The specifications are suitable for incorporation into contract documents as technical specifications.

This manual is also designed to be used in conjunction with a multimedia instructional computer program and video produced as part of this FHWA sponsored project. The goal of the program is to provide a comprehensive set of instructional materials for those interested in learning about heat-straightening repair.

History of Heat Straightening

The origins of heat straightening can be traced to the early days of welding. Steel fabricators observed how the heat from welding caused distortion in regular patterns. Some of these individuals began to experiment with ways to reverse this distortion by heating the steel in specific patterns

to counteract the initial distortion. With experience, some of these technicians developed skills at not only removing weld distortion, but repairing other damage as well. These heating procedures developed as an art form passed from one practitioner to the next.

During this period, the use of curved steel members gained popularity for both practical and aesthetic reasons. Primary examples include horizontally curved bridge girders and camber to negate dead load deflections. Heat curving techniques were developed for these applications. While many of the heating techniques are similar to those used in heat straightening, there is a distinction between the two. Heat curving is typically performed on undamaged steel, usually in the controlled environment of the fabrication shop. The typical radius of curvature for heat-curved members is quite large meaning that the curvature is usually very gradual. On the other hand, heat straightening is used on damaged steel in which the yield stress has been exceeded, and often excessively, well into the strain-hardening range. Most heat straightening is conducted in the field, under highly variable weather conditions, and often with the members at least partially loaded. These differences mean that techniques and criteria for heat straightening may sometimes differ substantially from those of heat curving.

Little information has been available in terms of quantification of the heat-straightening process. The earliest written information found was traced to Joseph Holt who defined some of the basic concepts of heat straightening in an unpublished manuscript in 1938. Over the years since, more publications began to appear which tended

to be more qualitative than quantitative in nature.

Well into the 1980's, the use of heat straightening was so little understood that one-half the States did not allow heat-straightening repair of bridges (Shanafelt and Horn, 1984). At that time there were reasons why heat-straightening repair had not been widely accepted. First, the basic mechanism of heat-straightening was not well-understood in that the effects of both external restraints (jacking) and internal restraints (redundancy) were considered to be of minor concern rather than fundamental to the broad application of the process. Second, as a result of not identifying the importance of these parameters, there had been little documentation of the behavior of vee heated plates subjected to varying degrees of constraint and even less on rolled shapes. Third, while a fair amount of research indicated that most material properties are relatively unaffected by heat straightening, two important aspects had been overlooked: the influence of strain aging on ductility; and residual stress distribution. Finally, the research information available was predicated almost entirely on laboratory studies of simple elements. The reported field investigations were qualitative rather than quantitative and thus could not serve as a building block for validating heat straightening. Because of these voids in heat-straightening research, it was indeed true that the artisan practicing the trade was much more important than the engineer. Consequently, heat-straightening repair was often not considered on engineered structures.

In recent years, considerable research has been conducted to quantify the heat-straightening process. The technical data

presented here represent a comprehensive evaluation of the heat-straightening process.

A scientific basis is provided which will enable an engineering evaluation of heat-straightening repairs. In turn, the methodology for conducting actual repairs is also presented.

In the past, heat straightening has been more art than science. While the fundamental principles and basic methodology will be presented here, heat straightening is a skill requiring practice and experience. The proper placement and sequencing of heats combined with control of the heating temperature and jacking forces distinguishes the expert practitioner.

Typical Types of Damage

The focus of this manual is on repairing damage to members of steel bridge structures. However, the principals are applicable to any type of steel structure. Damage to steel bridge members may result from a variety of causes. Among the more frequent are: vehicle impact, over-height trucks, unrestrained equipment on trucks, fire, and earthquake. While damage in structures may appear random, certain patterns and characteristics are distinguishable. A convenient way to classify damage is to define the four fundamental damage patterns, although typical accidents often include a combination of these types. The fundamental damage categories are:

1. Category S

This type refers to damage as a result of bending about the "strong" or major axis. For rolled or built-up shapes, the web element is bent about its strong axis with one flange element in compression and one in tension. In addition to plastic deformation,

the compression flange will sometimes exhibit local buckling due to the high compressive stresses. A typical example is shown in fig. 1.1.

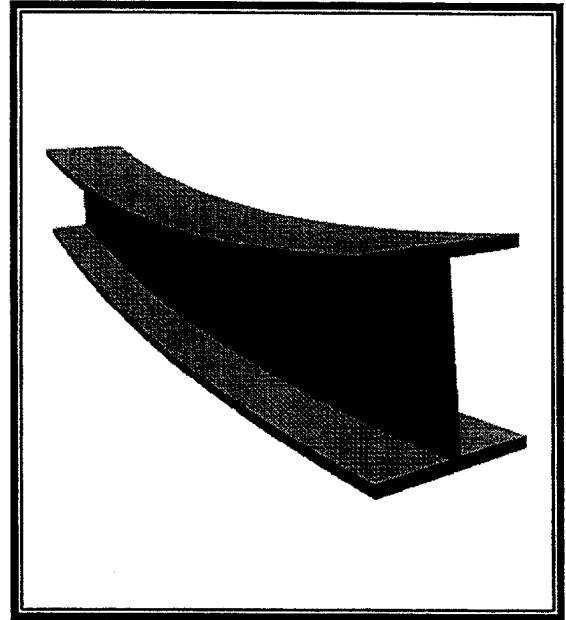


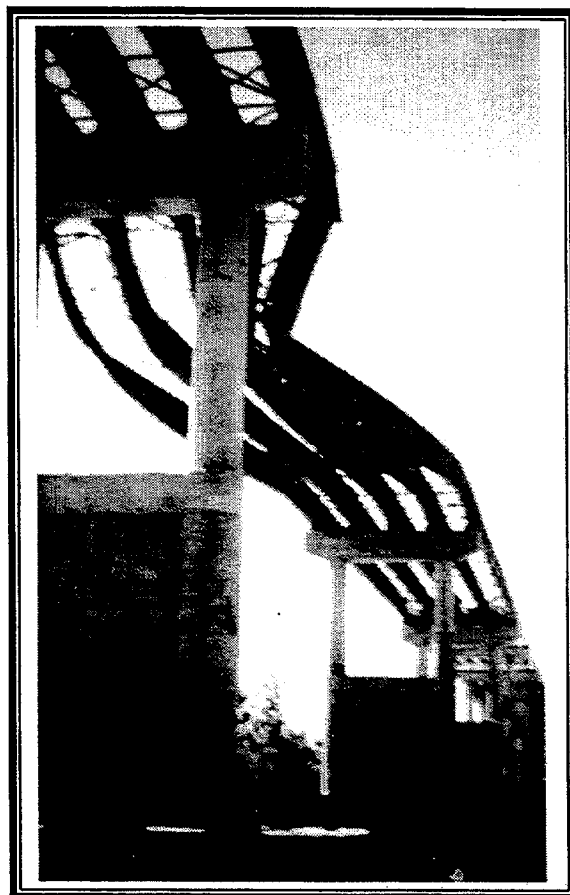
Figure 1.1 Graphic illustration of Category S damage.

2. Category W

This category refers to damage as a result of bending about the "weak" or minor axis. For rolled or built-up shapes the web is usually at, or near, the neutral axis. Consequently, it may be below yield and not deformed into the inelastic range. The flange elements are bent about their strong axes and usually exhibit classical flexural yield patterns. Typical examples are shown in fig. 1.2.



(a) Category W damage on a built-up double channel truss member. The damage was caused by a log falling from a truck on a bridge in North Louisiana.



(b) Category W damage to main girders caused by wind during construction of a Louisiana bridge.

Figure 1.2. Examples of Category W damage.

3. Category T

This type refers to damage as a result of torsion or twisting about the longitudinal axis of a member. For rolled or built-up shapes, the flange elements tend to exhibit flexural plastic deformation in opposite directions. The web is often stressed at levels

below yield. If one flange is constrained (such as the case of a composite bridge girder), then the unconstrained flange element is subjected to plastic deformation and yielding may also occur in the web. Examples are shown in fig. 1.3.

(a) Category T damage to a composite wide flange beam. Damage was induced by a jack as part of an experimental program at LSU.



(b) Category T damage on a composite bridge girder impacted by an over-height vehicle in Wisconsin.

Figure 1.3. Examples of Category T damage.

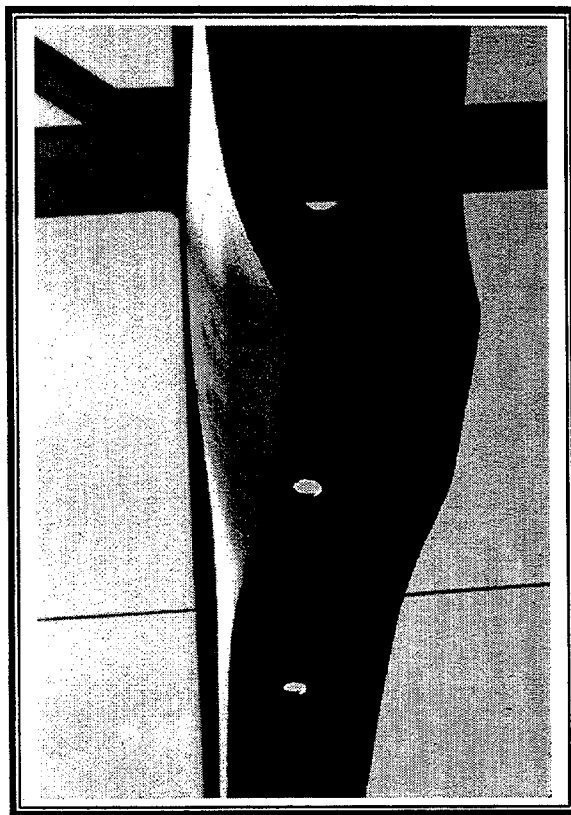


Figure 1.4. Category L damage showing flange buckles on wind bracing on Mississippi River Bridge in Greenville, MS.

4. Category L

This category includes damage that is localized in nature. Local flange or web buckles, web crippling and small bends or crimps in plate elements of a cross section typify this behavior. An example is shown in fig. 1.4.

The importance of this classification system is that well-defined heating patterns can be established for each category. Once these patterns are understood, they can be used in combination for damage that includes multiple categories.

Objectives of This Manual

The goals of this manual are to:

- Describe and quantify the fundamentals of the heat straightening process.
- Address specific methods for repairing the basic damage categories described above.
- Provide guidelines for repairing more complex combinations of the basic damage categories.
- Provide detailed technical research data for engineers and scientists.
- Provide guidelines for conducting and supervising heat-straightening repairs.
- Provide model specifications for conducting heat-straightening repairs.

How to Use This Manual

This manual is intended as a reference guide for conducting heat-straightening repairs. Part I, including Chapters 1, 2, and 3, contains an overview of heat straightening and is designed as an introduction for those unfamiliar with the process. Part II, including Chapters 4 through 10, is a technical guide in which the details of the process are presented. This part contains a detailed explanation of all important aspects of heat straightening. Research data is presented and analyzed. This part serves as a technical reference in which the interested reader can pursue specifics on any aspect of heat straightening. Part III contains an engineering guide, recommended specifications, a glossary, and a list of references. The engineering guide summarizes the heat-straightening repair process in the form of a manual of practice. This guide summarizes

the steps to be considered from assessment of damage to planning the repair process to supervising the repair. The technical specifications are given in a form which may be incorporated into contracts or may be suitable for inclusion in codes and standards.

In conjunction with the development of this manual, a multimedia instructional computer program and video have been prepared. The fundamentals of heat straightening are illustrated in both. The multimedia computer program is available on a compact disc (CD) and allows the user to

access material interactively. It contains an overview section as well as sections on management, design and techniques for heat straightening. An index provides a listing of commonly used heat straightening patterns. The program also provides a step-by-step example of how to conduct a bridge repair. The video is available in VHS format. It provides an overview of how to conduct heat-straightening repairs. This manual provides background material and more in-depth information as a supplement to the computer program and video.

Chapter 2. Heat Straightening Basics

What Is Heat Straightening?

Heat straightening is a repair procedure in which a limited amount of heat is applied in specific patterns to the plastically deformed regions of damaged steel in repetitive heating and cooling cycles to produce a gradual straightening of the material.

The process relies on internal and external restraints that produce thickening (or upsetting) during the heating phase and in-plane contraction during the cooling phase. Heat straightening is distinguished from other methods in that force is not used as the primary instrument of straightening. Rather, the thermal expansion/contraction is an unsymmetrical process in which each cycle leads to a gradual straightening trend. The process is characterized by the following conditions which must be maintained:

1. The maximum heating temperature of the steel does not exceed either (a) the lower critical temperature (the lowest temperature at which molecular changes occur), or (b) the temper limit for quenched and tempered steels.
2. The stresses produced by applied external forces do not exceed the yield stress of the steel in its heated condition.
3. Only the regions in the vicinity of the plastically deformed zones are heated.

When these conditions are met, the material properties undergo relatively small changes and the performance of the steel remains essentially unchanged after heat straightening. Properly conducted, heat

straightening is a safe and economical procedure for repairing damaged steel.

A clear distinction should be made between heat straightening and two other methods often confused with heat straightening: hot mechanical straightening and hot working. Hot mechanical straightening differs from heat straightening in that applied external force is used to straighten the damage. These applied forces produce stresses well above yield, resulting in large movements during a single heat cycle. Often the member is completely straightened by the continued application of a large force during a single cycle. The results of this type of straightening are unpredictable and little research has been conducted on this procedure. Specific concerns about hot mechanical straightening include:

1. Fracture may occur during straightening
2. Material properties may be adversely affected
3. Buckles, wrinkles or crimps may result

The Engineer should recognize that hot mechanical straightening is an unproven method which may lead to damaged or degraded steel. As such, its use should be considered only in special cases in which other methods are not viable.

Hot working is distinguished from heat straightening in that both large external forces and high heat are used. This method is similar to hot mechanical straightening in that external forces are used. In addition, the steel is heated well above the lower criti-

cal temperature and often glows cherry red indicating a temperature above the upper critical temperature. The results of this process are highly unpredictable and may result in:

1. Fracture during straightening
2. Severe changes in molecular structure which may not be reversible
3. Severe changes in mechanical properties including a high degree of brittleness
4. Buckles, wrinkles, crimps, and other distortions

Hot working should not be used to repair damaged steel.

Some practitioners will tend to over-jack and over-heat yet claim to be heat straightening. The reader is cautioned to be aware of these distinctions when specifying heat straightening as opposed to either hot mechanical straightening or hot working.

Why Heat Straightening Works

The basic concept of heat straightening is relatively simple and relies on two distinct properties of steel:

- If steel is stretched or compressed past a certain limit (usually referred to as yield), it does not assume its original shape when released. Rather, it remains partially elongated or shortened, depending on the direction of the originally applied force.
- If steel is heated to relatively modest temperatures (370-700°C or 700-1300°F), its yield value becomes significantly lower while at the elevated temperature.

To illustrate how steel can be permanently deformed using these two properties, consider the short steel bar in fig. 2.1a. First, the bar is placed in a fixture, much stronger than the bar itself, and clamped snug-tight (fig. 2.1b). Then the bar is heated in the shaded portion. As the bar is heated it tries to expand. However, the fixture prevents expansion in the longitudinal direction. Thus, the fixture exerts restraining forces on the bar as shown in fig. 2.1c. Since the bar is prevented from longitudinal expansion, it is forced to expand a greater amount laterally and transversely through its thickness than in an identical unrestrained bar. Consequently, a bulge will occur in the heated zone. Because the bulge has been heated, its yield value has been lowered, resulting in some yielding which does not occur in the unheated portions. When the heating source is removed, the material will cool and contract three-dimensionally. The clamp cannot prevent the bar from contracting longitudinally. As cooling progresses the bar shortens and the bulge shrinks. However, a portion of the bulge is permanent even after the bar has completely cooled and the bar has shortened from its original length, fig. 2.1d. In essence a permanent redistribution of material has occurred in the heated zone leaving the bar slightly shorter with a small bulge. This permanent bulge, or thickening, in the heated zone is called "upsetting". The redistribution of material is referred to as "plastic deformation" or "plastic flow". The clamping force is often referred to as a restraining force. Through cycles of clamping, heating, and cooling, the bar could be shortened to practically any length desired.

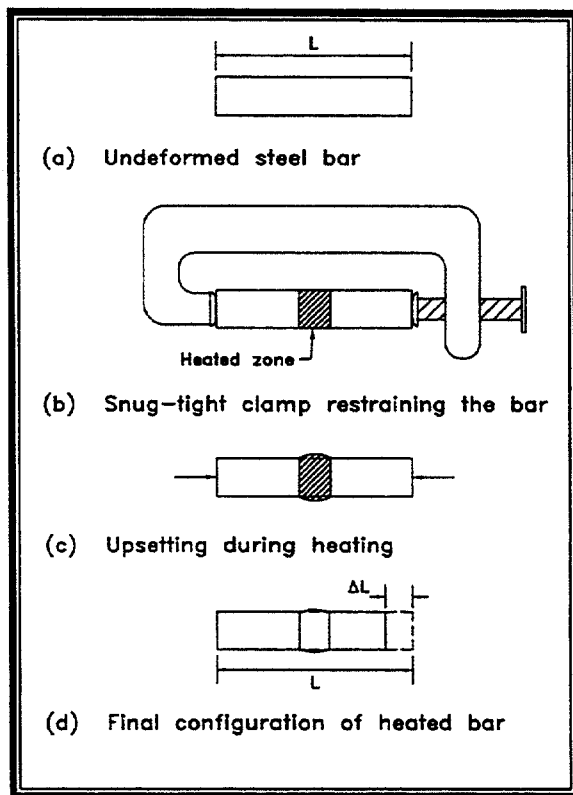


Figure 2.1. Conceptual example of shortening a steel bar.

This simple example illustrates the fundamental principles of heat straightening. However, most damage in steel members is much more complex than stretching or shortening of a bar. Consequently, different damage conditions require their own unique heating and restraining patterns.

The purpose of this chapter is to explain the basic techniques used in heat-straightening.

There are three key elements to the heat-straightening process. The first is to select proper heating patterns and sequencing to fit the damage. The second is to properly control the heating temperature, and rate of heating and cooling. The third is to provide appropriate restraints during the heating

cycle which can be relaxed or modified during the cooling cycle. The place to begin a discussion of heat straightening basics is with the first key: proper heating patterns and sequencing.

Fundamental Heating Patterns

Several types of simple heating patterns exist. When these patterns are combined into specific combinations, effective heat straightening results. As a starting point in understanding heat straightening, it is helpful to first consider a flat plate. Most steel bridge members are an assemblage of plate elements arranged to maximize strength and stiffness while minimizing material. Once an understanding of the heating patterns for a single plate is developed, these concepts can be extended to other shapes. There are several basic heating patterns used for flat plates.

Vee Heat.-The vee heat is the most fundamental pattern used to straighten strong axis (category S) bends in steel plate elements. As seen in fig. 2.2, a typical vee heat starts with a very small spot heat applied at the apex of the vee-shaped area using an oxy-fuel torch. When the desired temperature is reached (usually around 650°C or 1200°F for mild carbon steel), the torch is advanced progressively in a serpentine motion toward the base of the vee. This motion is efficient for progressively heating the vee from top to bottom. The plate will initially move upward (fig. 2.2a) as a result of longitudinal expansion of material above the neutral axis producing negative bending. The cool material adjacent to the heated area resists the normal thermal expansion of the steel in the longitudinal direction. As a result, the heated material will tend to expand, or upset, to a greater extent through

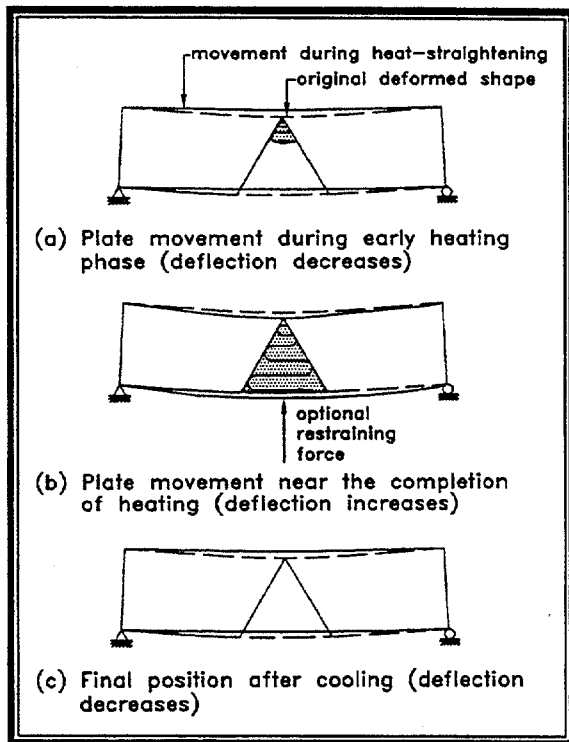


Figure 2.2. Stages of movement during vee heat.

the thickness of the plate, resulting in plastic flow. At the completion of the heat, the entire heated area is at a high and relatively uniform temperature. At this point the plate has moved downward (fig. 2.2b) due to longitudinal expansion of material below the neutral axis producing positive bending. As the steel cools, the material contracts longitudinally to a greater degree than the expansion during heating. Thus, a net contraction occurs. Because the net upsetting is proportional to the width across the vee, the amount of upsetting increases from top to bottom of the vee. This variation produces a closure of the vee. Bending is produced in an initially straight member, or straightening occurs (if the plate is bent in the opposite direction to that of the straightening move-

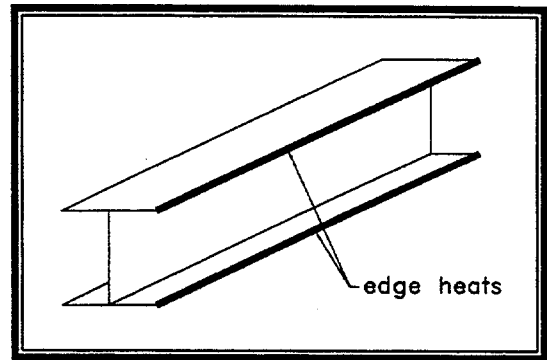


Figure 2.3. Schematic diagram of edge heats used to heat-curve a beam.

ment, fig. 2.2c). For many applications, it is most efficient to utilize a vee that extends over the full depth of the plate element but, partial depth vees may be applicable in certain situations. When using partial depth vees, the open end should extend to the edge of the element. The vee depth is varied by placing the apex at a partial depth location. The most typical partial depth vees are the three-quarter and half depth. Applications for partial depth vees will be discussed in later sections.

Edge Heats.-If a smooth gentle bend is desired, a line along the edge of the member is heated. The line may be continuous or intermittent, depending on the degree of curvature desired. This pattern is often used to heat-curve rolled shapes in the fabricating shop. A schematic is shown in fig. 2.3.

Line Heats.-Line heats are employed to repair a bend in a plate about its weak axis. Such bends, severe enough to produce yielding of the material, often result in long narrow zones of yielding referred to as yield lines. A line heat consists of a single straight pass of the torch, fig. 2.4. The restraint in this case is often provided by an external force although movement will occur

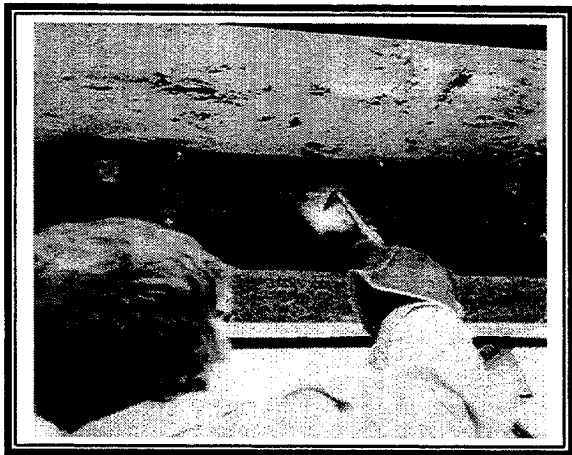


Figure 2.4. Line heat in progress on the web of a wide flange beam.

without external constraints. This behavior is illustrated in fig. 2.5. A line heat is applied to the underside of a plate element subjected to bending moments produced by external forces (fig. 2.5a). As the torch is applied and moved across the plate, the temperature distribution decreases through the thickness (fig.2.5b). The cool material ahead of the torch constrains thermal expansion, even if bending moment constraints are not present. Because of the thermal gradient, more upsetting occurs on the torch (or hotter) side of the plate. During cooling this side consequently contracts more, creating a concave bend on the torch side of the plate similar to that shown in fig. 2.5d. Thus, to straighten a plate bent about its weak axis, the heat should be applied to the convex side of the damaged plate. The movement can be magnified by the use of applied forces which produce bending moments about the yield line (fig. 2.5c). Referring to a section through the plate transverse to the line heat

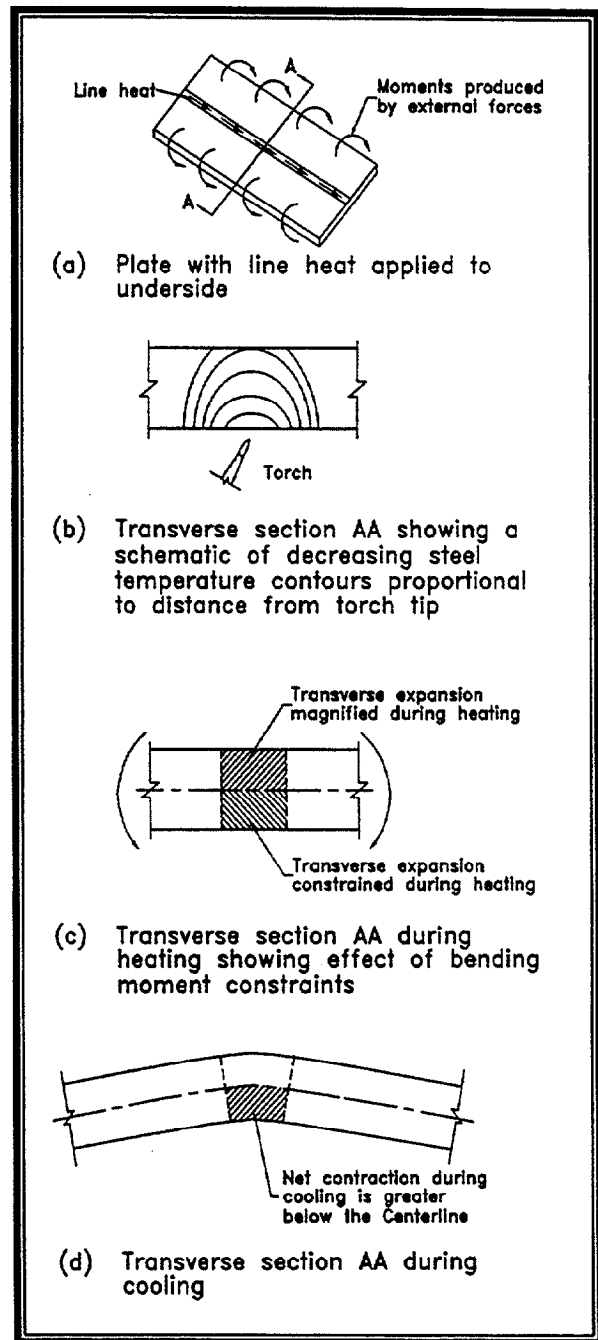


Figure 2.5. Schematic of line heat mechanism.

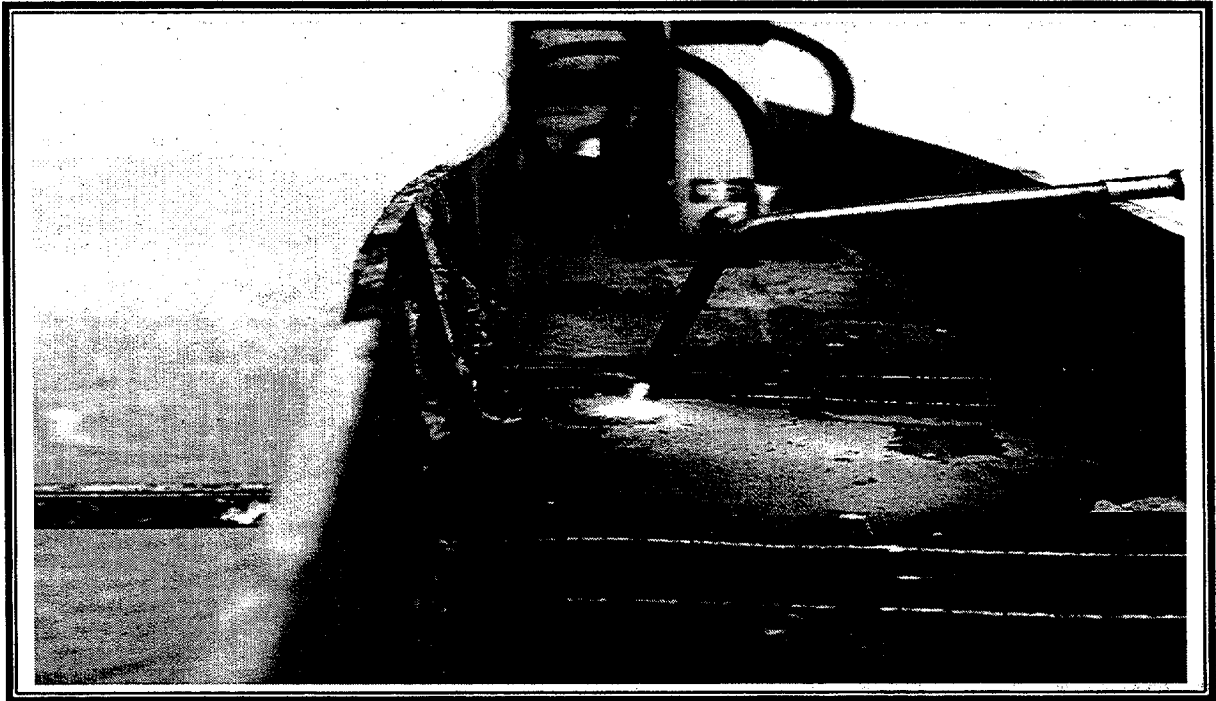


Figure 2.6. Strip heat in progress with a completed strip heat in the foreground.

(fig. 2.5c), the restraining moments tend to prevent transverse expansion below the plate centerline. In a manner similar to the vee heat mechanism, the material thus tends to expand through the thickness, or "upset". Upon cooling, the restraining moments tend to magnify transverse contraction (fig. 2.5d). The speed of the travel of the torch is critical as it determines the temperature attained. With proper restraints and a uniform speed of the torch, a rotation will occur about the heated line.

Spot Heats.-For a spot heat, a small round area of the metal is heated by moving the torch in a slow circular motion increasing the diameter until the entire area of the

metal is heated. A spot heat causes upsetting of the metal through the thickness due to the restraint provided by the cool surrounding material. On cooling, a spot heat leaves tensile stresses in all the radial directions across the heated area. During a spot heat, the torch should not be held at a particular point for too long, as the spot may get too hot and buckling may occur due to excessive thermal expansion on the heated side of the member. Spot heats are used to repair localized damage such as bulges, dents, bellies, or dishes in a plate element.

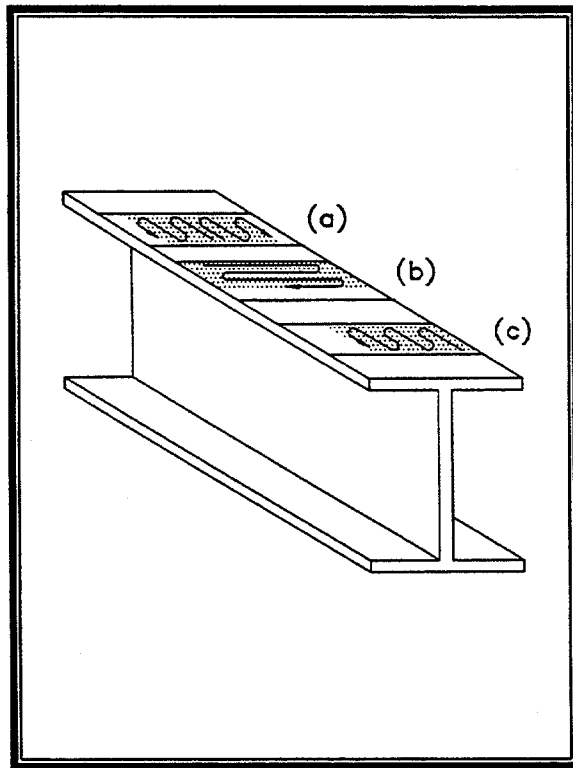


Figure 2.7. Schematic of strip heat on the top flange of a wide flange beam.

Strip Heats.-Strip heats, also called rectangular heats, are used to remove a bulge in a plate element or to complement a vee heat. Strip heats are similar to vee heats and are accomplished in a like manner. Beginning at the initiation point, the torch is moved back and forth in a serpentine fashion across a strip for a desired length, fig. 2.6 and 2.7. This pattern sequentially brings the entire strip to the desired temperature. The orientation can be an important consideration. The strip heat may be initiated at the midpoint and moved toward both edges si-

multaneously using two torches. This approach would minimize weak axis bending of the beam shown in fig. 2.7a. A second alternative with similar effect is shown in fig. 2.7b using a single torch and starting from one side. Depending on the structural configuration, the strip may also be started at a free edge as shown in fig. 2.7c. However, without restraints, this orientation may produce some weak axis bending. By alternating the initiation point to opposite edges in successive heating cycles, the weak axis bending can be minimized.

Defining Basic Damage Patterns and Yield Zones

The fundamental damage categories have previously been defined. A yield pattern is associated with each damage category. The yield zone of steel is that area in which inelastic deformation has occurred. It is important to recognize the region of yielding because heat should only be applied in the vicinity of the yield zones. Typical yield zones are shown in fig. 2.8. These sketches are schematic to depict the basic patterns. The yield zones may vary in length depending on the type of loading and degree of damage. Often, these zones can be determined by visual inspection and are identified by paint peeling or loosened rust and mill scale. Analytical methods are also available when necessary to accurately determine yield zones. The yield zone for category S damage to a wide flange beam is shown in fig. 2.9 along with the appropriate heating pattern.

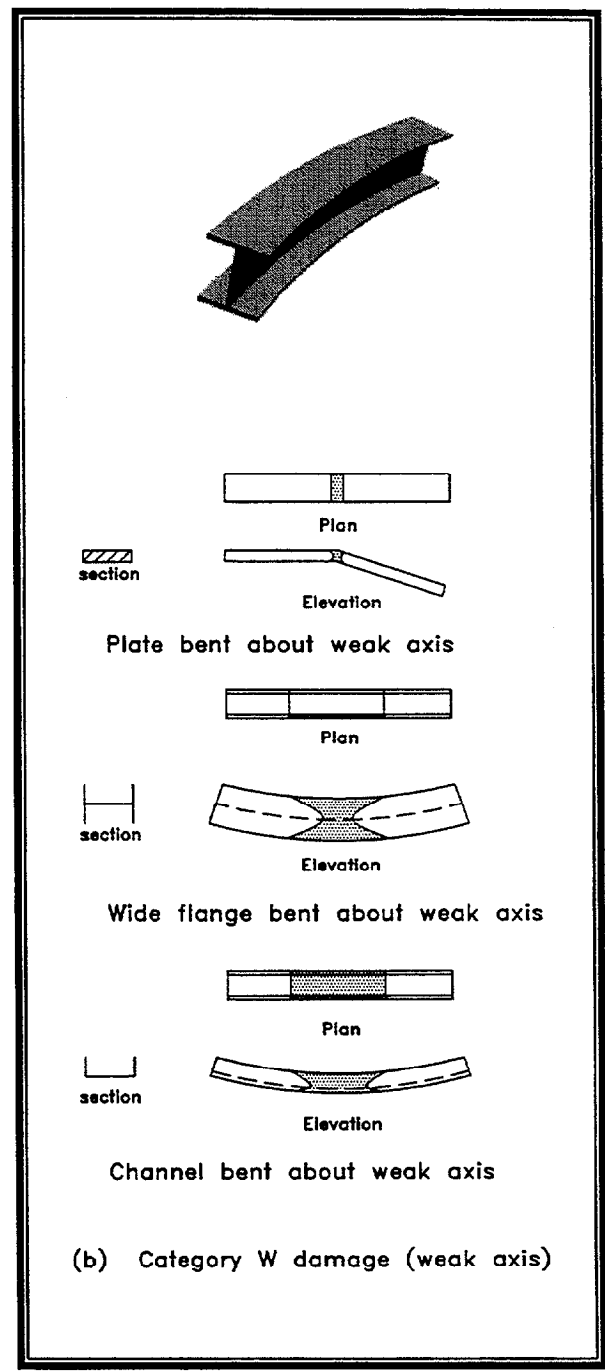
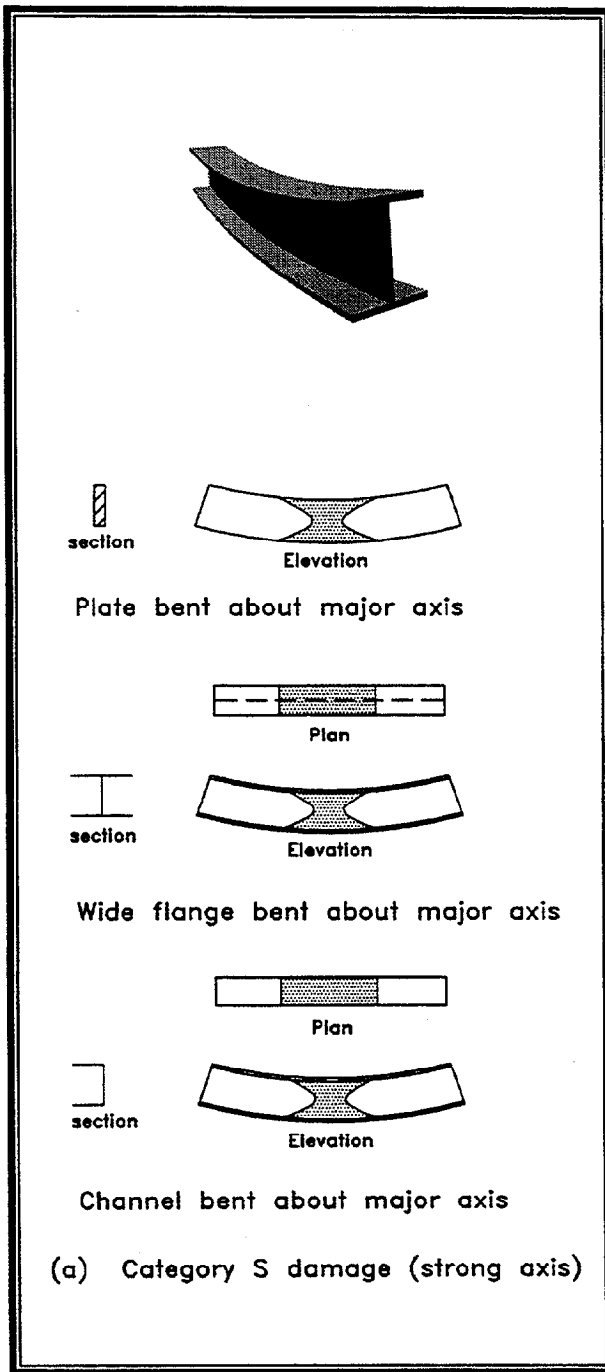


Figure 2.8. Yield zones for basic damage patterns.

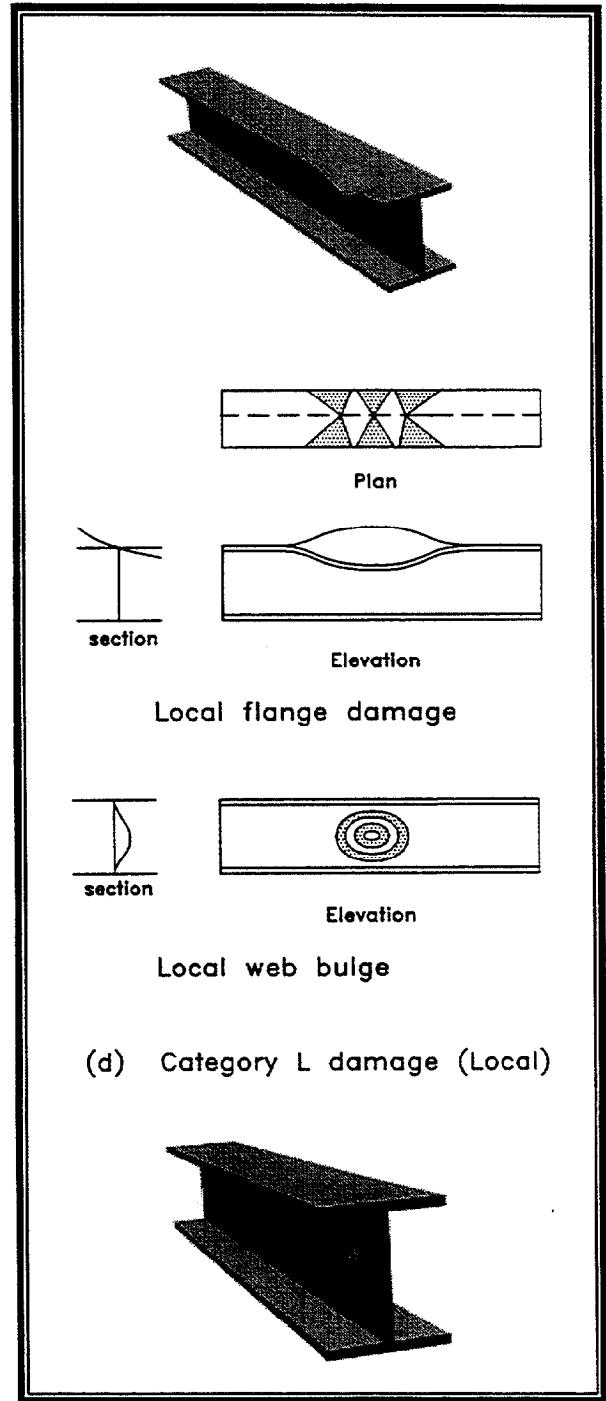
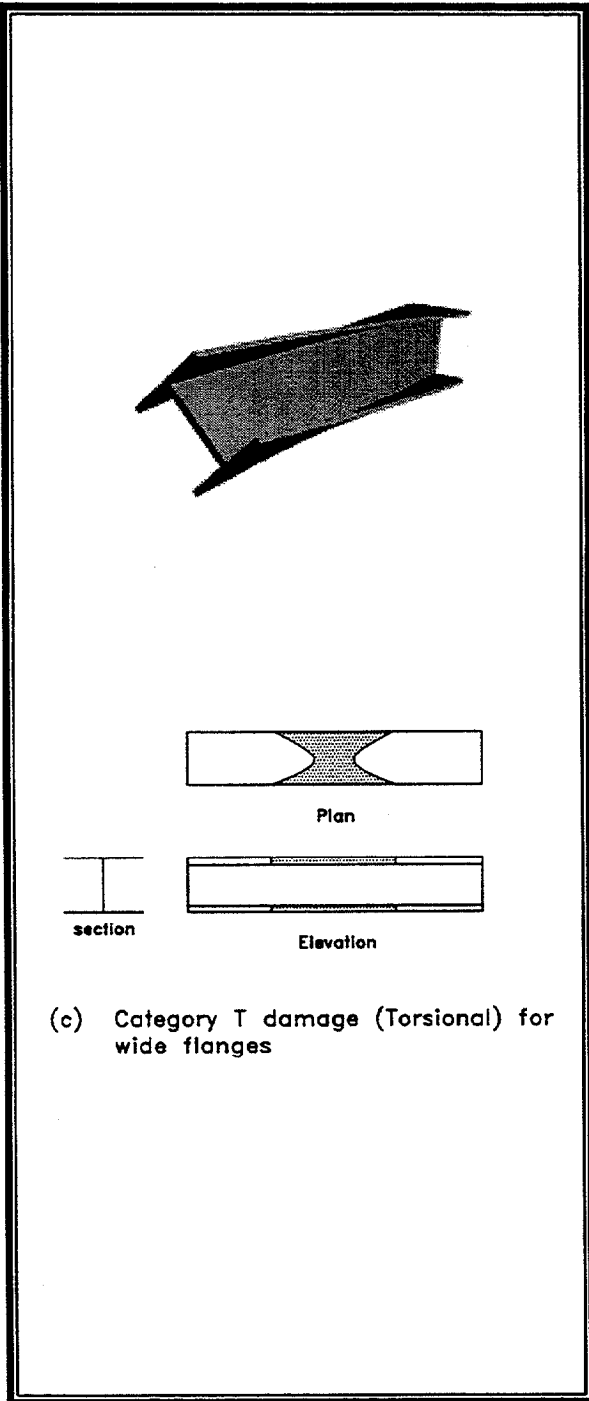


Figure 2.8. Continued.

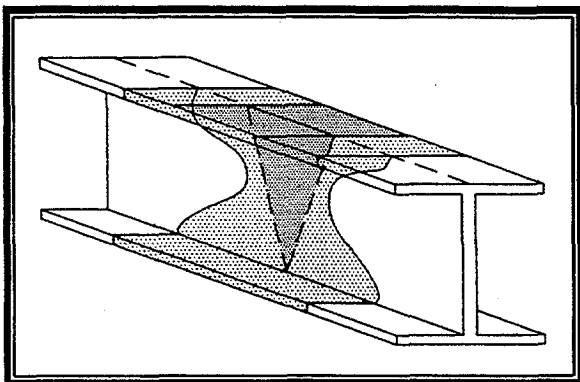


Figure 2.9. Yield zone and vee/strip heat layout for a category S I shaped beam.

Basic Heating Patterns

The repair of damaged steel members often requires a combination of vee, strip, line, or spot heats. A series of such heats, applied consecutively as a group, is referred to as a heating pattern. The order in which these individual heats are conducted is referred to as the heating sequence. The process of conducting a complete heating pattern and allowing it to cool is referred to as a heating cycle. Structural steel shapes for bridges can be considered as an assemblage of flat plates. Almost invariably, damage to these shapes involves the bending of some of these plate elements about their own major axes. Consequently, the heat straightening of steel begins with the application of vee heats to such plate elements. The application of a single vee heat to a flat plate has already been described. This basic vee heat is the building block upon which heat straightening of bridge members rest. The heating patterns used for the four fundamental damage categories are outlined in this section for typical rolled shapes.

Flat Plate Bent About Major Axis (Category S).-The deformed shape of the typical bent plate is shown in fig. 2.10. The heating pattern is the full-depth vee as shown. Because the net change in curvature after one pattern of heats is small, cycles of heating and cooling are required to completely straighten a damaged plate. For each cycle, the vee (or vees) should be moved to a different location in the vicinity of the yield zone region as suggested by the dashed lines in fig. 2.10 so that the exact same spot is not continually reheated. More heats should be placed in the central part of the yield region and fewer near the extremities to reflect the difference in damage curvature. This principle applies for all heating patterns in the following sections.

Structural Members Bent About Their Strong (Major) Axis (Category S).

As shown in fig. 2.11, the heating pattern for these cases consist of a vee and strip heat combination. For purposes of defining heating patterns, it is convenient to refer to the elements of a cross section as either primary or stiffening elements. The primary elements are those damaged by bending about their major axes, such as the webs in fig. 2.11. The stiffening elements are those bent about their minor axes, such as the flanges in fig. 2.11. Typically, vee heats are applied to primary elements while strip, line or no heat at all may be applied to stiffening elements. For the case under consideration here, a vee heat is first applied to the web. Upon completion, a strip heat is applied to the flange at the open end of the vee. The width of the strip heat always equals the vee width at the point of intersection. This procedure allows the vee to close during cooling without restraint from the stiffening element. No heat is applied to the flange at

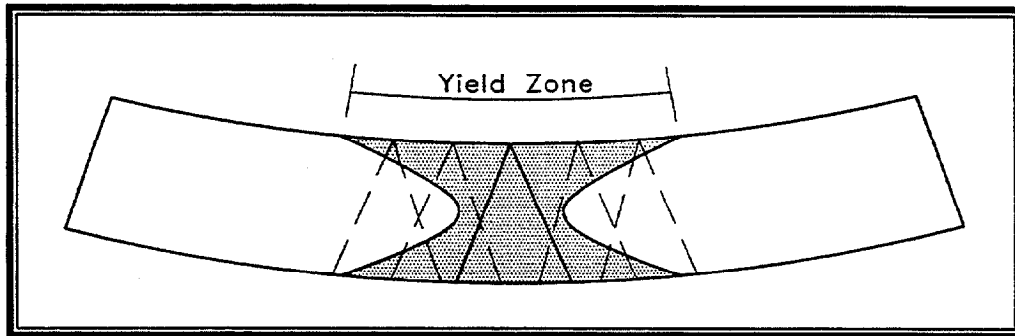


Figure 2.10. Plate vee heat pattern over yield zone.

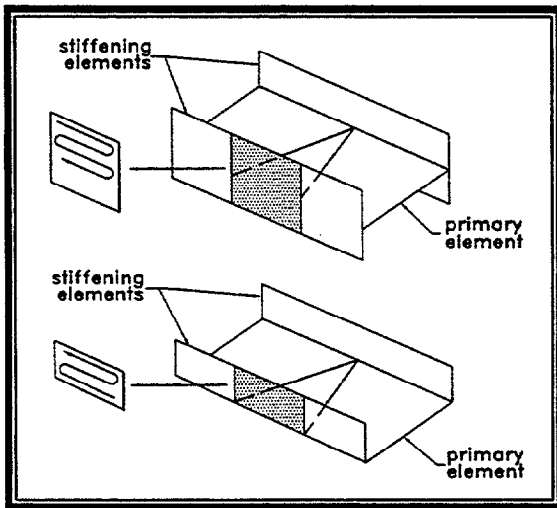


Figure 2.11. Heating patterns for wide flanges and channels bent about their major axes (Category S).

the apex of the vee. This vee/strip combination is repeated by shifting over the vicinity of the yield zone until the member is straight.

Structural Members Bent About Their Weak (Minor) Axes (Category W).-The heating pattern for these cases is similar to the previous case but note the primary and stiffening elements are reversed. The vee heat is first applied to both flanges (either

simultaneously or one at a time) as shown in fig. 2.12. After heating these primary elements, a strip heat is applied to the web. The only exception is that no strip heat is applied to stiffening elements located adjacent to the apex of a vee heated element since this element offers little restraint to the closing of the vee during cooling. Note that the width of the strip heat is equal to the width of the vee heat at the point of intersection. For all cases the pattern is repeated by shifting over the vicinity of the yield zone until the member is straight.

Structural Members Subject to Twisting Damage (Category T).-The heating pattern for this damage case is shown in fig. 2.13. The vees on the top and bottom flange are reversed to reflect the different directions of curvature of the opposite flanges. The vee heats are applied first and then the strip heat is applied. Note that for the channel, the strip heat need only be applied to half depth. This half depth strip allows the lower flange vee to close with minimal restraint from the web.

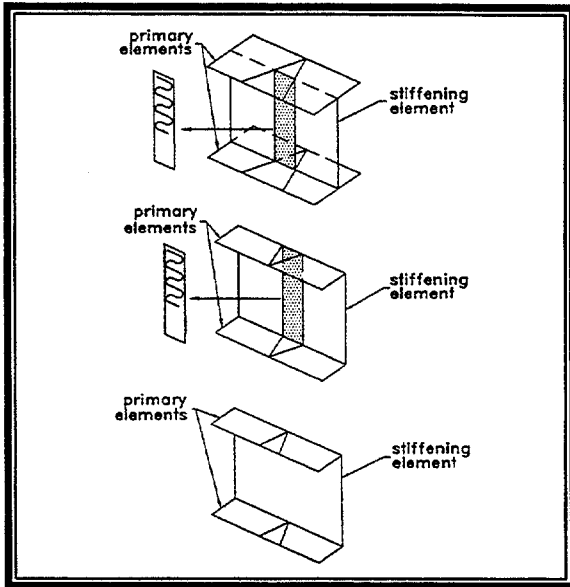


Figure 2.12. Heating patterns for wide flanges and channels bent about their minor axes (Category W).

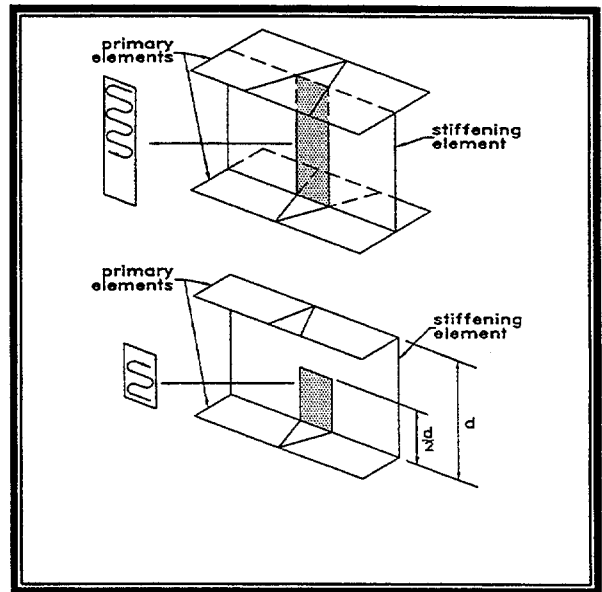


Figure 2.13. Wide flanges and channels with twisting damage (Category T).

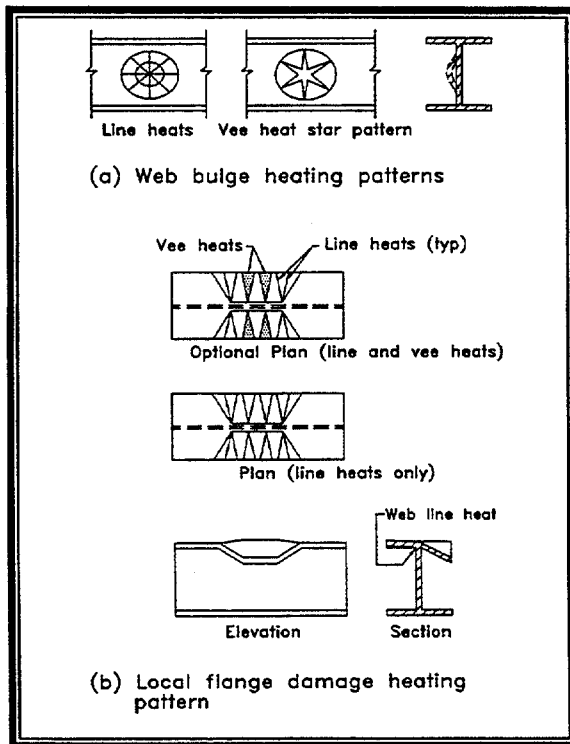


Figure 2.14. Typical heating patterns for local damage.

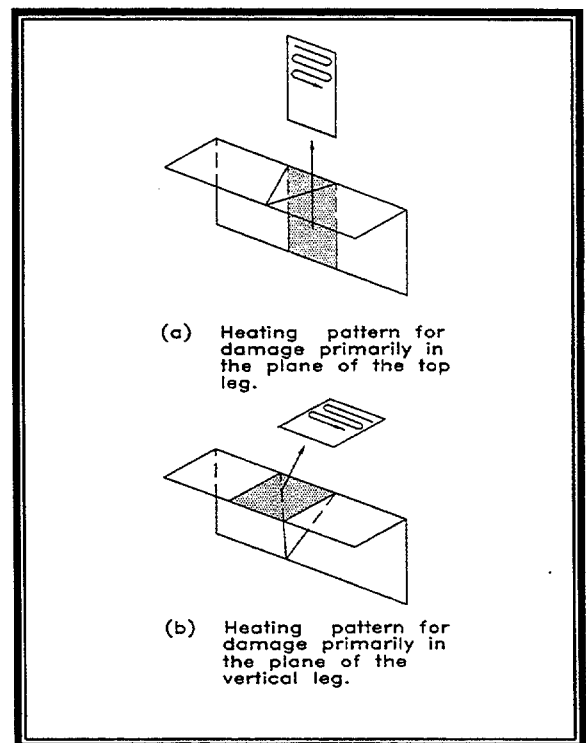


Figure 2.15. Heating patterns for angles.

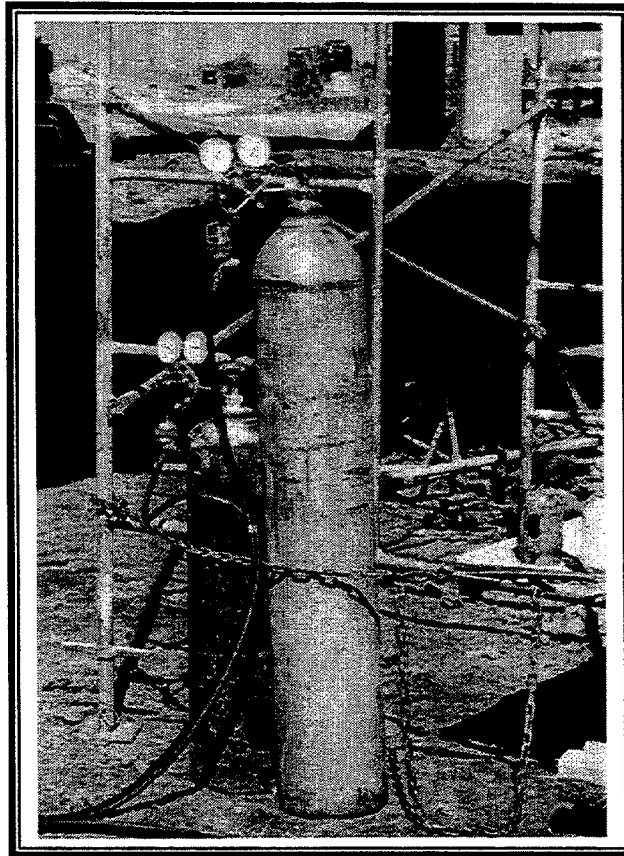


Figure 2.16. Oxyacetylene fuel system.

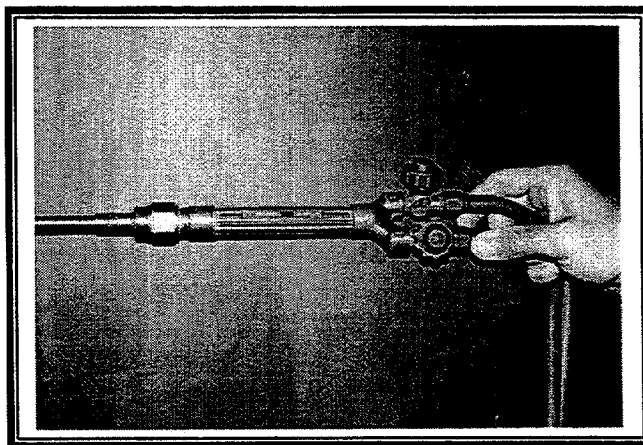


Figure 2.17. Fuel mixing nozzle.

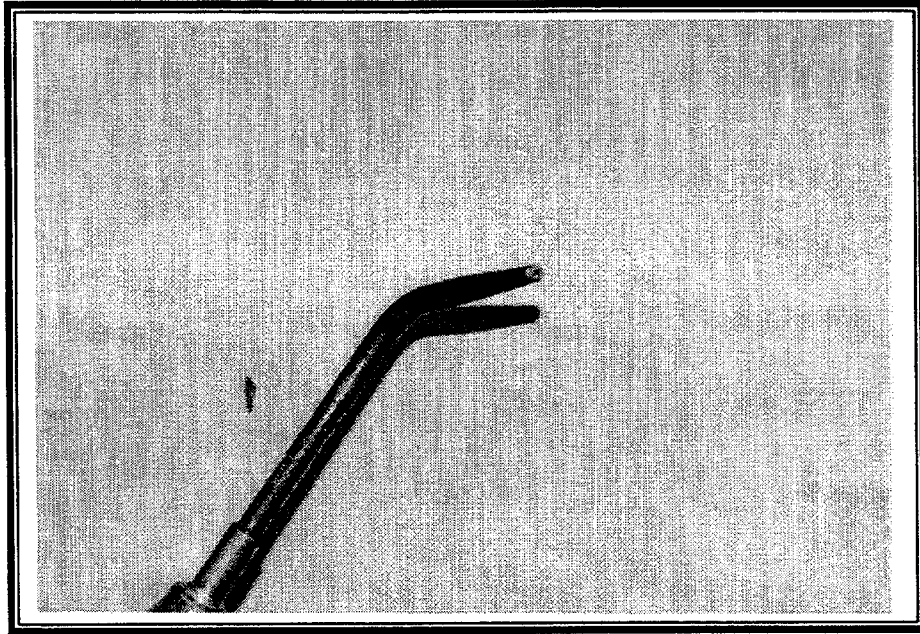


Figure 2.18. Single orifice tip.

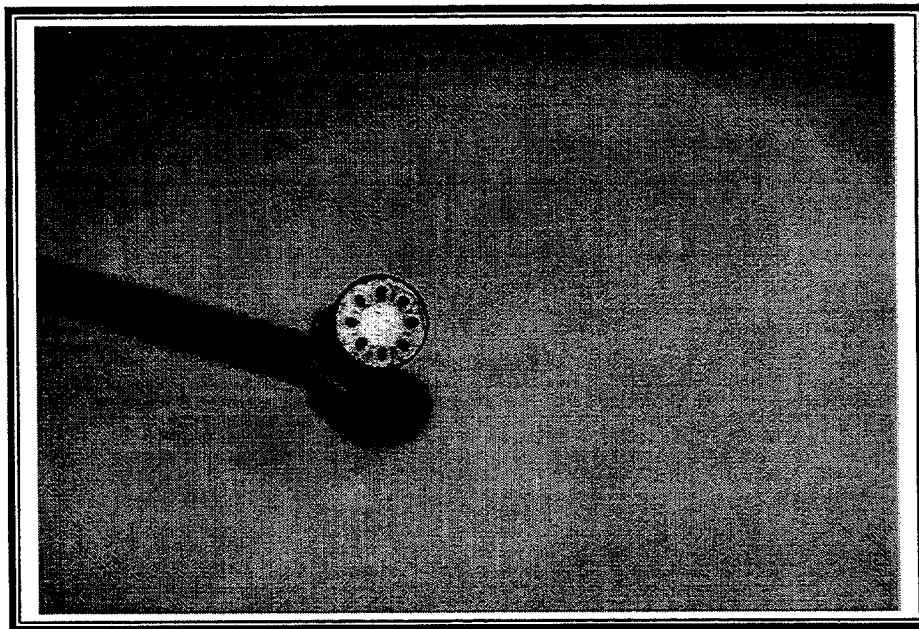


Figure 2.19. Rosebud tip.

Flanges and Webs with Local Buckles (Category L).-A local buckle or bulge reflects an elongation of material. Restoration requires the bulging area to be shortened. A series of vee or line heats can be used for this purpose as shown in fig. 2.14. These vees are heated sequentially across the buckle or around the bulge. For web bulges either lines or vees may be used.

If vees are used, they are spaced so that the open end of the vees touch. There is a tendency for practitioners to over-heat web bulges. For most cases, too much heat is counter-productive. The preferred pattern is the line heats in the spoke/wagon wheel pattern. For the flange buckle pattern (fig. 2.14b) either lines or a combination of lines and vees may be used. For most cases, the line pattern with few or no vees tends to be most effective. Since the flange damage tends to be unsymmetrical, more heating cycles are required on the side with the most damage.

Angles.-Since angles usually do not have an axis of symmetry, the heating pattern requires special consideration. Typically, the heating pattern is similar to that of a channel. However, the vee heat on one leg of an angle will produce components of movement both parallel and perpendicular to the heated leg. Thus, the heating pattern shown in fig. 2.15 may need to be alternated on the adjacent leg. Another method to minimize out-of-plane movement is to use the strip heat patterns suggested in fig. 2.15.

Equipment and Its Use

The primary equipment utilized for heat straightening is a heating torch. The heat source is typically an oxygen-fuel mixture. Typical fuels include acetylene, propane, and natural gas. The appropriate

fuel is mixed with oxygen under pressure at the nozzle to produce a proper heating flame. An oxygen and acetylene setup is shown in fig. 2.16 and the standard nozzle in fig. 2.17. A regulator is used to reduce pressures to working levels of 100-140 kPa (15-20 psi). Either a single orifice torch tip, fig. 2.18, or a multiple orifice tip, fig. 2.19, may be used. The size and type is dictated by the fuel selected and thickness of material to be heated. A No. 8 single orifice tip is generally satisfactory for thicknesses up to 20-25 mm (3/4 or 1 in) with acetylene. For thinner material a smaller tip is recommended. If heavy sections are being heated, a single orifice tip may not be adequate. For such cases a rosebud or multiple orifice tip is recommended. The size may vary depending on the material thickness. The determining factor is the ability to raise the through-the-thickness steel temperature to the specified level. Note that whether single or multiple orifice, the torch should be a heating torch and not a cutting torch.

The oxyacetylene fuel is preferred by many because it is a "hot" fuel. However, this fuel is also highly volatile. Some prefer a propane fuel, which is safer to handle. Since it does not burn as hot, a larger tip or rosebud orifice may be required. In either case the key is to be able to quickly heat a small area. Torch size and fuel must be adjusted to meet these criteria.

Safety Considerations

The fuel used in heat straightening is volatile and dangerous. Fuel tanks should always be handled with extreme care. Safety precautions include:

- Always place a protective cap on head of tank before handling.

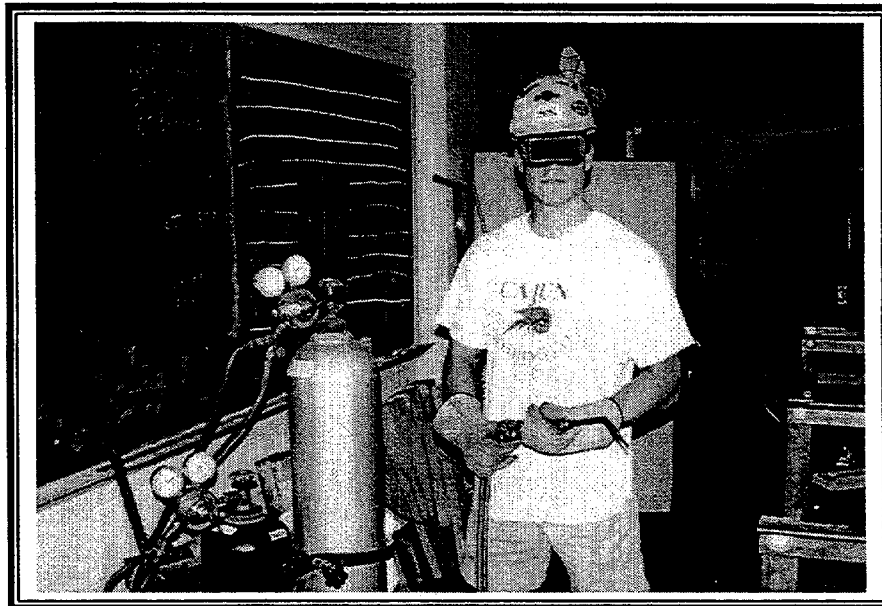


Figure 2.20. Technician preparing to heat straighten in a fabrication shop.

- Always secure tanks prior to heat straightening.
- Examine tanks for damage prior to each use.
- Check lines and fixtures for leaks or damage prior to each use and that proper check valves are installed.

In addition, the technician using the torch must be safety conscious at all times. Precautions include:

- Wear protective goggles while heating as shown in fig. 2.20 (a no. 3 lens is recommended).
- Be careful of where the lighted torch is pointed at all times.
- Wear protective gloves and clothing.
- Always be in a stable, secure position prior to opening valves and lighting the torch.

- Follow proper procedures when using scaffolding and use safety harnesses when working above the ground.

Temperature Control

One of the most important and yet difficult-to-control parameters of heat straightening is the temperature of the heated metal. Factors affecting the temperature include size and type of the torch orifice, intensity of the flame, speed of torch movement, and thickness and configuration of the member. Assuming that adequate control of the applied temperature is maintained, the question arises as to what temperature produces the best results in heat straightening without altering the material properties. Early investigators had different opinions on temperature control. However, more recent comprehensive testing programs have shown that the plastic rotation produced is directly proportional to the heating temperature, up to at least 870°C (1600°F).

The maximum temperature recommended by most researchers is 650°C (1200°F) for all but quenched and tempered high-strength steels. Higher temperatures may result in greater rotation but out-of-plane distortion becomes likely and surface damage such as pitting will occur at 760°-870°C (1400° to 1600° F). Also, temperatures in excess of approximately 700°C (1300°F) (metallurgically referred to as the lower phase transition temperature) may cause changes in molecular composition which could alter material properties after cooling. The limiting temperature of 650°C (1200°F) allows for about one hundred degrees of temperature variation, which was found to be a common range among experienced practitioners. AASHTO/AWS D1.5 (1996) specifies maximum heating temperatures of 590°C (1100°F) for quenched and tempered steels and 650°C (1200°F) for all others. For A514 and A709 (grades 100 and 100W), a minimum tempering temperature of 620°C (1150°F) is required. Thus, the 590°C (1100°F) limit provides a 30°C (50°F) safety factor. However, for A709 grade 70W the specified minimum tempering temperature is 590°C (1100°F). A maximum heating temperature of 565°C (1050°F) is recommended for this grade to provide a 30°C (50°F) safety factor and to avoid property changes.

To control the temperature, the speed of the torch movement and the size of the orifice must be adjusted for different thicknesses of material. However, as long as the temperature is rapidly achieved at the appropriate level, the contraction effect will be similar. Various methods can be used to monitor temperature during heating. Principal among these include: visual observation of color of the steel; use of special tempera-

ture sensing crayons or pyrometers; and infrared electronic temperature sensing devices. More details on the use of these techniques are given in Chapter 3 (Role of Engineer, Inspector, and Contractor.)

Restraining Forces

The term "restraining forces" can refer to either externally applied forces or internal redundancy. These forces, when properly utilized, can expedite the straightening process. However, if improperly applied, restraining forces can hinder or even prevent straightening. In its simplest terms, the effect of restraining forces can be explained by considering the previous plate element as shown in fig. 2.2. The basic mechanism of heat straightening is to create plastic flow, causing expansion through the thickness (upsetting) during the heating phase, followed by elastic longitudinal contraction during the cooling phase. This upsetting can be accomplished in two ways. First, as the heat progresses toward the base of the vee, the cool material ahead of the torch prevents complete longitudinal expansion of the heated material, thus forcing upsetting through the thickness. However, as shown in fig. 2.2, some longitudinal expansion occurs because the surrounding cool material does not offer perfect confinement. After cooling, the damaged induced distortion is reduced in proportion to the confinement level from the internal restraints.

A second method of producing the desired upsetting (usually used in conjunction with the vee heat) is to provide a restraining force. The role of the restraining force is to reduce or prevent longitudinal plate movements associated with expansion during the heating phase. For example, if a restraining force is applied as shown in fig.

2.2, the upsetting effect will be increased by constricting the free longitudinal expansion at the open end of the vee. A restraining force is usually applied externally, producing a bending moment tending to close the vee. Caution must be used in applying external forces, since over-jacking may result in fracture of the member. To minimize the cracking potential, it is recommended that an external force be calculated and set prior to actual heating and not be re-adjusted until the cooling phase of the cycle is complete.

In essence, a restraining force acts in a similar manner to the cool material ahead of the vee heat torch movement. The material behavior can be viewed as shown in fig. 2.21. A small element from a plate, when constrained in the x -direction and heated, will expand and flow plastically primarily through the thickness (fig. 2.21c). Secondary plastic flow will occur in the y -direction. However, this movement will be small in comparison with that of the z -direction, because the plate is much thinner than its y -dimension and offers less restraint to plastic flow. Upon cooling with unrestrained contraction, the final configuration of the element will be smaller in the x -direction and thicker in the z -direction (fig. 2.21d). The material itself cannot distinguish the cause of the constraint: either cooler adjacent material in the case of the vee heat or an external force in the case of a restraining force. In either case the plastic flow occurs in an identical manner.

Sometimes the structure itself provides additional restraint through redundancy. For example, if the simply supported beam depicted in fig. 2.2 were fixed at the supports, the member stiffness increases by 33 percent. This increased stiffness would provide additional restraint over the simply

supported case. In general, structural redundancy increases the movement per heat in a member.

In light of this discussion, a set of criteria for constraining forces can be developed. These criteria apply for internal as well as external constraints.

1. Constraints should be passive during the heating phase; that is, they should be applied before heating and not increased by external means during heating or cooling.
2. Constraints should not impede contraction during the cooling phase.
3. Constraints should not produce local buckling of the compression element during the heating phase.
4. Constraints should not produce an unstable structure by either the formation of plastic hinges or member instability during the heating phase.

From a practical viewpoint, these criteria mean that (a) the vee angle should be kept small enough to avoid local buckling, (b) the external restraining forces must be applied before heating and be self-relieving as contraction occurs, and (c) the maximum level of any externally applied forces must be based on a structural analysis of the complete structure that includes the reduced strength and stiffness of a member due to the heating effects.

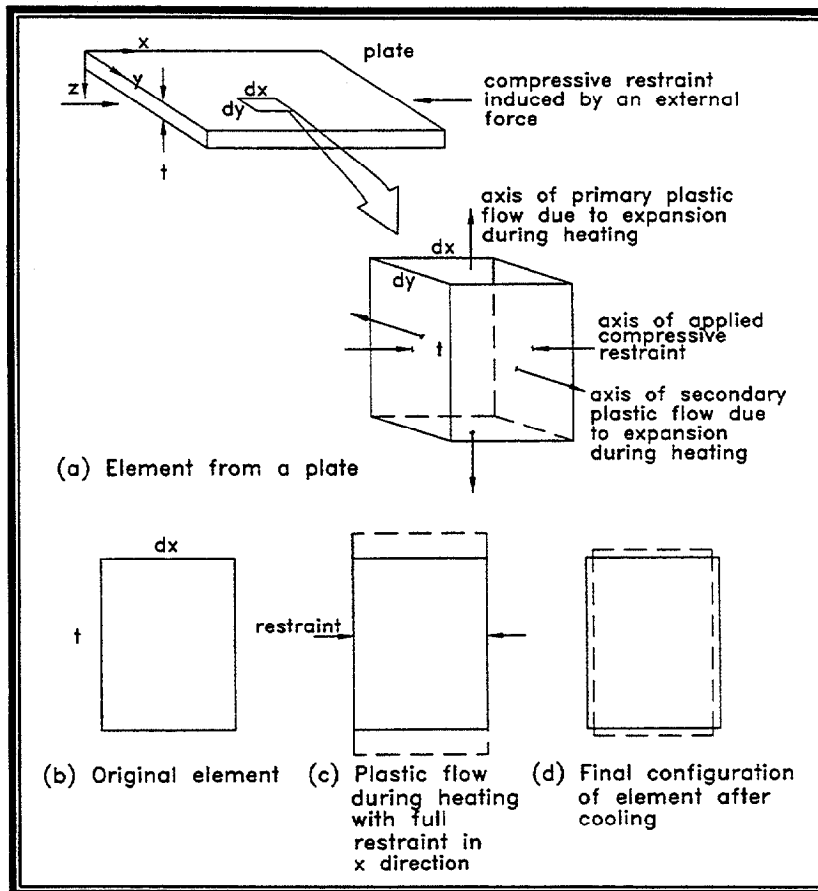


Figure 2.21. Characteristics of plastic flow and restraint during heat straightening.

Table 2.1. Recommended torch tips for various material thicknesses.

Steel Thickness		Orifice Type	Size
(in)	(mm)		
< 1/4	6	Single	3
3/8	10	Single	4
1/2	13	Single	5
5/8	16	Single	7
3/4	20	Single	8
1	25	Single	8
		Rosebud	3
2	50	Single	8
		Rosebud	4
3	75	Rosebud	5
> 4	100	Rosebud	5

Practical Considerations

This description of the heat straightening process provides the basic methodology. However, the proper application of heat is a skill requiring practice and experience and at this juncture, the art of heat straightening meets the technology. The practitioner needs to understand the variables involved in the process and how to control them. Some of the more important variables are discussed here.

Torch Tip Size and Intensity.-The amount of heat applied to a steel surface is a function of the type of fuel, the number and size of the orifices as well as the adjustment of the fuel pressure and intensity at the nozzle tip. Selecting the appropriate tip size is primarily a function of the thickness of the material. The goal is to rapidly bring the steel in the vicinity of the torch tip to the specified temperature, not just at the surface, but through out the thickness. Once this condition is obtained at the initial heating location, the torch should be moved along the path at a rate that brings successive sections of steel to the specified temperature. A tip that is too small for the thickness will result in an inadequate heat input at the surface that does not penetrate adequately through the thickness. If the tip is too large, there will be a tendency to input heat into the region so quickly that it is difficult to control the temperature and distortion. table 2.1 is a general guide for selecting a tip size. However, this table is only a guide. Intensity of the torch, ambient temperature, steel configuration, access, and fabrication details may influence the choice of tips. Adjustments can also be made in the torch intensity to improve the heating response. A hotter flame is helpful if the configuration of the steel tends to draw heat away from the spot

of heating. A less intense flame allows for a slower pace as the torch is moved along the path. The intensity may be adjusted so as to compensate for variables encountered in the field.

Material configuration.-The pace of moving the torch along the path will be a function of the configuration of the member, location of damage and fabrication details. At the initiation of heating, the torch typically remains on a single spot as the temperature rises. Once the heating temperature is reached, a steady movement along the path of heating can usually be maintained. However, backside attachments such as stiffeners may serve as a heat sink requiring the slowing of the torch movement over certain zones.

One typical example is the heating of the flange of a rolled beam where the web-flange juncture must be heated more slowly since the web draws heat away from the flange. Sometimes the pace must be quickened to maintain a uniform heat. A common example is at the conclusion of a vee heat at a free edge. By the last pass along that edge, the wave of heat moving down the vee almost overtakes the torch. As a result, the last pass is usually conducted very quickly. Practice heats will allow you to develop a feel for how to vary the torch speed over various configurations.

Judging the Temperature.-In theory, control of temperature may seem easy: watch the color of the steel and use temperature crayons. In practice, temperature control is quite difficult. First, the satiny silver color of steel indicating 650°C (1200°F) is often obscured. The torch flame often reacts with surface impurities including paint, oil or previous temperature crayon

marks themselves. When the flame hits these, it may burn bright yellow or orange and hide the surface near the tip. The available light also influences visual observations. In daylight or bright indoor light, the silver color is easier to read and no dull red can be seen. However, in outside shadow zones or on overcast days or with limited artificial light, the steel will emit a slight dull red glow at the same temperature. As a general rule, if you can see red in normal lighting, you're heating too hot. Many shop fabricators, erectors and welders operate on the principle that more heat is better. There is at least one book on heat straightening in which the author begins his description with: "First, heat the steel until it glows cherry red...". This is not heat straightening! Call it hot working, hot mechanical straightening, or even blacksmithing; but don't confuse it with heat straightening. When heat straightening is done properly the steel is not heated above its lower phase transition temperature. The steel's properties will not change significantly when the temperature is correctly controlled. Overheating may create brittle, fracture sensitive zones, which could result in a sudden failure. Constant vigilance is required to maintain the heating temperature in the correct range. It takes practice to develop the skill of recognizing and controlling the temperature

Jacking Forces.—Earlier in this chapter a clear distinction was made between hot mechanical straightening and heat straightening. The technique of hot mechanical straightening consists of lowering the yield strength by heating and then mechanically applying sufficient jacking loads in a single application to straighten the damage by inelastically deforming the section. Heat straightening on the other hand, re-

quires that the restraining forces result in stresses that are less than the yield stress at the elevated temperature. Movement occurs as a result plastic deformations during contraction, not by mechanical overload. Therefore, initial restraining forces are an integral part of heat straightening. First, you should always know how much external force is being applied to the system. Thus, all jacks should be gauged and calibrated. Second, the maximum jacking force should be calculated to insure that over-stress at elevated temperatures will not occur. Often, these computations require a structural engineering analysis, although for certain frequently encountered cases, some rules of thumb can be established. These issues are addressed in detail in the technical part of this manual (Part II). The practitioner must be aware that over-jacking may cause over-correction, buckling or a sudden fracture during the process. It might also result in difficult to detect micro-crack damage which could permanently weaken the repaired structure or greatly reduce fatigue resistance.

Heating Patterns.—One of the keys to heat straightening is appropriate heat patterns to fit the yield zones of the steel. Basic patterns were illustrated in figs. 2.10-2.15. Yield zones, where the steel has inelastically deformed, occur in regions of sharpest curvature. Some practitioners have a tendency to heat in a broader zone, but this again is a case of more being less—Stay with the recommended patterns and do not expand them. Heat straightening is a cyclic process. The movement occurs gradually by contraction during cooling. Sometimes 20 or more heating cycles are required to completely straightening a damaged member. Since a heating pattern usually covers only a portion of the yield zone, the pattern should be

shifted on a cycle-by-cycle basis. The significant portion of a single heating pattern array should be in the yield zone with fewer heating cycles near the edges and more near the center where curvature is the sharpest. Also, only make a single continuous pass through a given zone during one heating cycle. Going back and re-heating before the material has cooled interrupts the contraction process. The heat straightening predictability and effectiveness is consequently reduced.

Sequencing of Heats.-When a combination of vee, strip or line heats is used, the order of heating is referred to as the sequence. The sequencing of heats may be important in some straightening operations. However, little research has been conducted to verify its effects. Some practitioners feel that proper sequencing will accelerate the straightening and help keep residual stresses to a minimum. Consider the case of an I beam with Category S damage requiring a vee heat in the web and a strip heat in the flange as shown in fig. 2.11.

A common sequence is to heat the vee first, followed immediately by the strip. The resulting residual stresses and movements per heat are discussed in Chapters 4 and 6. An alternative used by some practitioners is to heat the web vee first and allow it to cool for a few minutes before heating the flange strip. It is felt by some that this approach will reduce the residual stresses significantly. The available research data and difference sequences used in practice indicates that more than one sequence can be successful for many cases. Since different sequences are successfully used in practice, it appears that heat straightening is not overly sensitive to the sequence used. At this time there is not adequate documenta-

tion to support one sequence over another for a particular heating pattern. The experience of the practitioner is the most reliable guide to proper sequencing. The sequencing patterns shown in this manual are based on those often successfully used in practice.

Lack of Movement.-One of the more perplexing aspects of heat straightening is that sometimes there is no movement. Should this happen, repeat the pattern for several cycles, making sure to shift it to a new location within the yield zone after each cycle. Sometimes there is a residual stress pattern tending to oppose movement. Several heating cycles will tend to redistribute or dissipate these opposing stresses and may lead to the desired movement. Should the problem persist, it is probable that the jacking forces are too low. A reanalysis of the jacking layout is recommended, particularly in light of redundancies that may exist. Finally, check the heating patterns to insure that they are consistent with the damage. For example, neglecting to heat all separate yield zones during one heat cycle could prevent movement. The key point is that if the steel doesn't move, there is a reason. It is a matter of finding the reason. Difficult problems may require a consultant more experienced in heat straightening. Over-heating or over-jacking is not a solution.

Cooling the Steel.-Ambient air cooling is the safest method. Rapid cooling is dangerous if the steel has been over-heated and may produce brittle "hot spots". However, once the steel has cooled below the lower phase transition temperature, rapid cooling is not harmful. Many practitioners allow the surface of all the steel to cool below 315°C (600°F) prior to accelerating cooling. Such a surface temperature reduc-

tion insures that the interior steel temperature has dropped. One approach to accelerated cooling is to use compressed air blown on the heated surfaces. Faster cooling can be obtained with water mist cooling. However, the steam generated could result in burns and the water runoff could lead to a clean-up problem especially if it covers areas which must be subsequently heated. The following cautionary measures should be taken when considering this option: (1) a mist applicator which allows the technician to remain at a safe distance; (2) protective clothing and goggles; and (3) a method for safely disposing of the waste water

Key Points to Remember

- Heat straightening is based on the principle of partially constraining the material expansion during heating while allowing unrestrained contraction during cooling.
- There are several fundamental heating patterns including the: vee, line, edge, spot, and strip heat.
- Fundamental heating patterns may be used separately or in combination depending on the damage type.
- Heating equipment usually consists of: oxygen and gas fuel tanks, heating torches, hoses, single or multiple orifice heating tips, and temperature monitoring crayons or equipment.
- Exercise safety precautions at all times.
- Familiarize yourself with the yield zone patterns associated with various damage

conditions:

- ◆ Category S: Strong axis bending
- ◆ Category W: Weak axis bending
- ◆ Category T: Twisting
- ◆ Category L: Localized damage
- Learn the proper heating patterns associated with each category of damage.
- Temperature of the steel should generally be limited to 650°C (1200°F) for carbon steels and low alloy (yield \leq 60 ksi or 400 mPa).
- For quenched and tempered steels the limiting temperature should be:
 - ◆ 590°C (1100°F) for A514 and A709 grades 100 and 100W
 - ◆ 565°C (1050°F) for A709 Grade 70W
- Proper restraining forces can expedite the heat-straightening process.
- Restraining forces (usually jacks) should be set to restrain the steel during heating but to allow free contraction during cooling.
- Restraining forces should be applied in a direction tending to restore the member.
- Restraining forces should be limited so that the material is not over-stressed during heating.
- Patience should be exercised in allowing the heated areas to fully cool below 120°C (250°F). Re-heating too soon may prevent the desired movement and result in additional damage to the steel.

Chapter 3. Assessing, Planning and Conducting Successful Repairs

As with other types of repair, a successful heat-straightening repair requires assessment, planning and design. Several procedures should be considered as part of the process. These aspects may include: determination of degree of damage, location of yield zones and regions of maximum strain, limitations for heat-straightening repair, selection of heating patterns, and selection of jacking restraints. Each requires the exercise of engineering judgement. Outlined in this chapter are some key aspects of assessing, planning and designing a repair. One of the primary keys is maintaining coordination between the engineer, field supervisor or inspector, and the contractor conducting the repair.

Role of Engineer, Inspector and Contractor

The engineer is responsible for selecting the most appropriate repair technique for the specific damage. Alternatives must be evaluated and the most effective solution determined. The key considerations include: cost, constructability, adequate restoration of strength, longevity of repair, time to complete repair, aesthetics, and impact on traffic. These aspects constitute the concept we refer to as design. Although frequently overlooked, repairs should be designed in a similar manner to new structures. The typical process includes: selecting a trial repair scheme, conducting a structural analysis (which may require assumptions of certain geometric or material properties), sizing the parameters of the repair (or verifying the capacity after repair), possibly re-analyzing

and re-designing, evaluating alternate repair or replacement schemes, and finally, providing complete details and specifications for the system selected.

Heat-straightening repair is not the solution for every damage situation. The engineer's role is to make an assessment as to its specific applicability. Aspects to consider are: current condition of the rest of the structure and other anticipated repairs, degree of damage, presence of fractures, cause of damage and likelihood of repetitive damage occurring, accessibility, and the repair method's impact on material properties. Once the heat straightening alternative is selected, then the repair parameters such as traffic control, contractor access and work areas, permitted hours of work, typical heating patterns, maximum restraining forces and locations, and maximum heating temperature must be chosen. Finally, plans and specifications should be developed which generally define how the repair is to be accomplished.

Since most heat-straightening repairs are conducted by contractors, the field supervisor (or inspector), representing the bridge owner, has major responsibilities. The supervisor must insure that the repair is being conducted according to plans and specifications. Of particular importance is insuring that procedures are followed which are not detrimental to the steel.

The third member of the team is the contractor who actually executes the repair. The ultimate success of the project hinges on the skills and understanding for the project

by the contractor's personnel. While others may have designed the repair plan, the details of execution lie with the contractor. Important considerations may include: (1) scaffolding arrangements; (2) selection of proper heating equipment; (3) implementing the restraint plan with appropriate jacks and come-alongs; (4) placing the heats in proper patterns and sequences; and (5) analyzing the progress of the repair. The contractor must be alert to the response of the structure and be prepared to suggest changes to expedite the process. In spite of our current knowledge and analytical capabilities, movements during heat straightening cannot always be predicted accurately.

The primary reasons for this difficulty are that: (1) damage patterns are often a complex mixture of the idealized cases and require experience to determine the details of the heating process; and (2) residual stresses and moments which may have been locked into the structure during the damage phase are sometimes difficult to predict and may prevent the expected movement. The contractor must be able to assess the reaction of the structure to the planned repair and suggest modifications if the structure is not performing properly. These modifications may range from changes in heating patterns and jacking arrangements to decisions on whether to remove secondary or bracing members during the repair.

Perhaps most important is that the engineer, the supervisor and the contractor maintain open and clear channels of communication. This interaction of the three key players in a heat-straightening repair will go a long ways toward insuring a successful project.

Keys to a Successful Repair

A successful repair requires the control and selection of certain specific parameters. The first key is the selection of the heating patterns and sequences. The combination of vee, line and strip heats must be chosen to fit the damage patterns. Heat should only be applied in the vicinity of those regions in which yielding of the material has occurred. Typically, vee heats should be relatively narrow. A good rule of thumb is to limit the open end of the vee to 250 mm (10 in) for one inch thick plates. However, a smaller limit should be considered for progressively thinner plates. These limits will minimize distortion which might occur due to local buckling of the plate element.

The second key is to control the heating temperature and rate. Temperatures should be limited to 650°C (1200°F) for carbon and low alloy steels, 590°C (1100°F) for A514 and A709 (Grade 100 and 100W) quenched and tempered steels and 565°C (1050°F) for A709 (Grade 70W) quenched and tempered steel. Higher heats may adversely affect the material properties of the steel and lead to a weaker structure.

The third key is to control the restraining forces during repair. One of the most critical factors is the applied restraining force. Research has shown that the use of jacks to apply restraints can greatly shorten the number of heating cycles required. However, over-jacking can result in buckling or a brittle fracture during or shortly after heat straightening. To prevent such a sudden fracture as illustrated in fig. 3.1, jacking forces should always be limited. The recommended procedure is to calculate the plastic moment capacity of the damaged

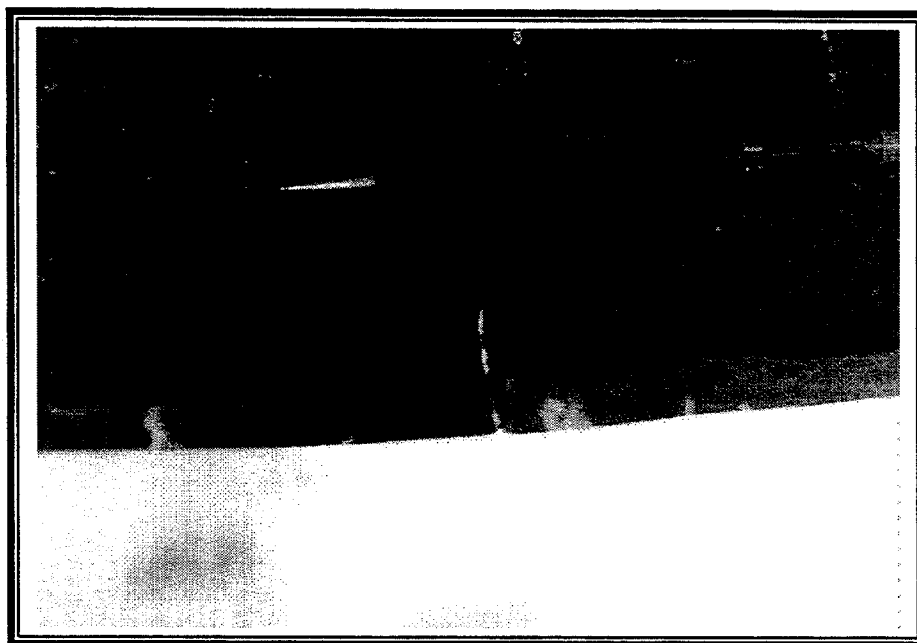


Figure 3.1. Brittle fracture during heat straightening.

member and limit the moment resulting from the combination of initial jacking forces and dead loads to one-half of this value. If practitioners do not take this precaution brittle fractures may occur. It is strongly recommended that jacks be gauged and calibrated with the maximum force limitation computed. Of course, the jacking forces should always be applied in the direction tending to straighten the beam. The execution of a heat-straightening repair that incorporates these keys must begin with the assessment of the damaged structure.

Steps in the Assessment Process

Many incidents resulting in damage to steel bridges produce an emergency situation to some degree. The first step in the rehabilitation process is to assess the degree of damage and the safety of the existing structure during a site investigation. The purpose of this section is to provide guide-

lines for damage assessment. These guidelines are in the form of steps required for a complete assessment. All aspects may not be required in each case. Judgement must be used when deciding if, and when, to eliminate a part of the process.

1. Initial Inspection and Evaluation for Safety and Stability

The purpose of the inspection is to protect the public and emergency service personnel. This inspection is often visual and conducted with special concern for safety. The major aspects of damage are recorded and documented with photographs and measurements. During this inspection, a preliminary list of repair options should be made. Particular attention should be paid to temporary needs such as shoring, traffic control, and other short-term considerations. A part of this evaluation may require a review of the design drawings and computa-

tions to determine the safety and stability of the bridge. Knowledge of the specific cause of damage may also influence the final decision on repair and should be investigated if possible. Typical damage causes are: (1) overheight or overwide vehicle impact; (2) overweight vehicles or overloads; (3) out-of-control vehicles or moving systems; (4) mishandling during construction; (5) fire; (6) blast; (7) earthquakes; (8) support or substructure movement; and (9) wind or water-borne debris.

2. Detailed Inspection for Specific Defects

The decision to conduct a heat-straightening repair depends on the type and degree of damage. Three aspects should be carefully checked: (1) signs of fracture; (2) degree of damage; and (3) material degradation.

Signs of Fracture.-While some fractures are quite obvious, others may be too small to visually detect. However, it is important to determine if such cracks exist since they may propagate during the heat-straightening process. When in doubt, one of the following conventional methods can be utilized.

The use of a dye penetrant is effective in detecting cracks. The process involves first thoroughly cleaning the surface. Then a liquid dye is sprayed on the surface and permitted to stand, during which time the dye is drawn into surface discontinuities. Excess dye is then cleaned from the surface and a developing solution applied. The developer reacts with dye remaining in the cracks. The dye can be observed because of the color change.

Another procedure is to use magnetic particle inspection. A magnetic field is introduced by touching the metal with a yoke or prods. A flaw in the steel causes a disruption of the normal lines of magnetic flux. If the flaw is at or near the surface, lines of magnetic flux leak from the surface. Fine iron particles are attracted to the flux leakage and indicate the crack location.

A third procedure is ultrasonic testing by one of several techniques. These procedures typically involve the analysis of pulses passing through undamaged versus damaged material.

Finally, radiographic testing may be utilized to produce a visual image of any flaws in the material.

Degree of Damage.-An evaluation of the degree of damage requires measurements to be taken. Two types of damage require measurements: (1) Overall bending or twisting of a member; and (2) localized bulges or sharp crimps. These measurements can be used to compute the maximum damage-induced strain or to determine the degree of damage. The usual procedure is to begin by measuring offsets from a taut line or straight-edge. A typical layout is shown in fig. 3.2. The idea is to use the unyielded adjacent regions as reference lines since their curvature is small in comparison to the plastic zones, or use the offsets in the damage zone to compute the degree of damage. For the first case, tangents from the straight portions define the angle or degree of damage between the tangents. If the offsets are taken in the elastic zone on either side of the damage as shown in fig. 3.2b, the degree of damage,

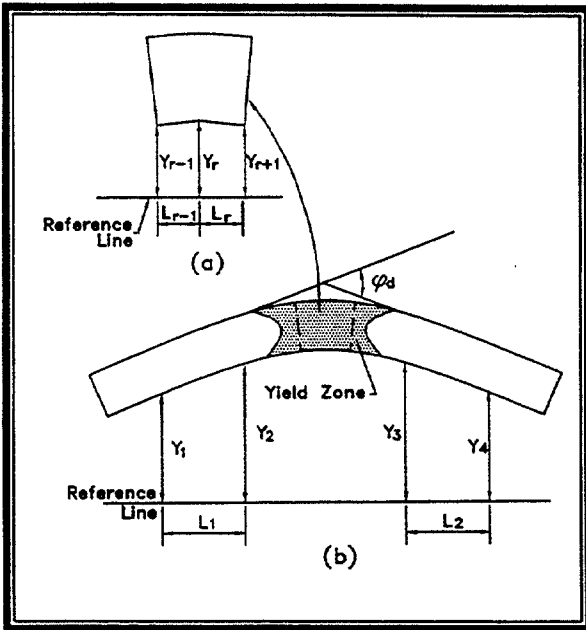


Figure 3.2. Offset measurements to calculate degree of damage and radius of curvature.

ϕ_d , can be computed. Based on measurements taken at the site, degree of damage can be calculated as follows:

$$\phi_d = \tan^{-1}\left(\frac{y_2 - y_1}{L_1}\right) + \tan^{-1}\left(\frac{y_3 - y_4}{L_2}\right) \quad (\text{Eq. 3.1})$$

where ϕ_d is the degree of damage or angle of permanent deformation at the plastic hinge and y_i is a measured offset as shown in fig. 3.2b. The length of damage, c_d , is defined by the chord connecting the tangents to the inelastically damaged region as shown in fig. 3.3. If ϕ_d and c_d are known, the radius of curvature can be computed as

$$R = \frac{c_d}{2 \sin(\phi_d / 2)} \quad (\text{Eq. 3.2})$$

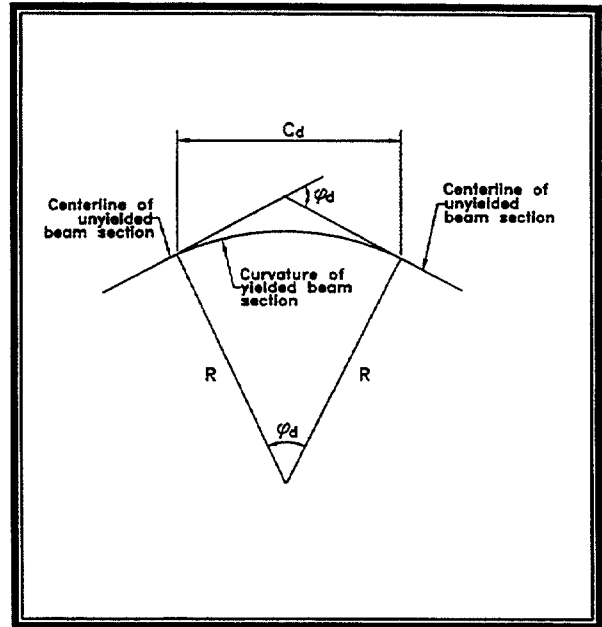


Figure 3.3. Relationship of degree of damage to radius of curvature and cord length.

In some cases direct measurements of ϕ_d can be made. One procedure is to stretch two taut lines forming tangents on either side of the damage. By stretching the lines until they intersect, the degree of damage can be measured with a protractor. For small zones of damage, two straight edges can be used to produce the tangent intersections. Again, the angle of damage can be measured with a protractor. While this method may seem somewhat crude, a reasonable degree of accuracy can be obtained.

For the case the offsets are taken in the damage zone (see fig. 3.2a). The radius of curvature, R , can then be approximated as

$$\frac{1}{R} = \frac{y_{r-1} - 2y_r + y_{r+1}}{L^2} \quad (\text{Eq. 3.3})$$

The degree of damage can then be calculated from:

$$\sin \frac{\varphi_d}{2} = \frac{L}{R} \quad (\text{Eq. 3.4})$$

or
$$\varphi_d = 2 \sin^{-1} \left(\frac{L}{R} \right) \quad (\text{Eq. 3.5})$$

It should be recognized that approximations are involved in using these equations. The assumption is made that the radius of curvature is constant over the entire length of the damage. However, the radius of curvature usually varies. If the damage curve is smooth, this assumption is fairly accurate. If the curve is irregular, the assumption becomes more approximate. For the more pronounced irregular curvatures, it is advisable to measure only the worst portion of the damaged region using the three-point offset procedure and the calculation of radius of curvature from eq. 3.3. In general, the approaches described here give a good estimate of the radius of curvature and, consequently, strain. The use of these parameters in the design of repairs will be described in a later section.

Material Degradation.-Certain aspects of material degradation will influence the decision to heat straighten. One area of concern relates to nicks, gouges and other abrupt discontinuities. Such flaws in the damage zone will be stress risers during the repair when jacking forces and heat are applied. It is recommended that such discontinuities be noted and ground to a smooth transition prior to heat straightening.

A second aspect relates to exposure to high temperature (such as a fire) when the damage occurred. As long as the temperature has not exceeded either the tempering temperature or the lower phase transition temperature, no permanent degradation would be expected to occur in the steel. However, if the damaged steel was exposed to higher temperatures, metallurgical tests should be performed to ensure material integrity before heat straightening is applied. Tests that should be considered include: (1) a chemical analysis; (2) a grain size and micro structure analysis; (3) Brinell hardness tests; (4) Charpy notch toughness tests; and (5) tensile tests to determine yield, ultimate strength, and percent elongation.

Several visual signs may suggest exposure to high temperature including: melted mill scale, distortion, black discoloration of steel, and cracking and spalling of adjacent concrete. Tests can then be conducted at suspicious regions. For example, a significant increase in Brinell hardness, in comparison to undamaged areas of the same member, indicates potential heat damage. Or, for the Charpy V Notch test at 4.4°C (40°F), a significant reduction in values over those from an undamaged specimen may indicate damage. The most definitive test is usually a micro structure comparison between damaged and undamaged pieces. Evidence of partial austenization and recrystallization into finer grain size indicates heating above the lower phase transition temperature.

Geometry of the Structure.-Often the bridge configuration is available from design drawings and it is a good policy to confirm that the system does conform to

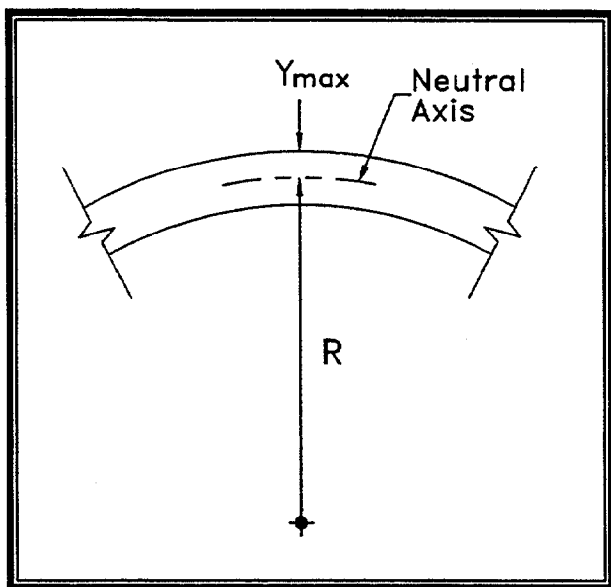


Figure 3.4. Radius of curvature for a damaged beam of curvature and cord length.

these drawings. If drawings are not available, then enough measurements should be taken so that a structural analysis can be conducted if required.

Steps in the Planning and Design Process

Once the damage assessment is complete, the repair can be designed. The following steps may be required as part of this planning and design process:

- Analyze the degree of damage and maximum strains induced.
- Conduct a structural analysis of the system in its damaged configuration.
- Select applicable regions for heat straightening repair.
- Select heating patterns and parameters.
- Develop a constraint plan and design the jacking restraint configuration.
- Estimate heating cycles required to straighten members.
- Prepare plans and specifications.

Each of these aspects are discussed in the following sections.

1. Analysis of Degree of Damage and Determination of the Maximum Strain due to Damage

Research data has shown that heat straightening can be successful on steel with plastic strains up to 100 times the yield strain, ϵ_y . There is reason to believe that even larger strains can be repaired. However, since no research data exists beyond the $100\epsilon_y$ range, engineering judgement is required. In order to evaluate whether the damage exceeds this level, the maximum curvature should be measured as previously described. Shown in fig. 3.4 is a damaged beam of uniform curvature. The radius of the bend is defined as radius of curvature, R .

Since strain is proportional to curvature and curvature can be computed from field measurements, it is often convenient to compare the radius of curvature to the yield curvature, R_y , expressed as

$$R_y = \frac{E y_{\max}}{F_y} \quad (\text{Eq. 3.6})$$

where E = modulus of elasticity, F_y = yield stress, and y_{\max} = the distance from the centroid to the extreme fiber of the element.

The radius of curvature is related to the strain by

$$\epsilon_{\max} = \frac{1}{R} y_{\max} \quad (\text{Eq. 3.7})$$

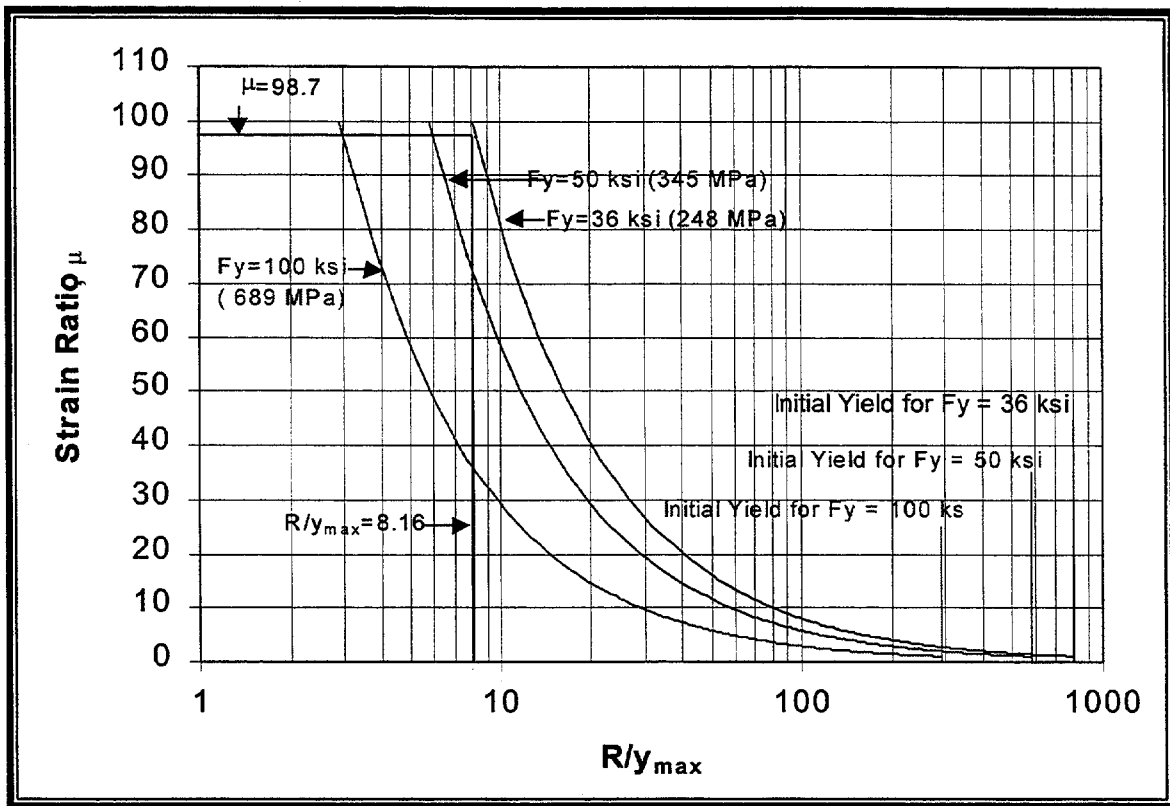


Figure 3.5. Strain ratio vs. normalized radius of curvature (μ vs. R/y_{max}).

where R is the actual radius of curvature in the damaged region.

Since damage measurements are taken at discrete locations, the radius of curvature can be approximated from eq. 3.2 or 3.3. Once the smallest radius of curvature is determined in the damaged region, the maximum strain can be computed from eq. 3.7 and compared to the yield strain

$$\epsilon_y = \frac{F_y}{E} \quad (\text{Eq. 3.8})$$

The ratio of maximum strain to yield strain, referred to as the strain ratio, μ , is used as

one measure of the extent to which the steel has been damaged. From eqs. 3.7 and 3.8, the strain ratio is

$$\mu = \frac{E y_{max}}{R F_y} \quad (\text{Eq. 3.9})$$

Since E is a constant for all steel grades (200,000 MPa or $E=29,000$ ksi), μ can be obtained graphically in terms of the ratio R/y_{max} and F_y for various steel grades as shown in fig. 3.5. A similar approach can be used for localized bulges, buckling or crimps.

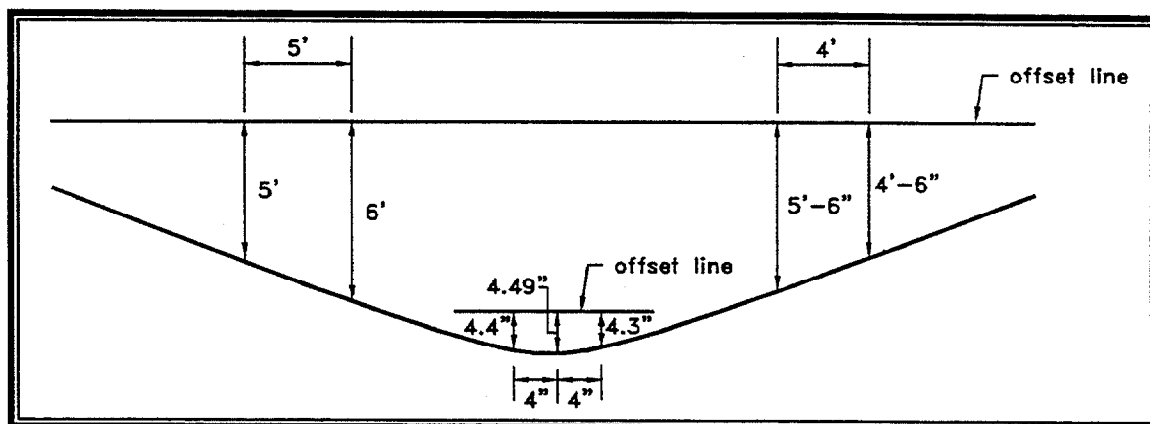


Figure 3.6. Offset measurements for example 3.1 (25.4 mm = 1 in and 0.305 m = 1 ft).

Heat-straightening repairs have been conducted for strains up to $100\epsilon_y$, or $\mu=100$. Repairs may be successful at even greater strains. However, research studies have not included strains in excess of $100\epsilon_y$. Engineers should use judgement in straightening beyond this range. Also, fire damage involving high temperature may be an exception to this limit. If the distortion is due to fire, it is probable that material properties have been affected. Repair decisions should be based on metallurgical analysis and engineering judgement as well as strain limitations.

As a rule of thumb for single curvature bends with a plate depth about the axis of bending of up to 305 mm (12 in), if the degree of damage is less than 12° , it is not necessary to measure for maximum strain. The only exception would be if the region of damage were concentrated over an extremely short length resembling a sharp crimp as opposed to a plastic hinge type of bend.

Example 3.1

Problem.-The bottom flange of an A36 steel composite bridge girder (W27 x 161 with a flange width of 356 mm or 14.02 in) was impacted by an over-height vehicle. The flange deflected laterally producing a plastic hinge at the impact region. Offset measurements are shown in fig. 3.6. Based on these measurements, compute the degree of damage, and the radius of curvature in the damaged region, the radius of curvature at initial yield and the ratio of maximum strain to yield strain.

Solution.-The offset measurements outside the yield zone are used to calculate degree of damage from eq. 3.1

$$\begin{aligned}\phi_d &= \tan^{-1}\left(\frac{6-5}{5}\right) + \tan^{-1}\left(\frac{5.5-4.5}{4}\right) \\ &= 25.35^\circ = 0.0224 \text{ rad.}\end{aligned}$$

The radius of curvature in the damaged region, R , is calculated from the offsets in the yield zone using eq. 3.3

$$\frac{1}{R} = \frac{4.4 - 2(4.49) + 4.3}{(4)^2} = -0.0175$$

$$R = 57.1 \text{ in. (1,451 mm)}$$

The radius of curvature at initial yield, R_y , is computed from eq. 3.6. Using $E=200,000$ MPa (29,000 ksi) $F_y=248$ MPa (36 ksi), and y_{\max} (one-half the flange width) = $14.02/2 = 178\text{mm}$ (7.01 in).

$$R_y = \frac{(29,000)(7.01)}{36} = 5647 \text{ in.} = 470.6 \text{ ft. (143.4 m)}$$

Since $R \ll R_y$, significant plastic deformations have occurred. The ratio of maximum strain to yield strain, is obtained from eq. 3.9

$$\mu = \frac{(29000)(7.01)}{(57.1)(36)} = 98.9$$

indicating that the maximum strain is 97.1 times the yield strain. This value can be obtained graphically using fig. 3.5. Entering the value of R/y_{\max} as

$$R/y_{\max} = \frac{57.1}{7.01} = 8.15$$

on the horizontal scale, the ordinate μ is the point at which R/y_{\max} intersects the $F_y=248$ MPa (36 ksi) curve as shown in fig. 3.4.

2. Conduct a Structural Analysis of the System

The strength of the damaged structure is usually evaluated by a structural analysis. This analysis serves two purposes:

(1) to determine the capacity in its damaged configuration; and (2) to compute residual forces induced by the impact damage. The analysis can be based on the undeformed geometry except when the displaced geometry of the frame or truss system (after damage) results in changes in internal forces by more than 20 percent. However, even if undeformed geometry is used in the analysis, the deformed geometry should be used when computing the member stresses. The allowable stresses should be based on the original properties of the material.

When a member has a significant change in shape due to damage, the section properties should be modified when calculating stresses. While each specific application must be considered on an individual basis, some general guidelines can be developed. Assuming that no fractures have occurred, bending and compression members are the most critical to evaluate. Forces due to applied loads in tension members tend to straighten out-of-plane damage (and are thus self-correcting), while such forces in bending or compression members tend to magnify the damage.

Change in cross section shape.-The primary variable in evaluating the stress level for a damaged bending member is the section modulus. Typically, the most serious strength reduction is due to deformations resulting from twisting or lateral distortion of the cross section. A good example is an impact on the bottom flange of a bridge girder by an over-height vehicle. Two ideal cases are evaluated here for two wide-flange sections. As shown in figs. 3.7 and 3.8, the damage is assumed to produce a rotation of the web about the juncture of the web and top flange.

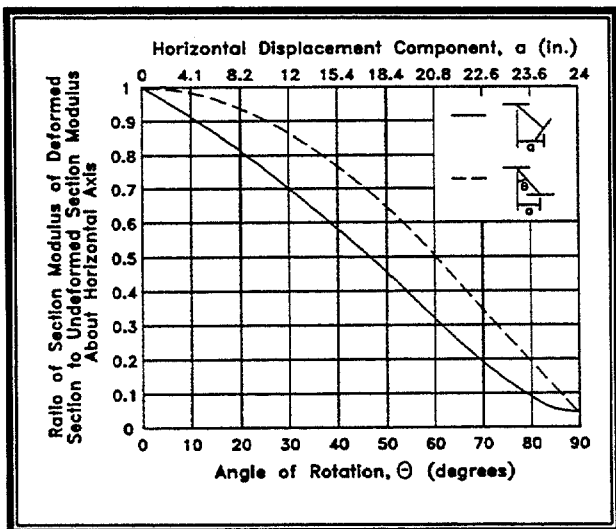


Figure 3.7. Reduction in effective section modulus for a W 24x76 beam subjected to varying degrees of idealized damage (Note: 25.4 mm = 1 in.).

The bottom flange is modeled in two ways: either it remains parallel to the top flange, or it remains perpendicular to the web. Actual combinations of damage often fall between these two conditions. Plotted in fig. 3.7 and 3.8 are the variations in the section modulus (for bending about the strong axis) associated with different levels of damage for two beams: a W24 X 76 and W10 X 39. The case of the bottom flange remaining perpendicular to the web is the more critical case for the comparison of section modulus values. As can be observed, the section modulus dips fairly rapidly with an increase in the cross section rotation. A 10° rotation results in a strength reduction within the range of 8-15 percent, depending on the section, while at 20°, strength reduction is between 18 and 29 percent. Although an engineer should evaluate the specific conditions and configuration of each case, a good general guideline is to repair the member if the section modulus is reduced by 10 percent. This level of damage typically corre-

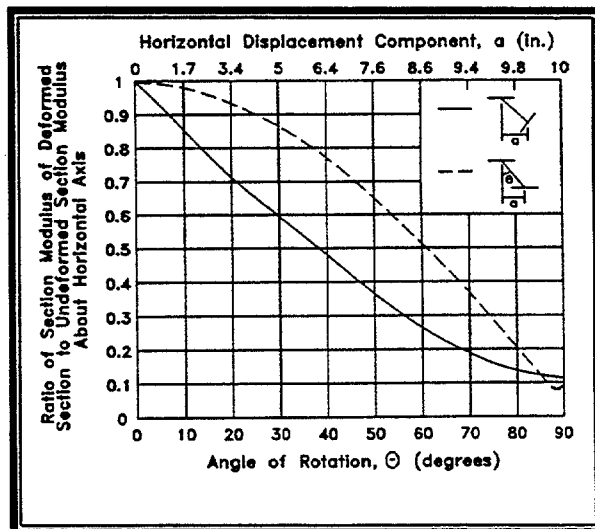


Figure 3.8. Reduction in effective section modulus for a W 10x39 beam subjected to varying degrees of idealized damage (Note: 25.4 mm = 1 in.).

sponds to a rotation of approximately 10°. In reference to the field tests conducted on the W10 X 39 and W24 X 76 beams as described in Chapter 7, the damage induced was considered to be moderate. In both cases the flange remained almost perpendicular to the web. The calculated bending strength reduction for the W10 X 39 beam was calculated in the range of 25 percent. The reduction for the W24 X 76 beam was on the order of 9 percent.

P-Δ Effects.-For compression members, the square of the minimum radius of gyration is the section property associated with the strength of the member. The effect of the two idealized cases of damage previously described is plotted in fig. 3.9 and 3.10. In this case, the configuration in which the bottom flange remains parallel to the top flange is the more critical. The curves are very similar for both wide-flange sections. The reduction in strength, as measured by the square of the radius of gyration, is not quite as large as the

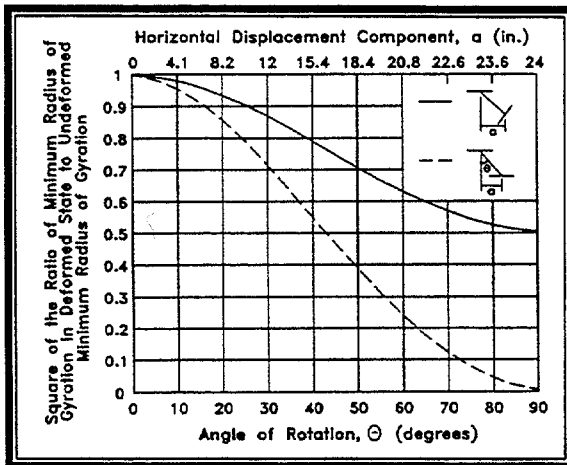


Figure 3.9. Reduction in the square of the effective minimum radius of gyration for a W 24x76 beam subjected to varying degrees of idealized damage (Note: 25.4 mm = 1 in).

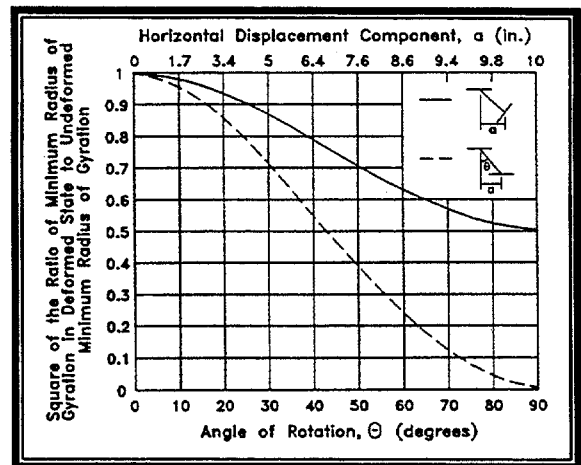


Figure 3.10. Reduction in the square of the effective minimum radius of gyration for a W 10x39 beam subjected to varying degrees of idealized damage (Note: 25.4 mm = 1 in).

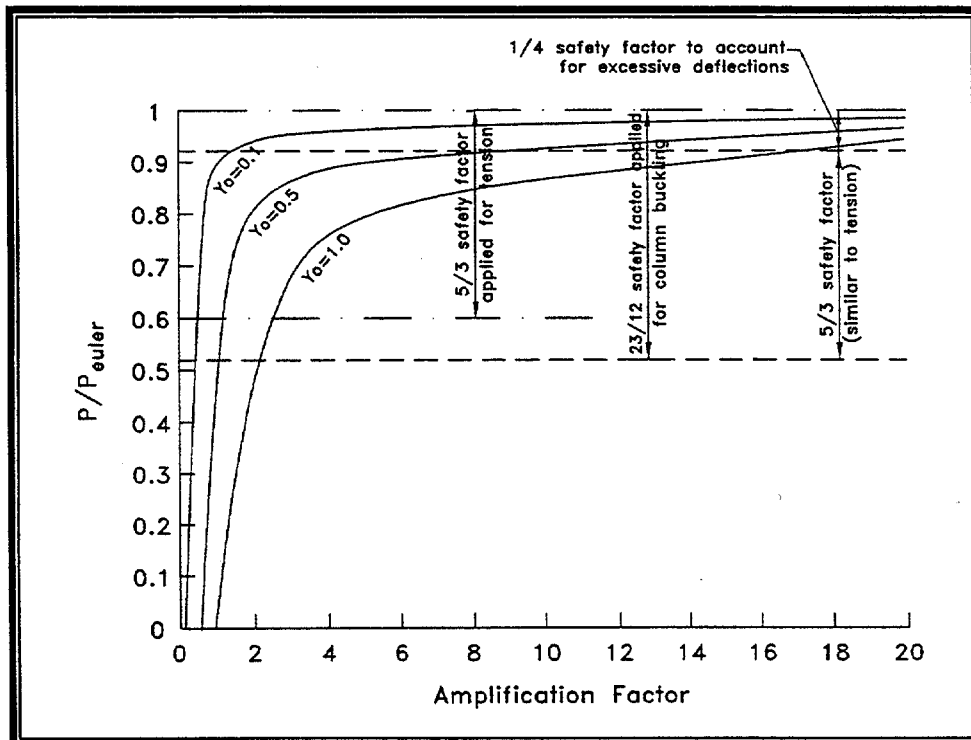


Figure 3.11. Effect of amplification factor for lateral deflections on compression members.

corresponding case for section modulus. The reduction is only about 5 percent for the 10° rotation and about 14 percent at 20° rotation. However, another aspect that must be considered when evaluating compression members is the strength reduction due to the P-delta effect. If a simply supported column has an initial midpoint deflection, y_o , due to impact damage, then the deflection (and bending moment) is amplified according to the amplification factor

$$A.F. = \frac{y_o}{1 - P/P_{euler}} \quad (\text{Eq. 11.6})$$

where P is the axial load and P_{euler} is the Euler buckling load. This factor is taken into account in design codes by an adjustment in the safety factor for columns.

Consider the AISC code (1989), for example. The long column formula (eq. E2-2) is the classical Euler buckling formula, divided by a safety factor of 23/12. Conversely, the safety factor for tension members is given as 5/3. The reason for the higher safety factor for compression members is to account for the P-delta magnification effect. A plot of the amplification factor is given in fig. 3.11. As the load approaches the critical buckling load, the deflection (and consequently the moment) approaches infinity. Failure must therefore be defined as the point where the deflection (and consequently the moment) remains finite but becomes excessively large. The safety factor for column buckling was therefore increased by 0.25 above that used in tension members. As can be seen from fig. 3.11, this extra safety factor accounts for 0.08 of the total load ratio reduction to al-

lowable values. In deciding upon this value, it was assumed that relatively small initial values of lateral deflections would exist due to lateral loads or fabrication imperfections, e.g., within the elastic range. When a compression member has larger permanent deformations well into the plastic or strain-hardening range due to damage, then the effective strength of the member is reduced by a larger factor than expressed by even the column safety factor.

In light of these considerations, even relatively small permanent deformations should be repaired for compression members unless additional bracing is added or a stability analysis is performed to justify that the strength reduction is small.

Residual forces.-The analysis of residual forces in damaged systems requires a plastic analysis. To illustrate the procedure, a bridge girder laterally supported by diaphragms will be used. For lateral impact, such as might occur with an over-height vehicle, the girder acts as a continuous beam with the diaphragms as interior supports. If an impact load occurs, the lower flange has positive bending at the impact point and negative bending at the adjacent diaphragm supports. A layout modeling this type of girder is shown in fig. 3.12. During impact, it is assumed that plastic hinges form at the impact point and at adjacent supports. These hinges form a mechanism from which the impact load can be computed. Using a plastic analysis, the load, P_u , can be calculated and a moment diagram constructed, fig. 3.12b. The impact load is now applied in the reverse direction and an elastic analysis performed, fig. 3.12c. The superposition of these two diagrams (b and c) give the

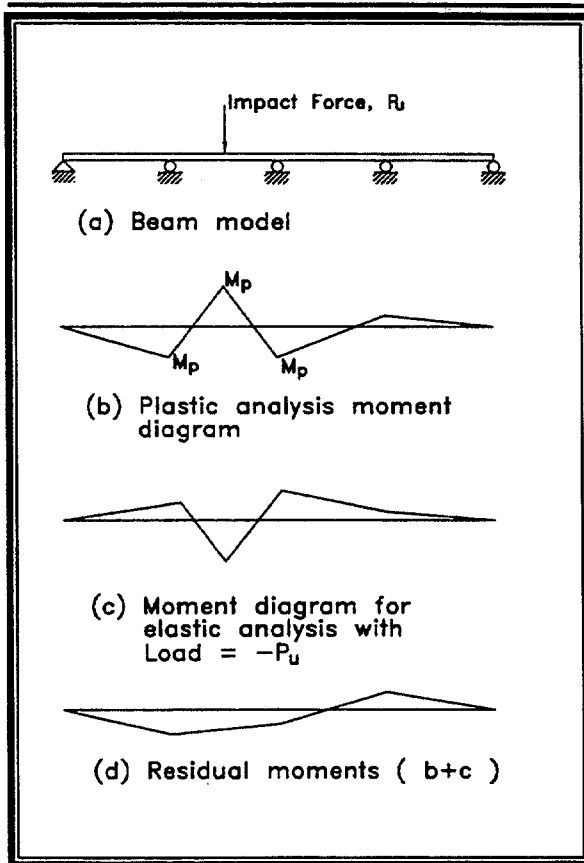


Figure 3.12. Plastic analysis for residual moments in a laterally impacted girder.

residual moments due to the impact which produces plastic deformation; fig. 3.12d. These resulting moments should be assessed in combination with other loadings such as the live and dead load on the bridge.

3. Select Regions Where Heat Straightening is Applicable

While the primary consideration for allowing heat-straightening repair is the degree of damage limitation, other criteria may also influence the decision. Of particular importance is the presence of fractures or previously heat straightened members. A fracture may necessitate the replacement of part, or all, of a structural member. In some cases it may be feasible to heat straighten

the suspect region and then repair it in-place by mechanical connectors. In other cases a portion of the member may be replaced while the remainder is repaired by heat straightening.

An example of combining heat straightening with replacement is when one or more girders are impacted by an over-height vehicle. This type of accident often displaces the bottom flange. If the impact point is near diaphragms, the diaphragms are often severely damaged. An example is shown in fig. 3.13. It is usually much more economical to simply replace a diaphragm rather than taking a lengthy time to straighten it. The recommended procedure is to remove the diaphragm (especially if it would restrain desired movement of the member) heat straighten the girder, and then replace the diaphragm with a new one.

In general, heat straightening can be applied to a wide variety of structural members. However, some have cautioned about straightening fracture critical members (Shannafelt and Horn, 1984). Although there is no research data to support a ban on heat straightening fracture critical members, practically no fatigue testing has been conducted. If careful control of heating temperature (including the limits imposed by section 12.12 of the AASHTO/AWS D1.5 Bridge Welding Code) and jacking forces are maintained, and if notches and nicks are ground smooth, there is no reason to expect problems. It is recommended that additional care be used for fracture critical members to insure that the heat straightening is properly conducted.

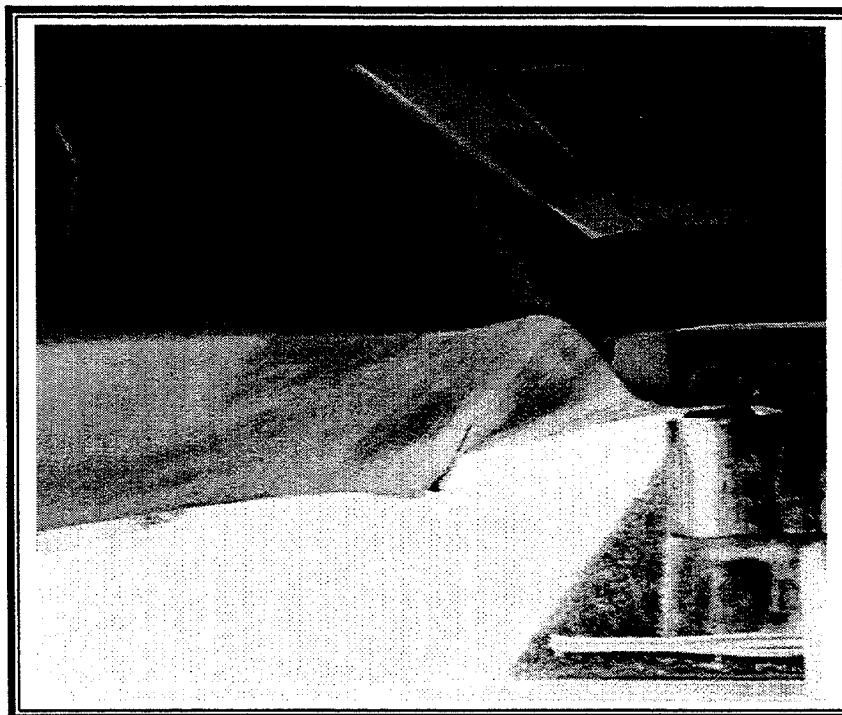


Figure 3.13. Diaphragm damage due to vehicle impact on girder.

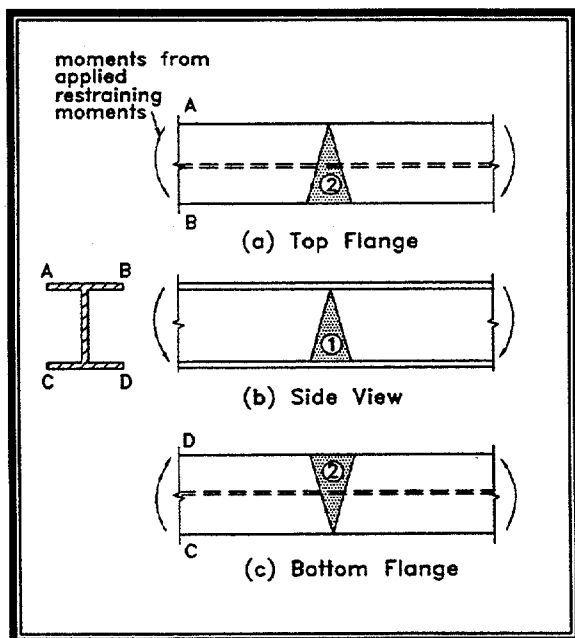


Figure 3.14. Heating pattern and sequence for bending combination about both the strong and weak axis.

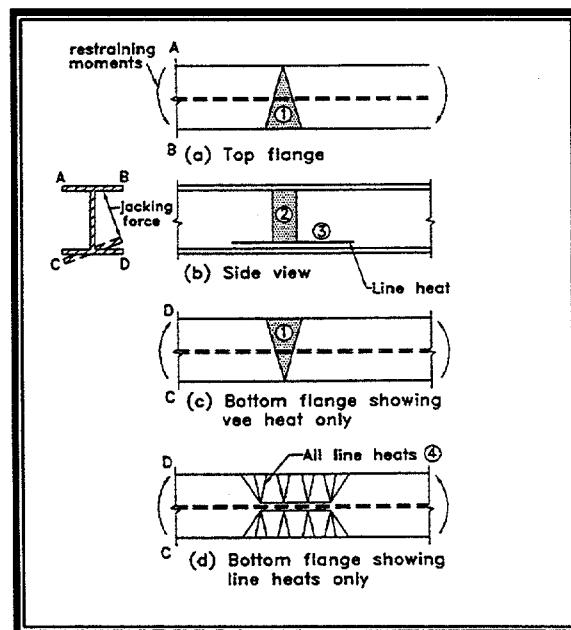


Figure 3.15. Heating pattern and sequence for combination weak axis bending and local flange bulge.

4. Select Heating Patterns and Parameters

Typical Heating Patterns.-The fundamental heating patterns have been described in Chapter 2. Since typical damage is often a combination of these fundamental damage types, a combination of heating patterns is often required. The key is to select the combination of patterns to fit the damage. When in doubt, a good policy is to address the attention to one of the basic heating patterns at a time. For example, remove the Category W damage prior to addressing the Category L damage. It should be noted that with proper combinations, several types of damage can be removed expeditiously. For example, suppose that a wide flange section is impacted such that the bending occurs about an axis at an arbitrary angle to the principal axes, i.e., bending occurs about both the strong and weak axis. The heating pattern, fig. 3.14, requires a vee heat on the web to restore the strong axis damage and vee heats on the flanges to restore the weak axis damage. The heats should be executed sequentially as numbered in fig. 3.14. Note that no strip heat is required on the web since a vee is used there. Restraining forces should be used to produce bending moments about both the strong and weak axis as indicated in fig. 3.14 tending to straighten the damage. Once the damage is corrected about one of the principal axes, the heating pattern should revert to one of the fundamental patterns until straightening is complete about the other principal axis.

As a second example, consider a wide flange beam with weak axis bending damage combined with a local bulge in one flange. The heating pattern is shown in

fig.3.15. Vee heats are used on the top and bottom flanges along with a web strip heat similar to the standard weak axis pattern. However, partial depth vees are used on the flange with the bulge along with a series of line heats along bulge yield lines. Since a yield line is likely to occur at the lower web fillet, a line heat is also needed on the web. Restraining forces are used to create bending moments about the weak axis as shown in fig. 3.15. In addition, a jacking force should be applied on the local bulge as shown on the cross section in fig. 3.15. The sequence of heats is also indicated in the figure.

A third example is damage resulting from impact of a composite bridge girder which produces weak axis damage to the bottom flange and twisting due to the restraint of the top flange. The heating pattern is shown in fig. 3.16 consisting of a bottom flange vee heat, a web strip heat and a line heat at the top fillet of the web. The heating sequence is shown in fig. 3.16 as well as the restraining moment required on the bottom flange.

A final example is the case of multiple plastic hinges formed about the weak axis such as might occur for a beam continuous over interior supports. The heating pattern is shown in fig. 3.17. Note the reversed direction of the vees to reflect the multiple curvature damage. The restraining moments must also reflect the reverse curvature nature of the damage as shown in the figure.

Vee Depth.-In general the vee depth should be equal to the width of the plate being straightened. Partial depth vees provide no advantages in reducing shortening as some have speculated. The primary situation

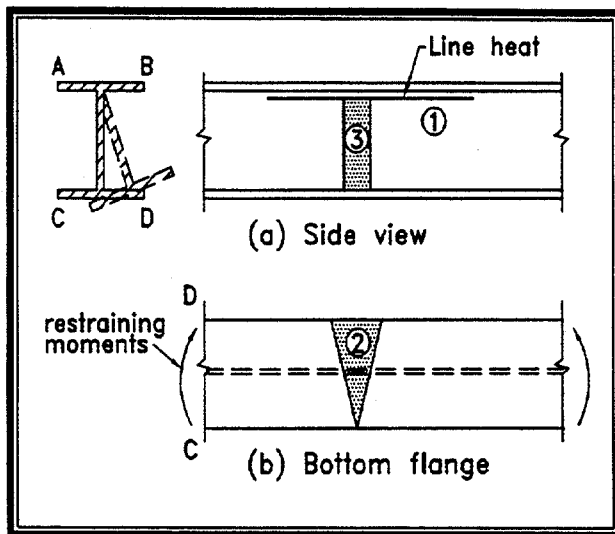


Figure 3.16. Heating pattern and sequence for combination of weak axis bending of lower flange and twisting.

for half depth vees is in the repair of local damage.

Vee Angle.-The angle of the vee is usually limited by practical considerations. It should be as large as practical for the specific application. If the open end of the vee is too wide, out-of-plane distortion often occurs. Likewise the vee area should be small enough to heat quickly so that differential cooling is limited. A good rule of thumb is to limit the open end of the vee to approximately one-third to one-half the plate width but not greater than 254 mm (10 in). These limits translate roughly to 20-30° vee angles. If the width of the open end of the vee, V , is selected, the vee angle is

$$\theta = 2 \tan^{-1} \frac{V}{2W} \quad (\text{Eq. 3.10})$$

where W is the plate width.

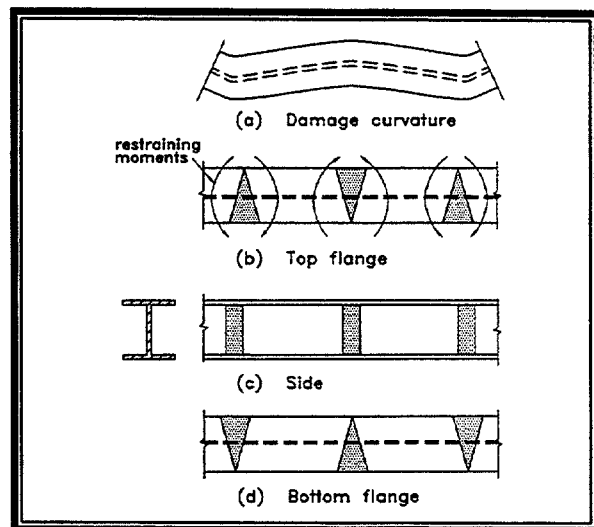
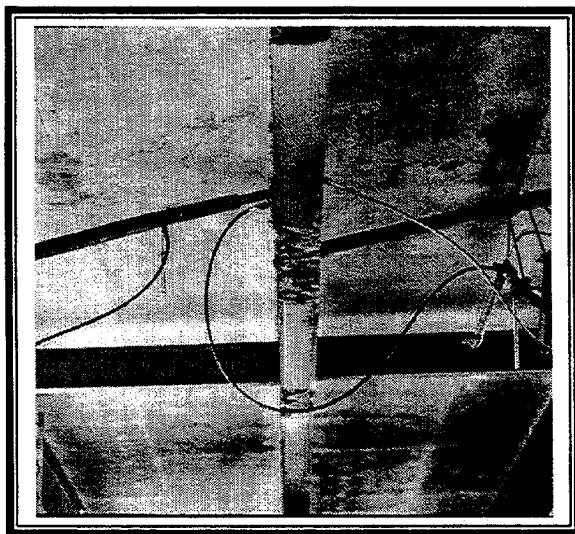


Figure 3.17. Heating pattern for reverse curvature bending.

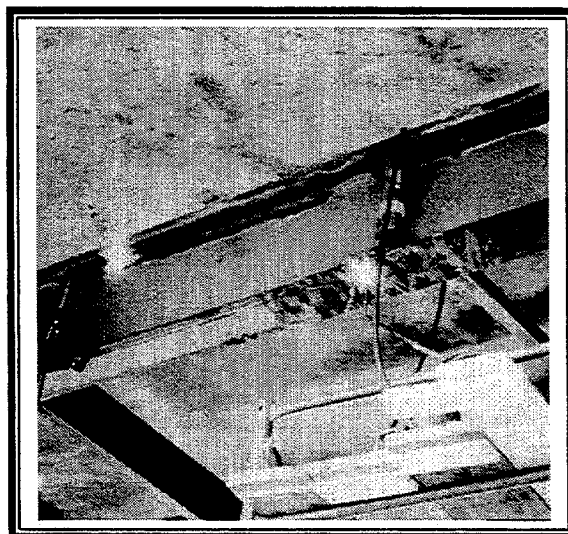
Number of Simultaneous Vee Heats.-Simultaneous vee heats may be performed with proper spacing. It is recommended that the vees be spaced at least one plate width, W , apart. Also, if multiple plastic hinges occur, each hinge may be heated simultaneously.

5. Develop a Constraint Plan

Since jacking forces can expedite repairs, it is recommended that such forces be utilized. Jacks should be located to produce their maximum effect in the zones of plastic deformation. It is recommended that jacks always be gauged and calibrated prior to use. Also, jacks must be properly secured so they will not fall out as pressure subsides during cooling. The loads applied to the structure should always be known and limiting values established. A jacking arrangement for a composite girder bridge is shown in fig. 3.18. Lateral forces are utilized on the lower flanges, fig. 3.18a, while jacks between flanges are used for local damage, fig. 3.18b.



(a)



(b)

Figure 3.18. Jacking arrangements for global and local damage on a composite girder bridge.

For cases where residual moments are small, the jacking moment, M_j , should be limited to

$$M_j \leq \frac{M_p}{2} \quad (\text{Eq. 3.11})$$

where M_p is the plastic moment capacity of the member.

For cases where residual moments exist, the jacking moment should be limited to

$$M_j \leq \frac{1}{2}(M_p \pm M_r) \quad (\text{Eq. 3.12})$$

where M_r is the residual moment and is positive when tending to straighten the member. Residual moments will be relieved during the first few heats. Rather than computing residual moments, an alternative is to

use a jacking moment of only $\frac{1}{4} M_p$ during the first two cycles.

On occasion, a hairline fracture will occur or become visible during an intermediate cycle of heat-straightening repair. The causes are believed to be: (1) excessive restraining forces being applied during the heating process; (2) repetitive repair of a re-damaged element; and/or (3) the growth of micro cracks initiated during the induction of damage. As item (1) is the primary cause, restraining forces should always be specified at safe limits and should be monitored during actual repair. For item (2) the repair of previously heat straightened material should be limited to only two damage/repair cycles.

One problem associated with the computation of jacking forces is that for indeterminate members, the bracing, diaphragms or other attachments may be difficult to model. In addition, it is sometimes necessary to make an estimate in the field as to the magnitude of jacking forces. The

jacking force limit can be approximated by measuring the deflection when the force is applied. Since end support restraint conditions will fall between the two ideal cases of simple and fixed supports, the deflection can be calculated by estimating the degree of restraint. The deflection that produces a maximum stress equal to 50 percent of yield for 248 MPa (36 ksi) yield strength steel on a center point loaded member can be expressed as:

(1) For 248 MPa (36 ksi) steel

(a) Simple supports

$$\delta_{\max} = \frac{1}{y_{\max}} \left(\frac{\ell}{140} \right)^2 \quad (\text{Eq. 3.13})$$

(b) For fixed supports

$$\delta_{\max} = \frac{1}{y_{\max}} \left(\frac{\ell}{200} \right)^2 \quad (\text{Eq. 3.14})$$

(2) For 345 MPa (50 ksi) steel

(a) Simple supports

$$\delta_{\max} = \frac{1}{y_{\max}} \left(\frac{\ell}{120} \right)^2 \quad (\text{Eq. 3.15})$$

(b) For fixed supports

$$\delta_{\max} = \frac{1}{y_{\max}} \left(\frac{\ell}{170} \right)^2 \quad (\text{Eq. 3.16})$$

where ℓ is the clear span length and y_{\max} is the distance from the centroid of the steel section to the extreme fiber. A safe jacking

force should produce a midpoint deflection within the range of these two values, depending on the level of end restraints.

Example 3.2

Problem.-For example, consider the case of a composite girder of A36 steel in which the lower flange (305 mm or 12 in wide) had been impacted by an over-height vehicle at a diaphragm location. In order to heat straighten the member, the damaged diaphragm was removed, leaving a clear distance between remaining diaphragms of 1.16 m (38 ft). Determine the limits of lateral displacement due to a jacking force if the jack is placed at the midpoint of the span at the point where the diaphragm was removed.

Solution.-For a 305 mm (12 in) flange $y_m = 152$ mm (6 in). Using eqs. 3.13 and 3.14, the range of deflections for a safe jacking force is 22-44 mm (7/8 – 1 3/4 in). A conservative limit would be to use the jacking force producing the 22 mm (7/8 in) deflection. However, if the bottom flange is continuous over the supporting diaphragms, a higher value may be used. One approach would be to use a jacking force associated with the average of these two values which, rounded to the nearest 6 mm (1/4 in), would be 31.8 mm (1 1/4 in). This type of approximation may serve as a useful guide when more accurate modeling techniques are not available.

6. Estimate the Heats Required to Straighten the Members

The estimate of number of heats provides a time line for the project. Comparing the estimated movement with the actual movement as it progresses also indicates whether the heating is being properly done.

The number of heats, n , can be completed as

$$n = \frac{\varphi_d}{\varphi_p} \quad (\text{Eq. 3.17})$$

where φ_p is the predicted plastic rotation per heat and φ_d is the degree of damage. Formulas for the plastic rotation associated with various structural shapes and damage conditions are provided in the Part II of this manual.

7. Repair Plans and Specifications

The final step is to prepare plans and specifications for the project. These plans will be the supervisor's guide as well as the contractor's directive. Suggested specifications are given in Chapter 12.

Example 3.3

Problem.-The truss section of A36 steel shown in fig. 3.19a was part of a bridge through truss. The continuous member ABC was damaged when a log fell from a truck and struck at the midpoint between AB which is 4.57 m (15 ft) in height. Section BC is also 4.57 m (15 ft). Member ABC is a W 12x40 arranged such that the impact produced bending about its weak axis. Determine the jacking force and heating pattern for the heat straightening repair of the member assuming that a plastic hinge formed in the member at the impact point and joint B and that adjacent members suffered minor damage.

Solution.-It will be assumed that the member can be analyzed as a continuous beam as shown in fig. 3.19a. A plastic analysis can be conducted assuming the mechanism shown in fig. 3.19b. From a plastic analysis, the relationship between the

collapse load, P_u , and the plastic moment, M_p , is

$$P_u = \frac{3M_p}{7.5}$$

For a W 12x40 bent about its weak axis, the plastic moment capacity, M_p , is

$$M_p = F_y Z_y$$

where Z_y is the plastic section modulus about the weak axis. Thus,

$$M_p = (36 \text{ksi})(16.8 \text{in}^3) = 604.8 \text{in} - k = 50.4 \text{ft} - k \quad (68.3 \text{kN} - m)$$

and

$$P_u = \frac{3(50.4)}{7.5} = 20.2 \text{kips} \quad (89.8 \text{kN})$$

The moment diagram resulting from the impact is shown in fig. 3.19c. The residual moments can be calculated by first applying P_u in the reverse direction, conducting an elastic analysis and obtaining the moment diagram in fig. 3.19d. The superposition of moment diagrams (c) and (d) gives the residual moments in the truss member as shown in fig. 3.19e. If residual moments are neglected, the maximum allowable jacking force will produce a maximum moment of

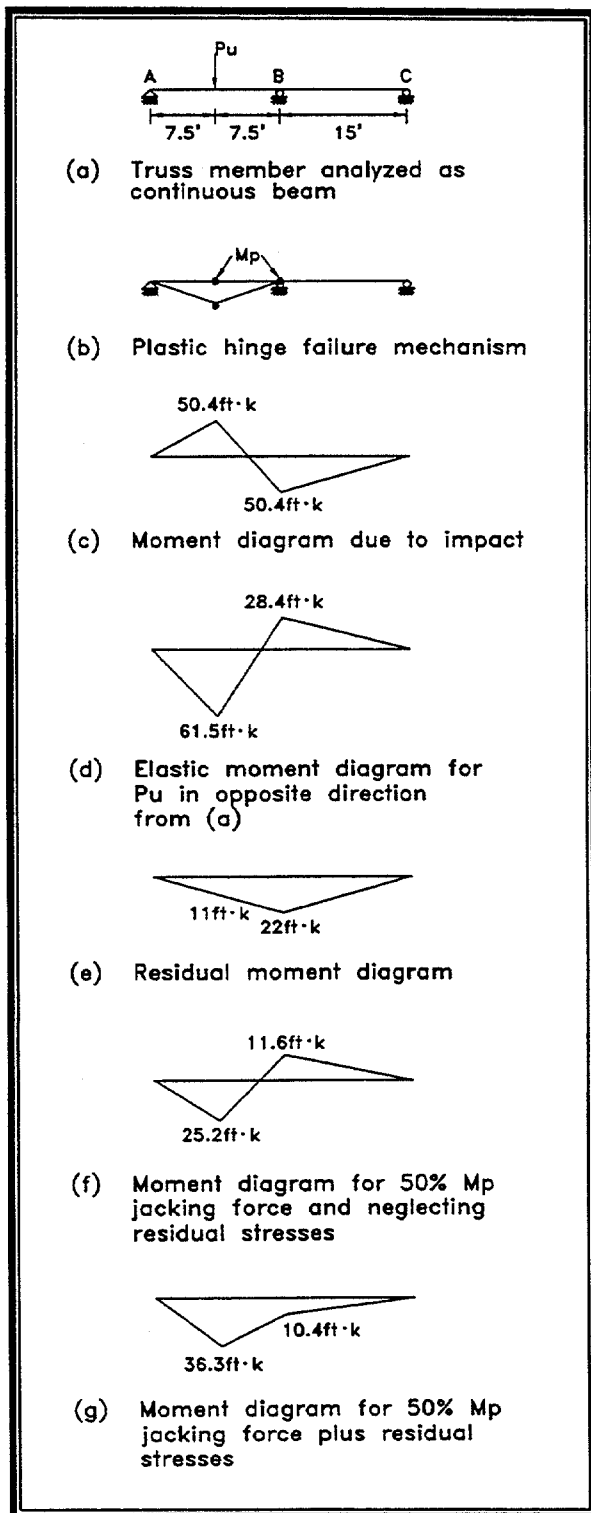


Figure 3.19. Schematic diagrams for example 3.3
 (Note: 0.305 m = 1 ft and 1.36 kN-m = 1 ft-kip).

$$M_j = \frac{M_p}{2} = 50.4 / 2 = 25.2 \text{ ft-k} \quad (34.2 \text{ kN-m})$$

Referring to the elastic moment diagram, fig. 3.19d, the jacking force can be obtained by proportioning the moments and applied force

$$\frac{P_j}{20.2} = \frac{25.2}{61.5}$$

$$P_j = 8.28 \text{ kips} \quad (36.8 \text{ kN})$$

The moment diagram for this load is shown in fig. 3.19f. It is recommended that the first 2 heats be conducted with a jacking force of one-half the maximum value ($P_j = 18.4 \text{ kN}$ or 4.14 kips) which allows the residual moments to be dissipated. If residual stresses are included, the moment diagram for $M_j + M_r$ is shown in fig. 3.19g. A reduction in the jacking force is required so that the maximum moment does not exceed 34.2 kN-m (25.2 ft-k). The value of $P_j = 18.4 \text{ kN}$ (4.14 k) provides a moment of 32.1 kN-m (23.7 ft-k) which satisfies this constraint. Defining the curvature after damage at the impact point as positive, the curvature at point B would be negative. Referring to fig. 3.17, the heating pattern at the impact point is that associated with the negative restraining moments and at point B the pattern is that associated with the positive restraining moments. Since the jacking plus residual moments at point B are negative, point B should not be heated during the first two cycles. Once the residual moments are relieved, the jacking moment is positive and point B can be heated simultaneously with the impact point. The degree of damage at

the impact point will be approximately twice that at joint B. Therefore, the jacking force should be placed near the impact point to maximize the moment at that location. Also, the moment at the impact point is approximately twice that at point B. Thus, the plastic rotation at B will be on the order of one-half that at the impact point and the member will straighten with about the same number of heats at each location.

If the open end of the vee is taken as one-half the flange width, that is 152 mm (6 in), the vee angle can be calculated from eq. 3.10 as

$$\theta = 2 \tan^{-1} \frac{V}{2W} = 2 \tan^{-1} \left[\frac{6}{(2)(12)} \right] = 28^\circ$$

Supervisor's Responsibilities

Monitoring the temperature.-

Excessive temperatures may cause surface damage or lead to increased brittleness. Temperature can be monitored in several ways. One of the most accurate is to use temperature-sensing crayons. These crayons melt at a specified temperature and are available in increments as small as 14°C (25°F) (fig. 3.20). By using two crayons that bracket the desired heating temperature, accurate control can be maintained. The crayons will burn if exposed directly to the flame of the torch. Therefore, the torch must be momentarily removed (one or two seconds) so that the crayons may be struck on the surface. An alternative is to strike the crayon on the backside at the point being heated.

Another temperature monitoring method is to use a contact pyrometer (fig. 3.21). This device is basically a thermocou-

ple connected to a readout device. It can be used in a manner similar to a temperature crayon by placing it on the surface. Because the pyrometer relies on full contact with a smooth surface, the readings vary with position and pressure, typically underestimating the actual temperature. It is recommended that the pyrometer be calibrated with temperature crayons prior to using.

Infrared devices are also available. These devices record the temperature and provide a digital readout.

To complement the crayons, pyrometer, or infrared devices, visually observe the color of the steel at the torch tip. Under ordinary daylight conditions, a halo will form on the steel around the torch tip, fig. 3.22. At approximately 650°C (1200°F) this halo will have a satiny silver color in daylight or bright lighting. The observation of color is particularly useful for the technician using the torch to maintain a constant temperature. However, this is the least accurate method of monitoring temperature and is approximate at best.

Controlling restraining forces.-

Another concern for the heat-straightening supervisor is the control of restraining forces. Typically hydraulic or mechanical jacks are used to apply restraining forces (see fig. 3.23 as an example) and should be calibrated so that the force being exerted can be determined. The maximum allowable force should be computed as part of the design process and specified in contract documents.

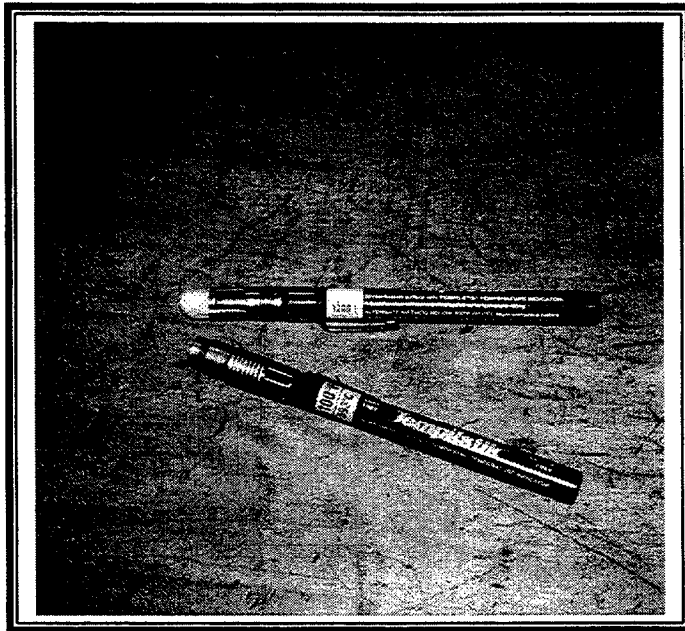


Figure 3.20. Temperature sensing crayons.

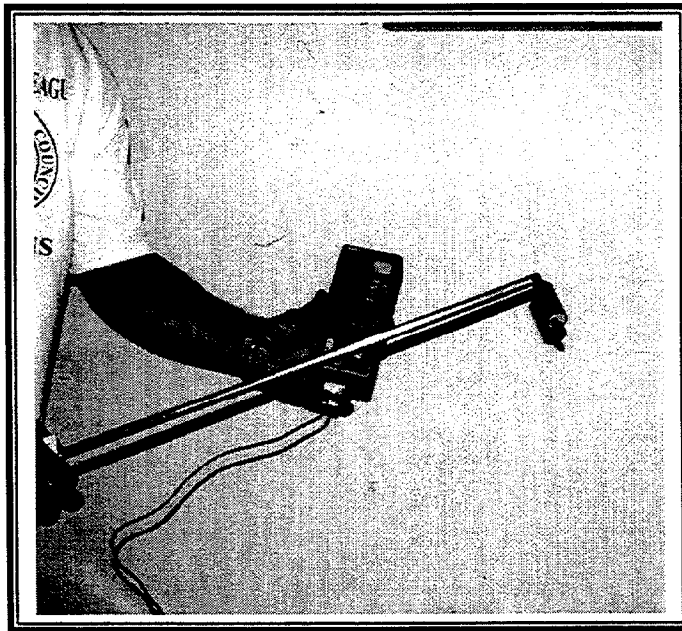


Figure 3.21. Contact pyrometer for measuring heating temperature.

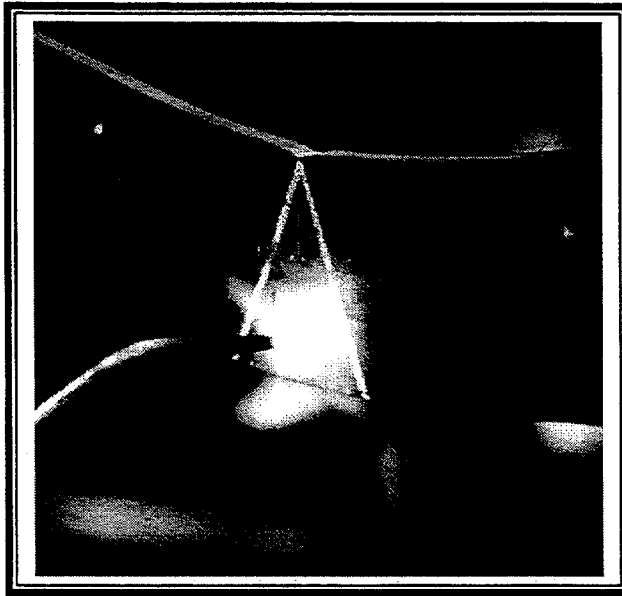


Figure 3.22. Heating in progress illustrating silver color around torch tip.

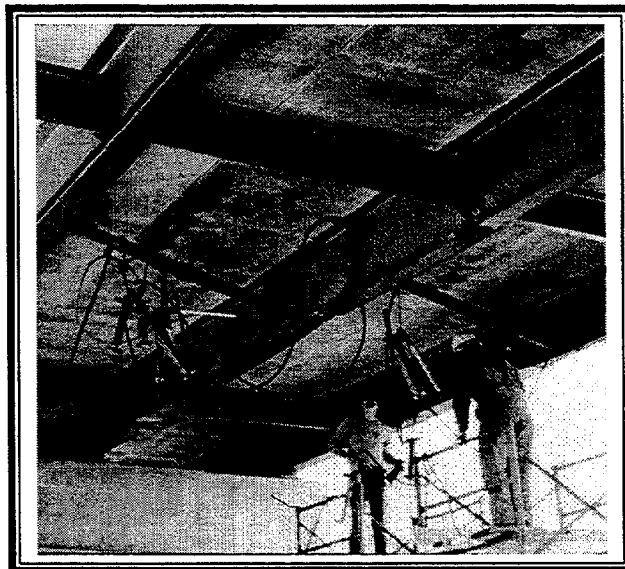


Figure 3.23. Jacks in place on a Wisconsin bridge.

Approving Heating Patterns.-The supervisor should approve the heating patterns and torch paths used. The general patterns can be set as part of the design of the repair. However, as heating progresses there may be a need to modify the patterns. The supervisor should understand the principles for using various patterns and approve modifications on site as required.

Checking Tolerances.-A significant concern is the tolerance for the completed repair. The contract documents should specify the allowable tolerances and the supervisor should verify that these limits either have been met or where (and why) exceptions were accepted. While tolerance levels similar to that of new construction may be used, often a looser tolerance level may be used to reduce the number of heat cycles required, especially in restricted areas and to minimize the cost of the repair. This decision should be made as part of the design process.

The above items relate specifically to heat straightening. The supervisor should also exercise normal control of the job site, as with any construction project, including monitoring of safety procedures.

Common Mistakes to Avoid

Because heat straightening has evolved as an art form, many practitioners have developed some skills. Most of these craftsmen have worked in steel fabrication or erection and many are experienced welders. They know methods to remove distortion in steel. However, many of their techniques are not heat straightening. The most common mistakes are:

Mistake No. 1: Heating the Steel Until it is Cherry Red

Such an approach is dangerous because the steel may pass through both the lower critical and the upper critical temperatures. The heating/cooling cycle may not result in a reversible molecular change. The heat-straightened steel may have brittle characteristics and not be suitable for bridge applications. Use temperature crayons to verify the heating temperature.

Mistake No. 2: Jacking the Girder Straight While it is Hot

Over-jacking can lead to a sudden brittle fracture. It may also result in micro cracks not readily visible which will weaken the structure. All jacks should be gauged and the forces limited to safe levels well below the material yield stress.

Mistake No. 3: Heating Too Large an Area

Some feel that the more surface area heated the better. However, the principle of heat straightening is to allow differential heating followed by contraction during cooling to move the steel. Heat straightening is most effective when small regions are heated. Narrow vee, strip or line heats, with unheated metal in between minimizes overall expansion yet allows contraction cooling to take place. In fact, heating too much area may prevent heat straightening.

Mistake No. 4: Heating Outside the Yield Zones

The goal of heat straightening is to gradually restore the yield zones to their original configurations. By limiting heat to only the vicinity of these areas, the damage

mechanism is reversible. Heating in non-yielded regions often results in a misaligned structure.

Mistake No. 5: Using Inefficient or Improper Heating Patterns

Certain heating patterns have been shown to be particularly effective: vee heats on major axis plate element bending, line heats for minor axis bending, and strip heats on stiffening elements. An understanding of the role of each heating pattern is essential to effective heat straightening.

Checking Procedures for Supervisors

Remember that the goal is not just to straighten the damage, but to straighten it safely. There are a number of checks that should be made by the supervisor as the repair progresses.

1. Review and approve all heating patterns prior to initiating the repair .
2. Periodically check the jack gauges to insure that excessive force is not being used.
3. Periodically monitor the temperature using temperature sensing crayons, a contact pyrometer, or other sensing device.
4. Constantly observe the color of the steel at the torch tip. In normal daylight lighting, the steel should have a satiny silver halo at the tip. At night or in heavy shadows, a slight dull red glow may be visible.
5. Establish reference points from which to measure movements. A taut line is useful although it must be moved aside during heating. In smaller regions a straight edge may be used. Sometimes it is convenient

to measure from a fixed part of the adjacent structure which will not move during the straightening process.

6. Always be sensitive to safety issues since the work is usually performed with at least some vehicle lanes open. Insure that jacks and other equipment are secured from falling.
7. Final approval should be based on meeting the specified tolerances.

Key Points to Remember

- The engineer's role is to design the repair.
- The field supervisor monitors the repair process to insure it meets plans and specifications.
- The contractor implements the design.
- Communication is essential between engineer, supervisor and contractor.
- Keys to a successful repair include:
 - ◆ Selection of appropriate heating patterns and sequences.
 - ◆ Controlling the heating temperatures and rates.
 - ◆ Using suitable restraining forces.
- Damage assessment includes:
 - ◆ Initial inspection and evaluation for safety and stability.
 - ◆ Detailed inspection for specific defects such as signs of fracture and material degradation.
 - ◆ Taking measurements to characterize damage.
 - ◆ Determining the cause of damage.

-
- ◆ Determining the presence of cracks, tears or other problems not amenable to heat-straightening repair.
 - Steps in the planning and design process include:
 - ◆ Analysis of degree of damage and determination of maximum strain due to damage.
 - ◆ Conducting a structural analysis of the system.
 - ◆ Selecting regions where heat straightening is applicable.
 - ◆ Selecting heating patterns and parameters.
 - ◆ Developing a constraint plan.
 - ◆ Developing repair plans and specifications.
 - Supervisor's responsibilities include:
 - ◆ Monitoring the heating temperature.
 - ◆ Monitoring restraining forces.
 - ◆ Approving heating patterns.
 - ◆ Checking Tolerances.
 - While some rational limitations exist when considering the heat-straightening option, engineering judgement is an essential ingredient for a successful repair.

PART II. TECHNICAL GUIDE FOR HEAT-STRAIGHTENING REPAIRS

Chapter 4. Effects of Heating on the Material Properties of Steel

Introduction

The potential for detrimental effects from heating damaged steel has limited the implementation of heat straightening. However, with an understanding of the properties of steel, heat straightening can be safely conducted. Heating steel reduces the yield stress as well as the elastic modulus but the coefficient of thermal expansion increases with temperature. The behavior of these parameters complicates attempts to understand the response of steel to heat straightening. In addition to these short-term effects, heat can result in long-term consequences which may be detrimental.

The large majority of steels used for bridge construction in the United States are either carbon or low alloy steel. At ambient temperature, these steels have three major constituents: ferrite, cementite and pearlite. The iron-carbon equilibrium diagram shown in fig. 4.1 illustrates the relationship of these components. Ferrite consists of iron molecules with no carbon attached, cementite is an iron-carbon molecule, (Fe_3C); and pearlite is a mixture of cementite (12 percent) and ferrite (88 percent). A low carbon steel has less than 0.8 percent carbon, too little carbon to develop a 100 percent pearlite compound, resulting in pearlite plus free ferrite molecules. High carbon steels (carbon content between 0.8 and 2.0 percent) have more carbon than required to form pearlite, resulting in a steel with additional cementite. Low carbon steels tend to be softer and more ductile because these are characteristics of ferrite. Cementite is hard and brittle

thus high carbon steels are harder and less ductile.

Temperatures greater than about 700°C (1300°F) begin to produce a phase change in steel. This temperature is often called the lower critical (or lower phase transition) temperature. The body centered cubic molecular structure begins to assume a face centered cubic form. With this structure, a larger percentage of carbon will be carried in solution. When steel cools below the lower critical temperature, it attempts to return to its body centered structure. Since this change requires a specified time frame, rapid cooling may not permit the complete molecular change to occur. Under these circumstances, a hard, strong and brittle phase called martensite occurs. The steel in this form may have reduced ductility and be more sensitive to brittle fracture under repeated loads.

The upper critical (or upper phase transition) temperature is the level at which the molecular change in structure is complete. At this temperature (around 815-925°C or 1500-1700°F for most steels, depending on carbon content) the steel assumes the form of a uniform solid solution called austenite. It is at temperatures between the lower and upper critical that a wide range of mill hot rolling and working can occur. As long as the temperature is lowered slowly in a controlled manner from these levels, the steel assumes its original molecular configuration and properties. This temperature control is more difficult to

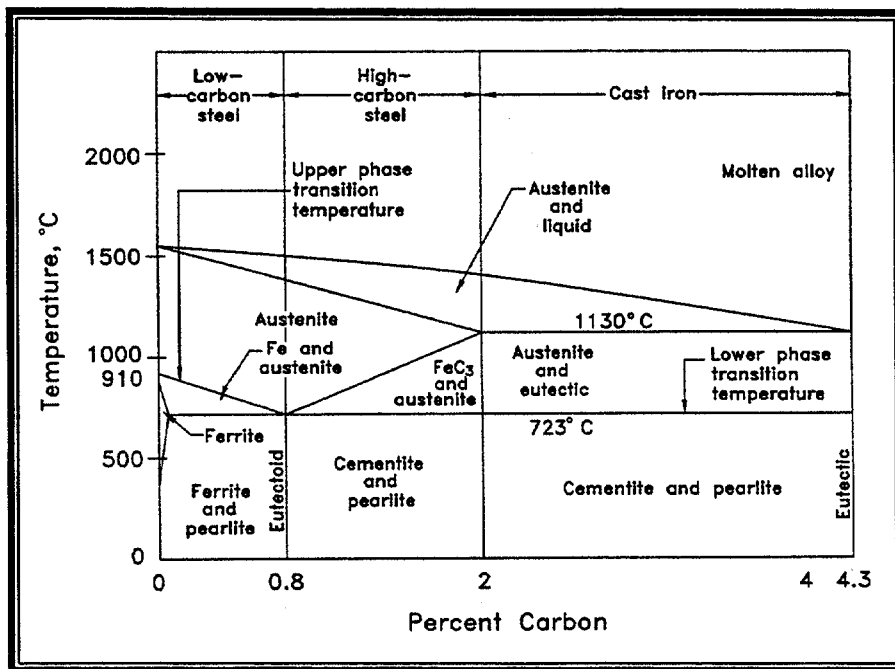


Figure 4.1. Iron-carbon equilibrium diagram.

maintain at a fabrication shop or in the field when conducting heat straightening repairs.

Consequently, if the temperature during heat straightening is not kept below the lower critical temperature, undesirable properties may be produced during cooling. It is this concern that has limited the application of heat straightening in many cases. A related issue is the question of residual stresses. When heated steel cools, the surfaces having the most exposure to the cooling environment contract more rapidly. This unequal contraction produces the residual stresses found in most steel shapes and it is important to understand how heat straightening affects these residual stress patterns. The purpose of this chapter is to first provide data on the residual stress patterns of heat-straightened steel, and second, to provide a summary of how heat straightening affects material properties.

Residual Stresses in Heat-straightened Plates

Although residual stresses are often mentioned in literature on heat straightening, there has been little documented research in this area. Past research was conducted in the context of heat curving (not heat straightening), and thus is somewhat limited in its applicability to heat straightening. Some of the most notable research was conducted at the University of Washington (Roeder 1985), where a finite element model was developed to predict the local behavior of a plate element subjected to a vee heat. Residual stresses were estimated using the model and experimental strains were also measured. An example of Roeder's results are shown in fig. 4.2.

Experimental research was conducted (Brockenbrough 1970b) to back up earlier theoretical residual stress studies

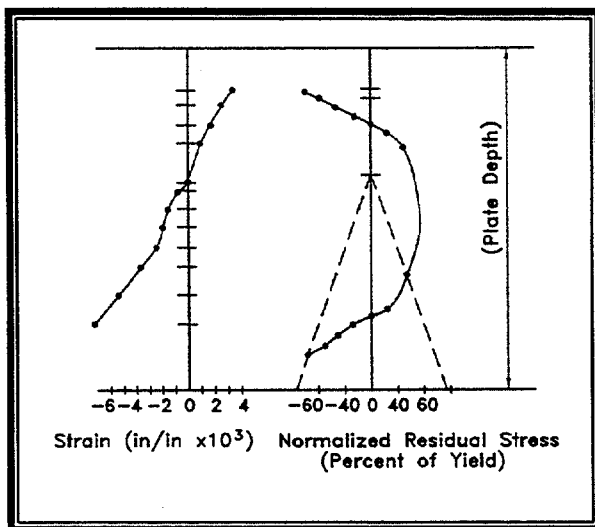


Figure 4.2. Experimental strain and theoretical residual stress distribution for 2/3 depth, 45° vee heated plate subjected to 1000°F temperature (Roeder, 1985).

(Brockenbrough 1970a) on heat-curved plate girders subjected to line heats. These stresses, determined by the “sectioning method”, were reasonably consistent with the theoretical values. Similar theoretical methods were used on vee-heated plate elements (Nicholls and Weerth 1972) and on wide flange beams (Horton 1973). However, the results were not supported by any experimental data.

Significant residual stresses occur in most structural steel members. Such stresses usually result from differential shrinkage during cooling in the manufacture of both rolled and welded built-up shapes. However, the cutting and punching process during fabrication may also produce residual stresses. Residual stresses are quite high and values may reach 50 percent of yield for some rolled shapes and approach yield for some welded built-up members. With one exception, residual stresses have been neglected in code requirements governing steel

design. The reasons for neglecting residual stresses relate to two characteristics: (1) The ductility of steel allows for a moderating redistribution of residual stresses when a member is subjected to large loads, and (2) since residual stresses are self-equilibrating, large compressive stresses at one location on a cross section are balanced by tensile stresses at another location. As a consequence, the stresses at a specific cross section produced by applied loads is additive to the residual stresses at some points and are subtractive at others. The result is that the ultimate strength of a member is usually not affected by residual stresses. The exception is compression members in which high residual stresses may reduce the buckling strength. American design codes account for residual stresses in compression members by assuming an average residual stress value of 50 percent of the yield stress. This assumption may lead to somewhat conservative designs for rolled shapes (which have smaller residual stresses) and slightly less conservative designs for welded built-up shapes (which have larger residual stresses). European codes have adopted the multiple column curve approach in which different formulas are used depending, on the magnitude of residual stresses. For these codes the level of residual stress affects the design capacity.

Avent, Robinson, et. al. (1993) have conducted research to provide insight as to whether heat straightening produces some negative effects due to residual stresses. The study included: both plates and rolled shapes; variations in vee angle, vee depth and level of external restraining forces; and degree of initial damage. Residual stress patterns were determined by using the “sectioning method”, a well-established, but

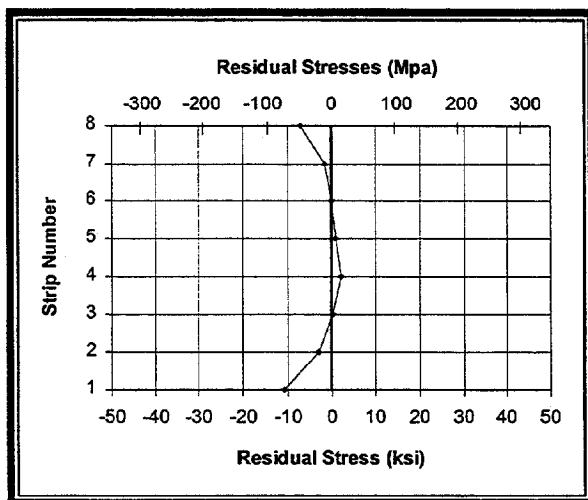


Figure 4.3. Measured residual stresses in a vee heated plate prior to heating.

destructive procedure. After taking initial distance measurements between two fixed points on the steel, a narrow strip containing these points is cut out (by milling to avoid heating the steel). The distance is re-measured and the change reflects the magnitude of residual stresses in that strip. Practical considerations limit strips to approximately $\frac{1}{2}$ in width and changes in length are quite small over the gauge lengths required; typically 4 in. These considerations limit the accuracy of the process. However, the results provide a reasonable assessment of residual stress patterns after heat straightening. For all residual stress values given in this chapter, a positive sign denotes tension and negative denotes compression stresses.

An unheated plate (Plate UH) was tested for residual stresses to provide the basis for determining changes resulting from vee heats. Stresses found in each strip are plotted in fig. 4.3. The values are fairly low and the shape compares reasonably well with standard residual stress assumptions and previous experimental measurements

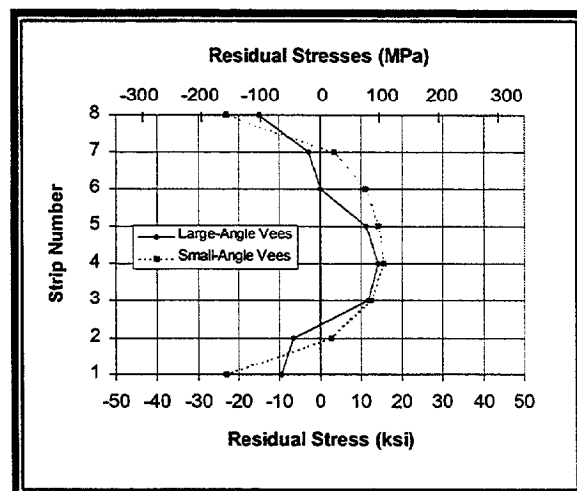


Figure 4.4. Average residual stress values for vee heated plates which were originally undamaged.

(Avent and Wells 1982). A series of 100 x 6 x 610 mm (4 x $\frac{1}{4}$ x 24 in) long, initially straight A36 steel plates were vee heated four times each. The heating parameters are shown in table 4.1. Residual stresses were measured across the vee heated zone for each plate with the 102 mm (4 in) gauge length centered on the vee for each strip. A distinction can be made by classifying "small vee angles" as those being less than or equal to 60° and "large vee angles" as those greater than 60° . These two categories have significantly different magnitudes of residual stresses, especially at the edges. The averages of all plates within each category are shown in fig. 4.4. The smaller vees exhibited considerably higher compressive stresses at the edges.

The residual stress patterns in all of the plates were similar in shape to Roeder's theoretical distribution (fig. 4.2), where normalized values were used. An evaluation of the individual results indicates that most vee heat parameters had little effect on residual stresses. The exception was that the largest vee angle cases (82°) had maximum

Table 4.1. Heating parameters for undamaged plates.

Plate	Vee Angle	Jacking Ratio	Depth Ratio
P-1	20	0.00	1.00
P-2	45	0.00	1.00
P-3	60	0.00	1.00
P-4	20	0.00	1.00
P-5	45	0.50	0.75
P-6	45	0.00	0.75
P-7	82	0.50	0.75
P-8	82	0.00	0.75

Table 4.2. Heating conditions and degree of damage for deformed plates.

Plate	Angle of Damage (deg/millirad)	Max Strain (Multiple of Yield Strain)	Vee Angle (degree)	Jacking Ratio (M_f/M_p)	Vee Depth Ratio	Avg. Plastic Rotation per vee heat (millira- dians)
P-9	6.40/111.8	30	45	0.25	1.00	4.63
P-10	23.62/412.2	100	45	0.25	1.00	3.82
P-11	5.58/97.4	30	45	0.50	1.00	5.94
P-12	11.80/205.9	80	45	0.50	1.00	5.60
P-13	18.7/327.6	90	45	0.33	1.00	5.56
P-14	5.99/104.5	30	45	0.50	0.75	4.69
P-15 ¹	21.12/368.6	80	20	0.50	0.75	3.81
P-16 ¹	25.06/437.4	90	20	0.50	1.00	3.41
P-17 ¹	18.21/317.8	100	60	0.50	0.75	6.43
P-18 ¹	25.02/436.7	100	60	0.50	1.00	6.56

¹The last four specimens were used just for plastic rotation data and were not straightened completely (20 heats were applied to each)

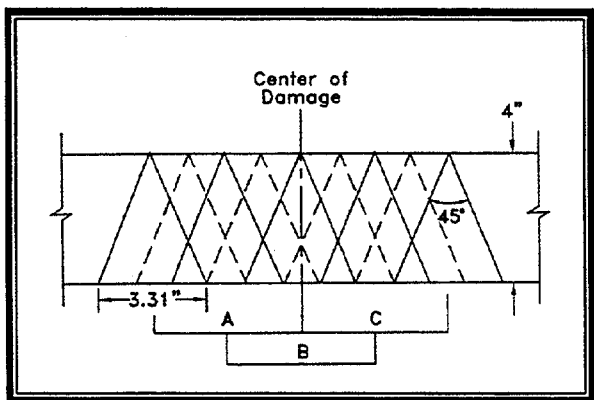


Figure 4.5. Regions utilized in residual stress measurements of damaged and heat straightened plates (Note: 25.4 mm = 1 in.).

stresses of 40-60 percent less than those with smaller vee angles. However, for vee angles from 20-60°, the residual stress variation was small. Similarly, neither the jacking ratios nor depth ratios significantly influenced residual stresses. In all cases the distribution of residual stresses were symmetrical. Thus, with the exception of vee angle, it appears that the heating/cooling cycle is the primary factor influencing residual stresses. Since the entire cross section was elevated to the same temperature, the residual stress distribution tended to be symmetrical. In comparison to the unheated plate, the maximum stresses were found to be over 100 percent larger. For vees in the 20-60° range, the maximum compression residual stresses were on the order of 172 MPa (25 ksi).

A second series of 100 x 6 x 610 mm (4 x ¼ x 24 in) long plates were initially damaged and then heat straightened. The parameters are shown in table 4.2. After straightening, average residual stresses were determined by the sectioning method for three different regions on the damaged plated: Regions A, B, and C (see fig. 4.5).

Typically, eight strips were cut from each plate. The plates were classified in groups of small degree of damage (6°) and large degree of damage (12 to 24°) where degree of damage, ϕ_d , is defined as shown in fig. 3.3. These two groups experienced slightly different residual stress patterns. The small degree of damage classification exhibited a maximum strain ratio (eq. 3.9) of approximately 30 times yield strain and the larger degree of damage cases 80 to 100 times yield strain. The residual stress distributions for both cases are shown in figs. 4.6 and 4.7.

Since all of these plates had significant damage, a large number of heats (25-100) were required to straighten them. It appears that the repetitive heating tended to reduce the residual stresses in comparison to the undamaged heated plates. All but one of the five plates exhibited the parabolic distribution predicted by Roeder (1985). The exception (plate II) had compression stresses at the center as well as the edges. As a result the average values for the two plates with the 6° damage did not follow the expected pattern. For all cases the maximum compressive stresses at the edges ranged between 83-179 MPa (12-26 ksi) and, the tensile stresses ranged between 55-83 MPa (8-12 ksi). The stresses were computed using the commonly assumed value of 200,000 MPa (29,000 ksi) for the steel's modulus of elasticity (E). It should be noted that a few of the gage holes were destroyed in the stripping process, thus rendering the strips unreadable.

Based on the measured residual stresses, a theoretical model can be developed by assuming the distribution to be parabolic. With a maximum tensile stress of

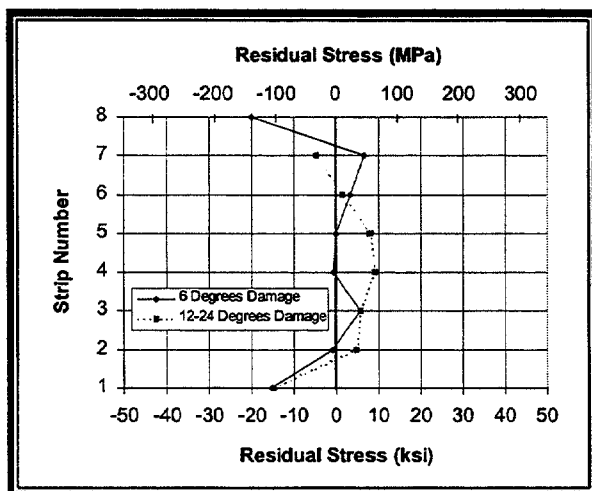


Figure 4.6. Residual stress distribution for damaged and vee heated plates in region B (assumed modulus = 200,000 MPa or 29,000 ksi).

69 MPa (10 ksi) and a maximum compressive stress of 138 MPa (20 ksi), the residual stresses can be approximated by

$$\sigma_r = 10(1 - 12x^2) \quad (\text{Eq. 4.1})$$

where x is the distance from the center of the plate to the residual stress location divided by the plate width and σ_r is the residual stress in ksi.

Residual Stresses in Rolled Shapes

Residual stress patterns have been experimentally determined for some representative samples of angles, channels and wide flange sections. The geometry of the shapes prevented measurements with the extensometer on both sides of certain strips. However, the continuity and consistency of the values indicate that by just measuring one side, sufficient accuracy was obtained. The residual stress values for angles are shown in fig. 4.8 – 4.11. The strip number

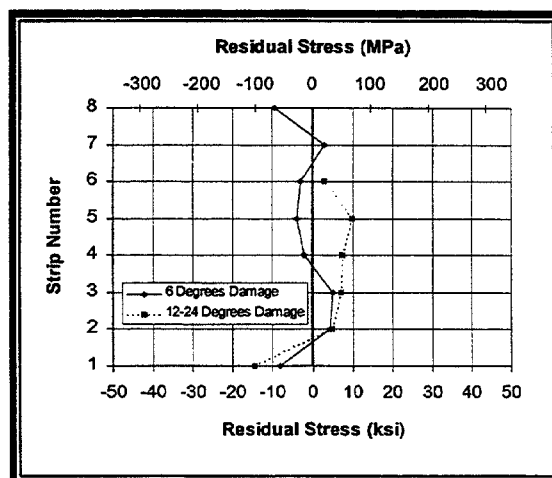


Figure 4.7. Residual stress distribution for damaged and vee heated plates in region A and C (assumed modulus = 200,000 MPa or 29,000 ksi).

locations are shown in the figures along with the location of the vee and strip heats.

In the two originally undamaged angles (figs. 4.8 and 4.9), the residual stress patterns were quite similar. Somewhat higher compressive stresses were found at the edges in Fig 4.9. The only difference between these two specimens was the vee angle used (20° and 45° , respectively). For these two cases the apex of the vee was located at the toe of one leg and a strip heat was used on the opposite leg.

The residual stresses for a $4 \times 4 \times 1/4$ angle that was damaged and then heat straightened is shown in fig. 4.10. An interesting fact is that the damaged angle specimen exhibited the same pattern of residual stresses as the undamaged angles although the damaged angle had somewhat higher values. For this case, the apex of the vee was located at the heel of one leg and a strip heat was not required on the opposite leg. It is apparent that the heating/cooling process in the angles results in quite high (around 280 MPa or 40 ksi) compressive stresses

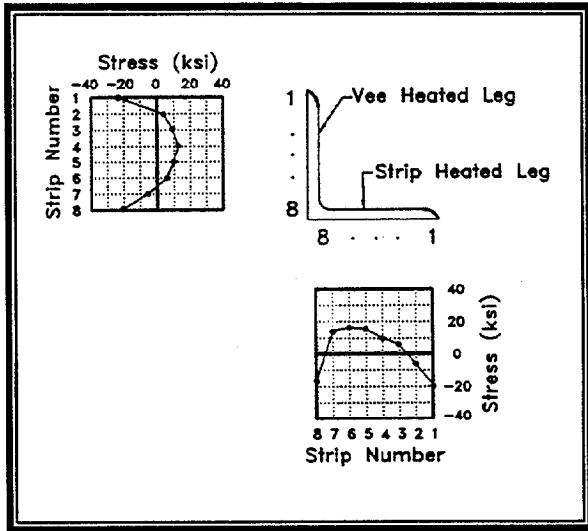


Figure 4.8. Stresses in angle VI-1 (20° vee, apex at toe, $M_f/M_p = 0.00$, depth ratio = 1.00).

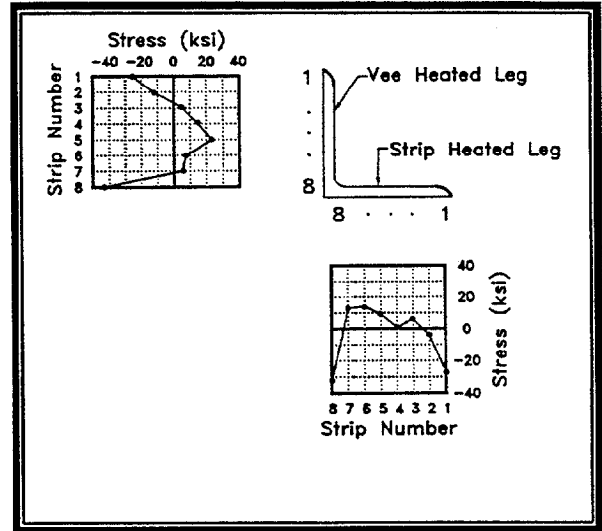


Figure 4.9. Stresses in angle VI-4 (45° vee, apex at toe, $M_f/M_p = 0.00$, depth ratio = 1.00).

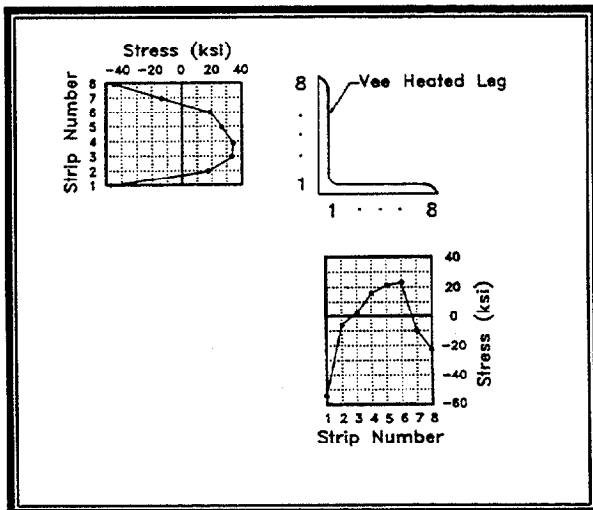


Figure 4.10. Stresses in angle L4x4 (45° vee, apex at heel, $M_f/M_p = 0.50$, depth ratio = 1.00).

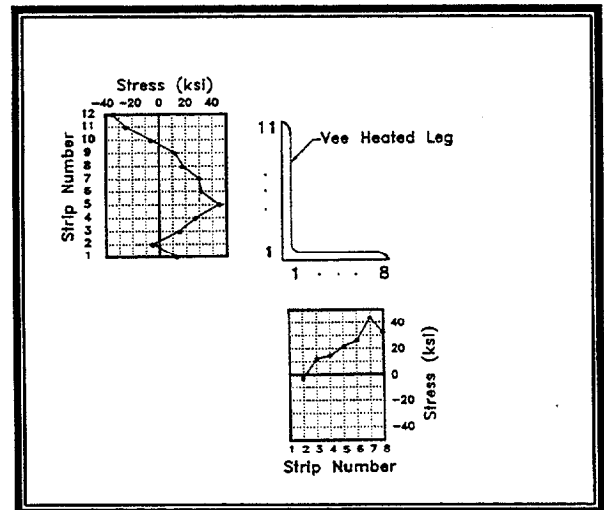


Figure 4.11. Stresses in angle L6x4x5/16 (45° vee, apex at heel, $M_f/M_p = 0.33$, depth ratio = 1.00).

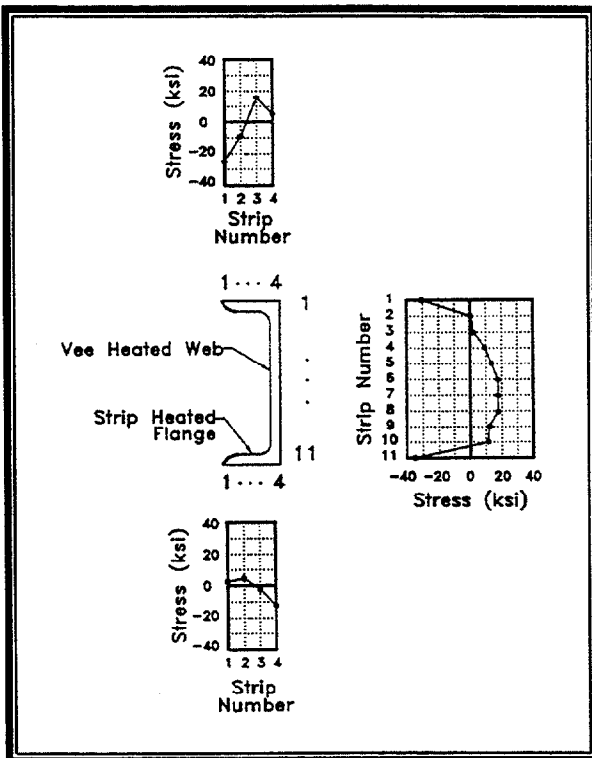


Figure 4.12. Stresses in channel IX-6 (45° vee, $M_f/M_p = 0.50$, depth ratio = 1.00).

near the toes, regardless of the location of the vee apex, relative to the stiffening element. For each of these cases the residual stresses were large compressive values at edges and corners and somewhat smaller tensile forces over the central portion of each cross section element.

The residual stress pattern for an unequal leg angle is shown in fig. 4.11. The angle was damaged and straightened with vee heats on the long leg. Since the apex of the vee was at the heel, no strip heat was required on the stiffening leg. Here the pattern varied from the equal leg angles, although the maximum values were of similar magnitude (approximately equal to the yield stress).

Of primary importance is the observation that residual stresses in heat

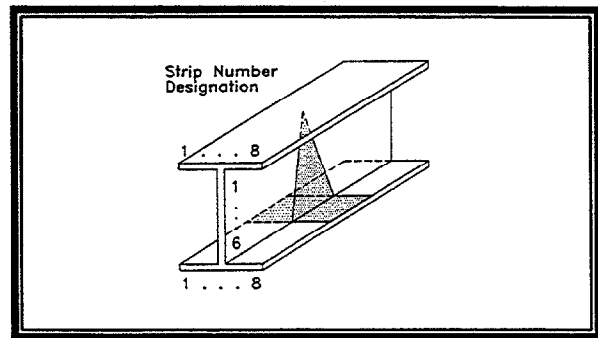


Figure 4.13. Residual stress strip locations (Category S heat).

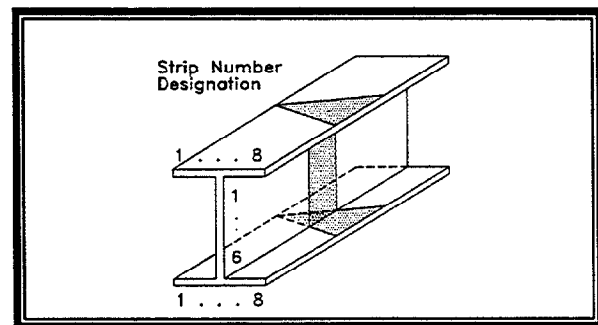


Figure 4.14. Residual stress strip locations (Category W heat).

straightened angles are quite high and approach yield stress at some points. While the distribution of these stresses may vary, the magnitudes are similar to that of welded built-up shapes.

The residual stresses for a category S heating pattern on an originally undamaged C 6x8.2 channel are shown in fig. 4.12. The pattern is not as well defined as for angles. However, significant residual stresses were found with the magnitudes approaching the yield stress.

Residual stresses were also experimentally determined in the heated region of W 6x9 wide flange beams using the sectioning method. In all of the beams, eight strips were cut from each flange, and six strips were cut from the web (see figs.

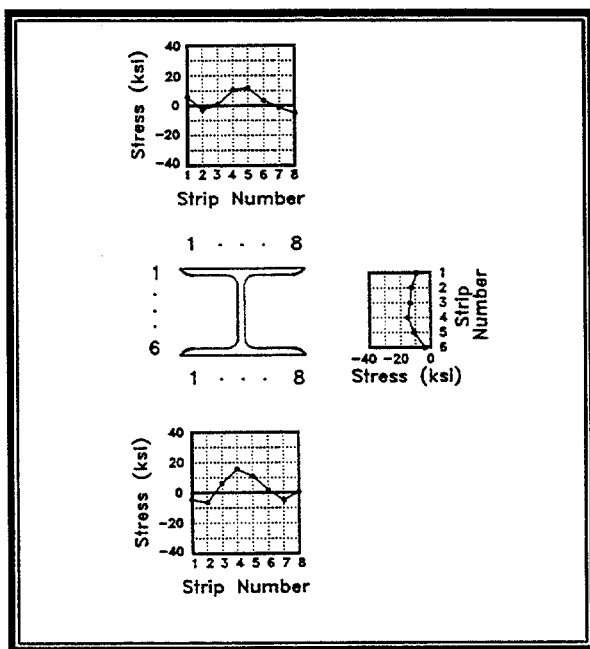


Figure 4.15. Residual stresses in unheated wide flange beam "UH".

4.13 and 4.14). The shape of the extensometer used to measure the gage lengths prohibited obtaining stresses in the web within about 1.5 inches from either of the flanges, thus limiting stress reading to six strips.

An unheated specimen (Beam UH) was tested for residual stress (fig.4.15), to compare with the heated specimens. These stresses closely matched a plot of the residual stresses in a roller straightened W6x20 shape shown in the Structural Stability Research Council's "Guide to Stability Design Criteria for Metal Structures" (1976). Roller straightening (or rotorizing) is a common mill practice for straightening small wide flange shapes to meet sweep and camber tolerances. The process redistributes and greatly reduces the initial residual stresses in the flanges (a characteristic evident in Beam UH, where these stresses are quite low).

Eight undamaged W 6x9 wide flange beams were heated using the standard patterns (five Category S and three Category W). Four heats were conducted for each beam. The heating parameters are shown in table 4.3. Plots of the residual stress patterns are shown in figs. 4.16-4.23. From the residual stress patterns in the heated undamaged beams, the following observations are made:

- The residual stresses are greatly increased when vee heats are applied to undamaged beams. The maximum values equal yield for Category S and approximately one-half yield for Category W heats.
- The patterns were significantly different in the Category S and Category W heated specimens.
- Jacking ratio and depth ratio were again found to not significantly change the stress patterns, when all other parameters were held constant.
- By classifying the 20- and 30-degree vee angles as small and the 45-degree vee angles as large, there were significant pattern differences in the two classifications in the Category S specimens (no significant difference in Category W specimens).

Four W 6x9 wide flange beams were bent about their weak axis (Category W) and repaired using the standard patterns. All beams were repaired with $\frac{3}{4}$ depth, 45° vees and a jacking ratio of 50 percent.

Table 4.3. Heating conditions for undamaged wide flange beams.

Beam	Vee Angle	Jacking Ratio	Depth Ratio	Category
B-1	20	0.00	1.00	S
B-2	30	0.00	1.00	S
B-3	45	0.00	1.00	S
B-4	45	0.25	1.00	S
B-5	45	0.50	1.00	S
B-6	20	0.00	1.00	W
B-7	20	0.50	1.00	W
B-8	45	0.00	1.00	W

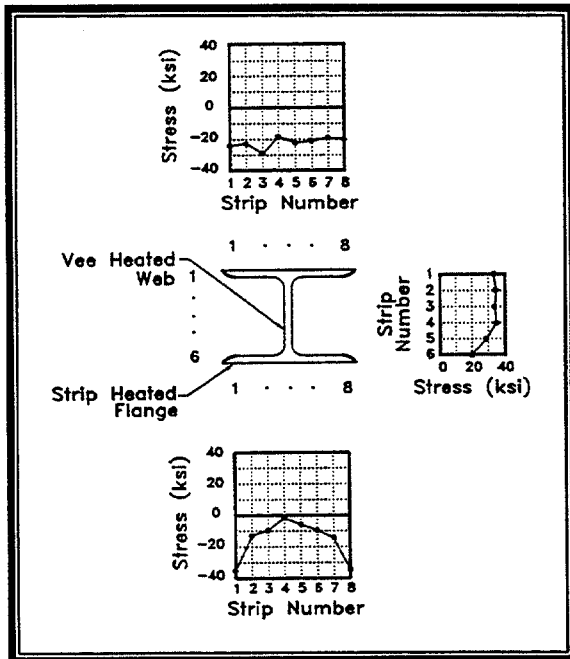


Figure 4.16. Stresses in beam B-1 (20° vee, $M_j/M_p = 0.00$, depth ratio = 1.00).

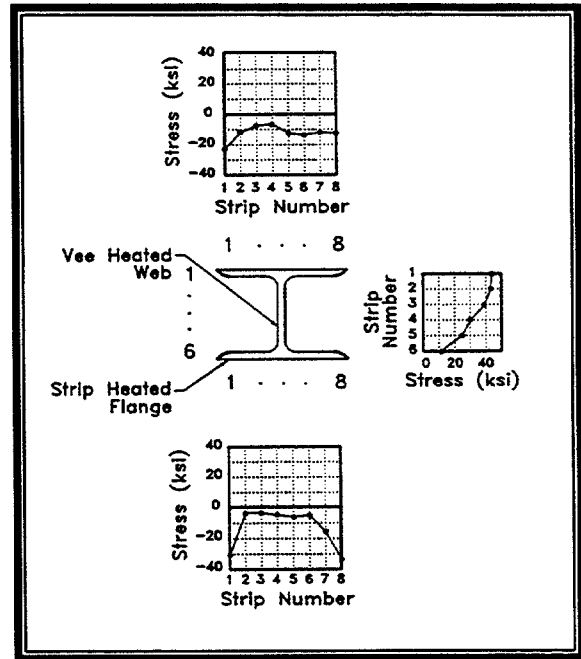


Figure 4.17. Stresses in beam B-2 (30° vee, $M_j/M_p = 0.00$, depth ratio = 1.00).

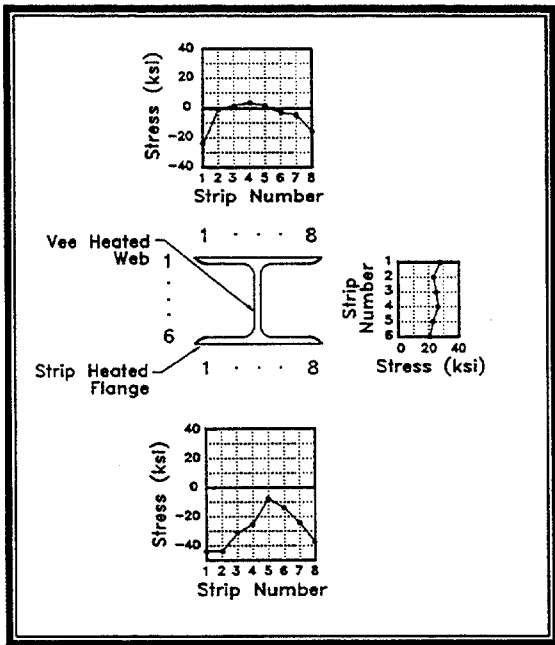


Figure 4.18. Stresses in beam B-3 (45° vee, $M_j/M_p = 0.00$, depth ratio = 1.00).

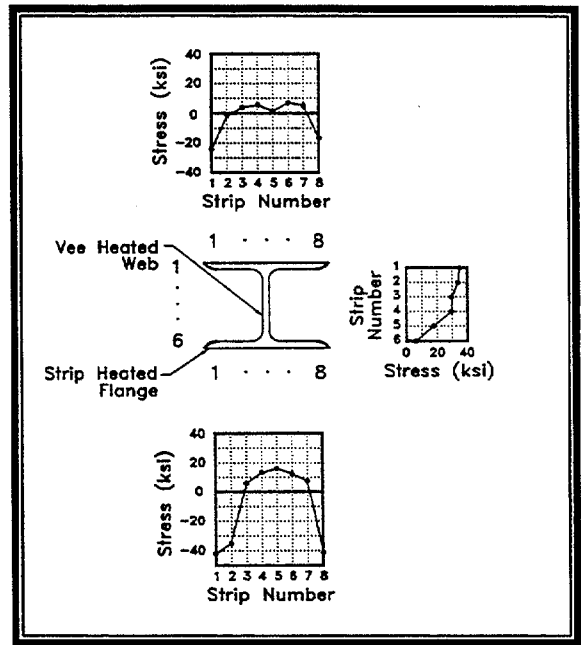


Figure 4.19. Stresses in beam B-4 (45° vee, $M_j/M_p = 0.25$, depth ratio = 1.00).

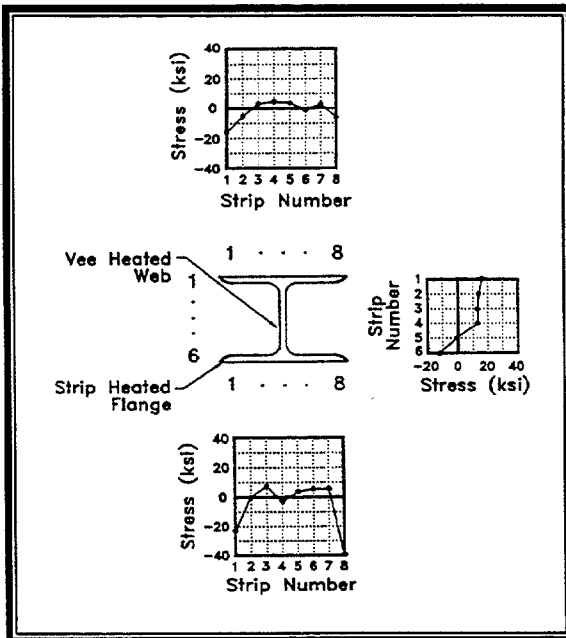


Figure 4.20. Stresses in beam B-5 (45° vee, $M_j/M_p = 0.50$, depth ratio = 1.00).

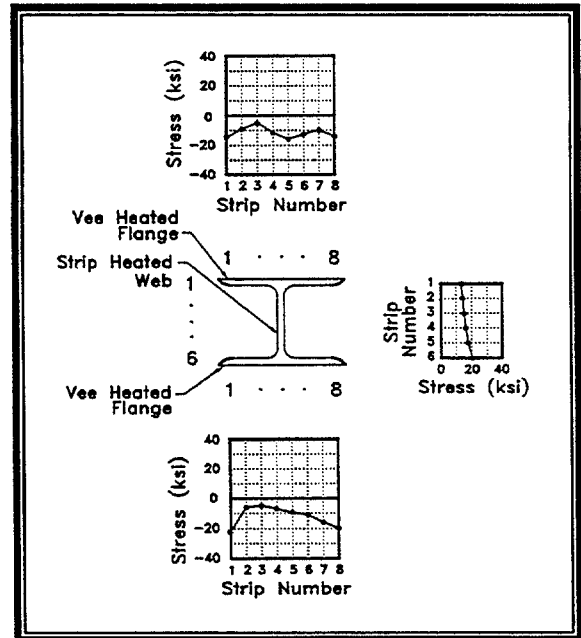


Figure 4.21. Stresses in beam B-6 (20° vee, $M_j/M_p = 0.00$, depth ratio = 1.00).

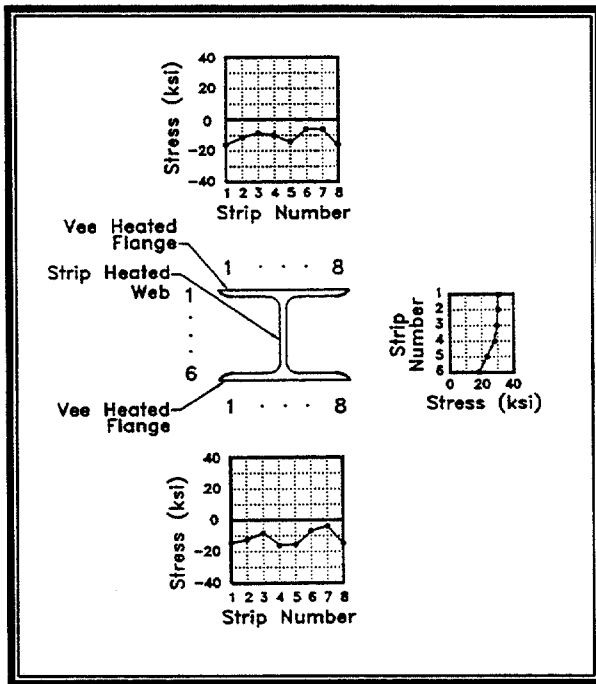


Figure 4.22. Stresses in beam B-7 (20° vee, $M_f/M_p = 0.50$, depth ratio = 1.00).

A unique part of these tests was that all beams except the first were re-damaged and repaired several times. Residual stresses were obtained after the last repair cycle for each beam. In each case the degree of damage was approximately 7° which required about 20 heats to complete the repair. Residual stress measurements were made on beams after 1, 2, 4, and 8 damage/repair cycles. Measurements were taken at the center of damage. Shown in fig. 4.24 are the average residual stresses in the flanges of the specimens for the different categories and locations (the shortening of the beams prevented the measurement of residual stresses in the webs, except for the single damage/repair cycle). The stresses were fairly consistent in the beams with one and two damage/repair cycles and fairly consistent in those with four and eight damage/repair cycles. This behavior indicates that the number of damage cycles

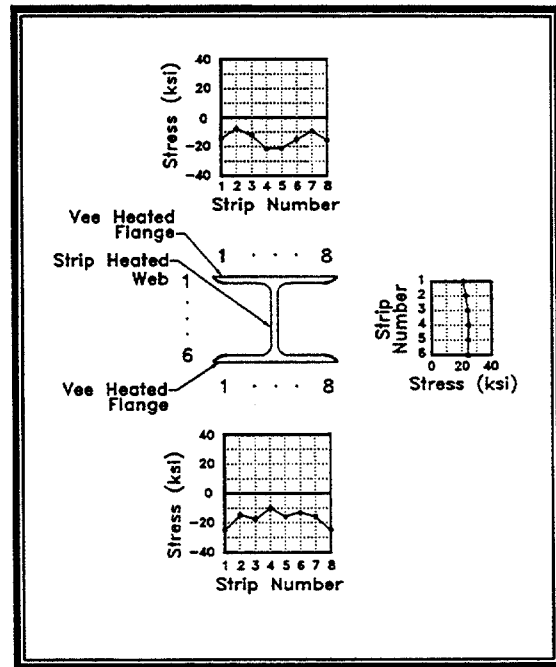


Figure 4.23. Stresses in beam B-8 (45° vee, $M_f/M_p = 0.00$, depth ratio = 1.00).

has some effect on the residual stress distribution. Values are shown, using an assumed modulus of elasticity of 200,000 MPa (29,000 ksi).

It is interesting to note that the residual stress patterns in all of these beams were exactly opposite in nature to that of the undamaged beams which had tension in the flanges and compression in the web. For the damage/repair cases, the large number of vee heats tended to shorten the flanges more than the strip heats shortened the web. Thus the flanges had tension stresses while the web had compression stresses. The web compression was obvious by severe web buckling which occurred after a number of damage/repair cycles (A correction factor was applied to account for curvature when computing the residual stress of each strip). Actual repairs would have required this local buckling to be heat straightened.

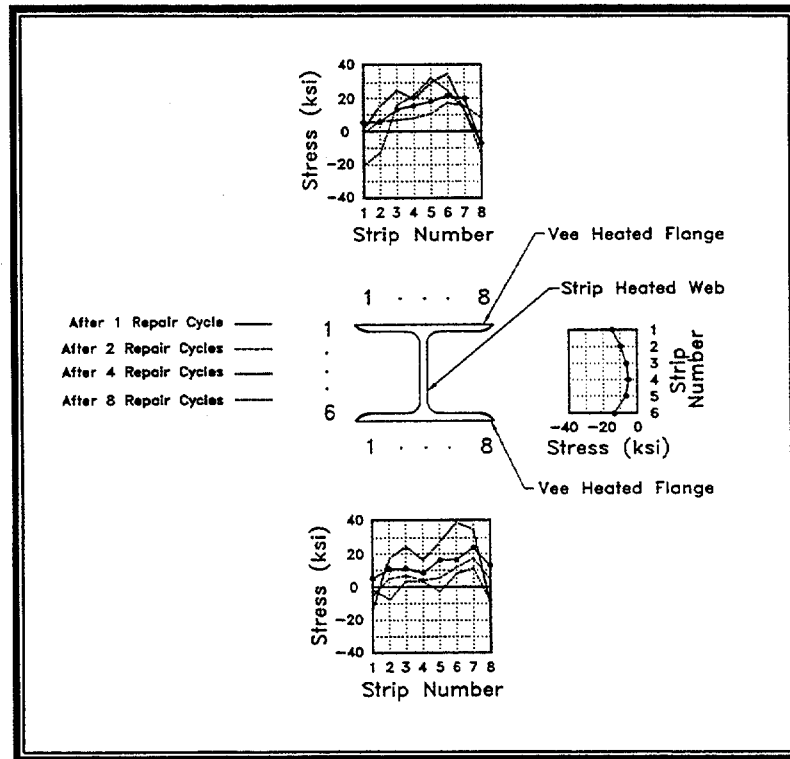


Figure 4.24. Residual stress distribution damaged, Category W side flange beams (assumed $E = 200,000$ MPa or 29,000 ksi).

Residual stresses were measured for a single W 6x9 beam with Category S damage which was repaired using the standard pattern. The residual stress patterns are shown in fig. 4.25. Both flanges were in compression while the web was in tension. The maximum compressive stresses in the flanges approached yield while those in the web were somewhat less. A comparison of the residual stresses for the undamaged and damaged beams showed a reasonably good correlation for Category S.

The large residual stresses created during heat straightening have several implications. First, if the member is a compression element, the high residual stresses are similar to welded built-up members. Since U.S. codes use a single column curve con-

cept, these members are all treated the same and no capacity reduction would be assumed. However, if multiple column curves are used (typical of many European countries), then heat straightened columns would fall in a lower strength curve after heating due to residual stresses. Consequently, there would be some loss of design strength.

Second, high tensile residual stresses reduce the effectiveness of jacking forces by effectively canceling out the compressive stresses in areas with externally applied force which causes compressive stresses. Movement could be reduced or even reversed, if the jacking force moment does not compensate for the residual stresses.

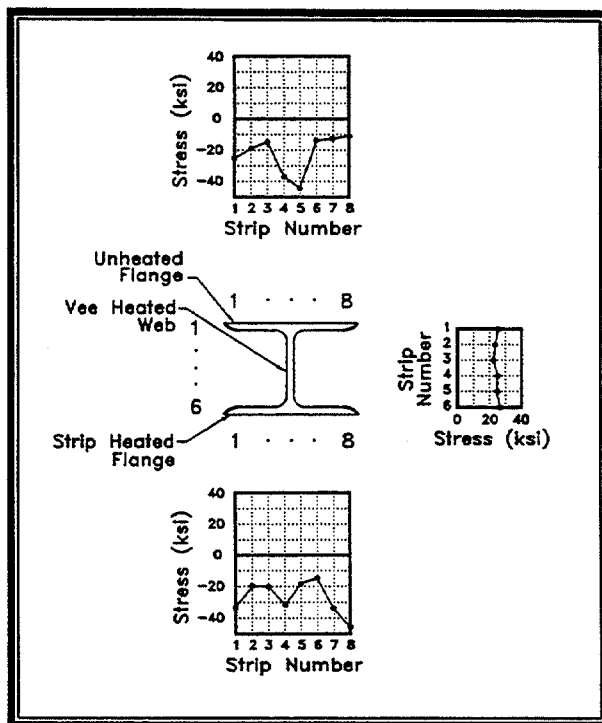


Figure 4.25. Residual stresses in Category S damaged wide flange beam (45° vee, $M_f/M_p = 0.50$, depth ratio = 1.00).

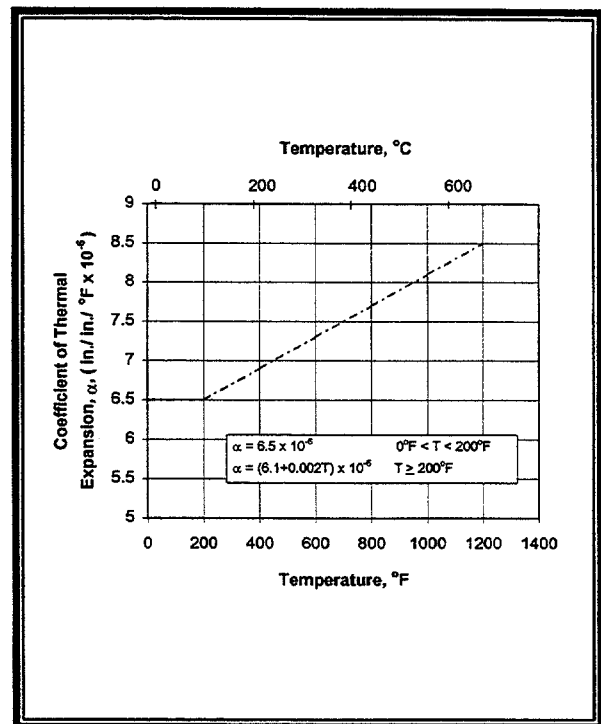


Figure 4.26. Variation of coefficient of thermal expansion versus temperature (Roeder, 1985).

Basic Material Properties From Laboratory Tests

Thermal Expansion.—One of the most fundamental aspects of heat straightening is the thermal expansion characteristics of steel. The coefficient of thermal expansion is a measure of the rate of strain per degree temperature. Between $65\text{--}650^\circ\text{C}$ ($250\text{--}1,200^\circ\text{F}$) this coefficient varies directly with temperature such that the rate of expansion increases as temperature increases (Blodgett, 1972; Ditman, 1961; Nichols and Weerth, 1972; Roeder, 1985). A plot showing the variation of the coefficient of thermal expansion for low carbon steels is shown in fig. 4.26 (Roeder, 1985). Most curves of this type do not exceed a temperature of $650\text{--}760^\circ\text{C}$ ($1200\text{--}1400^\circ\text{F}$)

because some research has indicated that the thermal expansion may become irregular over the range of temperatures between $700\text{--}870^\circ\text{C}$ ($1300\text{--}1600^\circ\text{F}$). This region is referred to as the phase transformation zone and the behavior is attributed to molecular change which might have detrimental effects on the steel properties. However, Roeder has shown that for vee heats the thermal expansion continues to increase in a well-behaved manner up to 870°C (1600°F) for carbon steels, although at this temperature, surface damage such as pitting becomes evident.

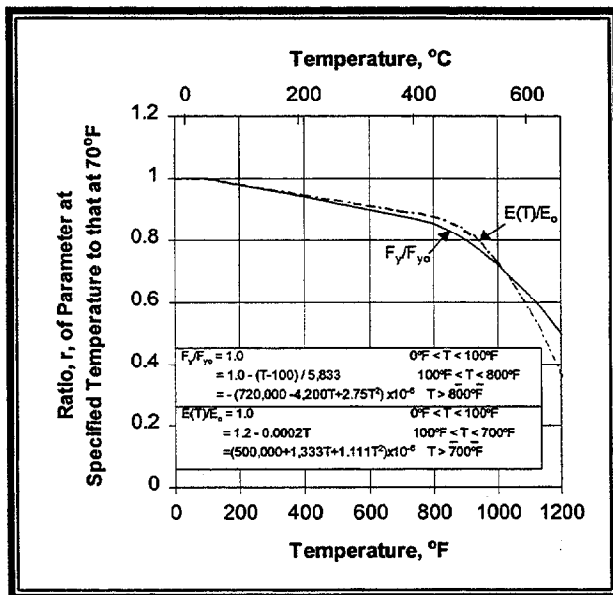


Figure 4.27. Normalized yield stress and modulus of elasticity versus temperature (Roeder, 1985).

Modulus of Elasticity.-Between 30-650°C (100-1200°F), the Modulus of elasticity decreases with increasing temperature. At 650°C (1200°F) the Modulus of steel typically decreases to one-half of its Modulus at room temperature. This relationship is shown in fig. 4.27 where E_o is the modulus at an ambient temperature of 21°C (70°F) which is 200,000 MPa (29,000 ksi) and T is in degrees Fahrenheit. Two investigators (Nicholls and Weerth, 1972 and Horton, 1973) have reported the results of measuring the Modulus of elasticity after the heat straightening. No appreciable change in the Modulus of elasticity was found after completing the heat straightening process and allowing the material to cool to ambient temperature.

Yield Stress.-Two aspects are important in relating the yield stress to the heat straightening process. The first is the variation in the yield stress during the heating

process. The second is the permanent effect heat straightening has on yield stress after the steel has cooled.

A plot of the yield stress versus temperature (Roeder, 1985) is shown in fig. 4.27 for carbon steel where T is the temperature in degrees Fahrenheit and F_{yo} is the nominal yield stress at 21°C (70°F). It can be seen that the yield stress may be on the order of 40 percent its original value when the temperature reaches the 650°C (1200°F) associated with heat straightening. This characteristic has the positive effect of enabling plastic deformation to occur at relatively low stresses during the straightening process. However, it may produce a negative effect in that the area being heated is temporarily weakened.

Of long-range interest is the effect on the yield strength after cooling has taken place. A number of researchers have measured the yield stress after the heating/cooling cycle to determine the modified characteristics. For the carbon steel tests representing over 25 specimens from various investigators (see table 10.1), the yield stress increases an average of 10 percent after heat straightening. Six specimens of high strength, low alloy steel showed a 2 percent increase in yield stress while eight specimens of heat-treated, high strength carbon steel showed an average increase in yield stress of 7 percent. The only steel that showed a decrease in yield stress was the quenched and tempered steel where the average of 12 specimens produced a 6 percent decrease in yield stress. This data indicated that the long term effects of the heat straightening process has a small but generally positive effect on the yield stress.

In addition, the tested specimens were heated for various lengths of time, cooled both by air and by quenching with a mist, and were subjected to various superimposed loads and residual stresses. None of these variables had significant effect on the yield stress with the possible exception of the quenched and tempered steel. In the case of quenching, the yield stress was, on the average, unchanged from the original yield.

Ductility After Heat Straightening.-Ductility has often been measured as the elongation over a two inch gage length expressed as a percentage. Test data (see table 10.1) shows that there is typically a 10-20 percent decrease in ductility after the steel has experienced a cycle of heat straightening. This range is the percent reduction and should not be construed as the actual reduction. The average decreases are: carbon steels, 8 percent; High strength, low alloy steels 18 percent; quenched and tempered steels, 14 percent; and quenched and tempered constructional alloy steels, 11 percent. While these changes in ductility characteristics are significant, the magnitude of the reduction is in an acceptable range.

Notch Toughness.-The Charpy V-notch test is widely used as a guide to the toughness of steels in structures susceptible to brittle fracture. A small rectangular bar with a specified V-shaped notch at its mid-length is simply supported at its ends as a beam and fractured by a blow from a swinging pendulum. The amount of energy required to fracture the specimen is calculated from the height to which the pendulum rises after breaking the specimen. The data is taken at a range of temperatures and a plot of energy versus temperature (on the ab-

scissa) is generated. The resulting curve is S-shaped with an upper limit asymptote of constant energy absorption as the temperatures increase above a certain upper critical temperature and a lower limit asymptote as the temperature goes below the lower critical temperature. These limits are referred to as the upper and lower shelf. Tests (see table 10.1) have shown that there is no significant change in the upper shelf energy absorption before and after the heat straightening process for any grade of steel.

A second measure of the notch toughness can also be obtained from the Charpy tests. The temperature at which 50 percent of the upper shelf energy was absorbed, T_{50} , is measured and the difference between the original T_{50} and the T_{50} after a completion of a heat straightening cycle is checked. Positive differences represent a decrease in notch toughness due to heat straightening while negative numbers represent an increase. Researchers (table 10.1) have found a considerable variation within a given steel grade. However, the average values indicate that only the quenched and tempered, low alloy steels have a significant positive shift (18°C or 32°F).

Another measure of notch toughness is the fracture transition temperature. This temperature is the one in which the percentage of shear fracture is 50 percent of the cross section. Pattee, et. al. (1969) used this criteria in evaluating several grades of steel that had been heat straightened. The Drop Weight Tear test was used instead of the similar Charpy test. The fracture transition temperature changes were modest for all cases except the A517-A steel where there was a significant positive shift indicating a fracture sensitivity.

Only one series of fatigue tests on flame straightened members were found in the literature (The shortening. . ., 1946). In this case three eye bars of A-7 steel were heat shortened and then fatigue cycled. When compared to similar specimens which had not been heated, the fatigue strength at both 500,000 and 1,000,000 cycles were similar. Although data is sparse, there is no indication that carbon steels will have a shortened fatigue life after heat straightening.

Shanafelt and Horn (1984) have recommended that fracture critical members (nonredundant tension members or components) not be repaired by heat straightening unless the member is fully strengthened by the addition of cover or splice material. No technical data was presented to back up this recommendation. The data presented here suggest that such restrictions are overly conservative with perhaps the only exception being the high strength quenched and tempered steels. The reductions in notch toughness are relatively modest otherwise.

Rockwell Hardness.-A few investigators have conducted Rockwell hardness tests on heat straightened specimens. Patee, et. al. (1969, 1970) indicated that the hardness test may be a better measure of material properties than tensile tests because the hardness test measures such a small area. Harrison (1952) also conducted hardness tests. Both of these researchers found that the hardness values did not change appreciably before and after heat straightening.

Mechanical Properties of Heat-Straightened Plates

Most testing for the basic mechanical properties of heat-straightened plates have been conducted on undamaged plates. These tests were typically conducted on undamaged plates which had been vee heated only 3 or 4 times. Researchers concluded from these tests that: (1) little change occurred in modulus of elasticity, (2) slight increases were found in yield and ultimate tensile stress, and (3) 10-25 percent reduction in ductility was observed. Of more significance are the properties of damaged plates (or rolled shapes) after experiencing the large number of heats required to fully straighten the member. To investigate this behavior, material properties tests were conducted on damaged plates in which a large number of heats had been applied.

Tensile tests were conducted on coupons taken from the residual stress strips described previously. Yield strength, tensile strength, percent elongation, percent reduction area; and modulus of elasticity were determined for plates P-9 through P-14. For each plate, coupons were taken from the heated area at the apex (strip 1 or 2), middle (strip 4 or 5), and open end (strip 7 or 8) of the vee. Also, a strip from an unheated region of the same plate (strip UH) was tested for comparison purposes.

Yield Stress and Tensile Strength.-The results of the coupon tests are shown in table 4.4. Some coupons exhibited significant increases in yield stresses over that of the unheated material (most notably at the top of the vee). The average increase for eight coupons at the vee apex was 17 percent. This value is nearly twice the increase

Table 4.4. Material properties of damaged plates.

Specimen/Strip	Yield Stress (MPa) (ksi)	Maximum Ten- sile strength (MPa) (ksi)	Percent* Elongation	Percent Red. In Area	Modulus of Elasticity (MPa x 10 ³) (ksi x 10 ³)
P-9 UH	323 46.8	474 68.7	45	58	199 28.9
	1 356 51.7	486 70.5	33	46	---- ----
	5 343 49.8	487 70.6	38	60	219 31.7
	7 345 50.0	485 70.3	39	60	222 32.2
P-10 UH	336 48.7	494 71.7	41	56	222 32.2
	2 361 52.3	491 71.2	30	62	209 30.3
	5 358 51.9	496 71.9	31	60	172 24.9
	7 356 51.7	481 69.7	34	64	125 18.2
P-11 UH	311 45.1	499 72.4	42	57	215 31.2
	1 382 55.4	507 73.6	30	60	219 31.7
	4 352 51.1	501 72.6	41	58	177 25.6
	8 333 48.3	491 71.2	36	57	158 22.9
P-12 UH	303 43.9	459 66.5	46	60	167 24.2
	2 359 52.0	472 68.4	34	63	154 22.3
	5 333 48.3	474 68.8	36	60	158 22.9
	7 324 47.0	476 69.0	36	60	117 17.0
P-13 UH	323 46.9	480 69.6	43	59	197 28.6
	2 345 50.0	487 70.7	32	57	250 36.3
	5 317 46.0	468 67.9	--	--	150 21.7
	7 301 43.7	466 67.6	35	65	126 18.3
P-14 UH	292 42.3	476 69.0	41	58	192 27.8
	2 414 60.1	521 75.6	28	51	301 43.6
	4 335 48.6	494 71.7	35	59	245 35.5
	8 351 50.9	487 70.7	34	56	199 28.9
Rates of strain=0.4545 in/in per minute up to yield					
=1.0714 in/in per minute up to failure					
*1-inch gage length					

found for the undamaged plates discussed in the previous section. It is obvious that the large number of repetitive heats provided a degree of heat treatment not reflected in a small number of heats on undamaged plates. The maximum tensile strength values were more consistent, having variations of less than 4 percent except for plate No. 14, which had a 10 percent increase. The net effect of heat straightening is to narrow the gap between yield stress and maximum tensile strength.

Modulus of Elasticity.-Based on limited data, it has been assumed that single vee heats on mild steel did not affect the modulus of elasticity. However, the results shown in table 4.4 indicate considerable variation in modulus of elasticity. Variations for a given plate ranged from 11-77 percent. The average values for plates P-9 and P-14 increased 11 percent and 30 percent, respectively. However, the average values for the other four plates decreased in the range of 13-31 percent. This evidence indicates that heat straightening tends to reduce the modulus of elasticity in the heated regions.

Ductility.-The percent elongation significantly decreased for all strips tested. This result is consistent with previous tests on undamaged vee heated plates. The elongation of the unheated strips ranged from 41-46 percent while the average for each of the heated plates ranged from 32-37 percent. Thus the elongation of heat-straightened plates tended to decrease by nearly one-third but all still met or exceeded material specification requirements.

An important observation is that the changes in material properties resulting from the damaging and straightening processes were very similar for each plate, in spite of

the differences in degree of damage, jacking ratio, vee depth and the number of heats applied. It appears that these parameters do not significantly affect material properties.

An independent sample t-test was conducted for each property in table 4.4 to attach a statistical significance to the effects of one damage/straightening cycle on these properties. This test is an excellent method to determine the confidence level for predicting changes from some process or event, even with a small number of samples. Table 4.5 shows the confidence levels of one damage/repair cycle causing an increase (or decrease) in the particular material properties of a steel plate specimen. A high level of confidence exists that yield strength will increase, and that percent elongation will decrease (at all positions within the heated region). However, the confidence level of increased tensile stress and decreased reduction of area are low since values under 95 to 97.5 percent are often rejected in hypothesis testing (Hicks 1982).

Considering only the high confidence levels for yield stress increase and ductility reduction, the respective percentages of these properties (for each specimen) in relation to those in the unheated specimens and the ASTM standards are listed in table 4.6. For yield stress, the ASTM standard minimum value is 248 MPa (36 ksi), and the standard for minimum percent elongation is 34 percent for a 50 mm (2 in) gauge length.

It should be noted that the highest values for yield stress (414 MPa or 60.1 ksi) was obtained in strip #2 of plate P-14. This was the only plate with a depth ratio of 0.75 for which tensile tests were conducted. Because this strip #2 is in a region that has undergone compressive deformation but has

Table 4.5. T-test confidence levels for material properties of heat-straightened plates.

Strip No.	Yield Stress*	Maximum Stress*	Percent Elongation**	Percent Red. In Area**
1 and 2	99.9	92.0	99.9	69.8
4 and 5	99.2	78.0	99.6	3.7
7 and 8	96.2	53.9	99.9	8.9

*Confidence level that heat straightening a deformed plate will cause an increase in the property shown over that of the same specimen before the damage/straightening cycle

**Confidence level that heat straightening a deformed plate will cause an decrease in the property shown over that of the same specimen before the damage/straightening cycle

Table 4.6. Comparison of material properties in heat straightened steel plates with unheated specimens and ASTM standard values.

Plate/Strip	Yield Stress		Percent Elongation	
	% of UH Specimen	% of ASTM Standard	% of UH Specimen	% of ASTM Standard
P-9 1	110	114	74	97
5	106	138	84	112
7	197	139	87	115
P-10 2	107	145	73	88
5	107	144	76	91
7	106	144	83	100
P-11 1	123	154	71	88
4	113	134	98	121
8	107	131	86	106
P-12 2	118	144	74	100
5	110	134	78	106
7	107	131	78	106
P-13 2	107	139	74	94
5	110	128	---	---
7	107	121	81	103
P-14 ¹ 2	142	167	68	82
4	115	135	85	103
8	120	141	83	100

¹ A three-quarter depth vee heat was used on this plate

not been directly heated, it is suspected to retain more strain hardening effects than if it were contained within the vee heated area (as other strip #2's are for full-depth vees). The minor restretching effect in the upper portions of this plate (addressed by Roeder, 1985) may have caused cyclic hardening not experienced if the material was heated. This specimen alone (among the plates) experienced a significant increase in tensile strength over the unheated specimen for that plate (10 percent). It should also be noted that similarly elevated yield and tensile strengths were experienced (near the vee apex) after the first damage cycle in the study of repetitively damaged wide flange beams, described in the next section where a depth ratio of 0.75 was also used.

Mechanical Properties of Heat-Straightened Wide Flange Beams

Tensile tests were conducted on strips taken from four W 6x9 beams damaged by bending about their minor axis (Category W). The residual stresses for these beams were discussed earlier and the results shown in fig. 4.24. In each case 45°, ¾ depth vees and a 50 percent jacking ratio were used. The standard Category W pattern of vee heats on both flanges and a strip heat on the web was employed. In addition to evaluating material properties, the purpose of these tests was to determine the effects of repetitive cycles of damage and repair. Consequently, Beam B-1 was damaged and repaired once, while Beams B-2 to B-4 were damaged and repaired twice, four times and eight times, respectively. In each case the degree of damage was in the range of 6-8° and required about 20 heat cycles to repair. After the last damage/repair cycle for each beam, one of the flanges was sectioned

and tensile tests conducted on strips near the apex, center and open end of the vee. The resulting properties are given in table 4.7 where UH indicates an unheated strip (see fig.4.14 for strip numbers).

Yield Stress.-A significant increase in yield stress and tensile strength occurred near the apex of the vee and it was progressively larger in proportion to the number of damage/repair cycles. A plot of the variation is given in fig.4.28. The yield stresses at other locations increased in the range of 9-21 percent and averaged a 13 percent increase (similar to the damaged plate results).

The data confirms that the apex of the vee is the most sensitive zone. Repetitive damage and repair cycles result in large increases in yield stress, especially after two or more cycles. Tensile strength followed a similar pattern as shown in table 4.7 and fig. 4.29. However, the tensile strength at the apex increased at only half the rate of the yield stress as shown in table 4.8. This narrowing of the normal gap between yield stress and tensile strength suggests that heat straightening should be limited to no more than 2 damage/repair cycles.

Modulus of Elasticity.-The modulus of elasticity averaged 8-23 percent lower for members with one or two damage/repair cycles. However an increase was observed for the beam with four cycles. In general, the level of variation was similar to that of damaged plates.

Ductility.-The elongation after one or two damage/repair cycles (31-32 percent) followed the trend of plates with about a one-third reduction. However, for four or eight cycles the elongation is proportionally reduced as shown in fig. 4.30 and table 4.8.

**Table 4.7. Mechanical properties of damaged and heat straightened W 6 x 9 Category W wide flange beams
(Vee angle=45°, jacking ratio=50 percent and depth ratio=75 percent)^{1,2}.**

Specimen/Strip	Yield Stress (MPa) (ksi)	Maximum Stress (MPa) (ksi)	Percent Elongation	Percent Red. In Area	Modulus of Elasticity (MPa x 10 ³) (ksi x 10 ³)
B-1 (UH)	313 45.4	465 67.4	43	63	223 32.3
1	398 57.7	507 73.6	30	62	234 33.9
5	372 53.9	506 73.4	36	64	166 24.1
7	340 49.4	484 70.2	29	64	218 31.6
B-2 (UH)	328 47.6	471 68.3	42	66	203 29.4
2	438 63.5	538 78.0	31	60	170 24.7
4	354 51.3	520 75.4	32	61	123 17.9
8	360 52.2	490 71.0	31	65	203 29.4
B-3 (UH)	311 45.1	469 68.0	43	65	185 26.9
2	489 70.9	569 82.5	22	59	232 33.7
4	390 56.6	519 75.3	26	57	199 28.8
8	363 52.7	523 75.9	27	42	267 38.7
B-4 (UH)	323 46.8	470 68.1	45	66	267 38.7
2	607 88.1	683 99.1	15	41	270 39.2
4	354 51.3	526 76.3	24	52	---- ----
8	343 49.8	493 71.5	23	61	---- ----
¹ Rates of strain=0.2206 in/in per minute up to yield =0.8824 in/in per minute up to failure					
² All values have been converted to represent an ASTM standard sized specimen (see ASTM A370 section 11.6.1) and a 1-inch gage length was used					

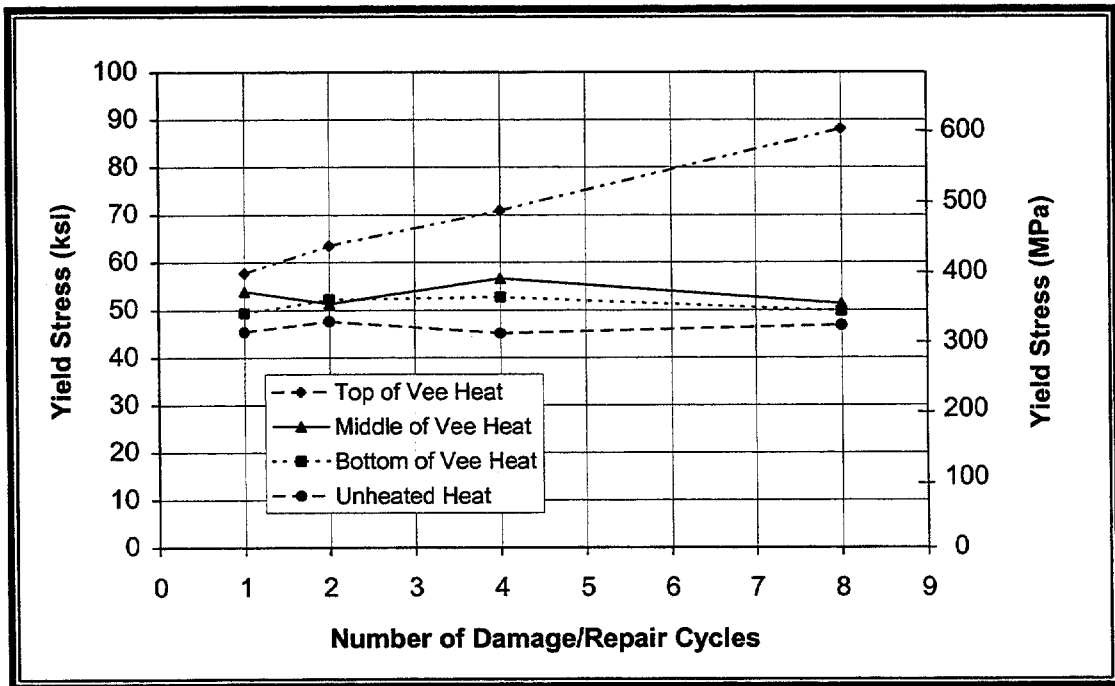


Figure 4.28. Yield stress versus number of damage/repair cycles.

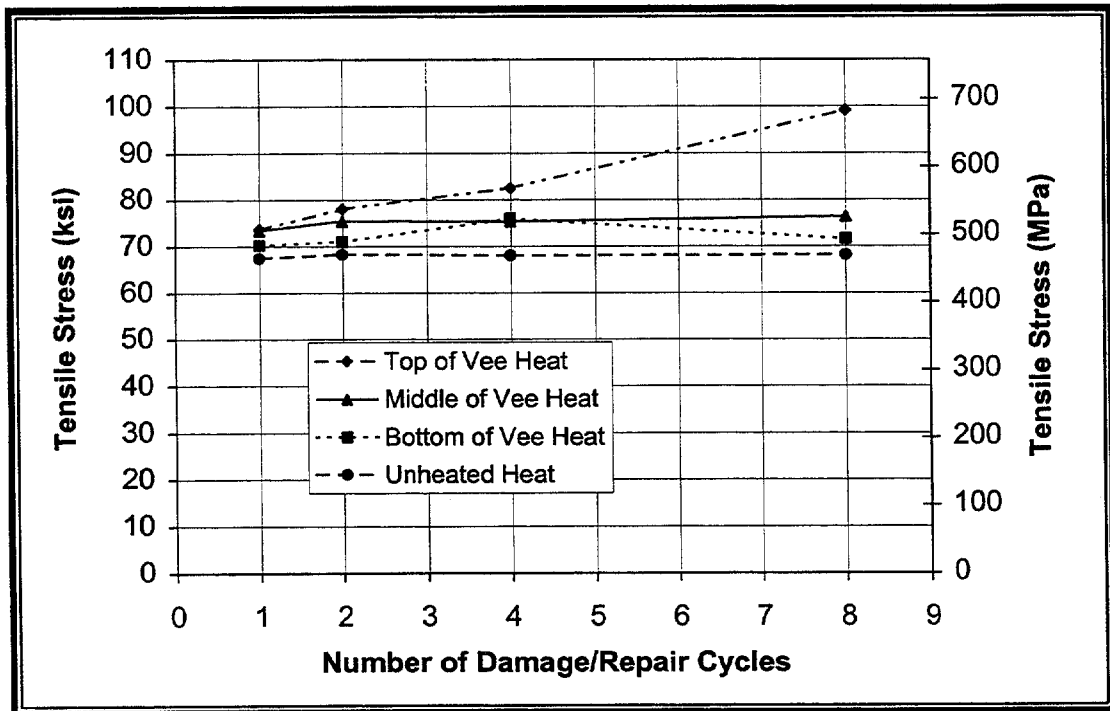


Figure 4.29. Tensile stress versus number of damage/repair cycles.

Table 4.8. Comparison of material properties in heat-straightened steel beams with unheated specimens and ASTM minimum standard values¹.

Beam/Strip	Yield Stress		Tensile Strength		% Elongation	
	% UH	% ASTM	% UH	% ASTM	% UH	% ASTM
B-1/2	127	160	109	110	69	88
B-1/4	119	150	109	110	85	106
B-1/8	109	137	104	105	69	85
B-2/2	133	176	114	116	74	91
B-2/4	108	143	110	113	79	94
B-2/8	110	145	104	106	74	91
B-3/2	155	197	121	123	51	65
B-3/4	124	157	111	112	62	76
B-3/8	115	146	112	113	64	79
B-4/2	188	244	146	148	33	44
B-4/4	110	143	112	114	54	71
B-4/8	106	138	105	107	51	68

¹Converted values for ASTM standard size specimens were used

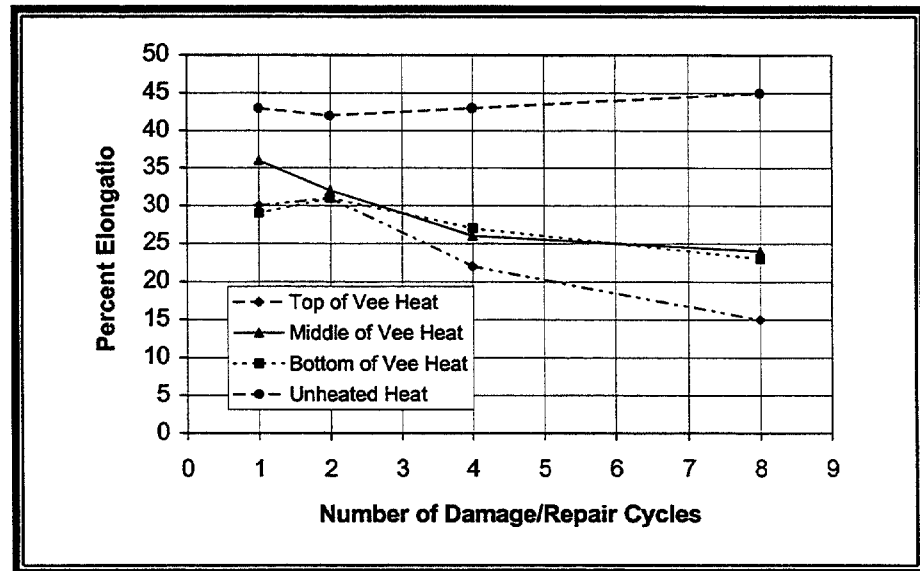


Figure 4.30. Percent elongation versus number of damage/repair cycles.

Table 4.9. Material properties taken from an improperly heat straightened girder of an Iowa bridge removed from service.

	FLANGE		WEB	
	Unheated Section	Heated Section	Unheated Section	Heated Section
Yield Strength (ksi)	37.4	59.0	45.3	57.4
Tensile Strength (ksi)	64.1	69.2	63.7	72.2
Ratio of Yield and Tensile	58%	85%	71%	80%
% Elongation 2" Gauge length	36%	26%	34%	22.5%
% Reduction in Area	62%	61%	60.4%	51.8%
Charpy V Notch @ 40°F.Ft.Lb.	19,22,16	6,7,9	16,11,10	*,4,6
Brinell (500 Kg) Hardness	119,114,107	139,143,143	119,114,109	150,158,143
Note: Chemical analysis percent by weight: Carbon-0.289; Manganese-0.647; Silicon-0.032; Sulfur-0.031; Phosphorus-0.009				

The data reinforces the conclusion of limiting the number of damage/repair cycles to no more than two.

Mechanical Properties from Heat Straightened Girders

Studies of mechanical properties for field straightened girders are rare. However, one such study was conducted by Putherickal, (1992). The Iowa Department of Transportation has allowed heat straightening of bridge girders for a number of years. One such girder (W 30 x 108) was removed from service several years after repair for reasons unrelated to the original heat straightening repair. Identical tests were conducted on a segment in the heat straightened zone and from an unheated segment.

A micro structure comparison between the heated and unheated specimens showed clear signs of recrystallization in the heat straightened area. The heated piece was partly austenitized and recrystallized into finer grains. This evidence indicates that the steel was heated above the lower critical temperature.

A summary of the mechanical properties measured is given in table 4.9. Both yield and tensile strength increased significantly but the increases were not proportional. Elongation decreased significantly and the Brinell hardness indicates that material became harder, indicating that the material was overheated. The Charpy V notch values in the unheated regions were poor. However, the values in the heated regions were even worse. All the data suggest that the material in the over-heated zone became more brittle. The need for careful control of material temperature during heating is reinforced by this field data.

This example illustrates that even though it is not advisable to overheat steel during heat straightening, it does not necessarily mean that the member should be scrapped if accidentally overheated. Rather, engineering judgement is required to determine the safety of the member based on data presented in this manual.

Member Shortening

The subject of member shortening due to heat straightening has been mentioned in the literature but little research has

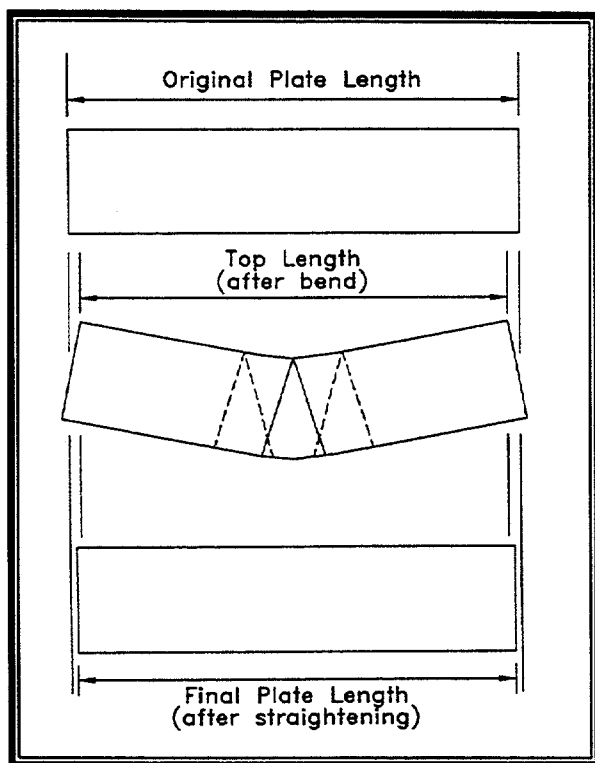


Figure 4.31. Shortening of a beam or plate after heat straightening.

been conducted. One researcher stated that using smaller vee depth ratios should result in less member shortening, given any particular damage situation (Moberg 1979). However, it could be argued that less shortening would occur when using full-depth vee heats, since the top fibers have been heated and are subjected to a tensile stress. In fact, the amount of shortening in a member can be quite significant, regardless of the vee depth used. Fig. 4.31 shows the basic concept of the shortening phenomenon. If the plate is damaged about its strong axis with a midpoint loading as shown, the top edge of the plate experiences compressive yielding (shortening) and the bottom edge of the plate experiences tensile yielding (stretching). As the plate is subjected to the heat straightening process, the top edge experiences some "restretching" in the longi-

tudinal direction (as evidenced by Roeder's strain distribution). However, these positive strains are small in comparison to the simultaneous shortening of the bottom edge of the plate. To quantify the amount of shortening experienced for a given amount of damage, measurements were made on some of the deformed plates. Cold bending will usually result in an increase in the centerline length of a member. To eliminate this factor, the initial lengths were measured before damage was induced and final measurements taken after heat straightening was completed. Regardless of initial and final lengths, all of the shortening occurs only within the damaged region (meaning shortening should not be expressed as a percentage of total length, but simply as a length itself).

A plot of shortening vs. degree of damage is shown in fig. 4.32 for 6 x 100 x 610 mm ($\frac{1}{4}$ x 4 x 24 in) plates bent about their strong axis. The shortening varies quite directly with degree of damage, up to a certain point (somewhere between 18 and 24 degrees), for the specimens studied. Shortening appears to be a function of plate width (since strain will vary with plate width for a given angle of damage). The shortening is also affected by the degree of damage itself, but does not vary with vee depth ratio, at least in the 0.75 to 1.00 range. The amount of shortening in the full depth vees of Plate P-14 was about the same as for deformed beams P-9 and P-11 in which the same amount of damage was experienced and $\frac{3}{4}$ -depth vees were used. All of the specimens with $\frac{3}{4}$ depth vees followed the same trend of shortening exhibited by those heated with full-depth vees. A formula for estimating shortening is:

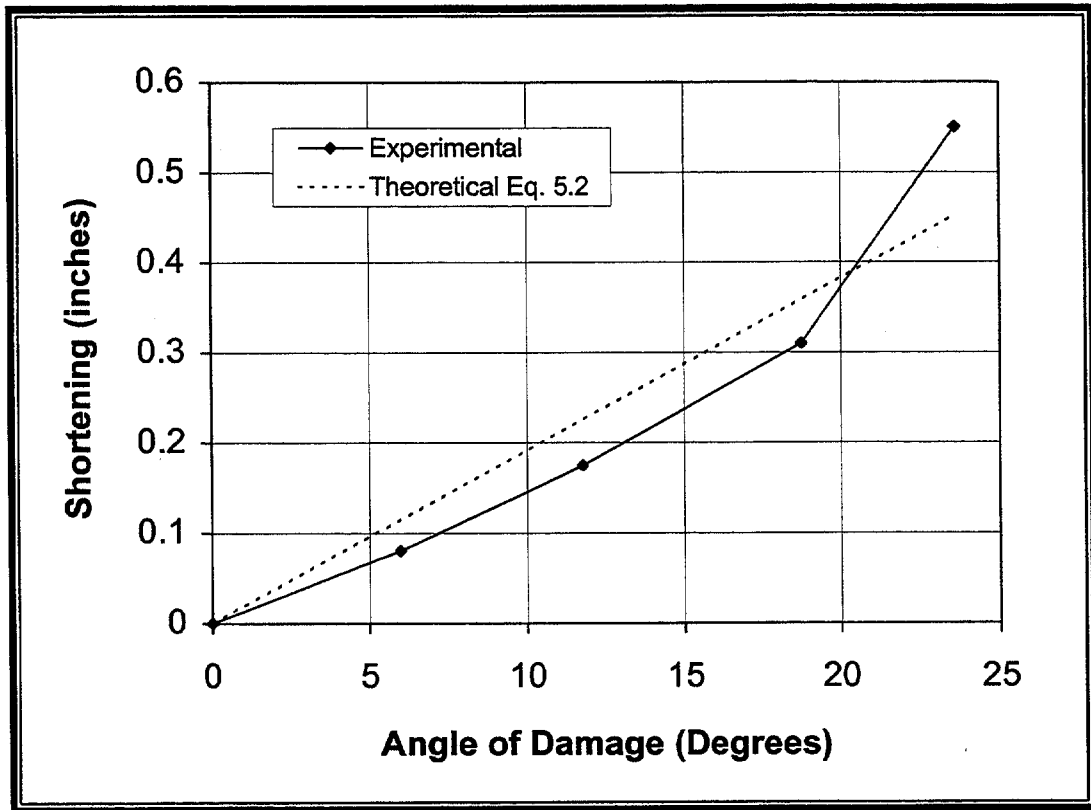


Figure 4.32. Shortening versus degree of damage for plate elements.

$$S = 0.005W\varphi_d \text{ for } 0 < \varphi_d < 24^\circ \quad (\text{Eq. 4.2})$$

where S = shortening in inches, φ_d = angle of damage in degrees, and W = plate width.

Four beams (W6x9's) were also investigated for shortening in the study. Each beam was damaged repeatedly about its weak axis to an angle of about seven degrees (approximately the same as the least damaged of the deformed plates). Each incident of damage was repaired using 45 degree vees with a depth ratio of 0.75 and a load ratio of 0.5. The number of damage/repair cycles varied for each of the beams but each repair cycle consisted of approximately 20 heat cycles. Each time a beam was damaged and straightened, a net shortening of about

2.5 mm (0.10 in) occurred in the heated region. These values agreed well with the plate shortening equation. It therefore appears that eq.4.2 can be applied to wide flange beams as well as plates.

Redistribution of Material

As a result of shortening, the heated portions of the deformed plate elements thickened (or upset) upon straightening. This fact becomes especially important in influencing future damage (if any) of the plate element. After the residual stress strips were cut from each plate element, thicknesses were measured at various locations along each strip. Thicknesses at five points on each of the eight strips were measured to 0.025 mm (0.001 in) accuracy.

Thickening was greatest for the plates damaged to the largest degrees. For example, in Plate P-10, which was the specimen with the greatest amount of damage (23.62°), the thicknesses (measured for each strip) along the center of damage averaged 16.6 mm (0.655 in). When compared to the average thickness of the plate before damage (12.3 mm or 0.485 in), the thickening resulted in a 32 percent increase in cross-sectional area. At points further away from the center of damage, thickening is less pronounced, but nevertheless, some thickening occurs within the entire yield zone. While a thicker cross-section results in a stronger member at that location, little structural significance should be placed on the thickening experienced.

For the damaged wide flange beams, thickening also occurred in the heated region. After straightening the first time, the thickening caused a spreading of the yield zone in each subsequent re-damage. The thickening resulted in a smoother distribution of curvature (due to thinner portions further from the centerline tending to yield first), although the total angle of damage was kept as consistent as possible for each bend. Due to the larger yield zone, the heat locations were spread over a greater length. The number of heats required to straighten each bend remained fairly consistent, just more widely distributed.

Impact of Heat Straightening on Mechanical Properties of Steel

Clearly, research data indicates that heat straightening does affect mechanical properties of steel. Early researchers used undamaged steel and a small number of heats to conclude that property changes were minimal. However, tests on damaged and

heat-straightened plates and beams indicate that some property changes may be of significance. Yield stress may increase by as much as 20 percent in some cases, especially in the vicinity of the apex of vee heats. Tensile strength also increases but at only one-half the rate of yield stress. The ductility as measured by percent elongation may decrease by one-third and the modulus of elasticity may decrease by over 25 percent in some heated regions.

The importance of increased yield stress and tensile strength and decreased ductility in the specimens lies in the areas of stress concentrations and fatigue. Stress concentrations often occur around discontinuities in structural members such as holes, fillets, welded stiffeners, and notches (Barsom and Rolfe, 1987). Structural designers rely on the ductility of the material to redistribute the load around a mild stress concentration, such as a drilled hole, within specification-imposed limits for fatigue. However, a decrease in ductility may reduce inelastic stress redistribution, thus the higher stresses remain concentrated.

Fatigue life is the total number of cycles (load fluctuations) required at a certain stress level to cause the initiation and propagation of cracks to a critical size. The "fatigue limit" is the maximum stress at which an infinite number of cycles can theoretically be applied without initiating and propagating a crack. Cycles of stress above the "fatigue limit" lead to a lower fatigue life for any given material and configuration and the presence of notches, holes, welds, and other stress concentrations lowers the fatigue limit.

Studies have shown that the fatigue-crack initiation threshold in various steels is

related to the yield strength as well as tensile strength (Barsom and Rolfe 1987). This threshold basically establishes a maximum stress for a given configuration geometry at which an infinite number of cycles can be applied without crack initiation. Equations basing the threshold on both tensile strength and yield stress have been formulated and agree well with each other for most structural steels (where the ratios of tensile strength to yield stress are fairly consistent). However, the tensile strength to yield stress ratio may be altered in heat-straightened members. In general, the fatigue-crack initiation threshold increases with tensile as well as yield strength, but tensile strength increases in the heat straightened plates were relatively small, when compared to ductility losses. Thus, improvement of the fatigue-crack initiation threshold, based solely on tensile strength, could possibly be more than offset by increased stress due to the reduced stress redistribution permitted by the ductility loss. Some reduction in the fatigue limit might occur as a result.

Like ductility, fracture toughness (a value proportional to the energy consumed during plastic deformation) may decrease as a material's yield strength changes during heat straightening. The ability of a particular flaw or stress riser to cause crack initiation or even catastrophic damage depends on the fracture toughness of the material. Because the subject of stress concentrations and brittle fracture depends of specific conditions, it is difficult to make recommendations without detailed analyses of the particular situations. In general, heat-straightening areas that will sustain high stress concentrations in service should be avoided when possible and only done after a sufficient analysis by a qualified engineer.

However, since varying degrees of damage seem to have similar material properties after heat straightening, degree of damage alone should not be the deciding factor on whether or not a member should be straightened. Therefore, the suggestion to use damage strain as made by Shanafelt and Horn (1984) to limit heat straightening in high fatigue areas (where strain hardening was the basis) are considered only as precautionary limits with little scientific rationale. Further study should be conducted to determine if heat straightening should be allowed for any degree of damage in areas with fatigue-sensitive details or very high cycles of fatigue loadings.

Since the effects of heat straightening on material properties do not relate to the degree of damage of plates and beams (at least past the initial strain hardening point), Shanafelt and Horn's suggested limit of five percent nominal strain in tension members (41.67 times yield strain, if assumed yield strain is 0.0012) has no basis. Recall that this constitutes a fairly small angle of damage in a plate element bent about its weak axis, especially with a large plate width. Research has shown that a strain of at least 100 times yield strain (ϵ_y) can be heat straightened with little difference in material properties from that of repairs with much smaller strains. Thus, except for severe fatigue sensitive areas, material properties should not be the primary determining factor when contemplating the use of heat straightening.

The data presented here provides guidance as to how many times a girder can be damaged and heat straightened in the same zone. Changes in all the material properties become more evident with the

increasing number of damage/repair cycles. These changes are particularly significant at the region associated with the apex of the vee. After two damage/repair cycles, the property changes are still relatively modest. But after four damage cycles, the increase in yield and tensile strength, and the loss in ductility were sharper. Since the variation in yield is larger, the gap between yield and tensile strength decreases as the damage/repair cycles increase. As shown in table 4.7 the ratio of yield-to-tensile strength is around 68 percent for unheated specimens. That ratio increases to 78 percent after one damage/repair cycle and to 88 percent after 8 cycles. This behavior combined with the ductility decreasing with each damage/repair cycle, results in an increasingly brittle material. This data illustrates why over-jacking during repairs may fracture the beam after a number of damage/repair cycles in the same zone.

As mentioned previously, the point at which loss in ductility becomes dangerous is case-specific. However, the extreme losses encountered in the repetitively damaged beams show that there is probably a limit to the number of times that any given member should be repaired. Material property changes were usually small after two cycles. Thus, whatever is safe to straighten once could usually be safely straightened twice under the same conditions. The changes become significantly greater after 4 and 8 damage/repair cycles, respectively. These findings are further substantiated by the fact that during one study of full-scale simulated bridge girders, one girder exhibited brittle behavior by cracking during a heat in its third damage/repair cycle. Based on this research evidence, redamaged members at the same location should not be sub-

jected to heat straightening more than twice, even for strains well under $100 \epsilon_y$.

Key Points to Remember

- At elevated temperatures the yield stress, tensile stress, and modulus of elasticity of steel is significantly reduced.
- The coefficient of thermal expansion increases with temperature.
- These property changes are reversible upon cooling if the heating temperature does not exceed the lower critical temperature of approximately 721°C (1330°F) for non-quenched and tempered steels
- Long-term effects of properly conducted heat straightening carbon steels may include:
 - ◆ Up to a one-third decrease in ductility.
 - ◆ Small changes in notch toughness characteristics.
 - ◆ Little change in fatigue limits.
 - ◆ Little change in hardness values.
 - ◆ A modest increase in yield and tensile strength.
 - ◆ A small decrease in modulus of elasticity.
- Residual stresses are large in heat straightened members with maximum values reaching yield at some locations. This characteristic is similar to that of welded built-up members.
- The high residual stresses in some heat straightened members may work against jacking forces and should be taken into account.

-
- Changes in material properties after heat straightening are unrelated to degree of damage (at least up to $100 \epsilon_y$).
 - The most sensitive area for material property changes is the region of the vee heat apex.
 - Repetitive damaging and repairing steel elements tends to increase brittleness and reduce ductility.
 - Heat straightening should be limited to a maximum of two repairs on the same heated region.
 - Records of heated zones should be kept for future reference in case the member is redamaged.
 - Member shortening will occur and should be anticipated. Full and three-quarter depth vee heats produce similar levels of member shortening.
 - The heated zone will thicken as a result of heat straightening.

Chapter 5. Heat Straightening of Flat Plates

Introduction

The fundamental element of any structural steel shape is the flat plate. Damage to bridge structures consists of these plate elements, in combination, bent about their strong and/or weak axes. The purpose of this chapter is to describe experimental and analytical research on heat straightening as applied to plates and to present related engineering design criteria for its use. This work forms the basis for extensions to heat straightening of rolled shapes.

Several detailed studies have been conducted for vee heats applied to plates. These studies have attempted to identify parameters which influence vee heats and to develop predictive models based on this data. Weerth (1971) and Nicholls and Weerth (1972) describe the bends produced by 211 vee heats whose apex angle varied from 24° to 60° in 6° increments applied to 10 mm (3/8 in) thick A36 steel plate. The vee depth was also varied over full depth, 3/4 depth, and 1/2 depth. No attempt was made to evaluate the effect of these parameters other than the general result that the greater the vee angle and depth, the greater the bend produced. Roeder (1986) also conducted a study on undamaged vee heated plates. He employed sophisticated monitoring equipment such as thermocouples, contact pyrometers, and strain gauges as well as more conventional tools such as a vernier caliper and a steel ruler. His work is particularly significant as the first attempt to both experimentally and analytically quantify heat straightening behavior for plates

over a wide range of parameters. The parameters included vee geometry, specimen geometry, heating temperature and rate, steel grade, restraining force, initial residual stresses, and quenching. Roeder's conclusions were based on approximately 60 heats over a wide range of parameters. As a result there were relatively few repetitive heats using identical parameters. While trends could be drawn from this data, its sparseness limited the quantitative value of the results. However, his research provided the initial basis for much of the later experimental work reported in this chapter. Roeder's most significant conclusions were:

- 650°C (1,200°F) is a practical and safe upper heating temperature limit.
- Changes in material properties are small when the heating temperature remains below the phase transition temperature of approximately 720°C (1330°F).
- The rotation produced by a vee heat is directly proportional to vee angle and heating temperature.
- The rotation produced by a vee heat is directly proportional to restraining forces which produce compression in the open end of the vee during heating.
- Quenching is effective and may increase vee heat rotations, but heating temperatures should be kept below the phase transition temperature (although some practitioners recommend quenching only if the steel temperature is below 700°F or 370°C).

- Plastic strain occurs primarily within the vee heat region.
- Plastic strain is somewhat sensitive to geometry of the plate. However, much of this sensitivity can be attributed to differences in rate of heating and heat flow.

The research described in this chapter (Avent, et. al. 1993) extends Roeder's work and includes enough repetitive data points to quantify these and other conclusions.

The actual method of heat straightening is easily learned; however, the handful of practitioners currently using the method rely extensively on their many years of experience to guide them through a repair. An engineer lacking this wealth of experience needs a set of analytical procedures to determine how best to apply the heat-straightening process to a particular repair. These analytical tools, for reasons of economy, should be relatively fast, easy to apply and allow for such considerations as different vee geometries, temperature ranges, external loadings, and support restraints. At present, two extremes exist: (1) overly simplistic models (Holt, 1965, 1971; Moberg, 1979) which cannot take into account the effect of either temperature variations or internal and external restraint; and (2) comprehensive computer models (Burbank, 1968; For Chin 1962; Horton, 1973; Roeder, 1985, 1986, 1987; Weerth, 1971) based on elastic-plastic finite element or finite strip stress analysis combined with a similar thermal analysis. While the former is too simplistic to accurately predict behavior, the latter requires such lengthy computational effort to not be practical for design office use. As a result, there is a need for an analytical model that offers both practicality

and comprehensive inclusion of all important variables to accurately predict behavior.

Of interest here are the currently available simplistic models. Referring to fig. 5.1, Holt (1965) developed one of the first and simplest methods for predicting plastic rotations, ϕ_p , in a vee heated plate. His model was derived from the geometry of the vee heat as shown in fig. 5.1. Recognizing that heat straightening merely reshapes the volume of material being heated, Holt assumed that the deformation through the vee was linear over the depth of the plate and that perfect single axis confinement existed longitudinally during heating. His resulting formula in terms of the plastic rotation, ϕ_p , was

$$\phi_p = \frac{S_p V}{W} \quad (\text{Eq. 5.1})$$

where S_p = the plastic strain resulting at temperature T for the single axis perfect confinement case (Holt used 1200° F or 650°C), V = the width of the open end of the vee heat and W = the plate width. Moberg (1979) modified the Holt equation to account for the depth of vee by considering the experimental work of Weerth (1971). In addition to Holt's assumptions, he assumed that the plastic rotation is proportional to the depth ratio d_v/W where d_v = the depth of the vee heat. The resulting equation was

$$\phi_p = \frac{S_p V d_v}{W^2} \quad (\text{Eq. 5.2})$$

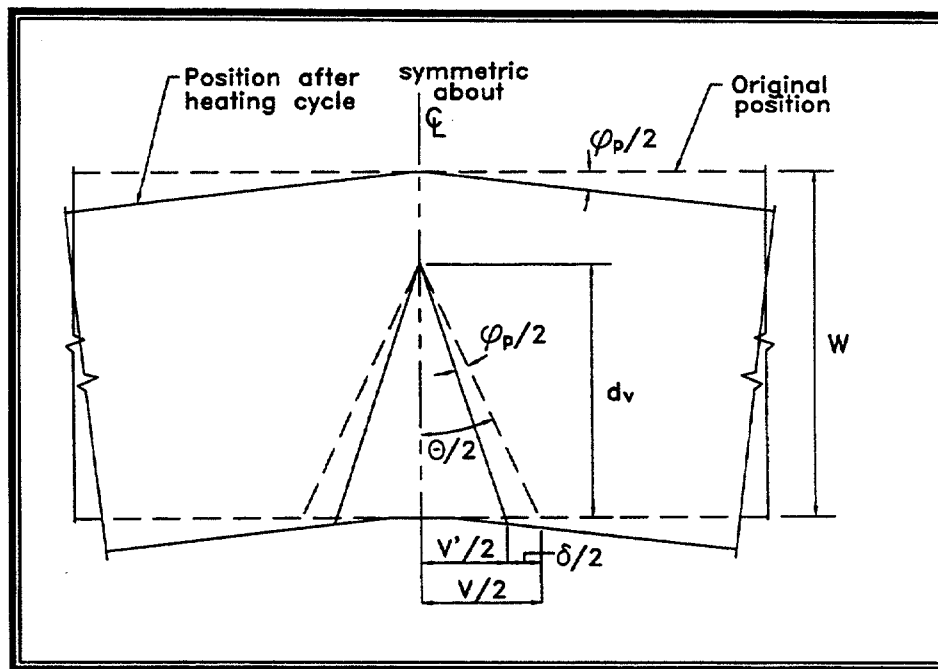


Figure 5.1. Illustration of vee heat geometry.

An important consideration not included in these formulations is the influence of external and internal restraining forces. The external forces, producing compression in the vee during heating, will increase the available confinement and therefore, increase the rotation produced per heat. The field applications cited by both Holt and Moberg involved the use of restraining forces. Since in most cases the material restraint alone will be less than perfect, it seems likely that any correlation between the predicted and actual movement in the structures being repaired, as noted by both Holt and Moberg, is primarily due to the influence of the external forces. An improved analytical model should include the effects of both internal and external restraints.

The research reported here (Avent, 1987, Avent, et. al., 1993) was part of a

project to experimentally and analytically develop engineering design criteria for heat-straightening repair of damaged steel structures. The portion of that study discussed here was devoted to the quantification of parameters and the development of simple yet efficient procedures for predicting the response of deformed steel plates during the heat-straightening process. The approach chosen was to first identify all parameters which have an important influence on the heat-straightening process. This phase was accomplished by studying the experimental data available from previous research as well as by conducting an extensive experimental program to provide additional data. After synthesizing this experimental data, an analytical procedure for predicting member response was developed. Since rolled and built-up sections are an assemblage of plates, this research is fundamental to the

understanding of more complex shapes. Vee shaped heats are used to repair plate elements with bends about their strong axis while line and spot heats are used to remove weak axis plate bends. Since damage usually includes strong axis plate bends, the vee heat can be considered the fundamental heating pattern for heat straightening. Only the behavior of vee heats on plates is considered in this chapter, but this material provides a basis for its extension to rolled shapes.

Experimental Program

The tests conducted in the experimental program consisted of first applying vee heats to straight (undamaged) specimens and measuring the resulting change in geometry. By using straight specimens as opposed to deformed ones, a larger variety and number of tests could be conducted more efficiently. A total 255 individual heating cycles were performed during this part of the study with three or four heat cycles per plate. While this data will be presented graphically here, specific results of all tests can be found in a research report (Avent, 1987).

The second phase of the study consisted of straightening mechanically induced strong axis bends. A center point loading on the simply supported plates was used to create various degrees of damage. The degree of damage was measured as the angle of the tangents formed by the edges of the unyielded portions of each plate on either side of the yield zone. The degree of damage ranged from 6 to 25 degrees resulting in extreme fiber strains ranging from 30 to 100 times the initial yield strain. Between 20 and 100 vee heats were applied to straighten the ten plates with differing degrees of dam-

age. A total of 336 individual vee heat cycles were applied. Detailed results of tests for each heat cycle are given by Avent, et al. (1992).

All plates were hot rolled A36 steel, and the majority of them had dimensions of 6 x 6 x 610 mm (1/4 x 4 x 24 in). The only exceptions to these dimensions were associated with tests on variations in plate thickness and geometry. Plate deformation measurements consisted of measuring the offsets between the plate edge and a reference frame.

As shown by Roeder (1986), the plastic deformation developed by a vee heat occurs primarily within the vee area. Thus, a very sharp but small curvature is obtained, which can be expressed in terms of plastic rotation, ϕ_p , as shown in fig. 5.1. For initially straight specimens, the portion of the plate from the ends to just outside the vee heat remains straight. This fact was used to compute the plastic rotation based on the straight line tangents. To reduce the influence of possible errors in the measured deflection, a straight line was first fitted through the four points on either side of the vee heat within the straight portion outside the yield zone using the least squares method. The change in the acute angle formed between these two lines is the angle of plastic rotation, ϕ_p .

Evaluation of Results of Experimental Program

The available data on plate behavior can be found in three studies: Nicholls and Weerth (1972), Roeder (1985), and Avent (1987, 1992). Indicated on plots presented here is the type or source of the data. Lack of a reference indicates that only the results

from Avent's research are used, while reference numbers are given for other data. An evaluation of each parameter is considered separately in the following sections.

Vee angle.- Researchers agree that one of the most fundamental parameters influencing the plastic rotation of a plate is the vee angle. The data shows a fairly linear relationship between plastic rotation and vee angle. For this reason, most data will be plotted with the vee angle as the ordinate and plastic rotation, ϕ_p , as the abscissa. A first order least squares curve fit will sometimes be shown. Plots in succeeding sections show a consistent proportional relationship between these variables.

Of particular interest is the scatter of the experimental results. In both Avent's results involving nearly 600 plate tests and in Roeder's research (1985) involving 59 plate tests, a similar level of scatter was observed. In both cases, special efforts were made to control the heating temperature using not only temperature sensing crayons, but also thermocouples or calibrated contact pyrometers. In spite of such efforts, a significant amount of variation occurred in nearly identical repetitive tests. Surprisingly, the smaller scale study by Nicholls and Weerth (1972) which included 21 tests showed no evidence of random scatter. The consistency of data points was such that smooth curves were produced with no curve fitting necessary. This pattern is even more remarkable when apparently the only temperature control was temperature sensing crayons. These data points are therefore viewed with some suspicion and omitted from most of the comparative studies herein.

Since a significant level of scatter does exist, an evaluation was conducted of data samples. The coefficients of variation for typical cases were on the order of 50 percent. Since the coefficient of variation is quite high, possible causes must be addressed. The most obvious source of the scatter would be the relative degree of control exerted over the parameters of the heating process, in particular, the restraining force and heating temperature. For the available equipment of this research, the accuracy of measurements could vary by 10-15 percent. Similarly, the control of the heating temperature could introduce an error of 10-15 percent. A third possible cause is the development of residual stresses. Both Holt (1971) and Roeder (1985) suggest that residual stress are not significant in the heat-straightening process. However, the results from Chapter 4 indicate that large residual stresses are possible as a result of the heating process. Thus, due to the difficulty in controlling the restraining forces and heating temperatures and the possible development of large residual stresses, a relatively large scatter in the data is not surprising.

Depth of Vee.- Past researchers (Nicholls and Weerth, 1972; Roeder, 1985) have concluded that the plastic rotation is proportional to the depth ratio, R_d , which is the ratio of vee depth, d_v , to plate width, W . A review of Roeder's test data in the range of 650°C ($\pm 80^\circ$) or 1200°F ($\pm 150^\circ$) or is inconclusive as to vee depth effect. Recognizing that the data was sparse, neither the depth ratio of 0.75 nor 0.67 produced plastic rotations that were consistently hierarchical. To further evaluate this behavior, a series of tests was conducted for depth ratios of 0.5, 0.75, and 1.0 and vee angles ranging from 20° to 60°. At least three heats were con-

ducted on initially straight plates for each case and the results averaged. The results are shown in fig. 5.2 for a combination of three depth ratios, three vee angles and two jacking ratios. The jacking ratios reflect that a jacking force was used to create a moment at the vee heat equal to either 25 percent or 50 percent of the ultimate bending capacity of the plate. As can be seen from fig. 5.2, the depth ratios of 75 percent and 100 percent track each other well. In fact the 75 percent depth ratio resulted in slightly larger plastic rotations in all but one of the six cases. The 50 percent depth ratio resulted in an erratic behavior when compared to the other two. In three of the six cases the 50 percent depth ratio produced much smaller plastic rotations. In the other three cases, the plastic rotations were similar.

To further verify this behavior, a series of plates was damaged and straightened. The degree of damage was large enough that at least 20 heats were required for most of these plates. Therefore, more statistically significant average plastic rotations were obtained from these tests. Results are compared in fig. 5.3 for a jacking ratio of 0.5 and two vee depth ratios: 0.75 and 1.0. Again the pattern of plastic rotations does not have a direct correlation to the vee depth ratios.

Therefore, even though it would seem intuitive that increasing the vee depth would increase the plastic rotation, there is no experimental justification for such a general statement. It can be concluded that the variation of vee depth ratios between 0.75 and 1.0 has little influence on plastic rotation. However, a vee depth ratio of 50 percent may reduce the plastic rotations.

Plate Thickness and Geometry.-

Researchers have generally considered plate thickness to have a negligible affect on plastic rotation. The only reservation expressed has been that the plate should be thin enough to allow a relatively uniform penetration of the heat through the thickness. The practical limiting value is on the order of 19-25 mm (3/4 to 1 in). Thicker plates can be heated on both sides simultaneously to ensure a uniform distribution through the thickness or a rosebud tip can be used. The results from tests involving different plate thicknesses are shown in fig. 5.4. Each bar represents the average of at least three heats. No jacking forces were used in these tests.

The results illustrate the level of variability that may occur among groups of heats. However, there is no discernable pattern among the plate thicknesses for the three different vee angles used. The randomness of these results indicates that plastic rotation is not a function of plate thickness. A similar plot is shown for data from Roeder's tests (Roeder, 1985) in fig. 5.5. In these tests only one vee angle was used ($\theta = 60^\circ$) along with several different jacking forces for plate thicknesses of 6, 10, and 19 mm (0.25, 0.375 and 0.75 in). Again, there is no discernable pattern among the plate thicknesses.

Roeder also investigated the effect of plate width on plastic rotations. Shown in fig. 5.6 is a comparison of the two plate widths of 150 and 200 mm (5.9 and 7.9 in). Only one or two heats were used in each case and several plate thicknesses were used. Relatively little difference in plastic rotations was observed for these two widths.

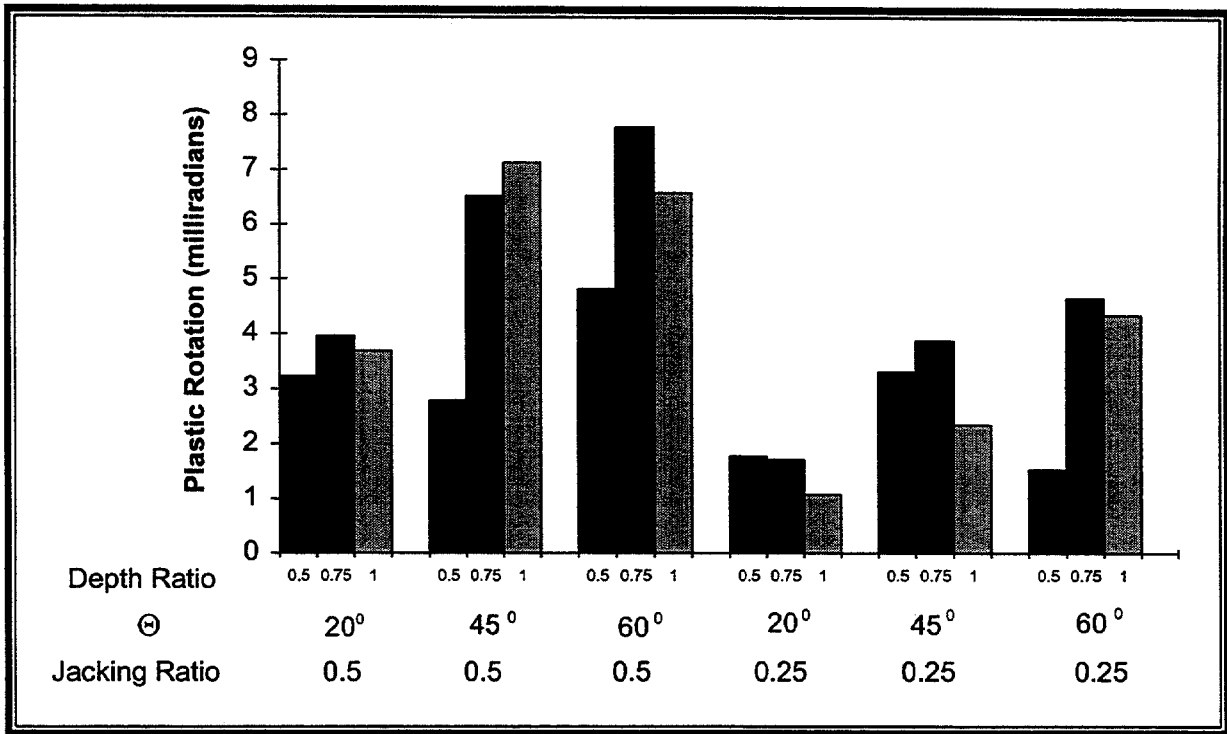


Figure 5.2. Influence of vee depth on plastic rotations of originally straight plates for various vee angles and jacking ratios (heating temperature = 650°C or 1200°F).

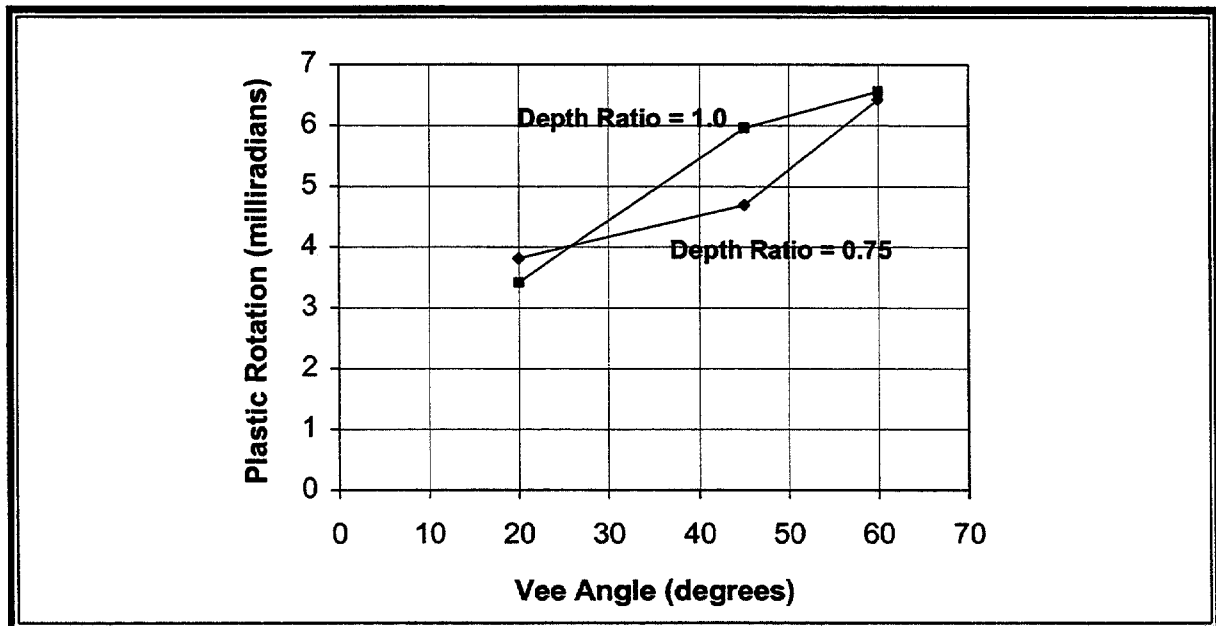


Figure 5.3. Vee angle versus average plastic rotation for damaged plates having different depth ratios (Jacking ratio = 0.5 and Temperature = 650°C or 1200°F).

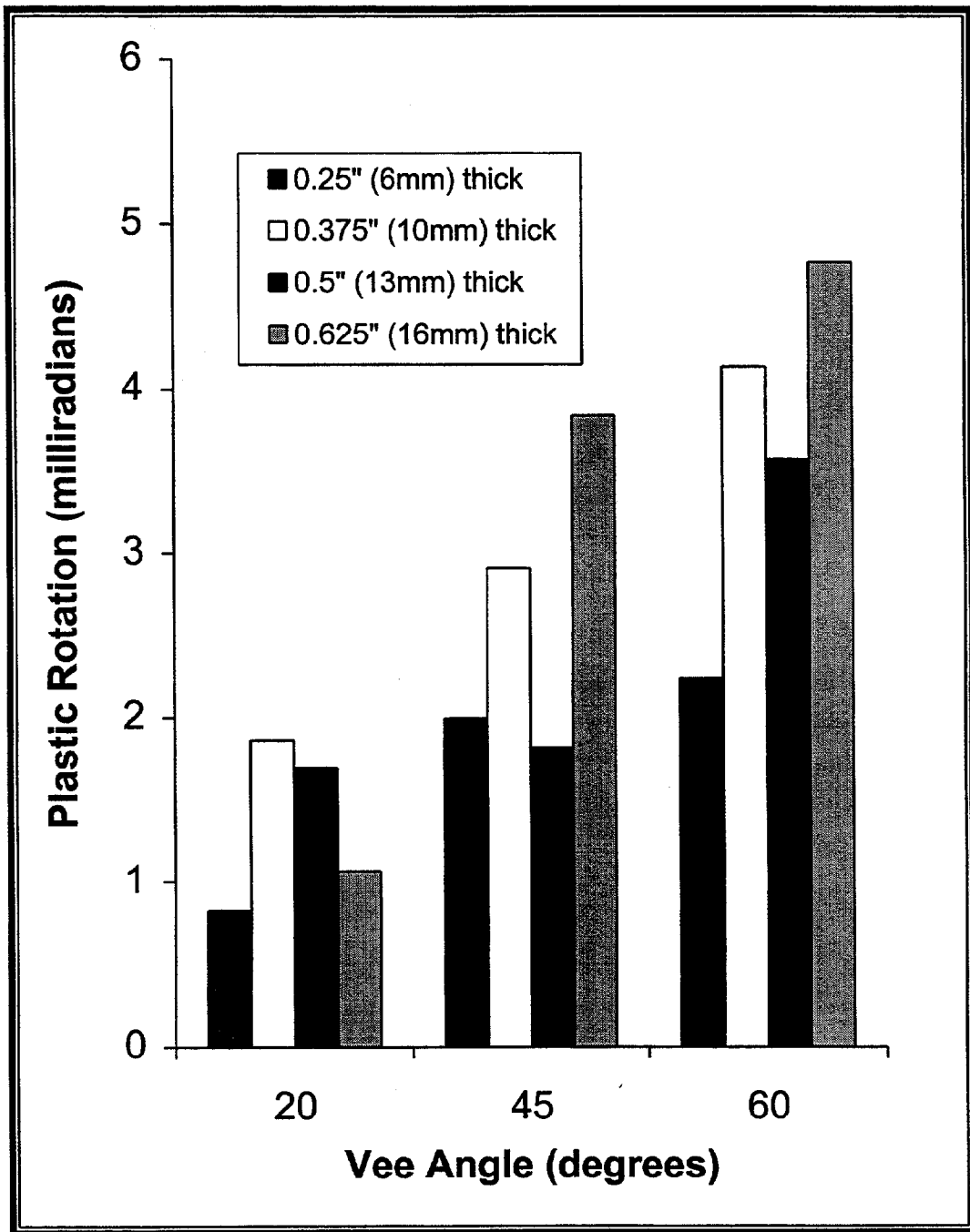


Figure 5.4. Influence of plate thickness on plastic rotation (average of 3 heats with depth ratio = 1, jacking ratio = 0, temperature = 650°C or 1200°F).

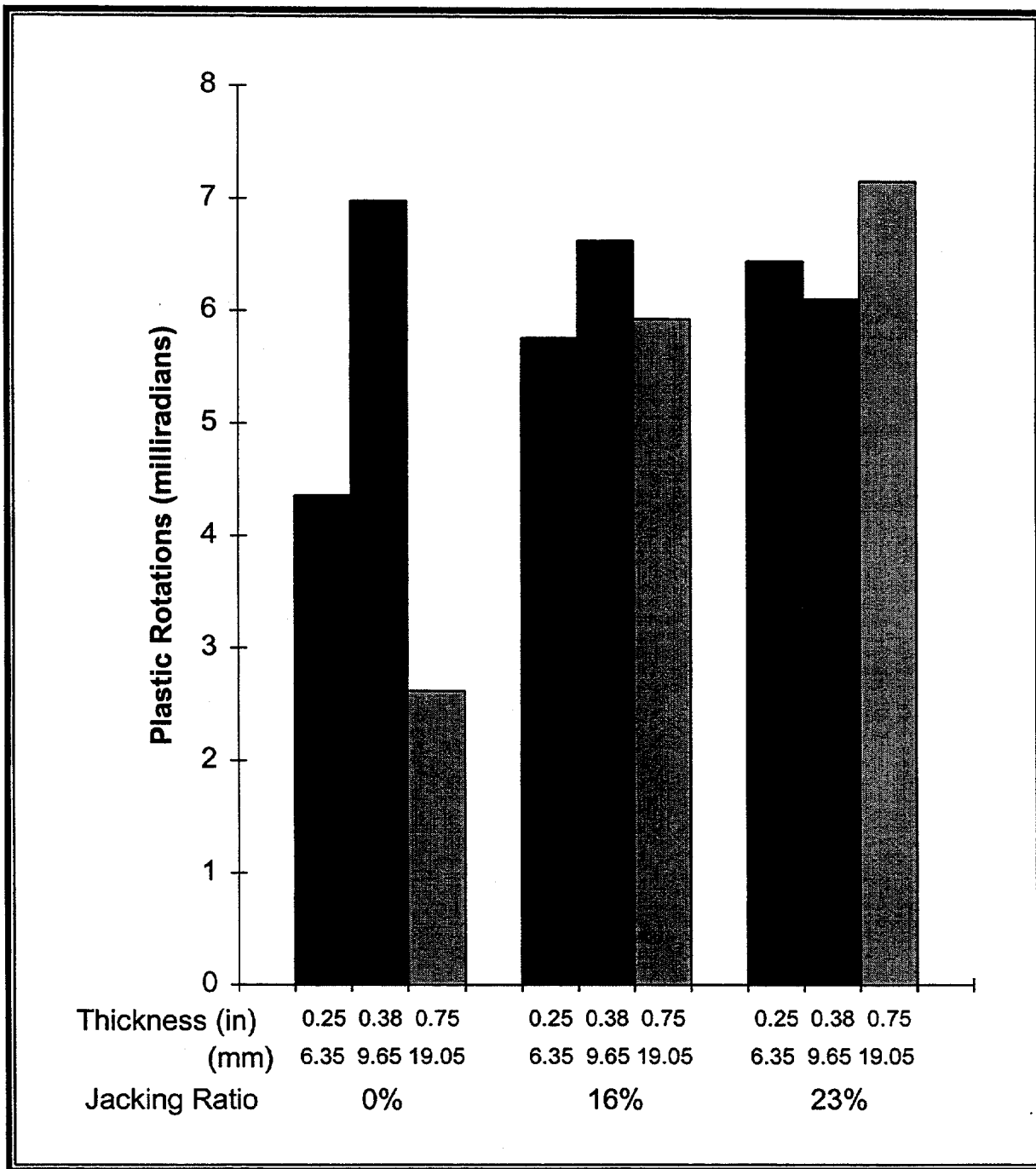


Figure 5.5. Influence of plate thickness on plastic rotations, Roeder, 1985 (single heats with $\theta = 60^\circ$, depth ratio = 0.67, heating temperature = 552-682°C or 1025-1260°F).

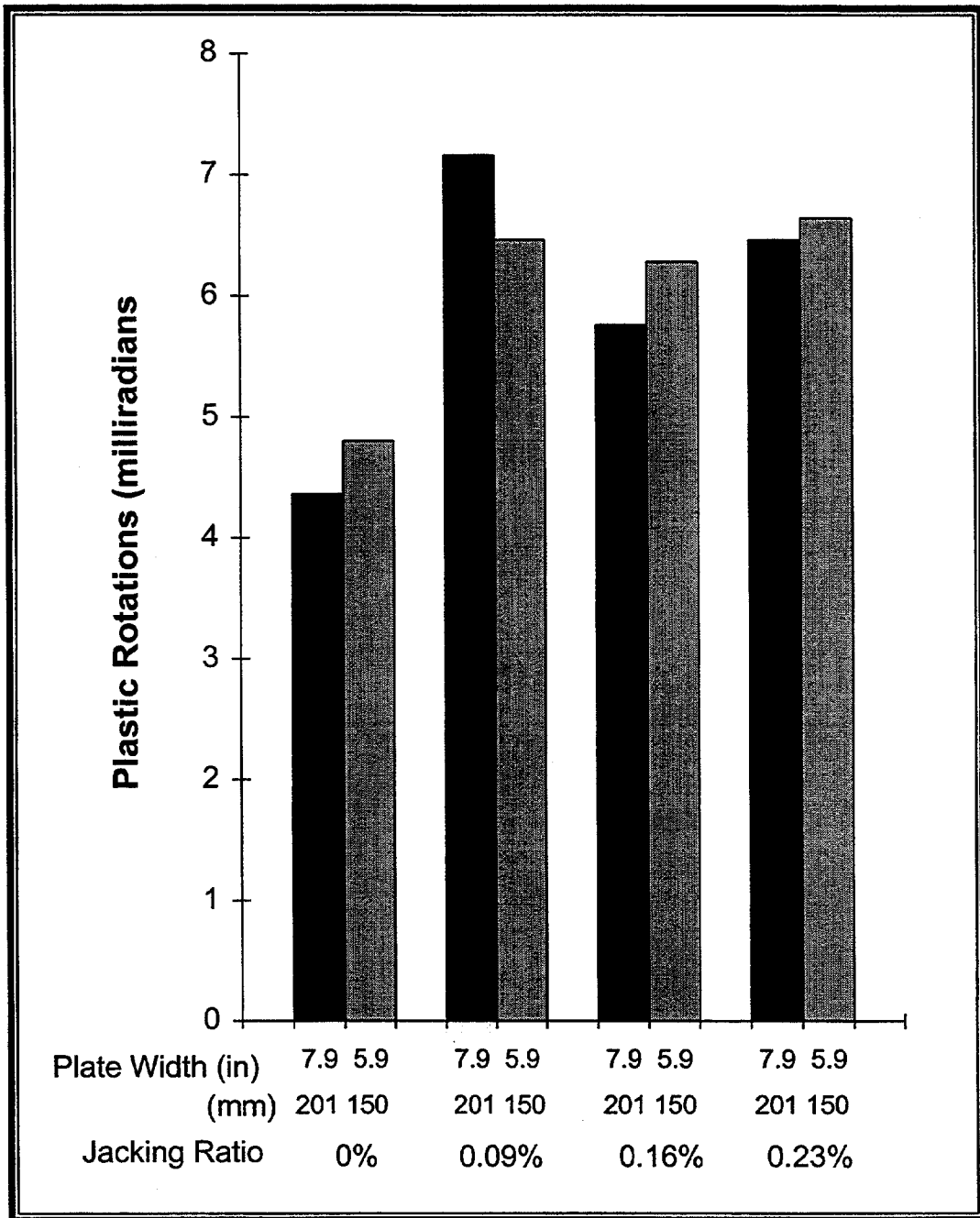


Figure 5.6. Comparison of plastic rotations for 150 mm (5.9 in) (average of 2 heats) and 200 mm (7.9 in) (single heat) plate widths, Roeder, 1985 ($\theta = 60^\circ$, depth ratio = 0.67, and heating temperature was approximately 650°C or 1200°F).

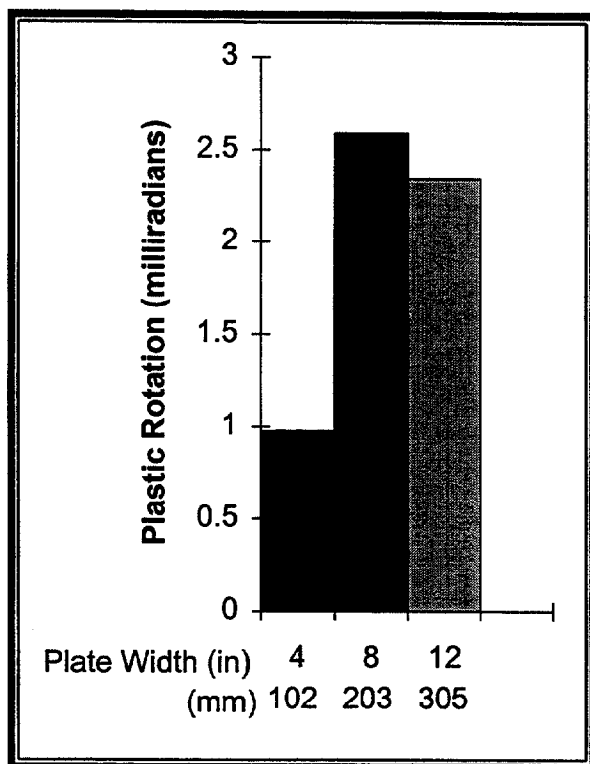


Figure 5.7 Comparison of average plastic rotation (for three 20° vee heats) for plates of three widths (jacking ratio = 0, depth ratio = 0.75, and heating temperature = 650°C or 1200°F).

In another test series conducted by Boudreaux (1987), three plate widths were studied as shown in fig. 5.7. The plastic rotations are the average of three heats. An unusually low average was observed for the 102 mm (4 in) width. However, little difference was found between the 8 in. (203 mm) and 12 in. (302 mm) widths. The results of these tests show no clear relationship between plastic rotation and plate width.

In summary, the parameters of plate thickness and width show little definitive influence on plastic rotations. The test results do illustrate the variability of response typical of heat straightening. It is probable that the fluctuations shown here reflect this variability characteristic rather than effects

of plate geometry. Thus, plate geometry is considered to be a minor factor influencing plastic rotation behavior.

Temperature.-One of the most important and yet difficult to control parameters of heat straightening is the through-thickness temperature of the heated metal. Factors affecting the temperature include: size of torch orifice, intensity of the flame, speed of torch movement, and thickness of the plate. In his experiments Roeder (1985) made careful temperature measurements of the heats produced by knowledgeable practitioners. He found that these individuals, when judging temperature by color, commonly misjudged by 56°C (100°F) and, in some cases, as much as 111°C (200°F). Thus, there are considerable variations in temperature control, even with knowledgeable users.

Assuming adequate control is maintained over the applied temperature, the question arises as to what temperature produces the best results in heat-straightening without altering the material properties. Previous investigators have differed in answering this question. For example, Shanafelt and Horn (1984) state that heats above 650°C (1200°F) on carbon and low alloy steels will not increase plastic rotation. Rothman and Monroe (1973) concluded that reheating areas where previous spot heats were performed will not produce any useful movements. However, Roeder (1985) has shown that the resulting plastic rotation is generally proportional to the heating temperature up to at least 870°C (1600°F). To more clearly define the behavior suggested by a limited number of data points in Roeder's study, a series of heats were applied to

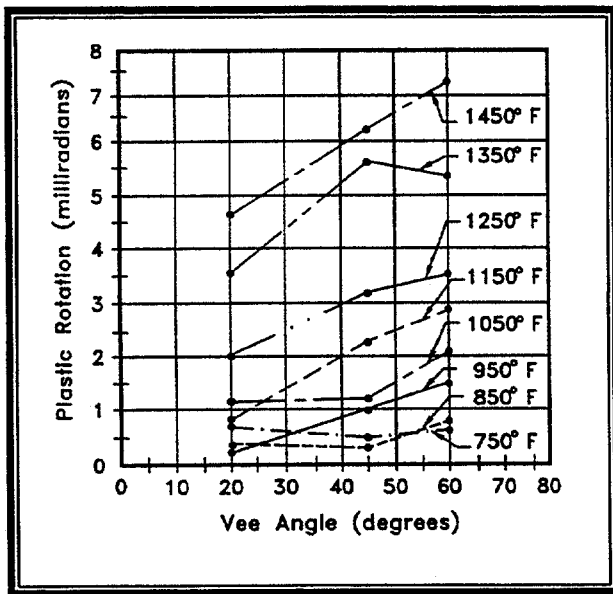


Figure 5.8. Influence of heating temperature on plastic rotation for 3/4 depth vee heats and a jacking ratio of 0.16.

plates in which the heating temperature was varied from 370-815°C (700° to 1500°F) in increments of 56°C (100°F). The results as shown in fig. 5.8 establish a clear and regular progression of increased plastic rotation with increasing temperature. Part of the reason for the regularity of the curve fits is that the same technician conducted all heats and varied the temperature in consistent step increments.

The maximum temperature recommended by most researchers is 650°C (1200°F) for all but the quenched and tempered high strength steels. Higher temperatures may result in greater rotation; however, out-of-plane distortion becomes likely and surface damage such as pitting will occur at 760-870°C (1400-1600°F). Also, temperatures in excess around 700°C (1300°F) may cause molecular composition changes which could result in changes in material properties after cooling. The limiting temperature of 680°C (1200°F) allows for a safety factor in

this regard. For the quenched and tempered steels, the heat-straightening process can be used but the temperature should be limited to 593°C (1100°F) for A514 and A709 (grades 100 and 100W) and 566°C (1050°F) for A709 grade 70W to ensure that the properties are not adversely affected. Permitting quenched and tempered steels to be heat straightened is contrary to recommendations of Shanafelt and Horn (1984); however, Roeder (1985) concurs with this recommendation.

To control the temperature, the speed of the torch movement and the size and type of orifice must be adjusted for different thicknesses of material. However, as long as the temperature quickly reaches the appropriate level, the contraction effect will be similar. This conclusion was verified by two test series on plates in which the intensity of the torch was varied. In one set, a low intensity torch moved slowly to achieve a 650°C (1200°F) temperature, while in the other a high intensity torch was moved more quickly while again attaining the same maximum temperature. The rotations in both cases were similar.

Restraining Forces.-The term "restraining forces" can refer to either externally applied forces or internal redundancy. These forces, when properly utilized, can expedite the straightening process. However, if improperly understood, restraining forces can hinder or even prevent straightening. The effect of restraining forces is explained in Chapter 2. The basic mechanism of heat straightening is to create plastic flow, causing expansion through the thickness (upsetting) during the heating phase, followed by elastic longitudinal contraction during the cooling phase.

While practitioners have long recognized the importance of applying jacking forces during the heat-straightening process, little research has been conducted to quantify its effect. A series of tests designed to evaluate this parameter involved applying a jacking force to a plate such that a moment is created about the strong axis in a direction tending to close the vee. This moment (at ambient temperature) is non-dimensionalized for comparison purposes by forming a ratio of the moment at the vee due to the jacking force, M_j , to the plastic moment, M_p , of the cross section, that is M_j/M_p . This term is referred to as the jacking ratio. The tests included jacking ratios ranging from zero to 50 percent with four different vee angles and the vees extending over either 3/4 or the full depth of the plate. The results are shown in figs. 5.9 and 5.10.

Roeder (1985) also studied the effect of the jacking ratio variation and found a similar pattern of behavior. However, the number of data points was limited. A plot of plastic rotation versus jacking ratio for 60° vee heated plates is shown in fig. 5.11 based on Roeder's study. It can be concluded from this data that the variation of plastic rotation is generally proportional to the jacking ratio and the proper use of external loads greatly expedites the heat-straightening process.

The results shown in figs. 5.9-5.11 are based on undeformed plates which were heated either three or four times with each data point representing the average. The total number of data points for any fixed set of parameters was typically six or less. While such data illustrate the trends associated with variations of basic parameters, the data set is too small to obtain statistically meaningful average values. To fill this void,

a test series was conducted on similar size 6 mm (1/4 in) thick plates which were initially damaged and then heated until straightened. Ten damaged plates were straightened with the number of heats required per plate ranging from 20 to 100 (See Chapter 4 for a discussion of residual stresses in some of these plates). A summary of the test parameters and resulting plastic rotations is given in table 4.2. The heating temperature was 650°C (1200°F). Some of the results are also plotted in fig. 5.12 illustrating the jacking ratio effect. Again, the plastic rotation is found to vary linearly with the jacking ratio.

An interesting phenomena that had not been noted in previous research was the relatively high (statistically significant) plastic rotations resulting after the first few heats, particularly the first. After these first few heats, the plastic rotations were consistently lower and showed no significant statistical variation with respect to heat number. A similar, but much less pronounced trend was noted on the undamaged plates. This behavior is attributed to the initial residual stresses induced during the damage process. The implications of this result is that theoretical formulations should be evaluated on experimental data with a large number of data points rather than on tests involving only a few heats.

A second type of constraint which may exert external forces on a member is axial restraint. A series of tests were conducted using a superimposed axial load on plates for various vee angles. The load created a 138 MPa (20 ksi) axial stress or an actual stress to nominal yield stress ratio of 56 percent. These results are shown in fig. 5.13 in comparison to the results from the

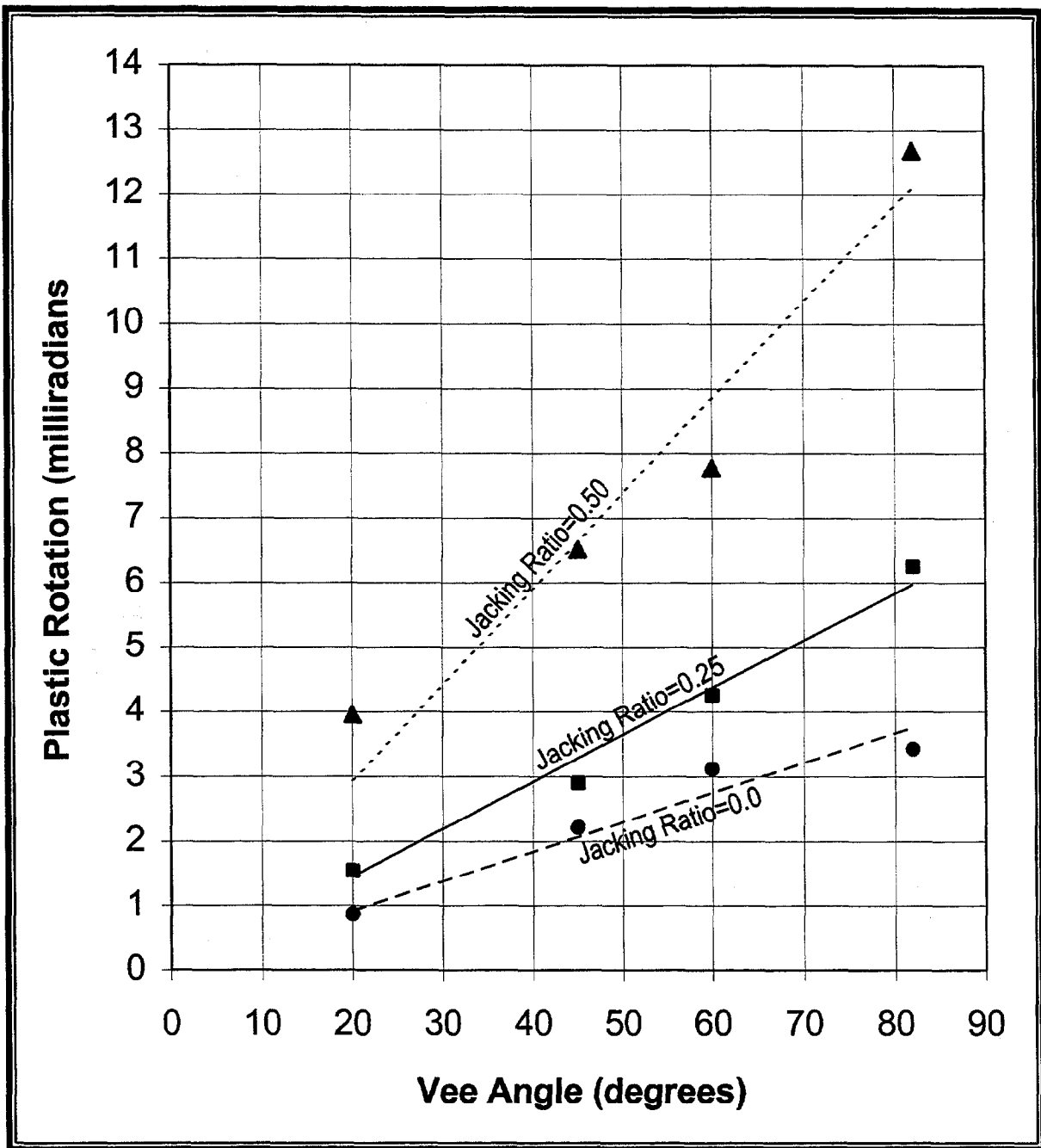


Figure 5.9. Influence of jacking ratio on average plastic rotation for $\frac{3}{4}$ depth vee heats and 650°C (1200°F) heating temperatures (lines represent a least squares curve fit).

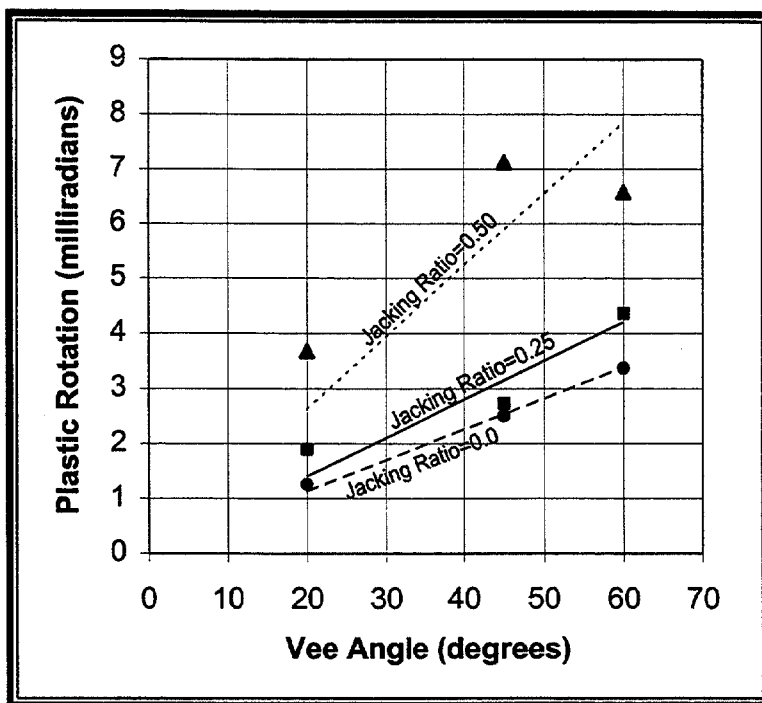


Figure 5.10. Influence of jacking ratio on average plastic rotation for full depth vee heats and 650°C (1200°F) heating temperature (lines represent a least squares curve fit).

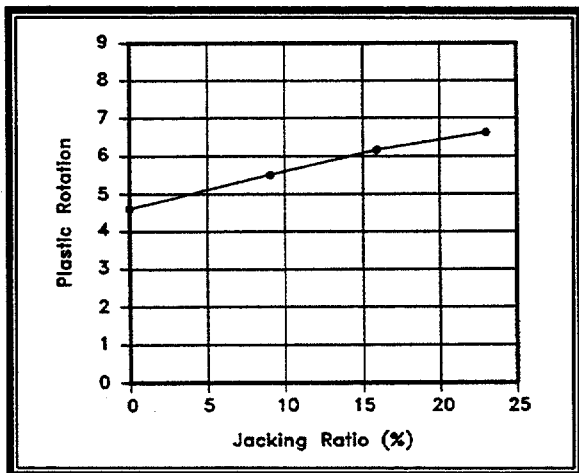


Figure 5.11. Average plastic rotation versus jacking ratio for 60° vee heated plates from Roeder, 1985 (depth ratio = 2/3 and heating temperature = 650°C or 1200°F).

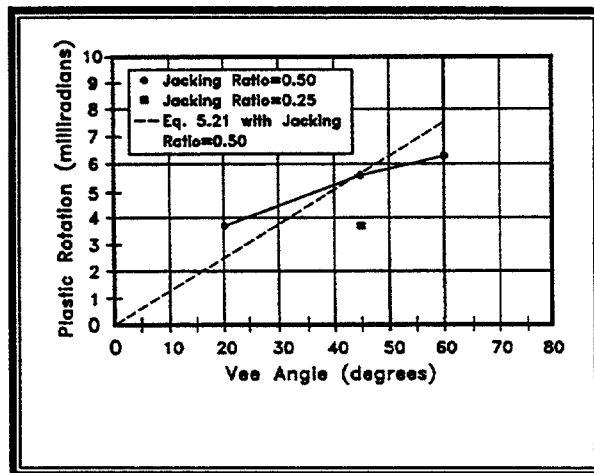


Figure 5.12. Jacking ratio versus vee angle for straightening damaged plates (Temperature = 1200°F or 650°C and depth ratio = 1)

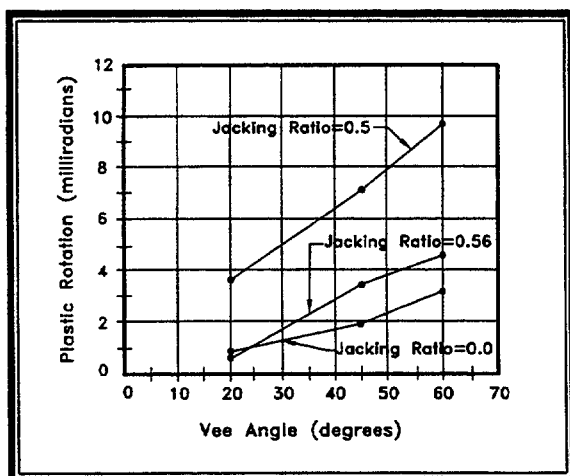


Figure 5.13. Influence of axial jacking force on plastic rotation of vee heated plates (Temperature = 650°C or 1200°F and depth ratio = 1).

previous flexural jacking ratios of 0 percent and 50 percent. The axial load may slightly increase the plastic rotation but the effect is limited.

In summary, the parameters which were found to have NA important influence on the plastic rotations produced by vee heats are: (1) vee angle, (2) steel temperature, and (3) external restraining force. The depth of the vee appears to have a small effect in the usual range of three-quarters of the plate width or greater. Likewise, the plate dimensions are of minor significance as long as the desired heating patterns and temperature can be attained.

Analytical Development

Two general approaches have been used to develop an analytical procedure for predicting member response during a heat-straightening repair. One approach involves finite element/finite strip thermal and stress analyses including inelastic behavior. The stress and strain equilibrium is evaluated over small time steps and takes into account the influence of the non-uniform tempera-

ture distribution. This approach is a lengthy computational task which is only possible using computer techniques and a typical analysis for a single vee heat can require extensive set up and computer time.

The other approach considers the global action of the vee. The Holt equation, eq. 5.1, is based on such an approach and assumes that perfect confinement is provided at all times during the heating phase. As a result longitudinal displacements through the vee are linear. With this equation the number of vee heats required to remove a bend in a steel member can be simply calculated. However, the Holt equation neglects the effect of restraining forces and temperature variation.

The goal of the analytical development is to obtain an equation which can be used to predict the angle of plastic rotation produced by a vee heat. Referring to fig. 5.14, the most common assumptions previously used in this type of development have been that: (1) longitudinal plastic strain occurs only in the vee heat zone (and in a reflected vee about the apex for partial depth vees); (2) at any specified distance from the neutral axis of the plate, the strains are constant in the longitudinal direction over the zone of the vee; (3) the planes defined by the sides of the vee remain planes after heating and rotate about the apex of the vee; and (4) confinement during heating is perfect single axis in the longitudinal direction. Roeder (1985) has been the only researcher to experimentally investigate the validity of these assumptions. He found that the statistical correlation of plane sections remaining plane was typically less than 0.5 although the apex of the vee was close to the center of rotation. While he found that most of the plastic

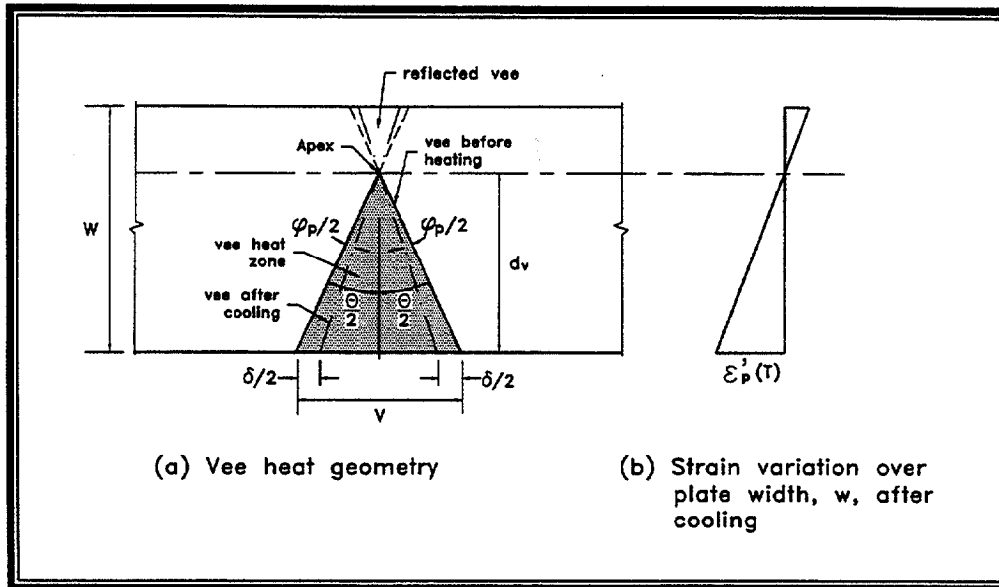


Figure 5.14. Geometric changes resulting from a vee heat on a plate.

strain occurred in the vee zone, the strain was not constant in the longitudinal direction. Rather, he found that most of the permanent strain occurs over the middle two-thirds of the vee. While it is recognized that the assumptions listed above are approximate, the poorest is that of perfect single axis confinement. This assumption can be improved using the experimental data as a guide. fig. 5.14 illustrates the geometry of a vee, before and after heating, based on the first three assumptions listed previously. The change in the width of the open end of the vee, δ , can be written as:

$$\delta = 2d_v \left[\tan \frac{\theta}{2} - \tan \left(\frac{\theta}{2} - \frac{\phi_p}{2} \right) \right] \quad (\text{Eq. 5.3})$$

If $\epsilon_p'(T)$ is defined as the final plastic longitudinal strain at the open end of the vee for a

specified maximum heating temperature, T , after a heating/cooling cycle, then,

$$\epsilon_p'(T) = \frac{\delta}{V} \quad (\text{Eq. 5.4})$$

or using trigonometric relations from fig. 5.14 to eliminate V :

$$\delta = 2d_v \epsilon_p'(T) \tan \frac{\theta}{2} \quad (\text{Eq. 5.5})$$

Equating eqs. 5.3 and 5.5 and using the trigonometric identity for the tangent function:

$$\varepsilon_p'(T) \tan \frac{\theta}{2} = \left[\tan \frac{\theta}{2} - \frac{\tan \frac{\theta}{2} - \tan \frac{\varphi_p}{2}}{1 + \tan \frac{\theta}{2} \tan \frac{\varphi_p}{2}} \right] \quad (\text{Eq. 5.6})$$

Since the experimental data shows that both φ_p and $\varepsilon_p'(T)$ are small, it is assumed that $\tan \varphi_p/2 \cong \varphi_p/2$, $\varepsilon_p'(T) \ll 1$ and φ_p is in radians. Eq. 5.6 can then be solved for φ_p :

$$\varphi_p = 2\varepsilon_p'(T) \sin \frac{\theta}{2} \quad (\text{Eq. 5.7})$$

However, Roeder (1985) carefully measured strain distributions over the vee heat areas of plates. He found that most of the permanent strains occurred within the inner two-thirds of the vee. This observation suggests using an effective vee angle of two-thirds the actual angle. By incorporating this assumption, the equation for plastic rotation becomes:

$$\varphi_p = 2\varepsilon_p'(T) \sin \frac{\theta}{3} \quad (\text{Eq. 5.8})$$

The actual plastic strain, $\varepsilon_p'(T)$, depends on the heating temperature (which is usually known) and degree of confinement (usually unknown). If the restraint is perfect single axis confinement with the strain designated as $\varepsilon_p(T)$, then $\varepsilon_p' = \varepsilon_p$. In terms of the total unconfined thermal strain, $\varepsilon_t(T)$, and the elastic strain, $\varepsilon_e(T)$:

$$\varepsilon_p(T) = \varepsilon_t(T) - \varepsilon_e(T) \quad (\text{Eq. 5.9})$$

where:

$$\varepsilon_t(T) = \int \alpha(T) dT \quad (\text{Eq. 5.10})$$

$$\varepsilon_e(T) = \frac{F_y(T)}{E(T)} \quad (\text{Eq. 5.11})$$

and $F_y(T)$ is the yield stress at temperature T , $E(T)$ is the modulus of elasticity at temperature T , and $\alpha(T)$ is the coefficient of thermal expansion at temperature T . In order to obtain values for ε_t and ε_e , equations are needed for F_y , E , and α as a function of temperature.

Roeder (1985) used the equations shown in figs. 4.26 and 4.27 to approximate $\alpha(T)$, $F_y(T)$ and $E(T)$ where T is in degrees Fahrenheit and E is in ksi. Substituting $\alpha(T)$ from fig. 4.26 into eq. 5.10, assuming that the ambient temperature is 21.1°C (70°F) and carrying out the integration gives

$$\varepsilon_t = (0.001T^2 + 6.1T - 415)10^{-6} \quad (\text{Eq. 5.12})$$

By substituting $F_y(T)$ and $E(T)$ from fig. 4.27 into Eq. 5.11, the unconfined elastic strain for $T > 424^\circ\text{C}$ (800°F) is:

$$\varepsilon_e = \frac{F_y(-720,000 + 4,200T - 2.75T^2)}{29,000(500,000 + 1,333T - 1.111T^2)} \quad (\text{Eq. 5.13})$$

Substituting eqs. 5.12 and 5.13 into eq. 5.9 and assuming $T = 649^\circ\text{C}$ (1200°F) and $F_y = 310 \text{ MPa}$ (45 ksi), which is the value for the steel plate tested, then $\varepsilon_p = 0.00735$. For the

perfect confinement case where the actual strain, ϵ_p' equals ϵ_p , eq. 5.8 gives the plastic rotation in the form:

$$\varphi_p = 0.0147 \sin \frac{\theta}{3} \quad (\text{Eq. 5.14})$$

This equation is plotted in fig. 5.15 along with the average value for each of the experimental vee heat test series. The plot includes both damaged and initially straight plates having jacking ratios of zero and 50 percent. A linear least squares curve fit is also shown for both jacking ratios. The average values shown represent over 500 vee heats conducted by at least five different technicians over a three year period. There is the characteristic scatter of data, particularly for the jacking ratio of 50 percent. However, the trend of the data is reflected by the least squares curve fit.

Note that the theoretical equation for the perfect confinement assumption, eq. 5.14, is nearly linear and falls between the zero and 50 percent jacking ratios. If it is assumed that the plastic rotation varies linearly with the jacking ratio, then the theoretical perfect confinement case corresponds to a jacking ratio of 20 percent. Using the experimental data, when the internal restraint is combined with this jacking ratio, the total constraint produced by the theoretical perfect confinement case is 31 percent of the full plastic moment capacity. Based on the reduction in yield stress at 650°C (1200°F) as shown in fig. 4.27, the uniaxial perfect confinement case is 36 percent. Thus, the theoretical equation for perfect confinement is consistent with the experimental data.

A theoretical model can be developed for various levels of jacking forces by introducing a jacking load factor, F_ℓ . Assume that: (1) the plastic rotation varies linearly with jacking ratio, (2) perfect confinement is equivalent to a 20 percent jacking ratio as observed in fig. 5.15, and (3) the zero jacking force equals 60 percent of the perfect confinement case as shown by the data in fig. 5.15. The jacking load factor can be expressed as:

$$F_\ell = 0.6 + 2 \frac{M_j}{M_p} \quad (\text{Eq. 5.15})$$

and the plastic rotation is:

$$\varphi_p = 2F_\ell(M_j)\epsilon_p(T) \sin \frac{\theta}{3} \quad (\text{Eq. 5.16})$$

Eq. 5.16 can be used to produce plots for a range of temperature from 400-565°C (750-1150°F). Such curves were compared to the temperature variation experimental data in fig. 5.8. While there was little discrepancy for the higher temperature heats, at the lower temperatures the predicated rotations were much larger than those of the experimental data. This phenomenon is not surprising because the computation of $\epsilon_p(T)$ assumes the entire vee has been instantaneously heated to a uniform temperature while the actual heating process is sequential and results in a non-uniform temperature distribution. Eq. 5.16 was modified to reflect this effect. The criteria used was to assume a linear variation in $\epsilon_p(T)$ from 427 - 650°C

Table 5.1. Plastic rotations for Example 5.1.

M_j/M_p (%)	F_ℓ	Plastic Rotation, ϕ_p (milliradians)						
		θ (degrees)						
		10	20	30	40	45	50	60
0	0.6	0.513	1.02	1.53	2.03	2.28	2.53	3.02
10	0.8	0.684	1.37	2.04	2.71	3.04	3.37	4.02
20	1.0	0.855	1.71	2.55	3.39	3.80	4.22	5.03
25	1.1	0.940	1.88	2.81	3.73	4.19	4.64	5.53
30	1.2	0.940	2.05	3.06	4.07	4.57	5.06	6.03
40	1.4	1.20	2.39	3.57	4.75	5.33	5.90	7.04
50	1.6	1.37	2.73	4.08	5.42	6.09	6.75	8.04

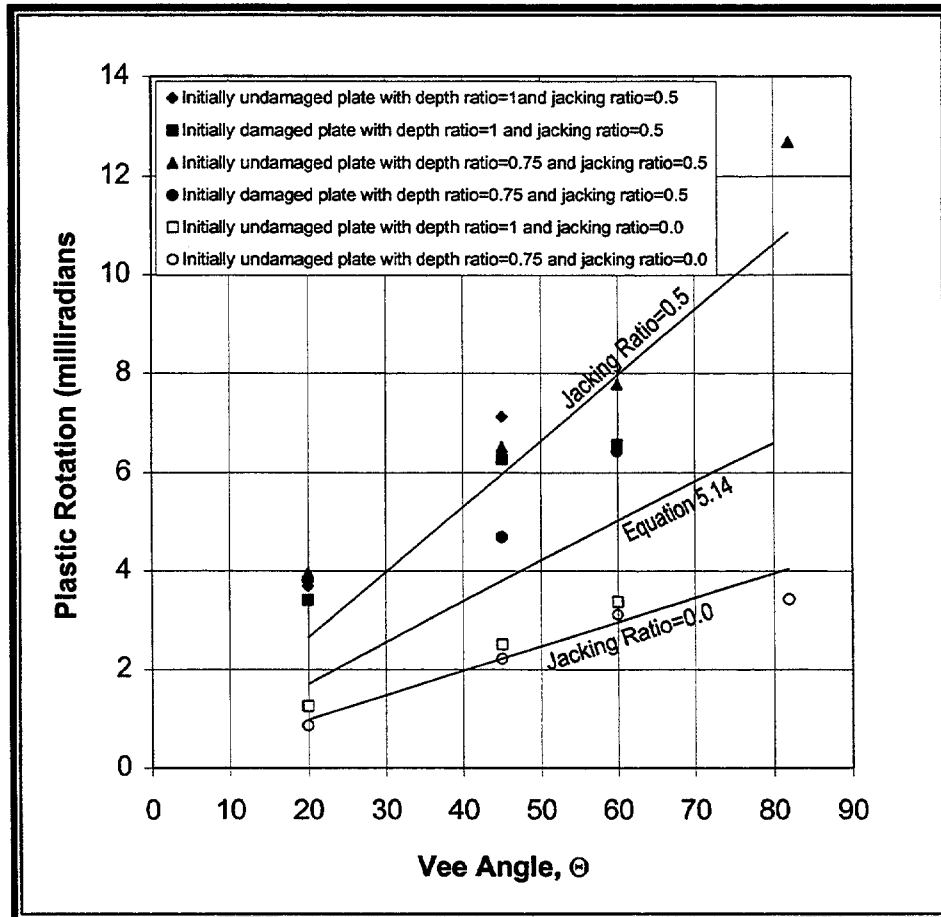


Figure 5.15. Plastic rotation versus vee angle for vee heated plates having a heating temperature of 650°C (1200°F).

(800-1200°F) with ϵ_p at 427°C (800°F) reduced by 50 percent. The resulting equation for ϕ_p can then be modified with temperature factor, $F_t(T)$, as:

$$\phi_p = 2F_t(T)F_t(M_j)\epsilon_p(T)\sin\frac{\theta}{3} \quad (\text{Eq. 5.17})$$

where:

$$F_t(T) = [0.5 + 0.00125(T - 800)] \quad (\text{Eq. 5.18})$$

or

$$F_t(C) = [0.5 + 0.00225(C - 427)] \quad (\text{Eq. 5.19})$$

where T is the heating temperature in degrees Fahrenheit and C in degrees Celsius, respectively. Eq. 5.17 correlates reasonably well over the temperature range of 390-650°C (750-1200°F).

However, the equation is not applicable for temperatures above 650°C (1200°F) because the equation for F_y is not valid beyond that point.

For carbon steel with a yield strength ranging from 230-345 MPa (33-50 ksi) and a 650°C (1200°F) heating temperature, ϵ_p varies by only 3 percent. Therefore, ϵ_p can be approximated as $\epsilon_p = 0.00735$. For this case $F_t(T) = 1.0$ and the equation for plastic rotation of a plate element becomes:

$$\phi_p = F_t\phi \quad (\text{Eq. 5.20})$$

where ϕ is the plastic rotation factor defined as:

$$\phi = 0.0147 \sin\frac{\theta}{3} \quad (\text{Eq. 5.21})$$

and F_t is defined by eq. 5.15.

Example 5.1

Problem.-For a heating temperature of 650°C (1,200°F), the plastic rotation of a plate heated with a full depth vee is a function of jacking force ratio and vee angle. Develop a table of values for plastic rotations for various jacking ratios and vee angles.

Solution.-The values for plastic rotation are obtained from eq. 5.20 and listed in table 5.2 in milliradians. This table is a handy reference as to estimated plastic rotations per vee heat for flat plates.

Significance of Plate Response to Heat Straightening

Since the plate is the basic element of any rolled or built-up shape, understanding its response to heat straightening is fundamental. The experimental behavior of heat-straightened plates has been documented with nearly 600 heating cycles on some 70 plate specimens. A number of factors were evaluated to assess their effect on the plastic rotation produced by a vee heat on a plate bent about its strong axis. In addition, a mathematical model was developed to predict these rotations.

The most important parameters affecting plastic rotations during heat straightening are angle of the vee heat, maximum temperature of the vee zone during heating, and restraining forces on the plate. Plastic rotations were verified to be directly proportional to vee angle, temperature, and restraining force. On the other hand, depth of the vee with respect to the plate width was not significant for vee depths equal to or greater than 75 percent of the plate width. Plate thickness was also shown to be insignificant as long as the heat application process allows for penetration of the heat through the thickness.

In order to aid engineers in predicting plate movements during heat straightening, a simple mathematical formula was developed. This equation relates the average plastic rotation per vee heat to vee angle, steel temperature, magnitude of restraining force, coefficient of thermal expansion, and yield stress. The formula compares well to the experimental data and is the first simple formula available that includes the parameters of heating temperature of the steel and magnitude of restraining force (jacking force). The form of this analytical approach will also lend itself toward future extensions to include the behavior of rolled shapes, axially loaded members, and composite and non-composite girders.

Key Points to Remember

- Changes in material properties of heat-straightened plates are minor when the heating temperature remains below the lower critical temperature of approximately 720°C (1330°F) for carbon steels. However, using a safety factor, a limit of 650°C (1200°F) is recommended.

- Plastic strain occurs primarily within the vee heated region.
- Due to the difficulty in controlling the many variables associated with heat straightening, the magnitude of movements for individual heats may vary considerably.
- Plastic rotation is defined as the change in angle of tangents located on either side of the damaged zone of a plate after the completion of a vee heat.
- The variation in vee depths between 75-100 percent of the plate width has little influence on the plastic rotation of a vee heated plate.
- Plate thickness and width do not significantly influence plastic rotations, provided the heat is applied to generate a specified consistent temperature within the vee.
- Plastic rotations are proportional to the angle of the vee heat.
- External restraints can significantly increase the movements per vee heat with the movement being proportional to the level of restraint.
- The movement associated with each of the initial few heats is often larger than subsequent heats due to internal restraints developed when a member is damaged severely enough to require a high number of cycles for straightening.
- Axial forces can be used as constraining forces, however bending moments are usually more efficient in producing movement.
- The plastic rotation per vee heat is proportional to the heating temperature used between 370-870°C (700-1600°F).

-
- A simple analytical formula for predicting the plastic rotation in a vee heated plate was developed as a function of: vee angle, heating temperature of the steel, restraining force, and the plastic strain at the elevated temperature. This plastic strain can be related to yield stress, modulus and coefficient of thermal expansion at the elevated temperature.
 - The influence of yield stress on plastic rotation is small for mild steel having an F_y between 230-345 MPa (33-50 ksi). Thus, the analytical formula of eq. 5.20 is applicable over this range.

Chapter 6. Heat Straightening Rolled Shapes

Introduction

The process of heat straightening damaged rolled shapes is based on a logical extension of the straightening of plates. Rolled shapes can be viewed as an assemblage of flat plate elements. When damaged, some plate elements are bent about their strong axis, some about their weak axis and some about both. The overall effect on a member results in damage which is a combination of one or more of the fundamental damage categories as follows:

- Category S: Denotes primary bending about the major or "strong" axis (see fig. 1.1).
- Category W: Denotes primary bending about the minor or "weak" axis (see fig. 1.2).
- Category T: Denotes torsional or twisting of a member about its longitudinal axis (see fig. 1.3).
- Category L: Denotes localized damage to plate elements in the form of bulges, buckles, and crimps (see fig. 1.4).

The first step in developing a methodology for heat straightening complex damage on rolled shapes is to understand the behavior of such shapes when subjected to single fundamental types of damage. The purpose of this chapter is to examine this behavior from an experimental and analytical perspective. The focus will be on categories S and W. Local distortions (Category L) will be addressed in Chapter 9 and tor-

sional distortions (Category T) in Chapter 7.

A distinction will be made between the primary elements and stiffening elements of a cross-section. The primary elements are the plate elements of the cross-section subjected to bending about their own local strong axes. The stiffening elements are perpendicular to the primary elements and are bent about their own local weak axes.

For example, consider the channel shown in fig. 6.1, which has been plastically deformed about its major axis, resulting in Category S damage. The web of this channel, a plate element bent about its major axis, is therefore a primary element. The two flanges are bent about their minor axes and are thus secondary elements.

For rolled shapes with flexural damage, the pattern of yielding usually differs for the primary and secondary plate elements. Typically, the primary plate elements develop plastic hinges. A plastic hinge defines a state of stress in which the entire cross-section has reached yield (F_y): Tensile yield in one region and compressive yield in the other as shown in fig. 6.2a.

The secondary elements of a damaged rolled shape may exhibit one of several scenarios. In the first, yielding does not occur because the secondary element is located near the neutral axis of the cross section, e.g., when a wide flange beam is bent about its minor axis, the web may not reach yield. In the second case, the secondary element is located near the extreme fibers of flexural yielding (such as the flanges of the channel shown in fig. 6.1). In this situation the

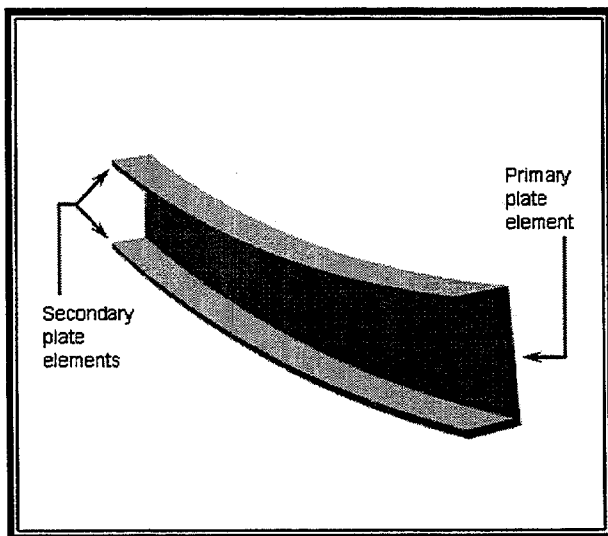


Figure 6.1. Primary and Secondary plate elements for a channel bent about its major axis (Category S damage).

flanges yield due to axial stress (either tension or compression) as illustrated in fig. 6.2b. In the third case, the secondary element is yielded in weak axis bending in which a region of yield is formed as shown in fig. 6.3. The stress distribution is similar to that shown in fig. 6.2a. However, the results are a narrow strip of flexural yielding often referred to as a yield line.

As a consequence of the various patterns of yielding which occur in damaged rolled or built-up shapes, the heating pattern for repair must be tailored to fit. While the vee heat is generally used on primary plate elements of a section bent about their major axes, the secondary elements may require a strip heat, line heat or no heat at all. These heating patterns introduce an additional degree of variability in that the time to complete a heat may be considerably longer than heating a single plate. Considerable cooling may have occurred at the initial heating locations before the last element is heated. Movement may be retarded in such cases

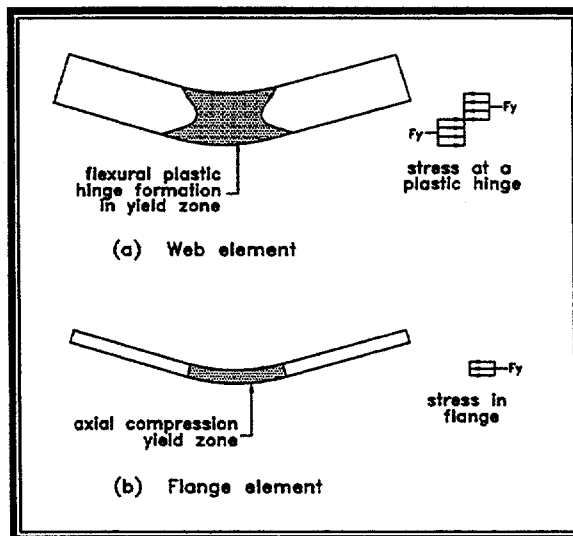


Figure 6.2. Typical yield zone patterns in the plate elements of the channel shown in fig. 6.1.

due to increased internal restraints. A good practice to minimize the heating time is by using more than one torch for complex patterns.

In addition to the jacking load factor, the various combinations of plate elements found in structural steel shapes introduces two other parameters that may affect the member's behavior during heat straightening. The first is a shape factor and the second is a stress factor. It is obvious that the shape may influence behavior. However, the stress factor requires an explanation.

For cases in which jacking forces are applied prior to heat straightening, the distribution of stress over the heated section will vary according to the shape of the cross section and the magnitude of the moment. As the torch moves over the section, the steel temperature rises and then falls in a manner somewhat analogous moving across calm water. The heat variation produces continuous and complex changes in the stress distribution. As a consequence, stress

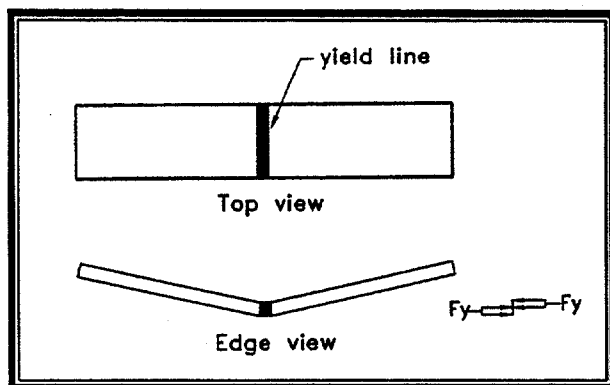


Figure 6.3. Weak axis bending resulting in a yield line in the plate element.

distributions may be quite different between two members of different shapes.

One measure of this effect is the ratio of plastic moment, M_p , to the moment at initial yield, M_y . For a constant yield stress this ratio is Z/S where Z is the plastic section modulus and S is the elastic section modulus. Since the moment due to jacking is usually expressed as a percentage of M_p , the degree of yielding during heating is often a function of this ratio. For example, $Z/S = 1.5$ for a rectangular plate and is only about 1.12 for typical wide flange beams. In other words, yielding is initiated at two-thirds of ultimate capacity for a plate but does not occur until 90 percent of capacity for most wide flange members. For a moment due to jacking in the range of 35-50 percent of M_p , some localized yielding will occur during heat straightening. The amount, and consequently the degree of straightening, will depend on the stress factor as a function of Z/S .

In this chapter, the behavior of common structural shapes subjected to heat straightening will be examined. In addition to considering the experimental data, an analytical method of predicting movement

will be presented. The basis for this model is the plate equation for plastic rotation developed in Chapter 5. For mild steel, the equation for plastic rotation of a structural shape can be expressed as

$$\phi_p = F_\ell F_s F_a \phi_b \quad (\text{Eq. 6.1})$$

where F_ℓ is the factor associated with the external jacking force, F_s is a factor reflecting the shape of the cross section, F_a is the stress factor, and ϕ_b is the basic plastic rotation factor derived for a rectangular plate (see eq. 5.14) and expressed as:

$$\phi_b = 0.0147 \sin \frac{\theta}{3} \quad (\text{Eq. 6.2})$$

In the following sections the experimental data on structural shapes will be evaluated and equations for the various factors used in eq. 6.1 will be presented.

Behavior of Channels with Strong Axis Damage (Category S)

When a channel has Category S damage, a flexural plastic hinge forms in the web and axial yield zones form in the flanges as illustrated in fig. 6.2. As shown in fig. 6.4, the heating pattern consists of a vee heat in the web followed by a strip heat on the flange that was subjected to tension (flange 1) during the damage phase. The reason for this pattern is that during heat straightening the vee will close, tending to reduce the damage curvature. However, flange 1 will tend to prevent this closure if unheated. By continuing the vee heat into the flange as a strip heat, the upsetting

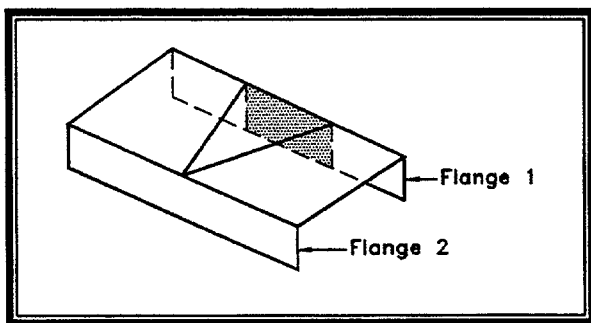


Figure 6.4. Heating patterns for channels bent about their strong axis (Category S).

process will include the flange and expedite the movement. The heating sequence is: (1) web vee heat and (2) flange 1 strip heat. Note that flange 2 is not heated.

One note of caution should be mentioned for both this and other heating patterns for structural shapes. The strip heat on the flange may produce minor curvature about the undamaged axis. Typically, this movement is small and can be corrected with a few heats directed toward removing this curvature.

A series of heats was conducted on a C 6x8.2 channel using the vee/strip pattern in fig. 6.4. Three heats each were conducted for jacking ratios of 0, 25, and 50 percent and vee angles of 20° and 45°. The average values of plastic rotations are shown in fig. 6.5. The results follow the same trend found in plates. The curvature caused by heat straightening is proportional to vee angle and jacking ratio.

The plastic rotation was first computed by the plate equation (eq. 5.20) using the dimensions of the channel web. The results were significantly lower than the actual channel plastic rotations suggesting that the shape of the channel magnifies the movement over that expected from an equivalent sized plate. An explanation for this behavior

can be developed by considering the geometry of the section. The channel can be considered as a folded plate as shown in fig. 6.6. First, consider the section in its unfolded position with the heat applied beginning with the vee and continuing across the strip. If the vee was extended across the web portion of the unfolded section, the result would be a standard vee heat having a vee depth equal to the channel web depth, d , plus the flange width, b_s . By using a strip heat on the flange portion, the effect is similar except that the heating pattern is somewhat narrower over the flange. Since most of the plastic deformation occurs over the middle two-thirds of a vee (Roeder, 1985), the difference between a vee and strip on the flange portion is small and can be neglected. Assuming that the longitudinal strain is small and varies linearly with distance from the vee apex, (fig. 6.6) the relationship between x_1 and x_2 is:

$$x_2 = \left(\frac{d + \frac{1}{2}b_s}{d} \right) x_1 \quad (\text{Eq. 6.3})$$

Now consider that the same heating pattern is applied with the flange in its folded position. The average longitudinal movement of the flange, x_2 , will tend toward the same value as in its unfolded position. However, in its folded position its distance from the apex has been decreased from $d + b_s/2$ to d . If the same movement, x_2 , occurs at a shorter distance from the vee apex, the change in curvature is magnified. From eq. 6.3 this magnification can be expressed as a shape factor:

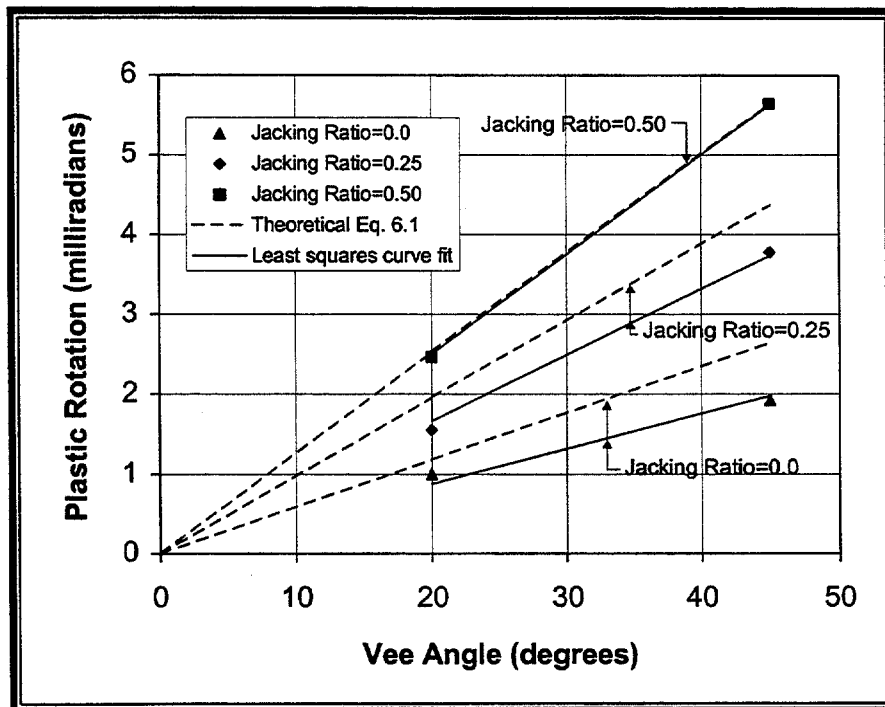


Figure 6.5. Experimental and theoretical plastic rotations for a C 6x8 channel with Category S damage.

$$F_s = \frac{d + \frac{1}{2}b_s}{d} = 1 + \frac{b_s}{2d} \quad (\text{Eq. 6.4})$$

Note that this analysis assumes a full depth vee heat. Since little difference has been noted between a full and three-quarter depth vee, the equation is valid in this range.

The stress factor, F_a , can be computed by normalizing the Z/S ratio for the channel bent about the major axis to that of the plate ($Z/S = 1.5$) since the plate equation is the basis for developing equations for rolled shapes. The stress factor should be unity for the zero jacking force case and is assumed to vary linearly to the maximum at the 50 percent jacking ratio case. The stress factor can be written as

$$F_a = 1 - 2\left[1 - \left(\frac{2}{3}\right)\left(\frac{Z}{S}\right)\right] \frac{M_j}{M_p} \quad (\text{Eq. 6.5})$$

where Z/S is the ratio of plastic to elastic section modulus for bending about the major axis, i.e., Z_x/S_x in this case. Since channels typically have a Z_x/S_x ratio of about 1.2, the stress factor for channels can be approximated as

$$F_a = 1 - 0.4 \frac{M_j}{M_p} \quad (\text{Eq. 6.6})$$

The jacking load factor is identical to that developed for plates, that is

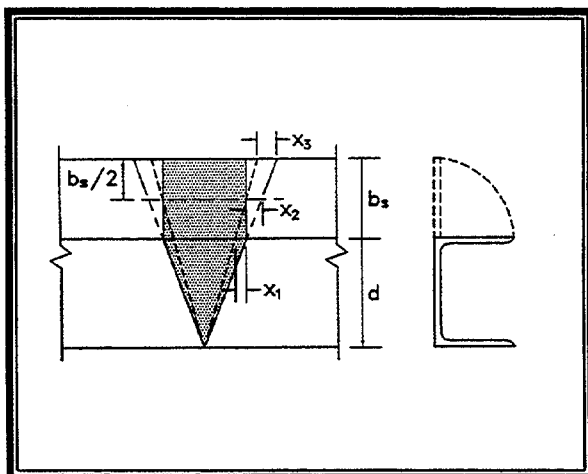


Figure 6.6. Unfolded flange for a Category S channel.

$$F_{\ell} = 0.6 + 2 \frac{M_j}{M_p} \quad (\text{Eq. 6.7})$$

and the shape factor, F_s , is given by eq. 6.4. Using these factors, the plastic rotation can be obtained from eqs. 6.1. and 6.2.

A comparison of the experimental and theoretical results for the C 6x8.2 is shown in fig. 6.5 indicating reasonably good agreement. From this investigation of Category S channels, it is seen that the plate equation for plastic rotation can be used as the basis for other rolled shape behavior.

Behavior of Channels with Weak Axis Damage (Category W)

A channel with Category W damage is more complex than the Category S due to lack of symmetry about the weak axis. Also, the heating pattern will differ depending on whether the compression zone induced by damage is in the web/flange junction or flange tips. The heat-straightening process is based on the open end of the vee

heat lying in the zone stressed in tension during the damage phase. Thus, the apex of the vee heat on the flanges may lie at either the flange tips or the web/flange junction depending on the direction of bending moment damage. The heating patterns are shown in fig. 6.7 for both cases. A combination of vee heats on the flanges and a strip heat on the web is required for case (a), here referred to as negative moment damage, and only vee heats on the flanges for case (b), positive moment damage. Experimental studies have been conducted for both damage cases.

A comprehensive series of tests was conducted on C 6x8.2 channels which were initially straight using the heat configuration shown in fig. 6.7a. The plastic rotation was measured after each heat cycle. The results are plotted in fig. 6.8 along with a linear least squares curve fit. The response of these channels generally corresponded to the typical pattern of behavior for heat-straightened plates although the variations were not as linear. The average values for plastic rotations were higher than expected for 20° vee heats and lower than expected for 45° vees.

This behavior illustrates that even under controlled conditions consistency in heating is difficult to maintain. Also, the amount of plastic rotation for a single heat significantly exceeded that expected of a plate of the same size as the flanges of the channel. Applying the plate equation to the vee heated flanges of the channel (and neglecting the web) leads to a prediction of plastic rotation much smaller than observed in the channel. In fact, the channel plastic rotations averaged 2.5 times more than an equivalent sized plate.

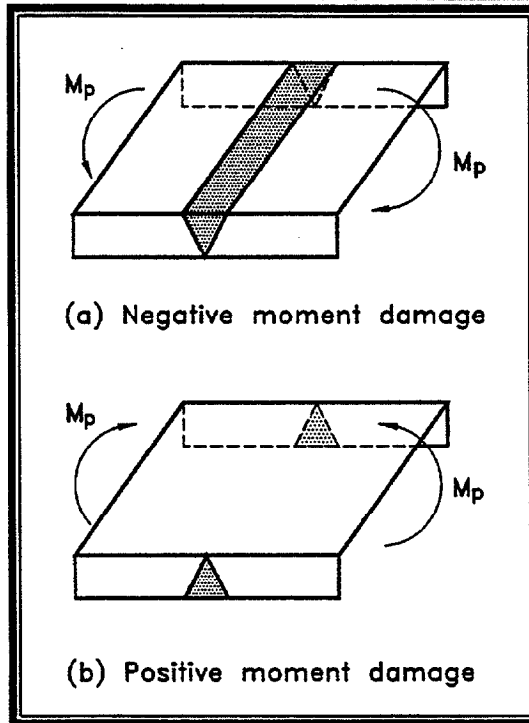


Figure 6.7. Heating patterns for channels bent about the weak axis (Direction of moment producing damage indicated by M_p).

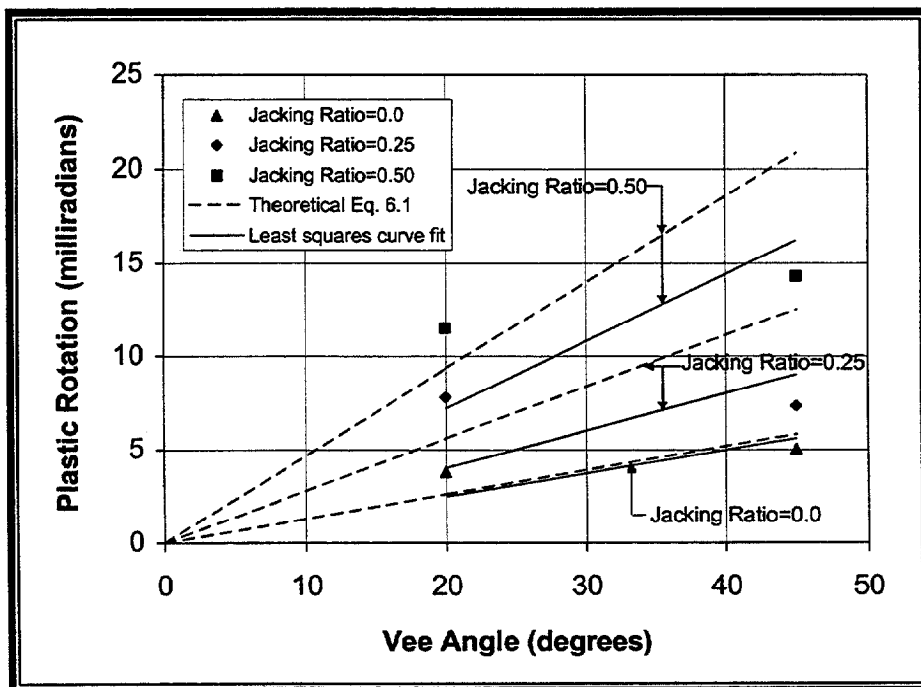


Figure 6.8. Experimental and theoretical plastic rotations for Category W damage of a C 6x8.2 with the open end of vees at flange-web-juncture as shown in fig. 6.7a.

Conversely, a C 6x8.2 was heated with the heating pattern shown in fig. 6.7b. Using a jacking ratio (M_j/M_p) of 50 percent and a 45° full depth vee, 14 heats produced an average plastic rotation per heating cycle of 5.78 milliradians. Use of the plate equation for the flange (and neglecting the web) predicts the nearly identical value of 6.09 milliradians. Thus, no magnification over the plate equation value was required for the case when the vee apex was located at the web/flange juncture.

The explanation for the seemingly contradictory results relates to both geometric and stress considerations. First, the most significant aspect is the geometry of the channel section. For the case of the vee/strip heat combination shown in fig. 6.7a, the channel section (fig. 6.9a) can be viewed in terms of its symmetrical component shown in fig. 6.9b. This component of the channel section can be considered as a folded plate in a manner similar to the category S channel. First consider the section in its unfolded position with the heat applied in the standard fashion: beginning at the apex of the vee, moving across the vee, and then continuing across the strip. If the vee is extended across the web portion of the unfolded section, the result would be a standard vee heat on the flange of depth d plus one-half the web, $d_w/2$. By using the strip heat on the web portion, the effect is similar except that the heating pattern is somewhat narrower.

Referring to fig. 6.9c, the maximum longitudinal shortening of the web portion of the section will occur at the axis of symmetry of the web portion as designated by x_2 . Because of the linear strain assumption, (similar to Category S damaged channels) x_1

and x_2 are proportional to the distance from the vee apex such that:

$$x_2 = \left(d + \frac{b_s}{2}\right) \frac{x_1}{d} \quad (\text{Eq. 6.8})$$

where d = vee depth (which equals the flange width) and b_s = width of stiffening element (or the web width).

Now consider that this same heating pattern is applied to the section in its folded position. The tendency will be for the same x_2 value as shown in eq. 6.8 to occur. However, since the channel is folded, this average movement, x_2 , acts over the distance d rather than $d + \frac{b_s}{2}$. Hence, the plastic rotation will tend to be magnified by the factor, F_s :

$$F_s = \frac{d + \frac{b_s}{2}}{d} = 1 + \frac{b_s}{2d} \quad (\text{Eq. 6.9})$$

For the C 6x8.2 channel, $d = 48.8$ mm (1.92 in) and $b_s = 152$ mm (6 in) thus $F_s = 2.56$. Consequently, a magnification of more than double would occur in comparison to an equivalent plate with the same dimensions as the flange of the channel. This analysis illustrates that the vee/strip heat combination does magnify the movement. On the other hand, for the case of the vee heat in the opposite direction and no strip heat required, fig. 6.7b, no magnification would be expected since the web is not heated. The experimental results showed no magnification which reinforces this conclusion.

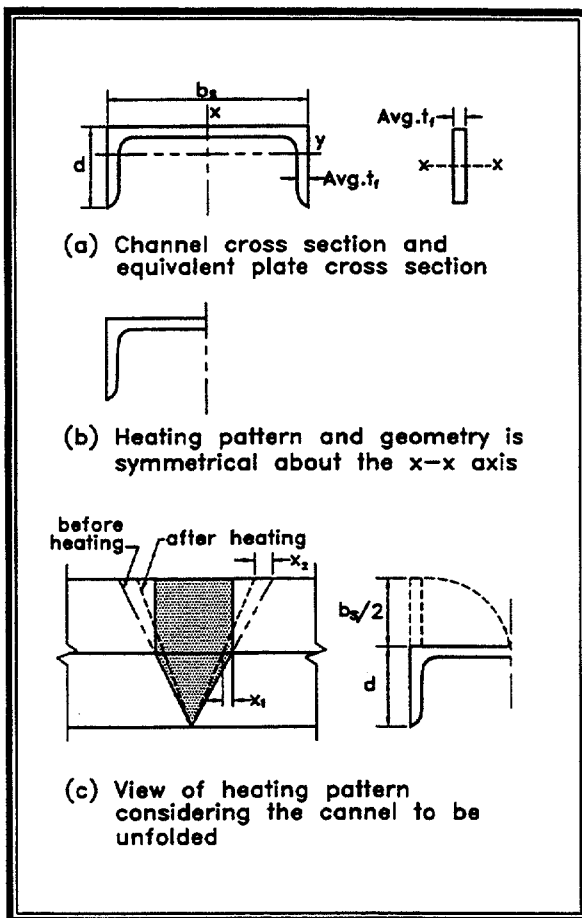


Figure 6.9. Geometric effects on heat straightening a channel with negative curvature damage.

The stress factor, F_a , can be considered in the form previously given by eq. 6.5 where the ratio Z/S is related to weak axis bending, i.e., Z_y/S_y . For typical cases Z_y/S_y is approximately 2.05. For example $Z_y/S_y = 2.02$ for the C 6x8.2. Therefore, using $Z_y/S_y = 2.05$ the stress factor can be approximated (for channels with weak axis damage) as:

$$F_a = 1 - 0.7 \frac{M_j}{M_p} \quad (\text{Eq. 6.10})$$

The shape factor, F_s , of Eq. 6.9 can be written as:

$$F_s = 1 + \frac{b_s d}{2d^2} \quad (\text{Eq. 6.11})$$

where d is the vee depth and b_s is the width of the channel web or stiffening element. The equation can be modified to include both positive and negative moment damage, if the term d in the numerator of the second term is replaced by d_s which is defined as the distance from the apex of the vee to the stiffening element (the web in this case), thus:

$$F_s = 1 + \frac{1}{2} \left(\frac{b_s d_s}{d^2} \right) \quad (\text{Eq. 6.12})$$

Consequently, $d_s = d$ for the case in fig. 6.7a and $d_s = 0$ for the case in fig. 6.7b. Note that since little difference was noted in plastic rotations for full and three-quarter depth vees, d should be taken as unity unless the vee depth ratio is less than 0.75. Research data is not available for more shallow depth vees. Applying these factors, the plastic rotation for a channel with flexural damage about the weak axis is given by eqs. 6.1 and 6.2 where F_s is defined by eq. 6.12, F_l by eq. 6.7, and F_a by eq. 6.5 (although F_a can be approximated by eq. 6.10 for most cases). The theoretical equation is shown for the negative moment damage case in fig. 6.8 for the three jacking ratios. The theoretical results tended to be larger than the least squares curve fit of the experimental data.

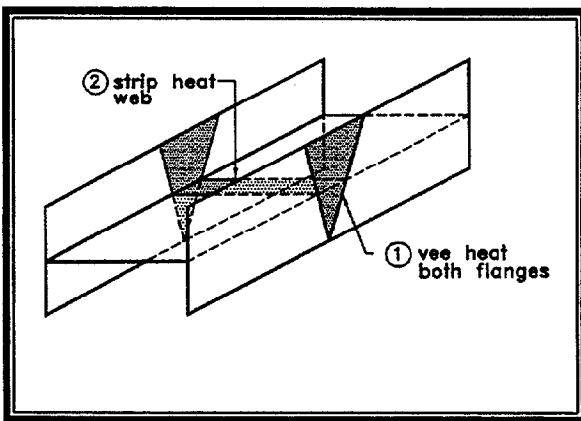


Figure 6.10. Heating patterns for weak axis damage to a wide flange beam (Category W).

Behavior of Wide Flange Beams with Weak Axis (Category W) Damage

For a wide flange beam bent about the weak axis, the flanges are the primary elements and the web is the stiffening element. The heating pattern consists of vee heats on each flange and a strip heat on the web as shown in fig. 6.10. In this case the stiffening element is located at the neutral axis of bending and introduces additional complexity in behavior. The yield pattern consists of a flexural plastic hinge on the two flanges. Since the web lies at the neutral axis of bending, it does not usually undergo significant yield. However, a strip heat is required on the web so that the closing of the flange vees will not be resisted by the web. This case is one example of when it is appropriate to heat a location where yielding may not have occurred.

Horton (1973) conducted tests on undamaged sections. The results of these tests are shown in fig. 6.11. Avent (1992), Avent and Fadous (1989) and Boudreaux (1987) also conducted tests on W 6x9 beams. In some cases the beams were undamaged prior to vee heating while others

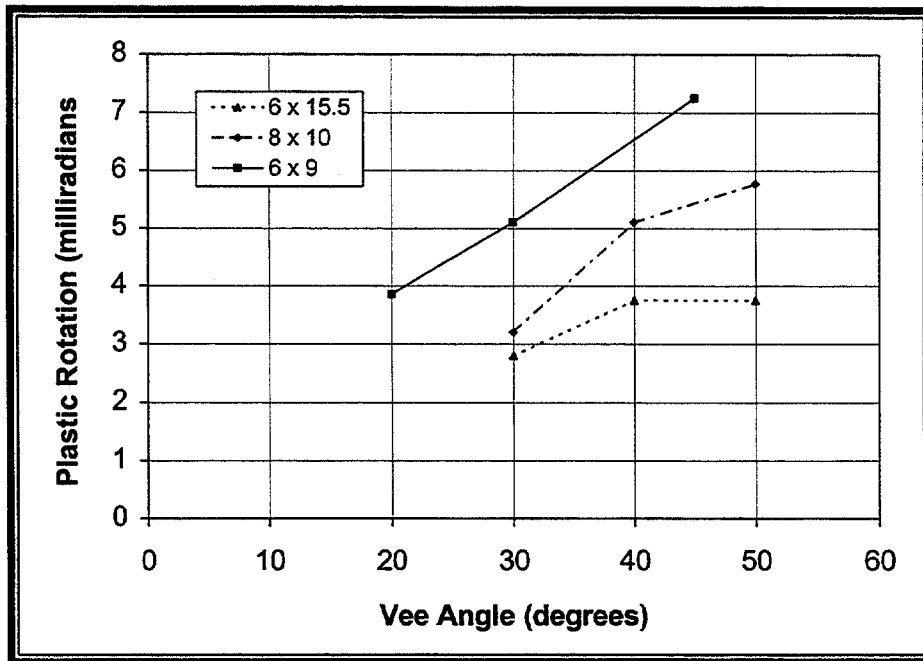
were damaged. The average plastic rotations are shown in fig. 6.12. The data from Horton's tests generally followed the pattern of increasing plastic rotation with vee angle.

Avent's tests showed the plastic rotation to be proportional to both vee angle and jacking ratio. The data was fairly linear with respect to vee angle for zero and 25 percent jacking ratios. However, considerable variation was found for the 50 percent jacking ratio.

The same model as used for Category W damaged channels is applicable for wide flange beams. The plastic rotation is given by eqs. 6.1 and 6.2 where F_l is defined by eq. 6.7, F_s is given by eq. 6.12 and F_a by eq. 6.5. The Z_y/S_y value for typical wide flange beams is around 1.5. Using this value, the stress factor can be approximated by $F_a = 1$. Also note that in this case, the stiffening element is located at mid-depth, thus d_s equals one-half the flange width ($d_s = 1.97$ in. or 50.0 mm for the W 6x9). This theoretical equation is also plotted in fig. 6.12. The results compare well with the least squares curve fit.

Repetitive Damage and Straightening for Category W Damage to Wide Flange Beams

A comprehensive study was conducted on rolled beam sections having multiple cycles of damage and repairs. The procedure was to damage the beam by bending about the minor axis. The beam was then heat straightened. After straightening was completed, the beam was re-damaged and again heat straightened. Up to eight cycles of damage were repaired in some cases. Four beams (W 6x9's) were used in the study. Each beam was damaged



6.11. Vee angle versus plastic rotation for wide flange beams using the Category W heating pattern, Horton (1973).

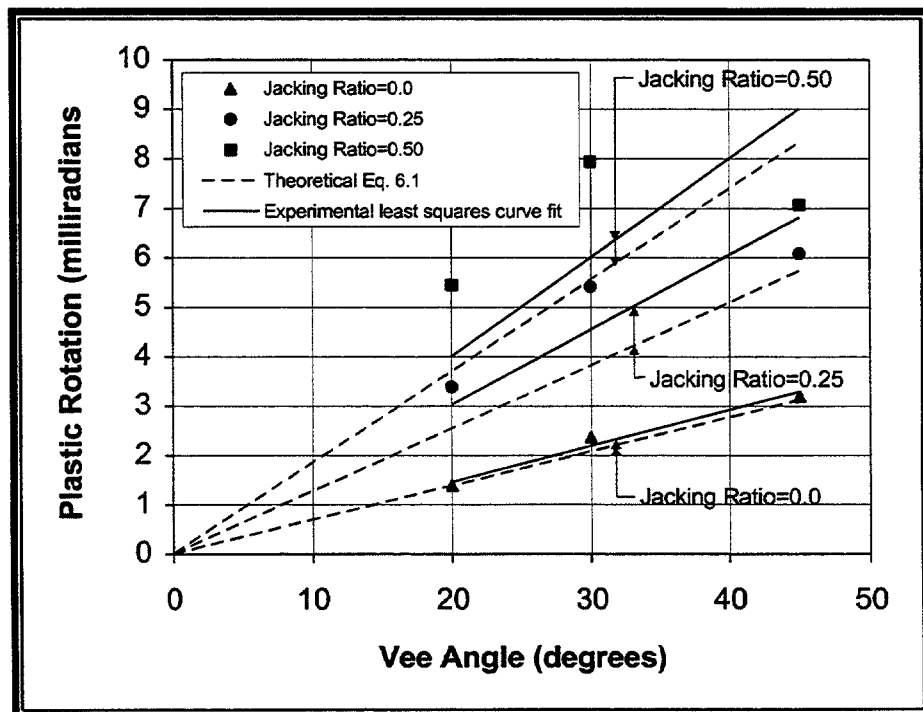


Figure 6.12. Plastic rotation versus vee angle for W 6x9 using the Category W heating pattern (Temperature = 650°C or 1,200°F).

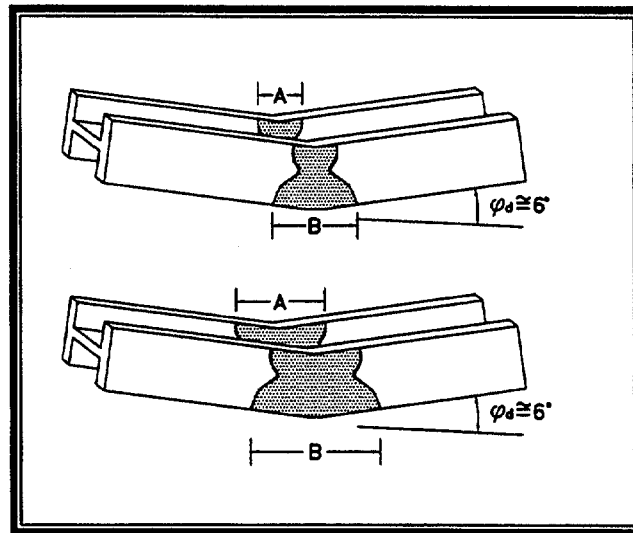


Figure 6.13. Spreading of yield zone in subsequent cycles of damage and repair for W 6x9 wide flange beam specimens.

Table 6.1. Summary of damaged beam data for W 6x9 beams with Category W damage.

Beam/Repair Cycle No.	Angle of Damage		No. of Heats	Avg. ϕ_p (milli- rad)	Coefficient of Variation
	(degree)	(millirad)			
B-1/1	7.34	128.1	20	6.85	0.28
B-2/1	7.67	133.9	20	6.65	0.30
B-2/2	8.22	143.5	23	6.70	0.26
B-3/1	7.15	124.8	18	6.64	0.16
B-3/2	7.21	125.8	22	5.93	0.26
B-3/3	7.14	124.7	19	6.19	0.28
B-3/4	7.17	125.2	21	6.30	0.29
B-4/1	7.06	123.2	18	6.42	0.28
B-4/2	6.56	114.4	17	6.52	0.17
B-4/3	7.50	131.0	21	5.91	0.33
B-4/4	7.20	125.7	20	6.12	0.39
B-4/5	6.87	119.9	21	5.68	0.39
B-4/6	6.42	112.0	13 ¹	8.13	—
B-4/7	7.16	125.0	16 ¹	8.14	—
B-4/8	7.27	126.9	14 ¹	9.47	—

¹Some heats included two vees due to time constraints

Table 6.2. Increasing yield zone after each damage/repair cycle for W 6x9 with Category W damage.

Beam	Length of yield zone (in) after Bend #: (Top row = A, bottom row = B)							
	1	2	3	4	5	6	7	8
1	---							
2	---	8.20						
	---	8.40						
3	5.90	8.05	9.75	10.30				
	6.00	8.65	10.40	11.65				
4	5.50	8.15	9.50	10.50	10.70	10.70	11.50	11.50
	5.80	8.40	10.20	12.00	13.20	13.30	15.25	15.25
Averages	5.70	8.13	9.63	10.40	10.70	10.70	11.50	11.50
	5.90	8.48	10.30	11.83	13.20	13.20	15.25	15.25

around its weak axis to a degree of about seven degrees. All beams were repaired using the heating pattern of fig. 6.10 and 45° vees with a depth ratio of 0.75 and a jacking ratio of 0.5. The number of damage/repair cycles varied for each of the beams. Each repair cycle consisted of approximately 20 heats, with the average plastic rotation shown for each repair cycle in table 6.1.

As the beams straightened, a thickening developed in the middle region, causing a spreading of the yield zone in each subsequent bend as seen in fig. 6.13 (values are shown in table 6.2). The thickening resulted in a smoother distribution of curvature (due to thinner portions further from the centerline tending to yield earlier than before), although the total angle of damage was kept as consistent as possible for each bend. Due to the larger yield zone, the vee heats were distributed over a longer length to accommodate the spread.

Since there were over 200 heats performed, statistical analysis can be used to evaluate trends in the data. DeBajar, et.al. (1992) addressed two questions: (1) Does the response to heat straightening vary if the member is re-damaged and repaired more than once; and (2) Is the response during a single repair cycle dependent on the heat number? An independent sample t-test (Hicks, 1982) was used to evaluate the response from different damage/repair cycles. The probability that the average plastic rotation in successive repair cycles was less than the average value of the first repair ranged from 71-87 percent. The results suggest that there may be a small trend toward larger plastic rotations in the first repair cycle.

To look at whether the amount of movement varied from heat to heat within a single repair cycle, a dependent samples t-test (Hicks, 1982) was used. The probability

values were high enough to conclude that the first heat does produce greater movement than successive heats, although there was no trend that another heat had preeminence over any other. This conclusion confirms observations in the field that the first heat produces more movement. The probable cause is that residual stresses are often created during the damage process. These stresses often act in a direction tending to reduce the damage thus magnifying the jacking force. The initial heat tends to relax these residuals so that successive heats are not affected. Because of this behavior it is recommended that the jacking force during the first two heats be limited to approximately 25 percent of the member capacity so as not to risk over-stressing the member.

The average value of plastic rotation for all damage/repair cycles (240 heat cycles) was 6.78 milliradians. The average value, considering the first damage/repair cycles only (75 heats) was 5 percent higher at 6.64 milliradians. These values were within 20 percent of the value predicted by the theoretical model of eq. 6.1.

Behavior of Wide Flange Beams with Strong axis (Category S) Damage

The heating pattern and yield zone for Category S damage is shown in fig. 6.14. Several researchers (Avent, 1992, Moberg, 1979 and Boudreaux, 1987) have conducted tests on Category S damaged and undamaged wide flange beams. The average plastic rotation for each case is shown in table 6.3 and values for the W 6x9 are plotted in fig. 6.15.

The results shown in table 6.3 follow the trend that plastic rotation is proportional to vee angle but are inconsistent. The W 10x33 values are far too low and suggest an

improper heating procedure. The values for the shapes heated with a 50° vee angle also appear low, again suggesting that the steel temperature was not adequate. The values for the W 6x9 with 20° and 30° vee angles appear too high suggesting either over-heating or lack of lateral restraint. The only values which appear consistent with other categories of damage are those with a jacking ratio of 50 percent. To evaluate these inconsistencies, a W 12x14 was vee heated. The temperature and jacking force were carefully controlled. The results are plotted in fig. 6.15.

A model to predict this behavior can be developed similarly to the channel. The flange of the beam is the stiffening element for the category S damage heating pattern. The flange at the open end of the vee provides a magnification effect similar to that of the channel. Using the folded/unfolded flange concept (fig. 6.16) similar to that of the channel along with the same assumptions, a shape factor can be derived identical to the channel of eq. 6.4 or 6.12 where for the wide flange beam d_s = beam depth, b_s = flange width and d = beam depth.

The equation for plastic rotation, ϕ_p , is given by eqs. 6.1 and 6.2, F_l is defined by eq. 6.7, F_s is given by eq. 6.12, and F_a by eq. 6.5. Note that Z_x/S_x is typically around 1.12 for wide flange beams. Using this value in eq. 6.5, the stress factor can be approximated by

$$F_a = 1 - 0.5 \frac{M_j}{M_p} \quad \text{Eq. 6.13}$$

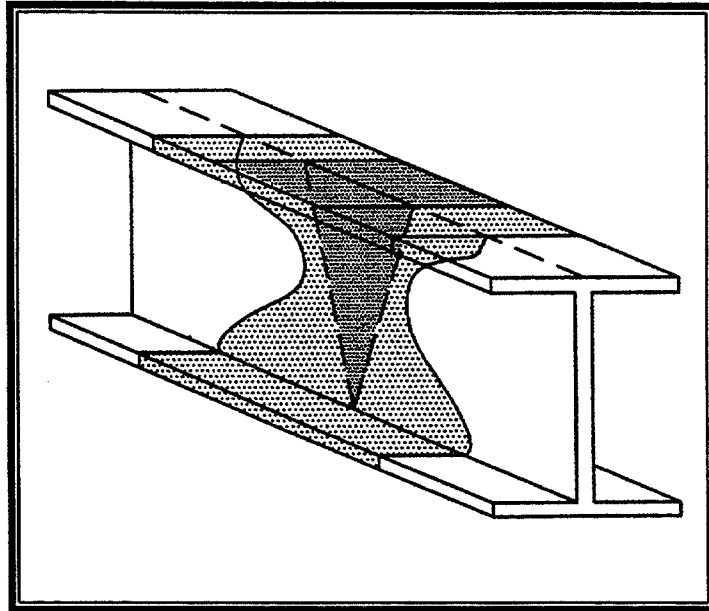


Figure 6.14. Yield zone and heating pattern for Category S damage to wide flange beams.

Table 6.3. Plastic rotations for Category S damage to wide flange beams (heating temperature = 650° or 1200°F).

Section Type	Number of heats	$\frac{M_j}{M_p}$ (%)	Plastic Rotations				
			Vee Angle (degrees)				
			20	30	40	45	50
W6x15.5	2	22		2.75	2.93		2.71
W6x15.5	2	22		2.80	3.10		3.01
W8x10	2	22		2.14	2.88		3.01
W10x33	2	22		1.14	0.26		1.01
W6x9	4	0	1.74	4.19		5.35	
W6x9	3	0	3.04	2.37		5.47	
W6x9	4	25	2.58			7.31	
W6x9	3	25		5.41		6.21	
W6x9	3	50	4.23	7.97		7.36	
W6x9	4	50				7.17	
W6x9	15	50				7.57	

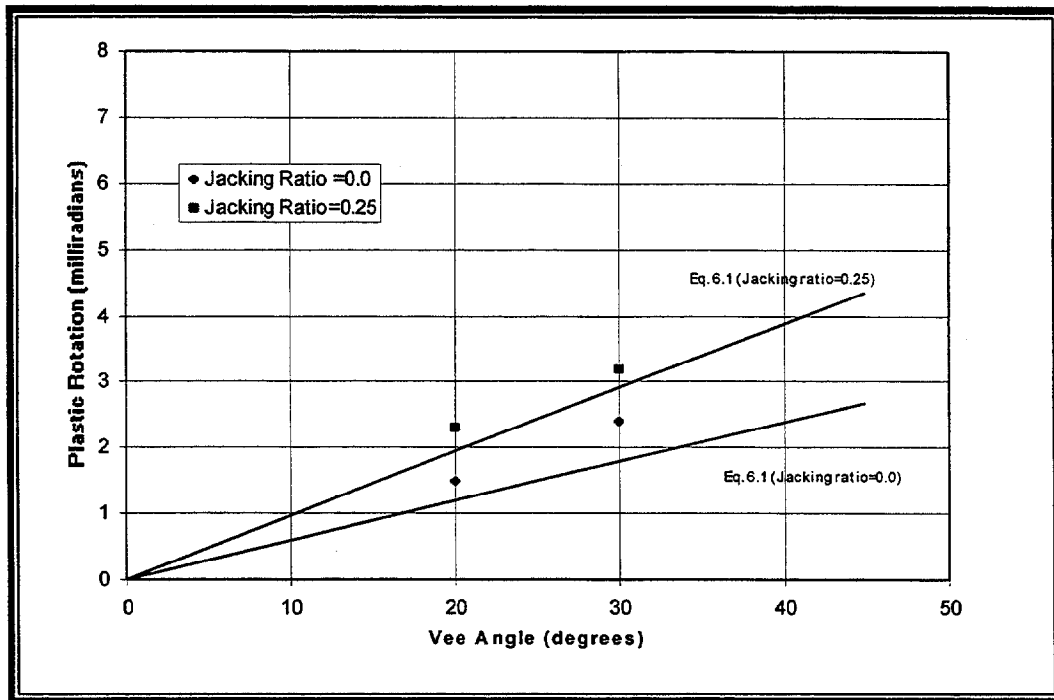


Figure 6.15. Influence of vee angle and jacking ratio on plastic rotation for W 6x9 (Category S damage pattern).

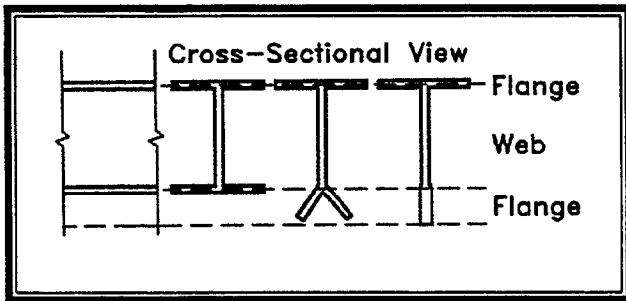


Figure 6.16. Geometric relationship between Category S wide flanges and plates.

The theoretical equation for the W 12x14 is plotted in fig. 6.15. The theory agrees reasonably well with the data.

Angles

Angles differ from other rolled shapes in that the plate elements of the cross section are not orthogonal to the principal axes. As a result, the damage to angles is often due to flexure about an axis other than a principal

axis. In addition, the jacking force applied during heat straightening often causes flexure about a non-principal axis. In one sense the angle is the most simple of rolled shapes which can be considered as a plate with a single fold. The heating pattern consists of a vee on one plate element and a strip on the other element as shown in fig. 6.17a or simply a vee heat if the apex of the vee is located at the stiffening element (fig. 6.17b). The results of tests on originally straight angles using the heating pattern of fig. 6.17a are shown in fig. 6.18. Other parameters included jacking ratios, M_j/M_p , of 0, 25 and 50 percent; vee angles of 20° and 45°; a depth ratio = 1.0; and a heating temperature 650°C (1200°F). In general the plastic rotations were significantly larger than for equivalent plates. The reasons for this

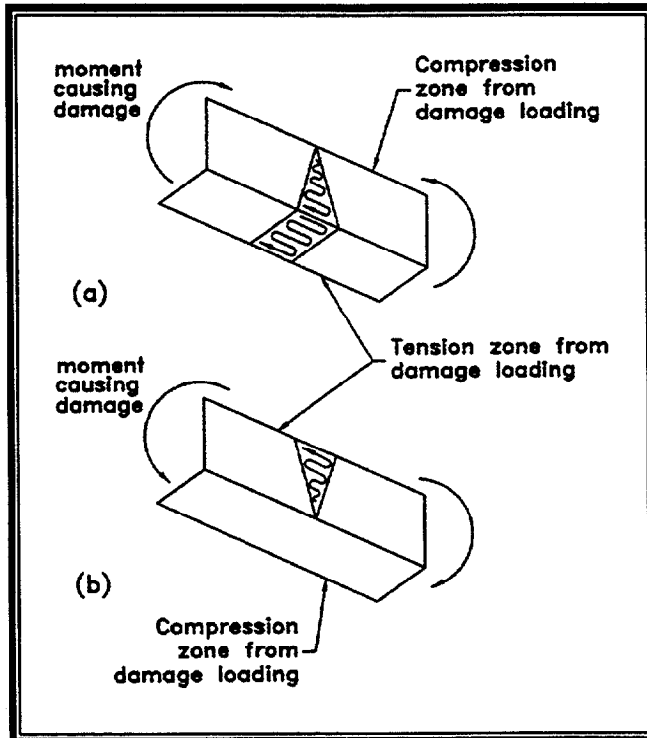


Figure 6.17. Yield zone and heating patterns for flexural damage of a typical angle.

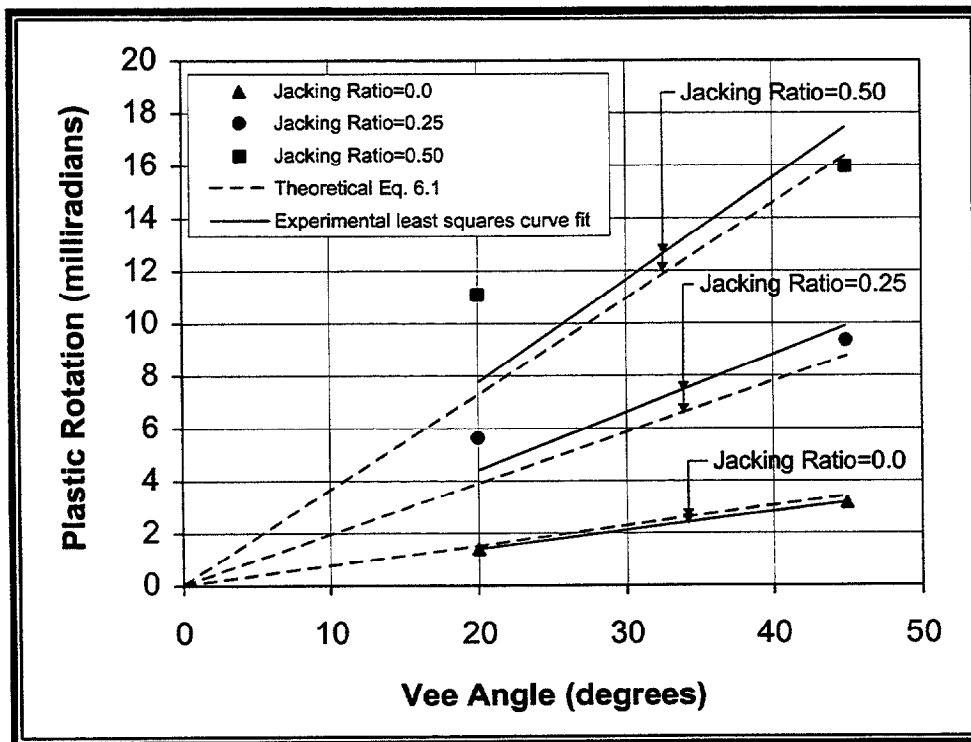


Figure 6.18. Influence of vee angle and jacking ratio on plastic rotation for L 4x4x1/4 angles with the heating pattern of fig. 6.17a.

behavior involve both geometric and stress considerations.

The geometric amplification for the angle is (with the apex at the toe per fig. 6.17a) the same as that of the category S channel. Using the same assumptions as for the channel (fig. 6.6), the shape factor, F_s , is the same as given by eq. 6.12 where $d_s = d$ = the leg length being vee heated and b_s = the width of the other leg.

If a jacking force is applied during the heating process, the stress distribution throughout the vee heat zone differs for an angle compared to a plate. First, the ratio of plastic to elastic section modulus is lower. Second, since the cross-section is not symmetrical, bending about the primary element is biaxial unless some type of lateral restraint is used. If no lateral restraint is provided, the simple bending stress formula, M/S , cannot be used to calculate stresses in the vee heated area due to the jacking force. Instead, the biaxial bending formula must be utilized. For example, an L 4 x 4 x 1/4 angle bent about the axis of one leg and having no lateral restraint has a maximum stress at the heel of 2.5 times that for the laterally restrained case.

In order to incorporate this behavior into the stress factor, the ratio of Z/S will be modified by the shape factor, F_s . The stress factor is defined by eq. 6.5 in which the ratio of Z/S is defined as

$$Z/S = F_s(Z'/S') \quad (\text{Eq. 6.14})$$

where Z'/S' is the ratio of plastic to elastic section modulus for the angle about the axis of bending.

The plastic rotation can thus be expressed by eqs. 6.1 and 6.2 where F_ℓ is given by eq. 6.7, F_s by eq. 6.12, and F_a by eqs. 6.5 and 6.14. This theoretical curve is plotted in fig. 6.18 and show relatively good agreement.

A series of angles were damaged and then heat straightened with the vee pattern shown in 6.17b and the results are shown in table 6.4. The magnitudes of plastic rotations were not magnified to the extent of the previous case since with the apex of the vee at the heel, the shape factor is one and only the stress amplification factor is needed. Thus the plastic rotation is given by eqs. 6.1 and 6.2 where $F_s = 1.0$ from eq. 6.12, F_ℓ is given by eq. 6.7, and F_a by eqs. 6.5 and 6.14. The theoretical values are shown in table 6.4 and compare reasonably well with most of the experimental values.

Out-of-Plane Movement.-Based on the geometric configuration of angles, an out-of-plane movement (in the direction perpendicular to the desired direction of movement) would be expected to occur. With the linear continuous strain concept for folded plates, even though the stiffening element is heated with a rectangle, its strain behavior resembles that of a vee heat and thus the stiffening element would shorten more on one edge than the other (at the free edge away from the vee heated leg in the case of the angle). For the angles shown in fig. 6.18 the average out-of-plane plastic rotations were measured and compared to the plastic rotations in the desired direction. These values and comparisons are shown in table 6.5. As can be seen from table 6.5, the out-of-plane movements are quite large in all cases, and they increase significantly with jacking ratio. However, when

Table 6.4. Damaged angle specimens with the heating pattern shown in fig. 6.17b¹.

Specimen/Damage Category	M_f/M_p	Depth Ratio	No. of Heats	Avg. Plastic Rotations (milliradians)	Theoretical Plastic Rotations (milliradians)
L6x4x5/16 (S)*	0.22	1.00	3	4.66	4.31
L6x4x5/16 (S)	0.50	1.00	16	9.10	7.31
L6x4x5/16 (W)	0.50	1.00	3	11.11	7.19
L4x4x1/4	0.33	0.75	2	5.57	7.28
L4x4x1/4	0.33	1.00	5	6.75	7.28

¹S denotes bending about axis of long leg, W denotes bending about axis of short leg. All vee heats were 45°, and all had the stiffening element at the vee apex and heating temperatures = 650°C (1,200°F)

Table 6.5. Comparison of out-of-plane plastic rotations to plastic rotations in the in-plane direction of movement for initially straight L 4x4x1/4 angles (in-plane movement shown in fig.6.18).

Vee angle (Deg)	M_f/M_p	Out-of-Plane Plastic Rotations (millirad)	Ratio of Out-of-Plane to In-Plane Movement
20	0	2.93	2.07
20	0.25	4.03	0.72
20	0.50	6.59	0.59
45	0	4.55	1.44
45	0.25	7.85	0.84
45	0.50	10.76	0.67

compared to the plastic rotations in the desired direction, the zero jacking ratio cases exhibited more relative movement. In fact, the out-of-plane movements were greater than the in-plane ones. The large out-of-plane movements are probably a result of the vee heated leg of the angle already being heated and offering less resistance to rotation. The lower ratios of out-of-plane to in-plane movement encountered at larger jacking ratios are probably due to an ineffective distribution of stresses in the outstanding leg.

Depending on whether or not the out-of-plane movements are beneficial to the overall repair of the given specimen, either bracing against this movement or using alternative heating patterns may be necessary to prevent or reduce them. The vee heat would be applied as normal, and the stiffening element would still need to be heated to allow rotation in the desired direction. However, instead of a rectangular heating pattern, it is likely a reverse vee heat (continuing from the open end of the original vee, and tapering down to a point) would encourage the desired rotation, while reducing the out-of-plane movement. In its "unfolded" position, the heating pattern would resemble a diamond shape, a pattern used by pipe welders to straighten pipe distortions. Heating in the proper fashion is essential for obtaining movement.

Example 6.1

Problem.-A beam is damaged in flexure producing a 4.5° degree of damage at the impact point. Compute the estimated number of heats to straighten the member for each of the following sections using a jacking ratio of 50 percent and 30° vee angle: (a) W 36x170 (weak axis bending), (b)

C 12x20.7 (strong axis bending), (c) L 5x3x5/8 (bending about the axis of the short leg with tension damage to short leg.

Solution.-The first step is to compute the expected movement per heat cycle using eq. 6.1. For all cases ϕ_b is computed from eq. 6.2 as:

$$\phi_b = 0.0147 \sin\left(\frac{30}{3}\right) = 0.00255 \text{ rad} = 2.55 \text{ millirad}$$

and F_ℓ is obtained from eq. 6.7 as

$$F_\ell = 0.6 + 2(.5) = 1.6$$

The other factors are dependent on the cross section and are calculated as follows:

(a) W 36x170 (Category W damage)

$$d_s = 12.03 \text{ in} / 2 = 6.02 \text{ in}$$

$$b_s = 36 \text{ in}$$

$$d = 12.03 \text{ in}$$

$$Z/S = 83.8 \text{ in}^3 / 53.2 \text{ in}^3 = 1.58$$

From eq. 6.5

$$F_s = 1 + \frac{1}{2} \left[\frac{(36)(6.02)}{12.03^3} \right] = 1.75$$

From eq. 6.12

$$F_a = 1 - 2 \left\{ 1 - \frac{2}{3} (1.58) \right\} (1.5) = 1.05$$

and from eq. 6.1

$$\phi_p = (1.6)(1.75)(1.05)(2.55) = 7.50 \text{ millirad}$$

(b) C 12x20.7 (Category S damage)

$$d_s = 12 \text{ in}$$

$$b_s = 2.94 \text{ in}$$

$$d = 12 \text{ in}$$

$$Z/S = 3.49/1.73 = 2.02$$

From eq. 6.5

$$F_s = 1 + \frac{1}{2} \left[\frac{(2.94)(12)}{12^2} \right] = 1.12$$

From eq. 6.12

$$F_a = 1 - 2 \left\{ 1 - \frac{2}{3} (2.02) \right\} (1.5) = 1.35$$

and from eq. 6.1

$$\phi_p = (1.6)(1.12)(1.35)(2.55) = 6.17 \text{ millirad}$$

- (c) L 5x3x5/8 (bending about axis of short leg with tension damage to short leg)

The vee heat should be located on the long leg with the apex at the toe.

$$d_s = 5 \text{ in}$$

$$b_s = 3 \text{ in}$$

$$d = 5 \text{ in}$$

$$Z/S = Z_x/S_x = 6.27/3.55 = 1.77$$

From eq. 6.5

$$F_s = 1 + \frac{1}{2} \left[\frac{(3)(5)}{5^2} \right] = 1.3$$

From eqs. 6.5 and 6.14

$$F_a = 1 - 2 \left\{ 1 - \frac{2}{3} (1.3)(1.77) \right\} (1.5) = 1.53$$

and from eq. 6.1

$$\phi_p = (1.6)(1.3)(1.53)(2.55) = 8.12 \text{ millirad}$$

The number of heats can be determined from eq. 3.15 where the degree of damage $\phi_a = 78.5$ milliradians as follows:

For the W 36x170

$$n = 78.5/7.5 = 10.5 \text{ or } 11$$

For the C 12x20.7

$$n = 78.5/6.17 = 12.7 \text{ or } 13$$

For the L 5x3x5/8

$$n = 78.5/8.12 = 9.7 \text{ or } 10$$

Summary

Summarized in this chapter is the response of rolled shapes to heat straightening. The focus was on the two fundamental damage conditions: weak axis bending (Category W) and strong axis bending (Category S). Over 300 heats were applied to 30 rolled shapes in order to document the behavior of heat-straightened, angles, channels and wide flange beams. This data formed the basis for developing simple analytical formulas for predicting the response of rolled shapes to heat straightening. These formulas can be used to design heat-straightening repairs.

Key Points to Remember

- There are four fundamental damage categories for rolled shapes:
 - ◆ Category S: Bending about the strong axis.
 - ◆ Category W: Bending about the weak axis.
 - ◆ Category T: Twisting.
 - ◆ Category L: Local bulges, dishes and crimps.

- The heating pattern for rolled shapes typically consists of vee heats on the primary elements and strip heats on the secondary elements.
- If a secondary element lies at the apex of the vee heat on a primary element, a strip heat is not applied.
- The amount of movement when heat straightening rolled shapes is a function of: the vee angle, heating temperature, magnitude of the externally applied jacking force, the shape of the cross section, and the distribution of stresses due to jacking.
- Typically, the factors listed above tend to magnify the movement above that expected from a vee heated plate of the same size as the primary element (or elements) of the rolled shapes.
- Heat straightening of angles produces components of movement in directions parallel to both legs even when only one may be desired.
- Rolled shapes can be damaged and repaired multiple times with similar movement response although it is recommended that the same area not be repaired more than twice.
- The first heat cycle often produces larger movements than successive cycles due to residual stresses.
- Analytical formulas were derived to predict movement during heat straightening of rolled shapes subjected to Category S and W damage.
- The analytical formula was based on the plate equation (eq. 5.21) modified by the addition of a shape factor, F_s , and a

stress factor, F_a , and can be generalized for rolled shapes as

$$\varphi_p = F_\ell F_s F_a \varphi_b$$

where the basic plastic rotation factor, φ_b , is defined as

$$\varphi_b = 0.0147 \sin \frac{\theta}{3}$$

and the modification factors are:

$$F_\ell = 0.6 + 2 \frac{M_j}{M_p}$$

$$F_s = 1 + \frac{1}{2} \left(\frac{b_s d_s}{d^2} \right)$$

$$F_a = 1 - 2 \left\{ 1 - \frac{2}{3} \left(\frac{Z}{S} \right) \right\} \frac{M_j}{M_p}$$

where

M_j = the moment at the heated zone due to the jacking force;

M_p = the ultimate plastic moment capacity about the axis of damage;

Z/S = The ratio of plastic-to-elastic section modulus about the axis of damage (except for angles in which the ratio is multiplied by F_s);

b_s = width of stiffening element;

d_s = distance from apex of vee heat on primary member to intersection of stiffening element; and

d = depth of the vee heated elements (assuming a vee depth of at least three-quarters of this depth).

Chapter 7. Heat-Straightening Repair for Composite Deck-Girder Bridges

Perhaps the most typical type of damage found on steel bridge members results from impact of vehicles or freight on the beams or girders of composite deck-girder bridges. Heat straightening is an attractive repair alternative because of its low cost and minimal disruption of traffic. However, little information has been available to guide either the Engineer or the heat-straightening technician on safe and acceptable implementation procedures. The purpose of this chapter is to provide such a guide.

The available literature shows little quantitative research related to heat-straightening repair of composite deck-girder bridges. Moberg (1979) described a limited field investigation of the heat-straightening behavior of damaged bridge members. Shanafelt and Horn (1984) addressed the general damage assessment of structures and suggested an approach for using heat straightening as one of several repair alternatives. A comprehensive summary of the state-of-the-art of heat straightening given by Avent (1989) emphasized the lack of quantified engineering data on heat-straightening repair procedures and addressed myths about heat-straightening repair. To provide quantified heat-straightening data, Avent and Fadous (1989) initiated a study of the behavior of composite girders followed with additional research conducted by Avent, et. al., (1993).

Several important questions arise in conjunction with heat straightening composite deck-girder bridges: What is the role

of internal and external constraints? What are the important parameters for straightening composite members? What is the basic methodology? Why do the members sometimes crack during repair? How much jacking restraint can be safely applied? And can movements be accurately predicted analytically?

One fundamental parameter that has been overlooked in previous studies is the internal redundancy of the structure. Often, the damaged steel member in the field displays an inherent redundancy due to its structural configuration, imposing an internal constraint on the potential heat-straightening mechanism for the member. An understanding of this behavior combined with knowledge of the role of jacking forces in heat-straightening is needed to answer these questions.

First, a detailed and controlled set of field experiments is summarized which were designed to provide a more comprehensive data base on the field behavior of damaged composite bridge members. Second, the heat-straightening behavior of those members is quantified both analytically and experimentally. Emphasis is placed on studying the interaction of the internal redundancy with both the external restraining forces and heat patterns. A number of heat-straightening tests have been conducted using two 6 m (20-ft) long, A-36 steel beams of different geometries (W10 x 39 and W24 x 76). Each beam was damaged and then repaired using the heat-straightening method. The level of jacking forces was

varied in the course of repair to evaluate the effect of external restraining forces. Based on these experiments, analytical models and guidelines for conducting such repairs are given.

Experimental Procedures

There are inherent problems associated with conducting research on actual bridges in the field. Among the most important are: public safety and traffic control; variability in the level and degree of damage; and limitations on conducting parameter studies. As a consequence, it was decided to simulate heat straightening of an in-service damaged member with a test facility capable of handling full-scale beams. In addition to mitigating the problems cited, the facility also provides a training facility for engineers and operators. The test frame has been designated as the **Heat-Straightening Evaluation And Testing (HEAT)** facility.

A prominent feature of the HEAT facility is the ability to control the damage-inducement process. Static as well as dynamic loading can be applied to distort the member plastically. Static loads were applied by the use of a hydraulic jack, while dynamic loads were created by an impact ram. In addition, a special U-shaped reference frame was constructed for specimen measurements. Eight measuring points were taken at each cross section: five points defining horizontal movement and three defining vertical movement.

Three primary parameters affecting heat straightening—vee angle, heating temperature, and depth ratio of vee to plate element—have been discussed in previous chapters and reported elsewhere (Avent 1987; Boudreaux 1987; Nichols and Weerth

1972; and Roeder 1986). However, three additional parameters have also been shown to play a central role in the heat-straightening process. One factor relates to the influence of restraining forces, a second to the heating patterns used, and a third to the damage-inducement pattern. The best way to evaluate these factors is to study actual structural systems.

The HEAT facility is unique in allowing, for the first time, a comprehensive evaluation of heat straightening as applied to prototype structures. Within the limits previously described for prototype experimental girders, five specific aspects of heat straightening were evaluated: (1) The degree to which restraining forces affect behavior during the process; (2) the effect of various heating patterns on movement; (3) the effect of successive heating cycles on damage restoration; (4) the effect of repetitive damage and straightening on material properties of the steel; and (5) an evaluation of whether dynamic (as opposed to static) damage inducement influences the heat-straightening process. Until these tests, there had been little documented evidence related to each of the characteristics.

Heat-Straightening Repair of a W 10x39 Composite Beam

An initially straight composite beam was statically loaded to produce a plastic lateral deformation of 70 mm (2.75 in) at mid-length of the bottom flange. A force of 125 kN (28,000 lb) was required. The pattern of damage shown in fig. 7.1 is typical for bridge girders and the level can be classified as light to moderate. Two yield zones were formed as a result of the load application. The lower flange yielded in flexure

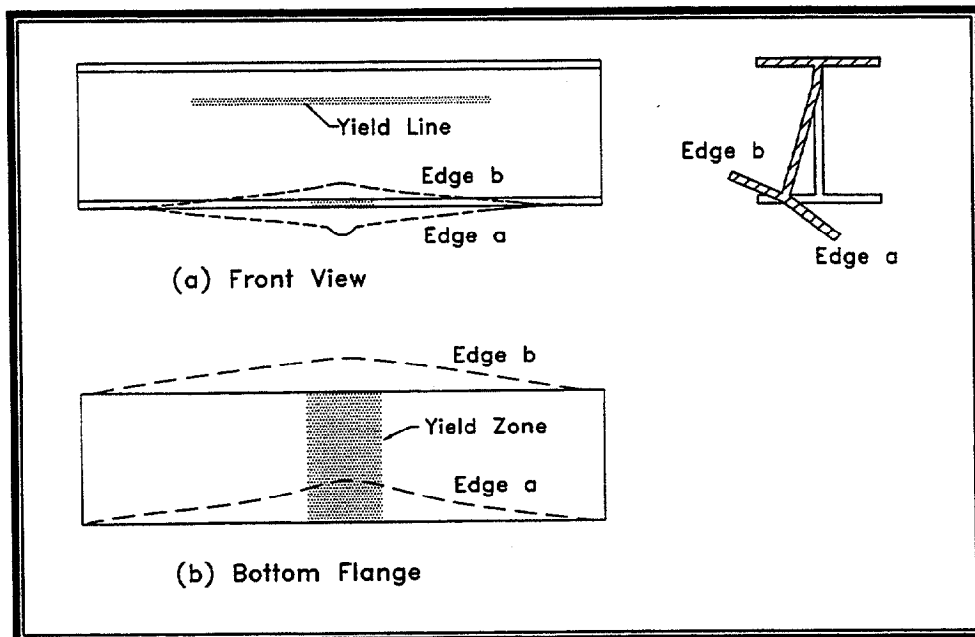


Figure 7.1. Typical deformed shape and yield zones in damaged composite girders.

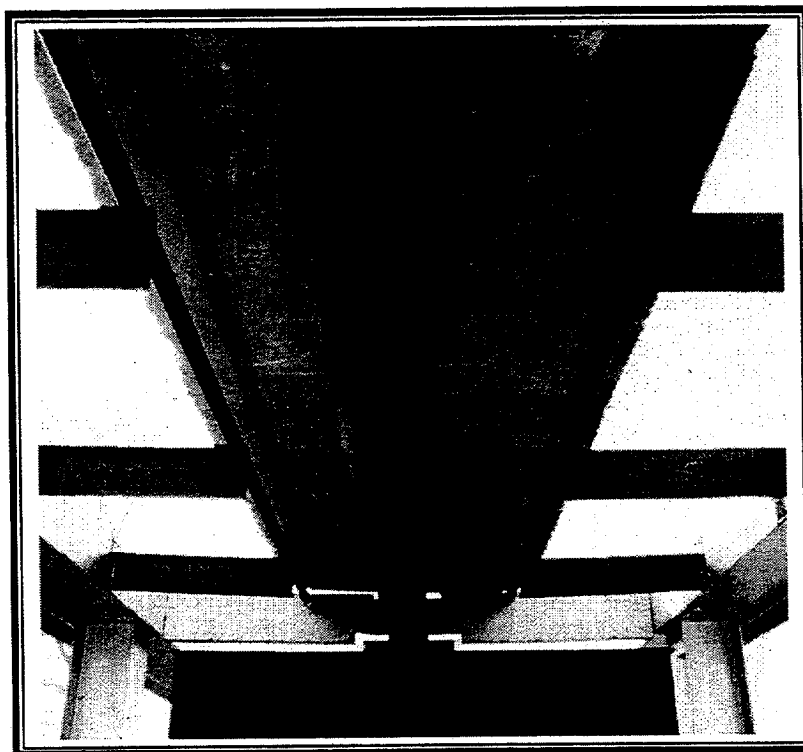


Figure 7.2. View from underside looking up at damaged beam SB-1.

(about the strong axis of the flange plate) over a short length and there was a local bulge in this region. A yield line also formed in the web approximately 57 mm (2-1/4 in) below the top flange, extending over the middle two-thirds of its length. A view of the damaged beam in the HEAT facility is shown in fig. 7.2.

Typically, a lateral jacking force is applied to the lower flange during heat-straightening repair. However, the determination of the jacking ratio is complicated for composite girders due to the internal redundancy of the system. First, when a lateral jacking force is applied to the lower flange, only a portion of that force produces a moment in the flange. Part of the force follows a load path through the web into the upper composite flange and is resisted by the concrete deck. The determination of the actual moment in the lower damaged flange is required to prevent over-stress during jacking and to predict the expected movement. Second, the moment capacity due to a laterally applied load is also influenced by the load path transfer making it difficult to compute the plastic moment capacity, M_p .

The procedure adapted here is to define the apparent moment due to jacking, M_j , as the moment carried by the lower flange assuming all the jacking force was transferred to the lower flange alone. Likewise, the lateral capacity of the beam, M_p , is defined as the plastic moment of the lower flange alone about its strong axis. The ratio of M_j to M_p will be referred to as the apparent jacking ratio. The actual moment in the lower flange due to the jacking force will be referred to as M_f and will be expressed as a percentage of M_j .

Five primary heating patterns/ jacking combinations were used in the repair, with a sufficient number of repetitions to establish the pattern of behavior. The basic heating pattern is shown in fig. 7.3. In two cases, a single vee heat on the bottom flange was used and the restraining force, applied laterally at the center of the bottom flange, produced an apparent jacking ratio (M_j/M_p) of either 56 percent or 112 percent. The other two cases were identical, except that a line heat was also applied to the center two-thirds of the web along the length of the girder at the damage-induced yield line. In all cases, the vee heats were identical: a vee depth of three-quarters of the flange width, a 30° vee angle, and a constant heating temperature in the range of 650°C (1,200°F) (as measured with contact pyrometer and multiple temperature crayons). The vee heat was always applied within the yield zone of the flange at the point of maximum curvature. A single-orifice oxyacetylene torch was used for the heating. Graduate students trained in heat straightening performed the heats.

After the completion of the repair process, the same W 10x39 girder was re-damaged by exerting a concentrated static force with a midspan jacking device. That force caused a permanent deflection in the bottom flange of 57 mm (2.23 in) in magnitude. A load-deflection curve was obtained during the process. Considering the elastic rebound, the initial yield load could be estimated as 71kN (16,000 lb). Based on this yield value, the external jacking force was limited to 35 percent of initial yielding. Since a 650°C (1,200°F) temperature can reduce the yield stress to approximately one-half to one-third its original value, this limit was intended to ensure that hot mechanical

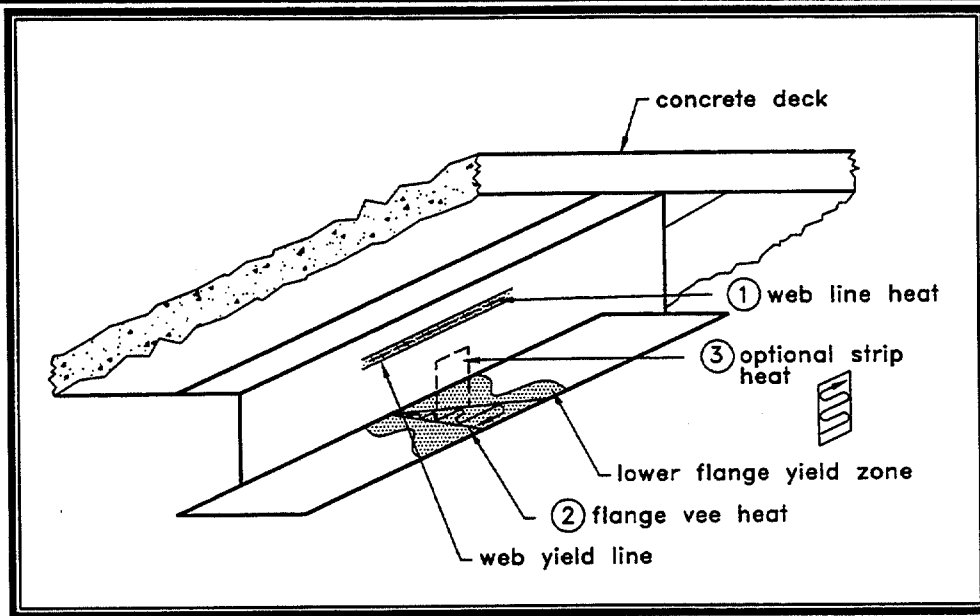


Figure 7.3. Heating patterns for composite girder.

straightening did not occur. This jacking force corresponded to a force which would produce approximately 100 percent of the plastic moment in the bottom flange acting alone. The damage was quite similar to that of the first case.

A number of combinations of vee heat, line heat and jacking ratios were used. A summary of all sequences of heats is shown in table 7.1 and comparisons of the average plastic rotation and the jacking ratio for seven sequences are plotted in fig. 7.4. An inspection of the data shows that certain heating patterns are much more effective than others. Two aspects accounted for behavior differences: (1) The magnitude of the restraining force; and (2) the inclusion of the line heat on the web in addition to the vee heat on the lower flange. While these conditions may seem independent, they are actually related. Both laboratory research (Boudreaux 1987; and Roeder 1986) and field experience (Moberg 1979) have shown

that applying a constraint force in a direction tending to reduce damage curvature expedites the heat-straightening process. Conversely, a constraining force applied in the opposite direction can result in little or no straightening effect after heating (Roeder 1986). The most effective combinations of heating patterns and restraining forces are ones that minimize any internal constraints inhibiting the straightening while maximizing the positive external constraint effect. For any damage condition, an analysis of these factors is required to optimize straightening effects. For the case under discussion here, the wide flange can be analyzed in terms of its web and bottom flange plate components as interacting elements. Each has plastically deformed so attempting to straighten the first component independently of the second leads to the second component acting as a negative constraining force rather than a positive one.

Table 7.1. Summary of plastic rotations for a damaged composite W10 x 39 beam after heat straightening with various heating patterns.

Damage Cycle	Heating sequence	No. of Cycles	No. of simultaneous vee heats	No. of web line heats	Apparent Jacking ratio	Average plastic rotation per vee heat (milliradians)
1	1	7	1	0	0.56	0.27 ⁴
1	2	8	1	0	1.12	0.93
1	3	8	1	1	1.12	3.53
1	4	4	1	1	0.56	0.96
1	5	5	1 or 2 ¹	1 ²	1.12	1.76
2	6	13	2 ³	1	1.00	1.32 ⁴

¹Two simultaneous vees were used in two cycles while only one vee was used in the other three
²Only a partial line heat was used omitting the center one-third of the web yield line since this portion was essentially straight
³The first heating cycle had only a single vee heat
⁴The movement from the first heat of each sequence after damage inducement was not included in the average

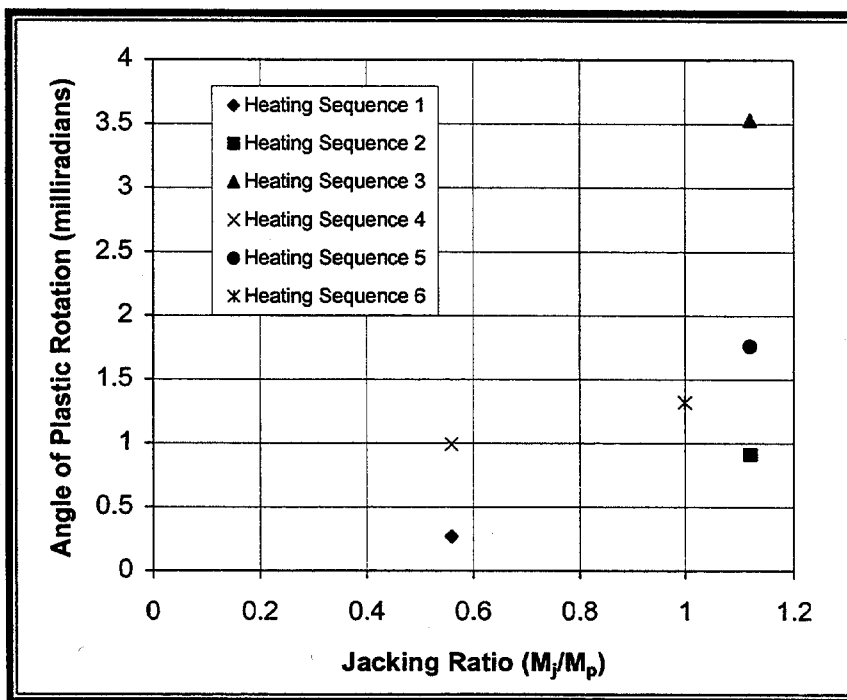


Figure 7.4. Comparison of average plastic rotation for various patterns and jacking ratios.

As a general rule, heat should be applied in the vicinity of every zone in which plastic deformation has occurred to reduce this negative restraint. The heating pattern should correspond to the specific type of damage. This principle is illustrated when comparing the first pair of heating patterns (1 and 2) to the second pair (3 and 4). In sequences 1 and 2, the vee heat was applied to the plastic zone of the bottom flange without a web line heat. Since the web was unheated, it tended to resist the straightening effect of the flange. Even with a positive external force applied to the flange, the restoring effect was relatively small.

In sequences 3 and 4, the yield line in the web was heated in addition to the vee heat in the flange. As a result, the restoring effect was more than doubled during each sequence. In a similar fashion, the application of an external restraining force acting in the direction of desired movement enhanced the process. Doubling the external force more than doubled the restoring movement for both heating patterns. A method of computing the safe limitations for such forces is discussed in a latter section.

Several interesting behavior patterns were noted when comparing the heating effect cycle-by-cycle. It was observed that a significantly larger amount of movement occurred from the first heat of a given sequence after damage was initiated than after successive heats of the sequence. Residual moments caused by the damage inducement are the primary cause of this phenomenon. After damage, the internal redundancy prevents full elastic rebound. Thus, there is a residual moment tending to straighten the beam in addition to the jacking force. The combination of forces results in larger

movement than expected. Most of the residual moment is relieved after one heat so that subsequent heats do not exhibit this behavior. In computing average values, the first heat of sequences 1 and 6 were excluded for this reason.

Careful measurements of the web were made and the length of the yield line was computed after each heating cycle. At the beginning of the 5th sequence, the central 635 mm (24-in) portion of the web yield line had been completely straightened. This portion corresponded in length to the yield zone of the flange where the inelastic deformation occurred. To have continued applying a line heat in this region would have produced some reverse curvature along the web yield line. Therefore, in sequence No.5, the center 0.635 m (2 ft) length of web was not heated. Rather, the line heat was only applied to those portions still showing plastic curvature.

The removal of the web curvature using the line heat is based on the same principle as the vee heat. The cold material ahead of the heat, along with the restraints of the lower flange and external force, holds the plate in its initial position creating the upsetting effect. Once the entire line is heated, the resistance to contraction is decreased and rotation occurs during cooling, tending to straighten the plate. By itself, the line heat produces movements which are small compared to those produced by vee heats. However, when the lower flange is also being straightened, this tends to pull the web plate even straighter. In contrast, when the line heat was applied without the lower flange vee heat, negligible movement was detected.

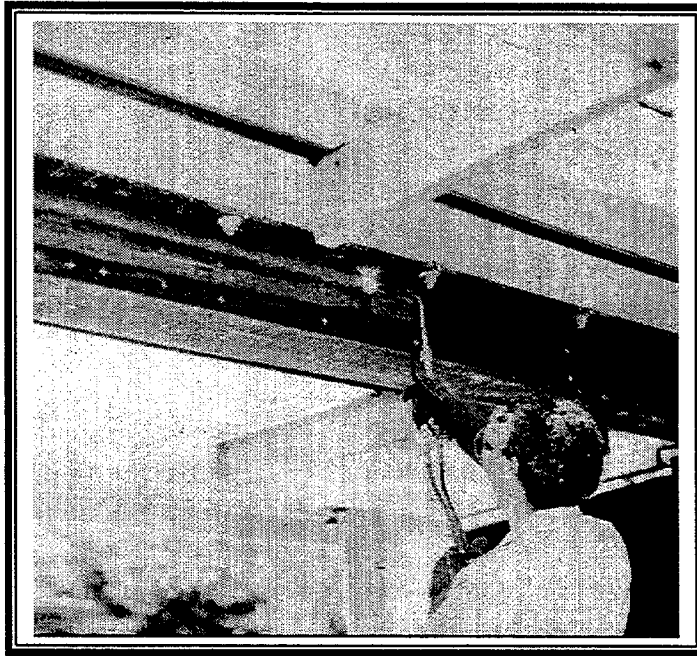


Figure 7.5. Line heat in progress on a composite girder.

Two single-orifice torches were used to perform the heating sequences with line heats. As shown in fig. 7.5, the line heat was applied first to the convex crest of the web yield line, starting from the outside ends and moving toward the middle in a longitudinal direction. Just before getting to the middle portion, one of the operators stopped heating the web and started heating the vee area in the bottom flange, while the other operator continued the line heat. This procedure allowed both operators to finish the heating cycle simultaneously. The heated areas in the middle portion of the beam, both in the web and in the flange, thus reached maximum temperature at the same time.

After successfully heat-straightening the lateral displacement of the bottom flange, two localized bulges still existed in that flange. To achieve a complete restora-

tion to the original undeformed shape of the girder, the bulges were removed. Both spot heats and circumferential line heats were applied to the "dish-like" bulge. As a result of removing the bulge, the lower flange deflected laterally backwards 7 mm (0.28 in) in a direction opposite to the earlier movements. That movement was expected, since the spot heats were acting similarly to small vee heats placed in the wrong location. A detailed discussion of straightening local bulges is given in Chapter 9.

The beam was re-damaged as described previously and heating sequence No. 6 was used to completely straighten the beam. The heating pattern was similar to that shown in fig. 7.3, except that two simultaneous vee heats were used on the lower flange. Essentially, only the most effective heating pattern from the previous case was used throughout. The first heating cycle was performed using one vee heat. All

subsequent cycles were applied using two vee heats simultaneously. The decision to apply two vee heats in the same heating cycle was made because the middle portion of the bottom flange contained two sharp regions of curvature. In addition to the vee heats, each heating cycle involved a line heat along the yield line in the web. A total of 13 cycles was required prior to removing the local flange buckles. At the end of the repair process, the "dish-like" distortion in the bottom flange was also removed using line and vee heats.

The values of the average plastic rotation per vee heat for sequence No. 6 is shown in table 7.1. Fig. 7.6 shows a plot of the progressive effect of heats on the behavior of the girder. After the application of the thirteenth heating cycle, the lateral displacement of the girder was eliminated. However, the "dish-like" distortion was still present in the bottom flange. A final sequence of line and spot heats was applied to remove the "dish-like" distortion which existed in the bottom flange. This process also produced a reverse lateral deflection of 4.6 mm (0.18 in). One additional heat cycle of sequence 6 was applied to remove the slight out-of-plane curvature which developed in the bottom flange during removal of the bulge. This last heating cycle removed most of the lateral deflection resulting from the removal of the bulges.

Heat-Straightening repair of W 24x76 Composite Beams

Rather than use gradually applied static loads to induce damage, a swinging ram was used in the first case of damage to a W 24x76 beam. The girder was supported similarly to the W 10x39: composite connection to the slab, simple supported ends

for resistance to gravity loads, and diaphragms at the ends for resistance to lateral loads. The ram was a 15kN (3,400 lb) steel section which was suspended from a 12 m (40 ft) crane boom. Damage was induced by swinging the ram in pendulum fashion such that the bearing plate impacted the lower flange of the beam. The type of damage was similar to that of the previous beam. The maximum deformation, which occurred at point of impact, was 110 mm (4.33 in).

The repair process was similar to the most efficient of the previous cases. The horizontal component of the jacking force applied as an external constraint produced an apparent $M_j/M_p = 0.33$. For each heating cycle, a single 650°C (1,200°F), three-quarter-depth, 30° vee heat was used to repair the damage. During each heating cycle, a line heat was used along the yield line. The location of the flange vee heat was varied from cycle to cycle over the 610 mm (2 ft) yield zone. The straightening process (sequence No.7) required 28 heating cycles for completion. The average value of the plastic rotation achieved during this sequence shown in table 7.2. Again, significantly larger plastic rotation angles were obtained during the first cycle.

The same girder was damaged a second time and then repaired (sequence No.8). In this case a gradually applied static load was used to induce the damage and a lateral load-deflection curve was obtained. The resulting damage was similar to the previous case with a bottom flange deflection of 53 mm (2.1 in). The girder was repaired in an identical manner, except that two vee heats were applied simultaneously during each heating cycle.

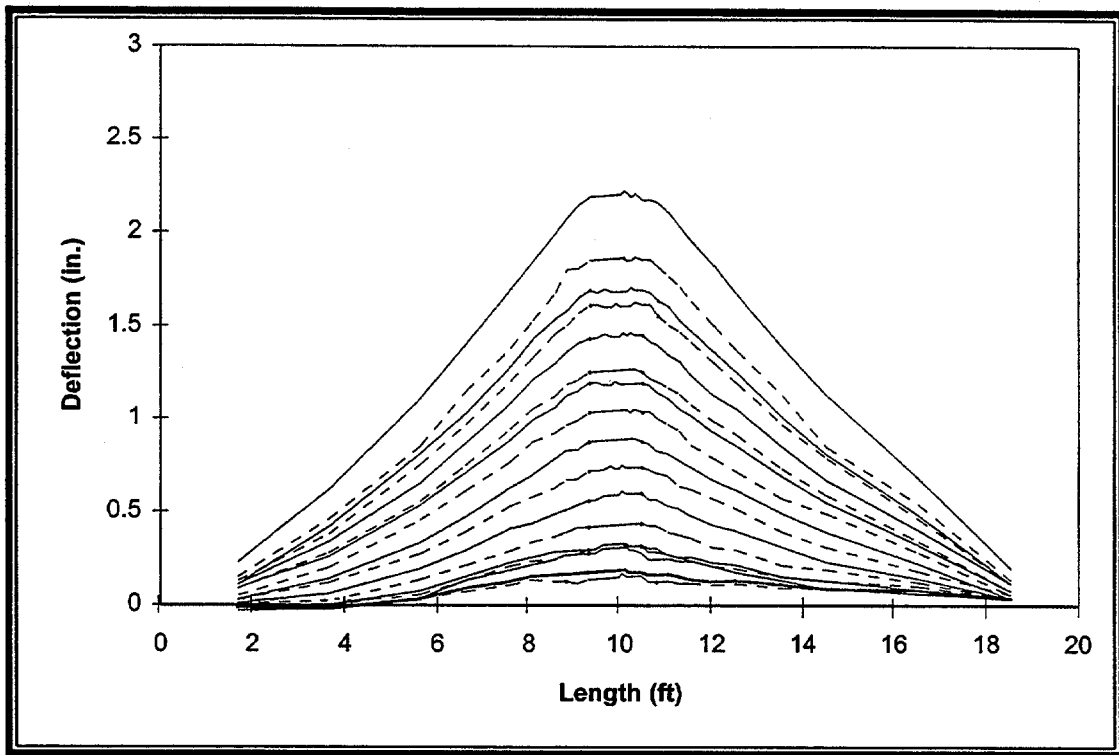


Figure 7.6. Heat straightening progression for a damaged W 10x39 beam using heating sequence No. 6 (25.4 mm = 1 in).

Table 7.2 Summary of plastic rotations for a damaged W24 x 76 beams after heat straightening with various patterns.

Damage Cycle	Heating sequence	No. of Cycles	No. of simultaneous vee heats	No. of web line heats	Apparent Jacking ratio	Average plastic rotation per vee heat (milliradian)
1	7	28	1	1	0.33	2.22 ²
2	8	12	2	1	0.33	2.48 ²
3	9	11	1	1	0	2.99 ²
3	10	9	1	1	0.5	3.89
3	11 ¹	10	1	1	0.5	3.75
4	12	8	1	1	0.33	4.33 ²
1	13	7	1	1	0.75	9.99 ²

¹A half depth web strip heat was also used in this sequence
²The movement from the first heat of each sequence was not included in the average

The results are tabulated in table 7.2 and were similar to those of sequence No. 7.

The same W 24x76 beam was damaged a third time. Damage was induced by statically loading the beam to obtain a flange lateral plastic deformation of 127 mm (5 in). At the midspan. Thirty heating cycles were conducted with three jacking ratio and heating pattern variations (sequences 9-11). A 30-degree vee angle, three-quarter-depth vee, and heating temperature of 650°C (1,200°F) were maintained throughout. The heat patterns consisted of a vee heat in the plastically deformed portion of the bottom flange accompanied by a line heat applied to the yield line in the web.

The heat-straightening parameters used and plastic rotations found are shown in table 7.2. Sequence No. 9 was conducted without a jacking force, and sequences 10 and 11 were performed with an apparent jacking ratio of 0.50. At the completion of nine heats of sequence No. 10, it was observed that the web had developed considerable bulging about the minor axis in the lower half of its depth, extending over a central span of 460 mm (18 in). The longitudinal contraction in the heated bottom flange had apparently created enough longitudinal residual stresses in the lower web section to cause buckling. Because the beam had been damaged and straightened several times, the flange shortening had become significant. To alleviate the problem, it was decided to apply half-depth strip heats on the web at the location of the vee heat. The width of the strip heat was kept equal to the width of the vee at the flange fillet. Sequence No. 11 consisted of this modified pattern with a 0.5 apparent jacking ratio. The application of the strip heats did not

significantly affect the plastic rotations. However, the strip heats effectively relieved the buckling in the web. At the end of 10 cycles of Sequence No. 11, the girder was restored to practically its original configuration. The plastic curvatures in the bottom flange as well as the web were corrected. Only a minor local kink remained in the bottom flange at the center of damage. The local bulge was still discernible in the web because of the earlier buckling, but it was less severe.

The same W 24x76 girder was re-damaged statically by a midspan jacking load for a fourth time. A permanent lateral deflection, 114 mm (4.5 in) in magnitude, was obtained at the center of the damaged flange. The heating patterns and repair procedures were identical to those shown in fig. 7.3. The strip heats were not included in the heat pattern, because the damage had stretched the web back into its unbuckled configuration. An apparent jacking ratio of 33 percent was selected for sequence No. 12 to establish a pattern of variation in the heat-straightening response of the beam with this specific jacking ratio and to compare the results with those obtained from the heat-straightening tests performed previously in the project by different operators. The purpose was to check for inconsistencies due to the human factor involved. Nine heating cycles were performed in this sequence. In the course of the ninth heating cycle, a crack, as shown in fig. 7.7, was formed on the convex side of the web yield line (on which the line heat had not yet been applied), extending over a length of 127 mm (5 in). The results from the ninth heating cycle were discarded. The reasons for the cracking will be discussed later.

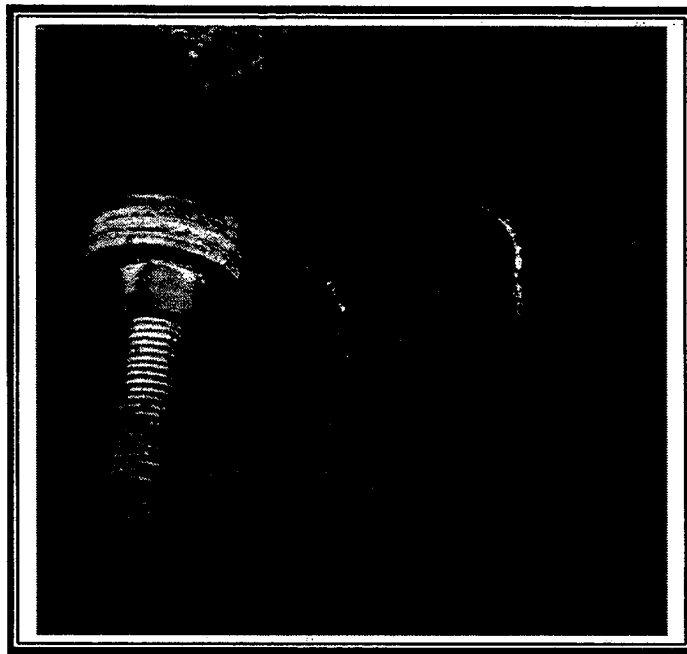


Figure 7.7. Crack in web of beam after heating sequence 12.

However, enough heating cycles had already been completed for evaluating the response of the girder under a 33 percent jacking ratio. The heat patterns and plastic rotations obtained as a result of the first eight heating cycles are shown in table 7.2.

A newly installed W 24x76 composite beam was damaged by a midspan static load to obtain the characteristic damage pattern of fig. 7.1. The repair was conducted using the previous methodology. The apparent jacking ratio was increased to 75 percent. This jacking ratio was rather high and had seldom been used in laboratory studies. It was applied in an attempt to find the limiting jacking ratio that would replicate the hot mechanical straightening phenomenon encountered in the past studies on W 10x39 composite girders. This sequence (No. 13) consisted of eight heating cycles. The average plastic rotations are given in table 7.2.

As expected, the plastic rotations encountered in this sequence were abnormally high, averaging 9.89 mrad. Thus, the average plastic rotation increased by 124 percent on raising the jacking ratio from 50 to 75 percent. This beam also fractured during the eighth heating cycle. The crack initiated on the convex longitudinal edge of the bottom flange at the point of application of the vee heat as shown in fig. 7.8 and continued over a length of 25 mm (1 in) to the apex of the vee. Causes for this cracking will be discussed later.

Evaluation of Factors Affecting Heat-Straightening Behavior of Composite Girders

Heat Patterns.—The term “heat patterns” refers to the combination and layout of vee heats, line heats, and strip heats used to conduct the heat-straightening repair. Conceptually, vee heats are used to

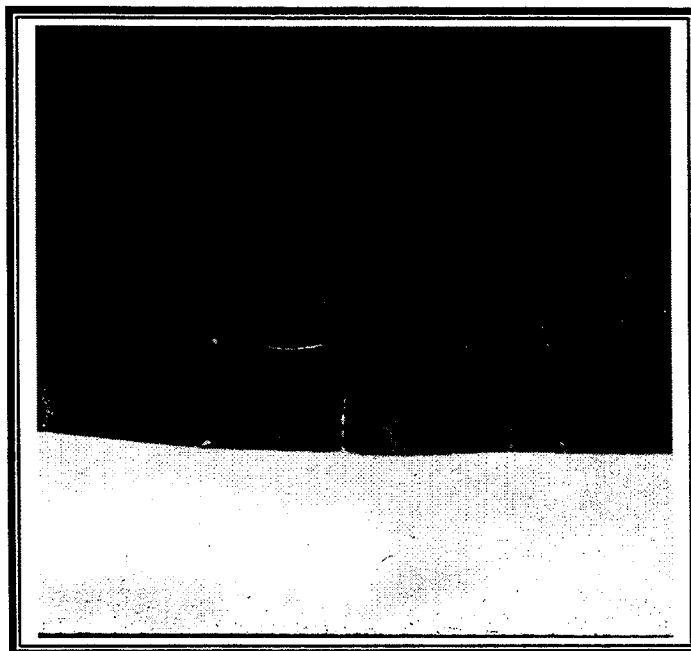


Figure 7.8. Crack in bottom flange of beam after heating sequence 13.

repair plate elements with plastic bending about the major axis, while line heats are applied to repair plate elements with flexural damage about the minor axis. Hence, a vee heat on the bottom flange in conjunction with a line heat on the web, applied to their respective plastically yielded portions, are the proper heat patterns to repair composite beams impacted by high loads. Care must be taken to continually adjust the span of the line heats, so that only those portions of the web are heated that show plastic curvature after the last heating cycle. Similarly, the vee heats are confined to the portion of the bottom flange with plastic deformations.

An important modification introduced in this study was the inclusion of a half-depth web strip heat during one sequence. The purpose of this heat was to reduce the differential shortening between web and flange. By heating the web with a half-

depth strip, the web can deform and relieve some of these stresses. The application of strip heats on the web in Sequence No. 11 did not influence the average plastic rotations appreciably but, it did tend to reduce the buckling of the web near the center of damage.

Residual Moments.-A characteristic of each damaged girder was the presence of residual moments. When damage is induced, the web acts as a spring resisting the movement. While a yield line typically occurs near the top of the web, there is also an elastic component of stored energy. This characteristic is often referred to as internal redundancy. The initial plastic rotation relieves the majority of this stored force. So, successive heats are not influenced significantly. During the first heat cycle, this restoring force acts as an additional jacking force tending to straighten the girder. Unless the external jacking ratio is reduced, the

plastic rotation during the first heat cycle is magnified. For example, the plastic rotation after the first heat cycle for all seven girders tested averaged over two and one-half times greater than the average of the succeeding values with the same jacking ratio. If the girder is externally indeterminate, residual moments are also created during the damage phase. For either case this behavior should be considered when developing a constraint plan. It is recommended that a reduced jacking force be used during the first two heats to minimize this effect and minimize the possibility of cracking. In order to eliminate this factor when computing the average plastic rotation for a specific set of parameters, the first heat after damage inducement was not considered when computing averages.

Restraining Forces.- The simplest way of providing restraining forces is to allow the unheated metal within the member to restrict thermal expansion by using a suitable heat pattern (as in the case of a vee heated plate). This is a form of an internal constraint. Internal constraint may also be imposed by the self-weight, axial loading, or statical indeterminacy of the member. Frequently, external restraining forces are used to complement or even substitute for the internal constraints required for the heat-straightening phenomenon. The importance of restraining forces in the heat-straightening process has been recognized in the field for many years. Hence, jacking forces have often been used to enhance the heat-straightening repair of a wide range of damaged structural steel members. The tests here were designed to evaluate the effect of external restraining forces on the heat-straightening behavior of damaged composite bridge girders.

Fig. 7.9 shows the effect of the applied apparent jacking ratios on the average plastic rotations for various heat sequences conducted. The average values for each jacking ratio were connected with a straight line. As shown in fig. 7.9, the jacking ratio-versus-plastic rotation curves exhibit a sharp discontinuity at higher loads for the W 24 x 76 beam. This behavior will be explained later.

Internal redundancy affects the heat-straightening response of a composite girder. Caused by the interaction of the bottom flange and the web, redundant forces are produced at the web-flange interface and impede the plastic rotations by acting as a negative internal constraint to the vee action in the bottom flange. Comparing the plastic rotations of the W10x39 and the W 24x76, the trend is apparent that plastic rotations are directly related to the jacking ratio, although not necessarily in linear proportion. However, there is something akin to a rigid body shift of the data with the W 24x76 showing consistently larger values than the W 10x39. It can be concluded that the redundant forces produced by the web-flange interaction in composite members inhibit the straightening effect more for a shallow beam than for a deep beam. The damage to the composite members produce plastic curvatures in the web about their minor axis along the yield line. This plastic deformation resists any elastic bending of the web about its minor axis during the straightening process of the bottom flange. Hence, the presence of the yield line in the web tends to magnify the counterproductive redundant forces and further inhibits the straightening effect of the bottom flange vee.

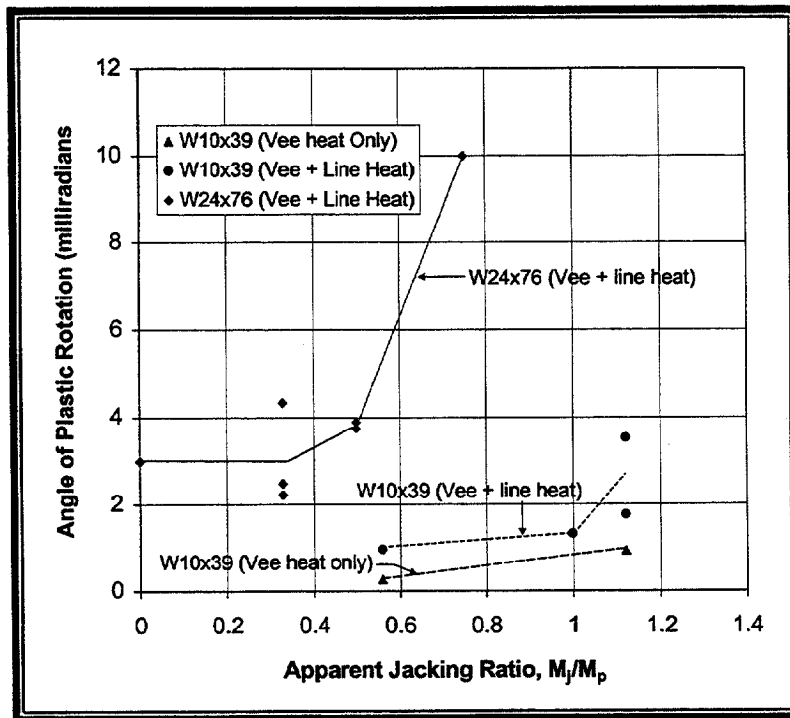


Figure 7.9. Apparent jacking ratio versus plastic rotation for composite girders.

By using a line heat on the web along with the vee heat in the bottom flange, these inhibiting forces are mitigated. This conclusion was verified in an appraisal of the influence of the web line heat on the heat-straightening response of the W 10x39 composite girder. Referring to table 7.1, the first two heating sequences 1 and 2 (without web line heats) result in very small plastic rotations in comparison to sequences 3 and 4 with web line heats.

When applying a lateral load to the bottom flange near the center of the composite girder, the moment produced is transferred to the end reactions by two mechanisms: the bottom flange acts as a flexural beam supported at the ends, and the web acts as a flexural plate (and, at large deformations, a membrane plate) supported by the deck and end diaphragms. A shallower

girder would be expected to have greater stiffness and thus smaller lower flange moments than that of the deeper girder subjected to the same lateral load. The data tend to verify these observations since the jacking ratio has less effect on the shallower girder. By adopting a jacking ratio definition with the plastic moment of only the bottom flange in the denominator, the implication is that most of the lateral stiffness is provided by the bottom flange. With the W 10 x 39 composite girder showing relatively small plastic rotations at jacking ratios greater than 100 percent, it is obvious that the web carries a significant portion of the jacking force. A primary question then becomes: how is the distribution of jacking forces between the flange and web to be determined?

Stiffening Effect of Web.- Correlating the jacking ratio to the plastic moment capacity of the bottom flange is misleading if the web interaction effects are significant.

Only the fraction of the total force that is directly carried by the bottom flange provides external restraint to the vee heat. Hence, the apparent jacking ratio as defined earlier for a composite girder does not reflect the true bending moment in the bottom flange and may be considered only as a nominal jacking ratio. It is more relevant to calculate the jacking ratio using the actual bending moment transferred to the bottom flange. This ratio will be called the effective jacking ratio.

Hot Mechanical Straightening.- A large increase in plastic rotations was observed using Sequence No. 13, when an apparent 75 percent jacking ratio was applied to the W 24x76 composite girder. The average plastic rotation obtained for this jacking ratio was almost three times the value extrapolated from the straight-line fit through the data points associated with the lower load ratios. The past studies on the temperature characteristics of steel have shown that the yield stress of steel decreases with increasing temperature. It is known from these studies that a heating temperature of 650°C (1,200°F) may reduce the yield stress in an A-36 steel member to as little as a third of its original value. Thus, the elevated temperatures associated with heat-straightening enable the member to yield at the relatively low stresses produced by the external jacking forces. In effect, during hot mechanical straightening of a steel member, the jacking forces are merely pushing the member mechanically because of the reduced yield stress. Consequently, large movements would result. It is concluded

that the large movements associated with the high jacking ratios involve some hot mechanical straightening.

Cracking.- An unusual phenomenon observed in the course of these experiments was the cracking in two of the girders subjected to heat-straightening. The crack that appeared at the end of sequence No.12 occurred during the fourth damage and repair cycle. It occurred in the web, parallel and adjacent to the line heat. The crack also corresponded to the tension side of the web with respect to the application of the jacking force. It was observed in Chapter 4 that the yield stress increases and ductility decreases dramatically after more than two damage-repair cycles. The implication is that the stress-strain characteristics become similar to brittle materials. It has also been found that high residual stresses occur in areas of concentrated heats such as the apex of the vee. Line heats are similarly concentrated. It is therefore concluded that repetitive damage combined with high residual stresses led to a brittle failure.

The crack at the end of sequence No. 13 occurred under quite different circumstances. The beam cracked during the first damage-repair cycle on the tension side of the bottom flange (as defined by the applied jacking force). An unusually high jacking force was used (75 percent apparent jacking ratio). Similar fractures have also been reported during field repairs. The probable causes were: (1) the high jacking force combined with the somewhat reduced ductility due to the heating; and (2) the residual stresses, which may tend to increase the total stress above ultimate. This behavior reinforces the concept that the jacking forces should be evaluated analytically and never

applied without a gauge to control the magnitude. Recommendations for maximum jacking forces are given in a later section. Adhering to these recommendations will greatly reduce the likelihood of brittle cracking. Should such cracking occur, the heat straightening must be stopped and the situation evaluated. An alternative is to finish the heat straightening with the crack present. Then a bolted splice plate can be designed for the flange to transfer load across the cracked area.

Theoretical Model for Heat-Straightening Response

Modeling of Simple Span Composite Girders.-The first step in modeling composite girders is to consider the case of the simply supported beam without diaphragms. The information required to develop this model is the amount of the applied lateral jacking force that is actually distributed to the lower flange as opposed to that which is transferred through the web to the composite deck. The apparent moment, M_j , is defined as the moment induced in the lower flange by the jacking force, P_j , as if the lower flange alone supported the lateral force (i.e., the web is neglected). If P_j is applied at the center of the span the apparent moment is:

$$M_j = P_j \ell / 4 \quad (\text{Eq. 7.1})$$

where ℓ is the span length.

The stiffness of the system can be expressed as:

$$K_j = \frac{4EI_j}{\ell} \quad (\text{Eq. 7.2})$$

where I_j is the equivalent moment of inertia that includes the bottom flange and the web stiffening effect. The deflection of a simply supported beam with a concentrated load at the center is:

$$\Delta = \frac{P_j \ell^3}{48EI_j} \quad (\text{Eq. 7.3})$$

or in terms of K_j

$$\Delta = \frac{P_j \ell^2}{12K_j} \quad (\text{Eq. 7.4})$$

Solving for K_j

$$K_j = \frac{P_j \ell^2}{12\Delta} \quad (\text{Eq. 7.5})$$

In the elastic range, K_j can be determined experimentally by measuring Δ for a specified applied load P_j .

The stiffness of the system includes both the effect of the lower flange and the web stiffening effect due to connectivity with the upper composite flange. Thus, only a portion of the moment generated by the jacking force is actually distributed to the lower flange. An estimate of the actual moment can be obtained by assuming that the moment in the flange, M_f , is equivalent to that produced by the application of a por-

tion of the jacking force to the lower flange with the web effect neglected. The moment in the flange can be written as:

$$M_f = P_f \ell / 4 \quad (\text{Eq. 7.6})$$

where P_f is the portion of the jacking load transferred to the lower flange. The lateral deflection of the flange can be written as

$$\Delta = \frac{P_f \ell^3}{48EI_f} = \frac{P_f \ell^2}{12K_f} \quad (\text{Eq. 7.7})$$

where I_f is the flange moment of inertia about the axis of bending and K_f is the flange stiffness, $4EI_f/\ell$. Since the deflections from eqs. 7.4 and 7.7 are identical, then,

$$\frac{P_f \ell^2}{12K_f} = \frac{P_j \ell^2}{12K_j} \quad (\text{Eq. 7.8})$$

or

$$\frac{P_f}{K_f} = \frac{P_j}{K_j} \quad (\text{Eq. 7.9})$$

using eqs. 7.1 and 7.6 to eliminate the forces P_f and P_j , Eq. 7.9 can be written as:

$$\frac{M_f}{M_j} = \frac{K_f}{K_j} \quad (\text{Eq. 7.10})$$

or

$$M_f = \bar{\gamma} M_j \quad (\text{Eq. 7.11})$$

where the distribution factor, $\bar{\gamma}$, is given by

$$\bar{\gamma} = \frac{K_f}{K_j} \quad (\text{Eq. 7.12})$$

Since K_f can be calculated for a given lower flange and K_j obtained from experimental measurements, the value for $\bar{\gamma}$ can be found. The lateral deflection, Δ , was measured for known applied loads so that K_j could be determined experimentally. Consequently, $\bar{\gamma}$ can be determined from eq. 7.12. For the W 10x39, the distribution factor $\bar{\gamma}$ was determined to be 0.183 and for the W 24 x 76, $\bar{\gamma} = 0.427$. These factors are appropriate when the effect of the web line heat on bottom flange stiffness is neglected. However, a comparison of results for sequences 1-5, (with and without line heats) indicates that the line heat significantly reduces the web's restraining stiffness. As a result, more jacking force actually goes into the bottom flange when the line heat is not neglected. By measuring the shift in the plastic rotation value for identical cases without and with the line heat, the stiffness reduction effect produces a magnification on the order of 160 to 190 percent. Therefore a reasonable approximation is to assume that the distribution factor, $\bar{\gamma}$, is increased by an average value of 175 percent when a web line heat is used. Consequently, the modified factor, γ , for the W 10 x 39 and the W 24 x 76 is 0.320 and 0.747, respectively,

where γ is the reduction factor including the line heat effect. Thus, the relationship between the apparent moment, M_j , associated with the jacking force and the actual moment in the bottom flange, M_r , (after the line heat to the web is applied) is:

$$M_j = \gamma M_r \quad (\text{Eq. 7.13})$$

Applying this distribution factor, the data from fig. 7.9 is replotted in fig. 7.10 for an effective load ratio M_j/M_p .

The plate equation is also plotted in fig. 7.10 for comparison purposes. It falls between a curve fit of data for the W 10x39 and the W 24x76. Comparing to the plate equation, it can be concluded that the web stiffening effect significantly reduces plastic rotations for shallow beams. As the stiffening effect is lessened for deeper beams, the plastic rotations tend to be magnified in a pattern similar to that of damage category W wide flange beams. Consequently, the stiffness factor would be expected to be a function of the square of d/t_w where d is the beam depth and t_w is the web thickness. Assuming that the plate equation is a reasonable model for the composite girder, a factor can be introduced to incorporate the web stiffening effect. Since the plate equation tends to fall between the values for the two girder types, a stiffness modification factor can be approximated as:

$$F_a = \left(\frac{d/t_w}{46}\right)^2 \quad (\text{Eq. 7.14})$$

The measured experimental values of

$\bar{\gamma}$ (prior to web line heat) can be translated to values of γ (after web line heat) as:

$$\gamma = 1.75(\bar{\gamma}) \quad (\text{Eq. 7.15})$$

The measured values for the W 10x39 and W 24x76 are plotted in fig. 7.11 with respect to d/t_w ratio. Also plotted is the value for a W36 x 170 taken from Avent and Brakke (1996). An equation can be obtained for the stiffness reduction factor, γ by assuming a second order curve fit between the known data points:

$$\gamma = \frac{d/t_w}{10,000} (15 + 2.75 d/t_w) \quad (\text{Eq. 7.16})$$

This equation is plotted in fig. 7.11 for comparison to the measured data.

Utilizing these factors, an equation for plastic rotation of composite girders (including web line heats) can be written in a form similar to that of rolled shapes in Chapter 6, that is,

$$\varphi_c = F_a F_t \varphi_b \quad (\text{Eq. 7.17})$$

where φ_b is the basic plate plastic rotation factor of the lower flange acting as an independent plate, eq. 5.21, and is given by

$$\varphi_b = 0.0147 \sin \frac{\theta}{3} \quad (\text{Eq. 7.18})$$

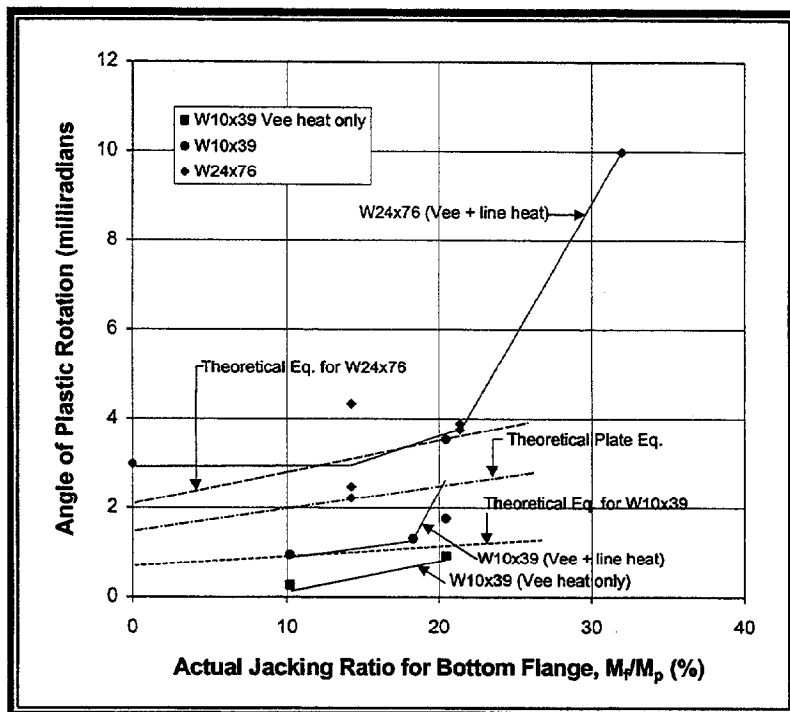


Figure 7.10. Actual load ratio versus plastic rotation for composite girders.

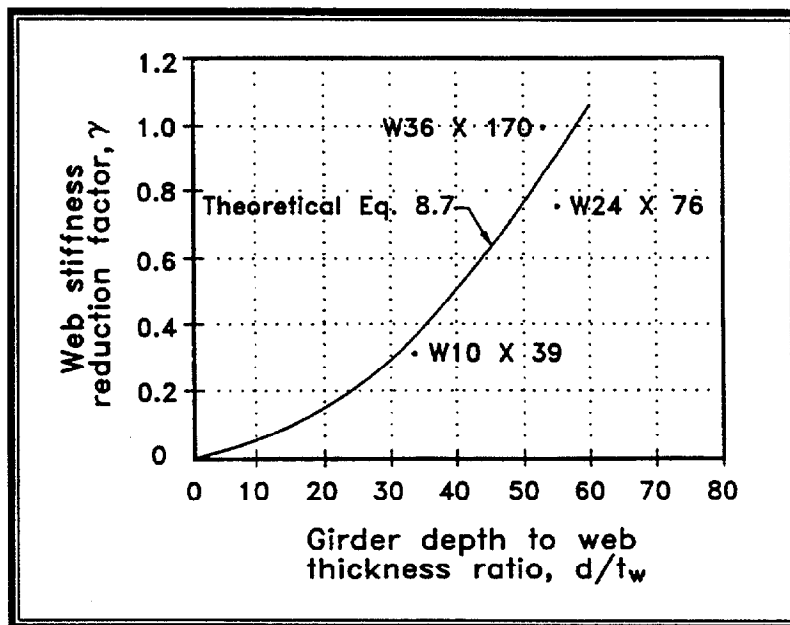


Figure 7.11. Web stiffness reduction factor versus d/t_w ratio.

F_a is given by eq. 7.14, the load factor, F_ℓ is:

$$F_\ell = (0.6 + 2 \frac{M_f}{M_p}) \quad (\text{Eq. 7.19})$$

or using eq. 7.13

$$F_\ell = 0.6 + 2\gamma \frac{M_j}{M_p} \quad (\text{Eq. 7.20})$$

where M_p is the plastic moment capacity of the lower flange about its strong axis. The theoretical plastic rotations, eq. 7.17, for the W 10x39 and W 24x76 composite girders were superimposed on the experimental plots in fig. 7.10 in which effective jacking ratio was the ordinate. Excluding the high jacking ratio data point associated with the hot mechanical straightening phenomenon, the analytical formula provides a reasonable approximation.

The experimental evidence indicates that the degree of plastic rotation per heat cycle is proportional to the magnitude of the restraining force up to a certain limit. For higher forces, the behavior becomes nonlinear with increased plastic rotations, as illustrated in fig. 7.9. This phenomenon is attributed to a combination of (1) the jacking forces creating stresses greater than the reduced yield stress in portions of the flange heated zones (often referred to as hot mechanical straightening); and (2) the spreading of the yield zone and the associated redistribution of moments. Since little evidence exists as to the safety of such high jacking forces, a load limit is necessary.

An approximate limiting value of the jacking force can be estimated from the data presented here. Since the W 10 x 39 and W 24 x 76 composite girders represent a range of section geometries, a conservative value can be chosen from the two cases. It is recommended that the actual jacking ratio in the heat-straightening of composite girders be limited to 33 percent, thus:

$$M_f \leq \frac{M_p}{3} \quad (\text{Eq. 7.21})$$

The apparent jacking ratio can be obtained using eq. 7.13 as

$$\frac{M_j}{M_p} \leq \frac{1}{3\gamma} \quad (\text{Eq. 7.22})$$

Modeling Statically Indeterminate Spans Due to Intermediate Diaphragms.- Practically all spans over roadways have intermediate diaphragms. When the lower flange is impacted, its behavior resembles that of a beam continuous over several supports with the diaphragms acting as these supports, fig. 7.12a. The impact usually produces a plastic hinge mechanism as shown in fig. 7.12b. The three plastic hinges produce reverse curvature bending and yield zones at the impact point and adjacent supports as shown in fig. 7.12c. The vee heat pattern is also shown in fig. 7.12c. Both the positive and negative curvature sections should be heated either simultaneously or in quick succession. Plastic rotation will occur at all three locations with relatively little restraint from adjacent plastic

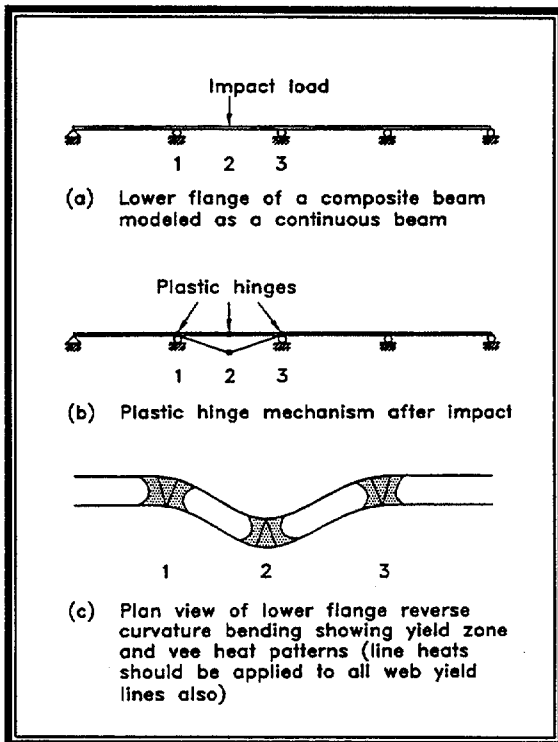


Figure 7.12. Lower flange of composite girder modeled as a continuous beam.

hinges. Consequently, the model for the single span case should provide a reasonable approximation of this more complex situation. An important consideration for composite girder repair is the residual stresses induced during both the damage and the repair phase. For diaphragm-braced members, the result of the damage inducement process is the creation of residual moments. These moments can be computed by first performing a plastic analysis on the continuous beam to determine the ultimate load (impact force), P_u , and the plastic moment diagram, M_u . A modified stiffness of $K_j = 1/\bar{\gamma} K_f$ can be used for these computations. The second step is to take the computed P_u , apply it in the opposite direction, and compute an elastic moment diagram, M_e , even if the stresses are greater than F_y . Finally, the superposition of these two moment diagrams yields

the residual moment distribution, M_r , due to the impact loading. These residual moments may either aid or hinder heat straightening depending on their directions. The moment in the flange is $M_f + M_r$, where M_f is positive when the residual moment has the same sign as the moment due to jacking. Using the limit of $M_p/3$:

$$M_f + M_r \leq \frac{M_p}{3} \quad (\text{Eq. 7.23})$$

or

$$M_f \leq \frac{M_p}{3} - M_r \quad (\text{Eq. 7.24})$$

The apparent jacking moment is found by substituting eq. 7.23 into eq. 7.13 and solving for M_j , thus

$$M_j \leq \frac{1}{\gamma} \left(\frac{M_p}{3} - M_r \right) \quad (\text{Eq. 7.25})$$

and the apparent jacking force can be found from eq. 7.1. Note that the movement associated with the first several heats will eliminate the residual moment. Care must be taken not to over-jack on the first few heats. If the residual moments are not computed, then the maximum jacking ratio should be reduced during the first two heats. The recommended limit is one-half the standard limitation or 16 percent. After two heats the 33 percent limit can be used.

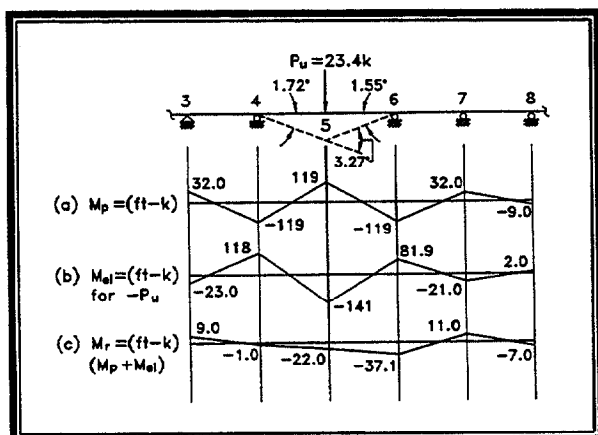


Figure 7.13. Deflected shape and structural analysis of damaged beam.

Example 7.1

Problem.—The lower flange of a composite A36 steel beam (W 36x170) was impacted by a crane boom which broke its moorings as the truck carrying it passed under the bridge. The deflected shape of the lower flange is shown in fig. 7.13 after the degree of damage at the three plastic hinges had been calculated. Compute the maximum jacking force that should be used in the heat straightening repair assuming that the diaphragm at joint 5 is removed prior to repair. Shown in fig. 7.13 are the results of the plastic analysis, (a), the elastic analysis, (b), and the residual moments, (c).

Solution.—For a W 36x170, the d/t_w ratio is 53.2. From eq. 7.16:

$$\gamma = \frac{53.2}{10,000} [15 + 2.75(53.2)] = 0.858$$

The limiting moment in the flange during heat straightening from eq. 7.21 is:

$$M_f \leq \frac{119}{3} ft - k = 39.7 ft - k \quad (53.8 \text{ kN} - m)$$

The apparent jacking moment can be found from eq. 7.25 if residual moments are included, as:

$$M_j \leq \frac{1}{0.858} \left(\frac{119}{3} - 22 \right) = 20.6 ft - k \quad (27.9 \text{ kN} - m)$$

and the apparent jacking moment if residual moments are neglected, is:

$$M_j = \frac{1}{0.858} \left(\frac{119}{3} \right) = 46.2 ft - k \quad (62.6 \text{ kN} - m)$$

Based on the elastic analysis, these moments translate to jacking forces, P_j , as follows:

For residual moments included

$$P_j = 3.42 \text{ K} \quad (15.2 \text{ kN})$$

For residual moments neglected

$$P_j = 7.67 \text{ K} \quad (34.1 \text{ kN})$$

Summary

Presented in this chapter have been experimental and theoretical results for the behavior of heat-straightened composite bridge girders damaged by impact to the lower flange. The typical damage pattern was defined and a recommended heating pattern described. Because of the web/flange interaction, the moment in the bottom flange due to jacking forces cannot be directly calculated. A methodology was developed for determining the actual moment transferred to the bottom flange by a

jacking force during heat straightening. This formulation included the influence of the web line heat on the moment transfer. The procedures described here are effective means to repair composite bridge girders.

Key Points To Remember

- Laterally deformed composite girders are complex, internally indeterminate structures.
- The primary damage mechanism is a plastic hinge at the impact point of the lower flange and a yield line in the web near the upper fillet.
- Secondary damage frequently occurs in the form of flange bulges at the impact zone, web bulges in the vicinity of diaphragms, and crushed or buckled diaphragms.
- The movement per repair heat is proportional to the magnitude of the jacking forces applied.
- The heating pattern primarily consists of vee heats in the flange and line heats in the web. Strip heats in the web may be needed in special cases.
- The response to repair is not influenced by whether the damage is statically or dynamically induced.
- Larger movements often occur as a result of the first heat, as opposed to successive heats, due to relieving residual moments in the girder.
- Over-jacking may produce hot mechanical straightening and lead to brittle fracture.
- Repetitive damage and repair cycles may lead to brittle fracture. Therefore, a composite girder should not be repaired more than twice.
- The moment induced in the lower flange by jacking forces can be computed using a distribution factor, γ , (eq. 7.16).
- The plastic rotation per heat (eq. 7.17) can be estimated by modifying the plate equation with a jacking ratio factor (eq. 7.20) and a stiffness modification factor (eq. 7.14).
- Jacking should be limited to a value that produces an actual flange moment of 16 percent of yield during the first two heats (unless residual moments are directly computed).
- After the first two heats, jacking forces should be limited to values that produce an actual flange moment of 33 percent.
- The actual jacking force must include the web stiffening effect.

Chapter 8. Heat Straightening Trusses and Other Axially Loaded Members

Introduction

The stress condition of a member plays a major role in its behavior during heat straightening. Yet, practically no research has been conducted on this effect. In some cases the loads on a structure can be reduced to the point that member stresses are a minor factor. However, for other cases, even after the removal of live loads, the dead loads produce significant stresses. A primary case in point is the truss bridge. Typically, the dead load stresses on such structures may range from 25-50 percent of maximum in some members. It is thus necessary to examine the stress distribution of a structure prior to initiating heat straightening.

First, consider the beam shown in fig. 8.1 in which the dead loads produce bending about the minor axis of the wide flange beam. The dead load can have a neutral, positive or negative effect depending on the type of damage. For example if the damage is a result of bending about the major axis in fig. 8.1, but dead loads produce moments about the minor axis, the web vee heat is in a region of nearly zero stress. The dead load stress will have little effect on movement after heating. If the damage is the result of bending about the weak axis (in the direction of the dead loads), then the flange vee heats will be working against the dead loads. Without the use of jacking forces to overcome the dead load moments, the straightening will be reduced or possibly be zero. If the damage was opposite to the direction of the dead load, the movement

after heat straightening would be enhanced by the dead load.

For columns and axially loaded members it is important to consider the $P-\Delta$ effect. If an axially compressed member is damaged by lateral loads as shown in fig. 8.2, a moment is generated which is equal to $P\Delta$. This moment is in the opposite direction to the moment generated by a jacking force during the straightening process. If the lateral deflection is large, the moment due to the $P\Delta$ effect could retard or prevent the restoration movement during heat straightening.

For truss members the internal stresses are typically axial tension or compression. Compression stresses act as a positive constraint during heat straightening and may be expected to generate larger plastic rotations than if no compression was present. Likewise, tension would be expected to retard movement. To investigate this behavior, a series of tests were conducted for axially loaded compression members damaged about either the major (Category S) or minor (Category W) axes. The purpose was to evaluate the $P\Delta$ effect and the jacking ratio on the magnitude of plastic rotations during heat straightening.

Response of Columns to Heat Straightening

A study of the response of two steel girders was conducted. An HP 12X53 was tested for weak axis damage (Category W) and a W 10X39 was tested for strong axis damage (Category S). During the repair,

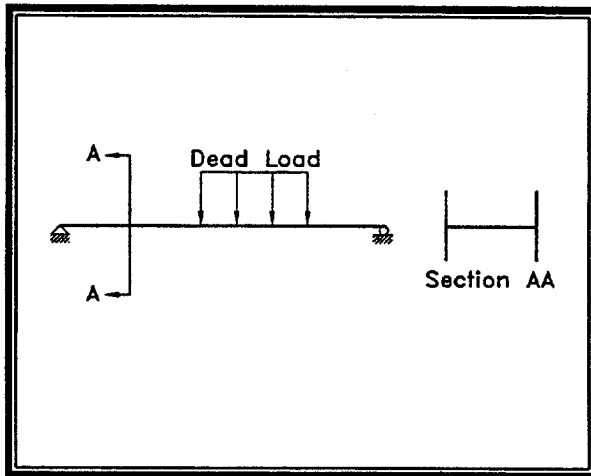


Figure 8.1. Dead load conditions on a simply supported beam.

both beams were subjected to axial compression of 0.35 times the AISC (1989) allowable axial load. A total of 70 heating cycles were performed. Jacking ratios ranged from zero to 50 percent. A zero jacking ratio sequence with an axial load of 0.175 times the allowable axial load was also conducted in the case of the Category W damage.

The specimens used were 6 m (20 ft) long, A-36 steel members. In four cases the member was damaged about the minor axis while in three cases the damage was about the major axis. The damage was statically induced at the center of the member using hydraulic jacks. The members were simply supported and diaphragms were placed only at the ends. No axial loads were applied during the damage process. Prior to heating, the axial force was applied by means of the tension rods attached to end plates on the members (fig. 8.3). Lateral jacking forces were applied by means of hydraulic jacks. One heating pattern was $\frac{3}{4}$ depth, 45° vees on the flanges and a strip heat on the web. This pattern is the standard pattern for Category W damage (see fig. 2.12). For the

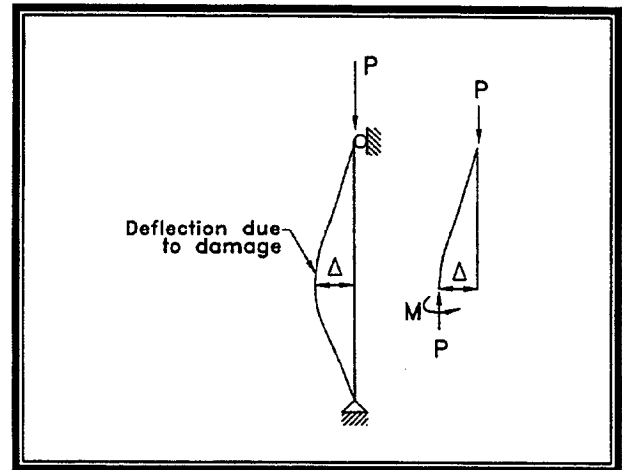


Figure 8.2. $P\Delta$ effect on an axially loaded column.

Category S cases the standard pattern was a full depth, 30° vee on the web followed by a strip heat on the flange at the open end of the vee (see fig. 2.11).

Heat Straightening Response of Columns with Category W Damage

With the axial load applied, a moment in the member is created due to the $P\Delta$ effect. This moment tends to impede the heat straightening process as it acts to magnify the damage. The approach used here was to cancel out this moment with the application of the lateral jacking force. After each cycle, the moment resulting from the $P\Delta$ effect was computed. The jacking force was adjusted to include the specified jacking ratio plus a moment to cancel out the $P\Delta$ moment at the center of damage. Thus, the jacking ratio for these tests is defined as the ratio of the moment at the center of damage due to both the $P\Delta$ effect and the jacking force, M , divided by the plastic moment capacity of the cross-section about the axis of damage, M_p . The HP 12X53 had an axial load, P , of 362 kN (81.4 kips), producing a compressive stress of 36.2 MPa (5.25 ksi),

which is 35 percent of the maximum allowable compression of 103 MPa (15 ksi). For the first damage inducement case, a maximum deflection of 85 mm (3.36 in) was obtained. The axial load of 362 kN (81.4 kips) will produce a moment of 30.9 m kN (22.8 ft kips) at the point of damage or 23.5 percent of the plastic moment, M_p . This is equivalent to the moment produced by a lateral load at the point of damage of 20.3 kN (4.56 kips). For a jacking ratio of 50 percent the lateral force required is 43.1 kN (9.69 kips). Thus, to compensate for the $P\Delta$ moment acting to hinder movement during straightening, the actual jacking force used for this case was the sum of these two, or 63.4 kN (14.25 kips). For each heating cycle the jacking force was reduced to compensate for the reduced $P\Delta$ moment.

To generalize for a simply supported beam-column with the damage at an arbitrary location, the applied jacking force, P_a , is

$$P_a = P_j + P_{ec} \quad (\text{Eq. 8.1})$$

where P_j is the jacking force to create a specified moment at the damage location as a percentage of M_p , or

$$P_j = \frac{R_\ell \ell M_p}{ab} \quad (\text{Eq. 8.2})$$

and ℓ = column length, a and b = distances from end supports to the applied jacking load, and R_ℓ = the jacking ratio, M_j/M_p . P_{ec} is the additional jacking force required to

cancel the eccentric moment due to the axial load, P , or

$$P_{ec} = \frac{\ell P \Delta}{ab} \quad (\text{Eq. 8.3})$$

This effect is illustrated in fig. 8.4 where the stress distribution at the damaged cross section is shown before (fig. 8.4a) and after (fig. 8.4b) the jacking force is applied. Recall that the purpose of the jacking force is to create compressive stresses on material at the open end of the vee. The $P\Delta$ moment produces stresses that tend to reduce this compressive stress (fig. 8.4a) and will produce a tensile stress if the stress due to the eccentric moment is greater than that due to compressive axial load effects. In contrast, the application of the jacking force cancels the $P\Delta$ effect and increases the compressive force at the open end of the vee above that caused by the axial force (fig. 8.4b). If the axial stress is greater than the maximum bending stress due to jacking, then the entire cross section is in compression.

Four Category W tests were conducted on an HP 12X53 section with various jacking ratios. In all cases, including the zero load ratio cases, the jacking force included a component to cancel out the $P\Delta$ effect. This component was re-computed after each cycle to reflect the reduced deflection as the girder straightened. For each heating cycle, both flanges were heated simultaneously using 45° vees. Next the web was heated with a strip heat. The axial load was maintained at 35 percent of the allowable except for Case 4 in which it was reduced to 17.5 percent. The results are shown in table 8.1. Both flanges were

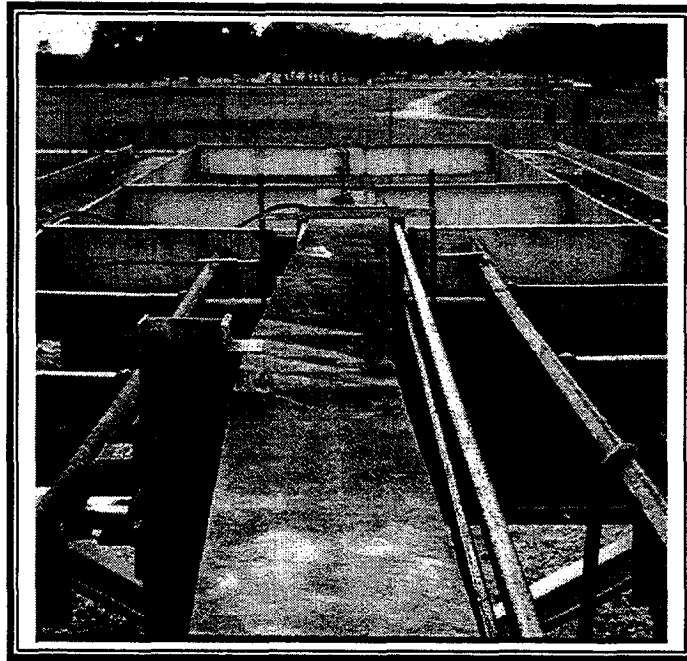


Figure 8.3. Jacking force applied to axially loaded column in test frame (Tension rods are visible on right side of column).

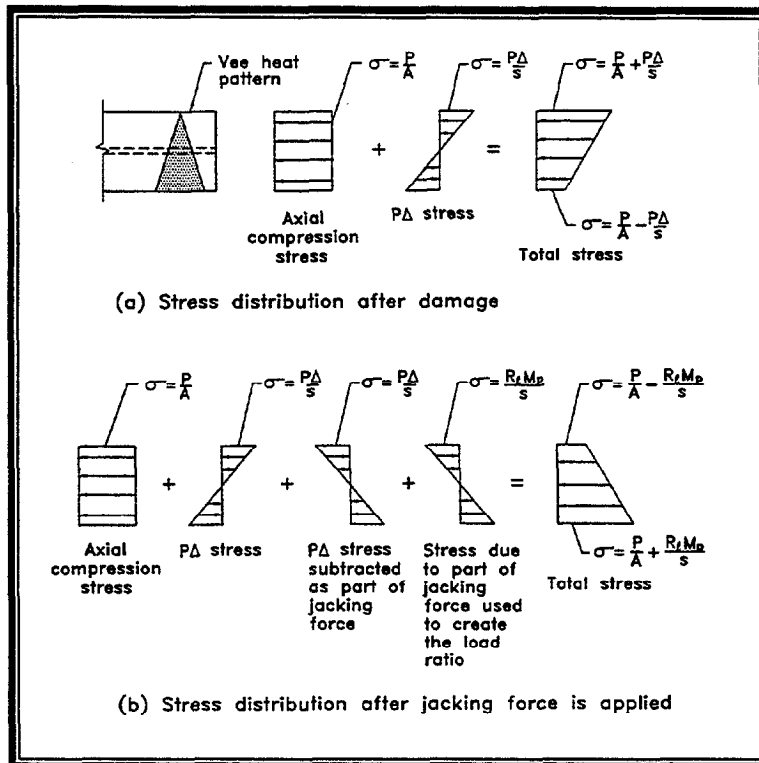


Figure 8.4. Stress distribution in axially loaded column (A = cross section area and S = section modulus).

Table 8.1. Plastic rotations for category W damaged HP 12x53 beam with compression axial loads (45° vee heats and 650°C (1200°F) temperature).

Beam	No. of Heats	Jacking ratio	Axial stress/ allowable stress	Max. stress ¹ (MPa/ksi)	Min. stress ¹ (MPa /ksi)	Avg. Plastic Rotation (millirad)
1	10	.50	0.35	-226.0/-32.8	154.0/22.4	5.54 (4.94) ²
2	10	.25	0.35	-131.0/-19.0	59.2/8.58	3.85 (3.32) ²
3	10	0	0.35	-36.0/-5.22	-36.0/-5.22	1.48 (1.27) ²
4	10	0	0.175	-18.1/-2.62	-18.1/-2.62	0.64

¹Tension is positive
²number in () is average neglecting the first heat

measured and the average is shown in the table. In general the plastic rotations of both were similar. The response of beam No. 1 to heat straightening is shown in fig. 8.5 and was typical in form to all category W columns tested. For the cases in which the jacking ratio was zero (the jacking force was only used to cancel the $P\Delta$ effect), there were several heats where the resulting movement was in the opposite direction to that expected. However, successive heats produced positive movement. This behavior illustrates a facet that occasionally occurs during heat straightening. Small or reverse movements sometime occur when low or zero jacking forces are used. The probable cause is the build-up of unfavorable residual stresses which are relieved in successive heats. A similar behavior was observed in the category S tests for a zero jacking ratio, which is described in the next section.

As found in other applications the residual moments resulting from damage inducement caused the plastic rotation from

the first heat to be exceptionally large. In order to compare the data to theoretical values, the average plastic rotation was also computed excluding the first heat. The results are plotted in fig. 8.6. Also shown is the theoretical curve for the beam without axial load based on the same parameters. The plastic rotations varied linearly with the jacking ratio. However, they tended to be smaller than those predicted for the same beam without axial load (eq. 6.1). It appears that the axial force tends to reduce the expected values over those without axial loads.

While more research is needed, the limited data suggest that the previously developed equations for plastic rotations is applicable here with a modification factor applied. If the movement is proportionally reduced with higher axial loads, the stress factor, F_a , of eq. 6.5 can be modified as

$$F_a = \left\{ 1 - 2 \left[1 - \left(\frac{Z}{S} \right) \frac{M_j}{M_p} \right] \right\} \left(1 - \frac{f_a}{F_a} \right) \quad (\text{Eq. 8.1})$$

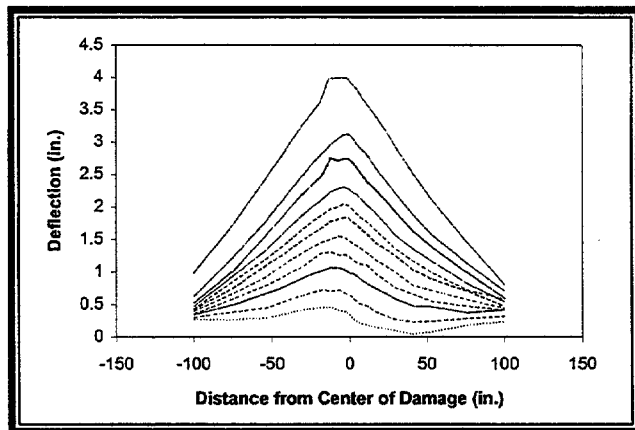


Figure 8.5. Deformations of one flange over 10 heating cycles for compression member No. 1 (45° vee heats, 650°C (1200°F) temperature, and modified jacking ratio of 50 percent).

where f_a = the axial compression stress in the member and \bar{F}_a = the allowable axial stress.

The equation for plastic rotation is in the form of eq. 6.1, that is

$$\varphi_p = F_\ell F_a F_s \varphi_b \quad (\text{Eq. 8.2})$$

where F_ℓ is given by eq. 6.7, F_s is given by eq. 6.12, F_a by eq. 8.1 and φ_b by eq. 6.2. A plot of this equation for the HP12 x 53 also is shown in fig. 8.6 and shows good agreement with the measured data.

Response of Columns to Heat Straightening for Category S Damage

A W 10X39 column, which had been damaged about the strong axis, was damaged and repaired three times using jacking ratios of 0.00, 0.25 and 0.50. In order to prevent lateral torsional buckling of the column during the damage phase, the beam was laterally braced at the third points. There was a tendency for lateral torsional

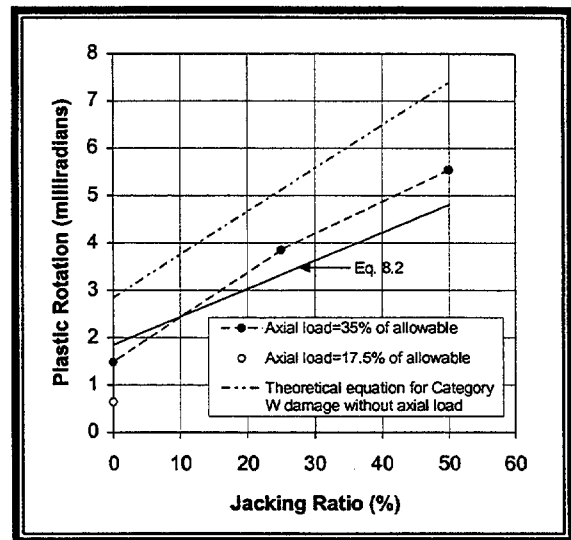


Figure 8.6. Plastic rotation versus jacking ratio for axially loaded Category W columns ($f_a/\bar{F}_a = 0.35$ except as noted, vee angles = 45° and heating temperature = 650°C or 1200°F).

buckling to occur due to the large load required to induce major axis damage on a full-scale beam. The bracings were removed during the repair sequence so as not to influence the plastic rotations. The three sequences are represented as beam Nos. 5-7 in table 8.2. A load of 129 kN (29 kips) was required to induce a deflection of 43.2 mm (1.70 in) on the initially straight column. Thirteen heating cycles were performed on Beam 5 using a jacking ratio of zero. A vee angle of 30° was used for all cases. The standard category S heating pattern was used consisting of a web vee heat followed by a flange strip heat at the open end of the vee (see fig. 2.11). The columns were not completely straightened in each test series. Rather, ten heating cycles (13 on No. 5) were conducted in order to define the response. The average plastic rotations are shown in table 8.2 and plotted in fig. 8.7. Because the first heat after re-damage often

Table 8.2. Plastic rotations for Category S damaged W10X39 columns (30° vee angle and 650°C or 1200°F heating temperature).

Beam	No. of Heats	Jacking Ratio	Ratio of Axial Stress to Allowable Stress	Max. Stress ¹ (MPa /ksi)	Min. Stress ¹ (MPa/ksi)	Average Plastic Rotations (milli-rad)
5	10	0	0.35	-48.0/-6.23	-43.0/-6.23	1.15
6	9	0.25	0.35	-139.0/-20.2	53.6/7.77	2.74
7	9	0.50	0.35	-206.0/-29.9	121.0/17.5	4.93

¹Tension is positive

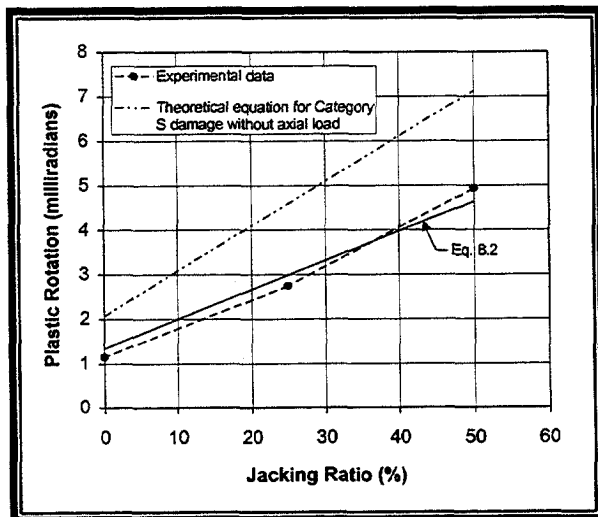


Figure 8.7. Plastic rotation versus jacking ratio for Category S columns (30° vee angle and 650°C or 1200°F heating temperature).

results in larger than usual movements, this heat was not included in the average values shown.

As with the Category W damage, the Category S damage plastic rotations fell well below those predicted by the theoretical equation without axial load. The use of eq. 8.2 is shown in fig. 8.7 and agrees well with the data. Thus, eq. 8.2 can be used to predict plastic rotations for repair of Category S

axially loaded compression members where F_t is given by eq. 6.7, F_s by eq. 6.12, F_a by eq. 8.1, and ϕ_b by eq. 6.2.

Summary

A series of full scale tests were conducted on both Category W and S damage axially loaded columns. Seven straightening procedures were conducted with at least 10 heats used for each set of parameters. The axial load imposed during the straightening process was typically 35 percent of the design allowable value. The jacking force was modified to cancel the $P\Delta$ moment effect in addition to providing the specified jacking ratio. The response for both cases was significantly less than that predicted for a wide flange beam without axial load. A suggest theoretical model agreed well with the data.

Key Points to Remember

- Heat straightening is effective for axially loaded columns using the same patterns as for cases without axial loads.
- The movements after heating will tend to be smaller than the case of zero axial loads on the same member.

-
- The jacking forces used should include, as a minimum, a component producing a moment at the damaged section equal and opposite to the moment produced by the axial force acting through the deflection at the damaged section.
 - A Theoretical model for plastic rotations was developed and is given by eq. 8.2.

Chapter 9. Heat-Straightening Repair of Localized Damage

Damage in steel members can be broadly classified as global and local damage. Different methods are required for the heat-straightening repair of these types of damage. Global damage is the overall deformation of the damaged section with respect to its supports. Local damage is characterized by plastic strain occurring only in the region of impact. It includes small bulges, bends or crimps in single elements of the cross section. The two most frequently encountered patterns can be categorized for convenience as flange bulges and web buckles as shown in fig. 9.1. Flange bulges are associated with local damage to unstiffened cross section elements such as a flange of a girder. Web buckles are associated with local damage to stiffened cross section elements such as the web of a girder.

All are classified as Category L damage. However, two sub-classifications will be used: Category L/U for local damage to unstiffened elements, and Category L/S for damage to stiffened elements.

The focus of past heat-straightening research has been on various aspects of repairing global damage. However, it is a rare situation when localized damage doesn't occur concurrently with global damage. Yet, little published information has been available on how to repair local damage by heat straightening. As a result, localized damage is often repaired improperly by cold mechanical straightening and hot mechanical straightening, as well as heat straightening.

In cold mechanical straightening, the steel is restored to its original shape by ap-

plying external loads in excess of the plastic capacity of the section while the steel is still at ambient temperature. In hot mechanical straightening, the steel is heated to very high temperatures (often greater than 927°C or 1700°F) causing a severe reduction in yield strength and plastic capacity. The steel is then straightened by external forces. The forces used are smaller than those used in cold mechanical straightening but are still in excess of the yield capacity of the heated steel. Both methods involve straightening of the steel by mechanical means. As a result, these techniques may involve strain hardening which results in a loss of ductility and increased brittleness. The safe alternative is heat straightening. Described in this chapter are methodologies for repairing localized damage using heat straightening.

Local damage patterns display two main characteristics: large plastic strains (usually tensile) in the damaged zone, and bending of plate elements about their weak axis. If the local damage is to be repaired, shortening must be induced in the damaged area equal to the elongation caused when the element was damaged. In addition, the distortion along the yield lines must be removed as part of the repair process. Studies on global damage repair have shown that vee heated regions shorten significantly during cooling and that line heats can be used to induce bending about the yield lines. Thus a combination of line and vee heats can be used to repair localized damage.

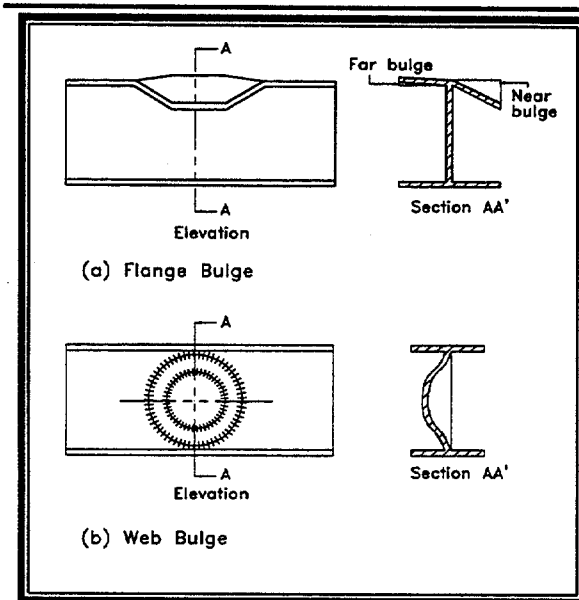


Figure 9.1. Typical localized damage classified as Category L.

The purpose of this chapter is to describe the basic procedures for heat-straightening repair of localized damage. This methodology will be illustrated using elements in which the damage was induced in the laboratory with a controlled loading system. The resulting damage tended to be more symmetrical and less severe than sometimes encountered in practice. The repair procedures described here illustrate the general principles used to repair localized damage. The heating patterns suggested can be adapted to the more complex and irregular actual damage patterns often found in practice.

The first of the two commonly observed local damage types investigated in this study is the flange bulge. For example, this type of damage was observed during a heat-straightening project executed on the Mississippi River Bridge at Greenville, Mississippi, fig. 9.2 and 9.3. Three sway struts

of the through truss had been damaged from underneath by a passing vehicle. Category L/U type local damage is typical in cases where the impact takes place on a plate element with one free edge such as a flange of a beam. fig. 9.4 shows the typical flange bulge pattern. Often, distinct yield lines are formed as well as some zones of flexural yielding where curvature is the highest.

Category L/U damage is commonly caused by impact to a flange on one side of the web. An idealized zone of damage is shown in fig. 9.4. The impacted side of the damaged flange will be referred to as the near side (N). The non-impacted side of the flange on the other side of the web will also typically incur damage. This damage on the far side of the flange (F) has a geometry similar to that of type N but usually of lower magnitude. The damaged flange typically undergoes rotation about a clearly defined yield-line near the fillet of the web. The impacted side of the flange (side N) usually deforms in a folded plate pattern. This flange is shown deforming toward the web in fig. 9.4b. The deformation usually results in yield lines which define the edges of the folded plate (fig. 9.4c). In some cases, particularly in regions of high curvature, the deformation pattern may be one of a flexural yield zone rather than a series of yield lines.

These zones result from plate element flexure and tend to spread over the surface as the degree of damage increases. Such zones will be referred to here as yield surfaces. The other half of the same flange usually deforms in a similar pattern in the opposite direction, even if not directly impacted. The folded plate pattern, fig. 9.4d, tends to have smaller deformations, thus $\delta_n > \delta_f$. Because

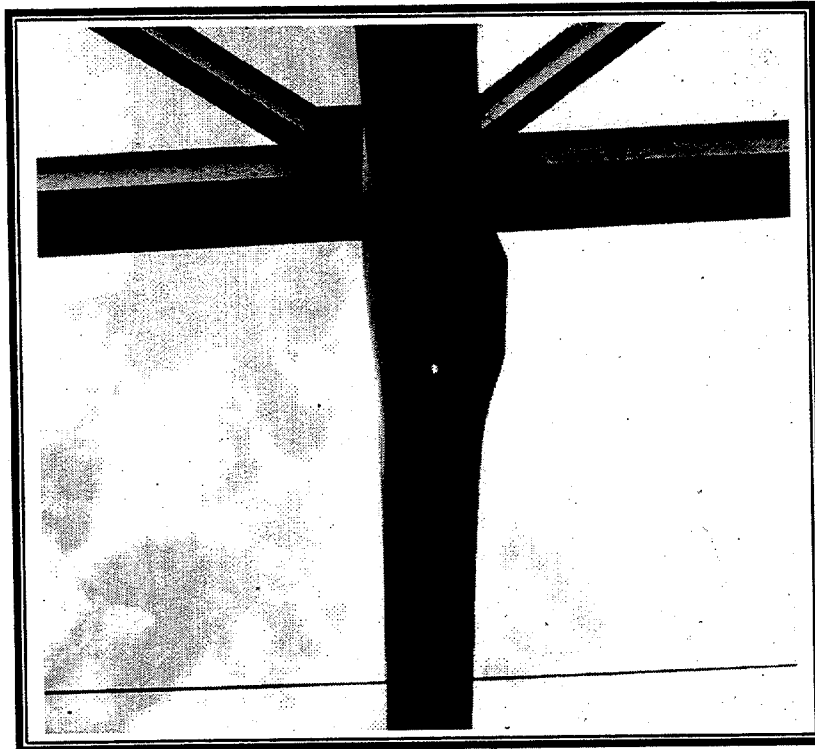


Figure 9.2. Category L/U flange bulge damage on Mississippi River Bridge at Greenville, MS.

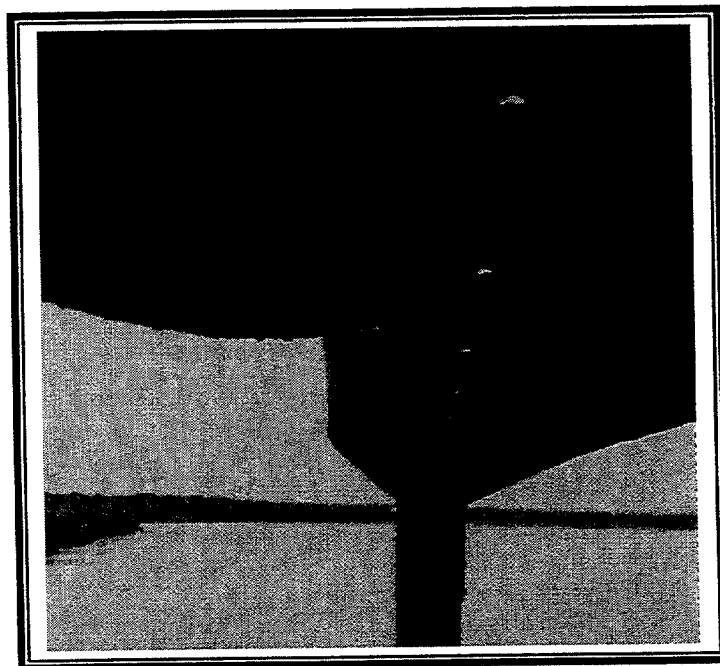


Figure 9.3. Typical Category L/U damage.

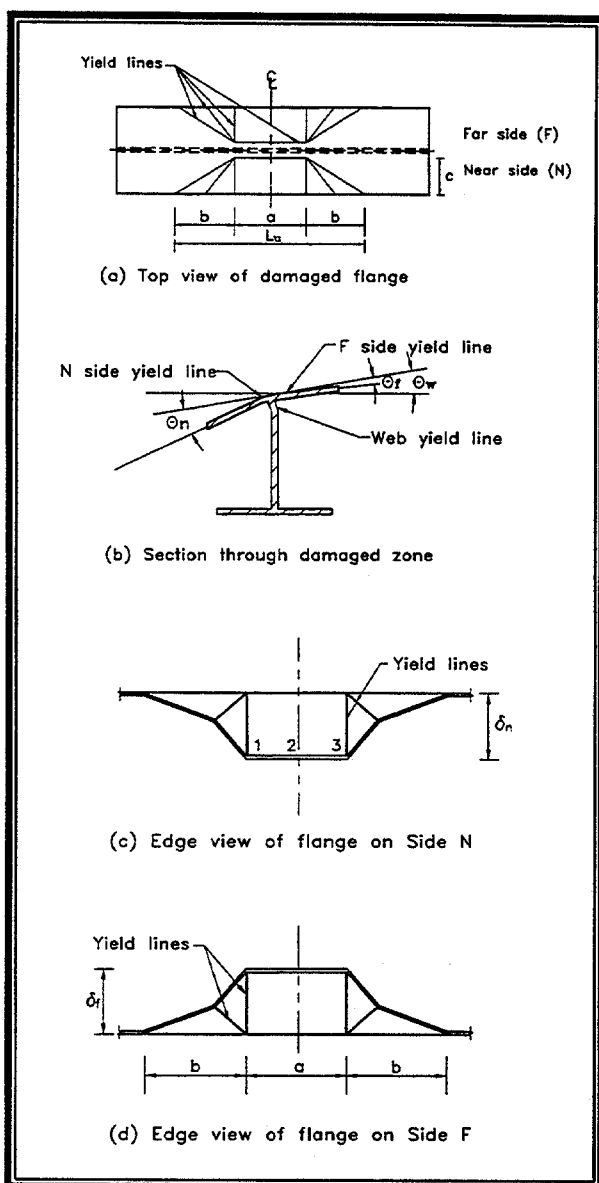


Figure 9.4. Heat straightening local flange damage (Category L/U).

the web is thinner than the flange, a yield line often forms in the web near the fillet. The section shown in fig. 9.4b illustrates this behavior. The tee section at the flange/web juncture remains a rigid right angle. The yield line forming in the web fillet allows this tee to rotate through an angle θ_w . The yield line at the flange fillet on the impacted side of the flange (side N) results from the

additional rotation, θ_n , thus the total rotation of the N flange is $\theta_w + \theta_n$. The other half of the flange (side F) tends to act as a reaction against rotation thus a second flange yield line may form at the F side fillet. The angle formed by this yield line is θ_f and the rotation of the F flange is $\theta_w - \theta_f$. The identification of these yield lines is important in the repair procedure.

Category L/U Damage of Unstiffened Elements

Damage Assessment of Category L/U damage.-While flange bulge type damage may not result in a collapse, if severe, it does reduce the capacity of the structure. The reduction in safety can be caused by either a local reduction of section properties resulting in reduced bending strength or, by local buckling resulting in instability under a compressive load.

In general, four values can be used to define bulge geometry as shown in fig. 9.4. The values are: (1) maximum out-of-plane deflection (δ) of the bulge; (2) original length (L_o) of the free edge of the bulge; (3) width of the bulge (c); and (4) length of the free edge after damage (L_d), which can be approximated by

$$L_d = [a + 2(\delta^2 + b^2)^{1/2}] \quad (\text{Eq. 9.1})$$

It should be noted that this is not the exact length of the damaged free edge since the small curvatures are neglected. Two parameters can be used to classify the degree of damage based on the geometry. The parameters are:

1. **Span/Deflection Ratio**-The ratio of the length over which damage occurs, L_u , to the deflection, δ , where L_u equals $a + 2b$. The severity of damage varies inversely with this ratio.
2. **Flange edge elongation**-The elongation ($L_d - L_u$) caused by damage equals the shortening required at the free edge of the bulge to restore the flange to its undamaged shape. The average plastic strain at the free edge is given by

$$\varepsilon_d = \frac{(L_d - L_u)}{L_u} \quad (\text{Eq. 9.2})$$

A large average plastic strain indicates extensive local damage.

Experimental Results for Category L/U Repairs.-In order to evaluate the most effective heating patterns, a series of tests was conducted on W8 X 13 beams. The load was applied through a spreader plate as shown in fig. 9.5a. Stiffeners were placed 381 mm (15 in) apart in order to limit the damage to the immediate vicinity of the load. Four beams were damaged in this manner to produce a maximum deflection of approximately 25 mm (1 in). A series of yield lines formed as shown in fig. 9.5b which is typical of such damage in the field. The portion of the flange edge at which the maximum deflection occurs, δ_n or δ_f in fig. 9.4, was used to measure the effect of straightening. Rather than taking a single point, similar deflections at three locations (points 1, 2, and 3 in fig. 9.4b) were averaged with these values designated as Δ_n and Δ_f . A summary of the flange damage is shown in table 9.1. The load producing the

yield pattern was approximately 133 kN (30 kips) in each case.

Each beam was straightened using various combinations of jacking forces and heating patterns. One of the fundamental concepts of heat straightening is to heat only in the vicinity of the yield zones. In the case of flange damage, these zones may include a series of yield lines and some yield surfaces on the flange. Yield lines are often distinct and easy to identify. However, sometimes the yield lines merge and form a surface of continuous plastic flexural curvature. For example, in the flange portion over the distance b in fig. 9.4a, the yield lines were difficult to distinguish. Even harder to distinguish was the flange elongation in the plastic range. The strain at initial yield for A36 steel, ε_y , is 0.00124. The average plastic strain over the 381 mm (15 in) damaged length is shown in table 1 in terms of multiples of ε_y . The values range from 5 to 12, indicating significant plastic behavior. As a result, most heats on the outer portion of the flange will be in a yield zone.

This type of yield surface implies that a variety of heating patterns may be applicable. However, for heat straightening to be effective, two key aspects must be considered: (1) the sharp curvatures at yield lines require straightening, and (2) flange shortening must occur to allow the longitudinal plastic strain to be removed. From this discussion it seems logical that line heats should be placed at all yield lines. For the yield surfaces, the longitudinal contraction may be accomplished using half-depth vee heats on the flange with the apex located at the yield line near the web/flange juncture and/or additional line heats in these regions as needed.

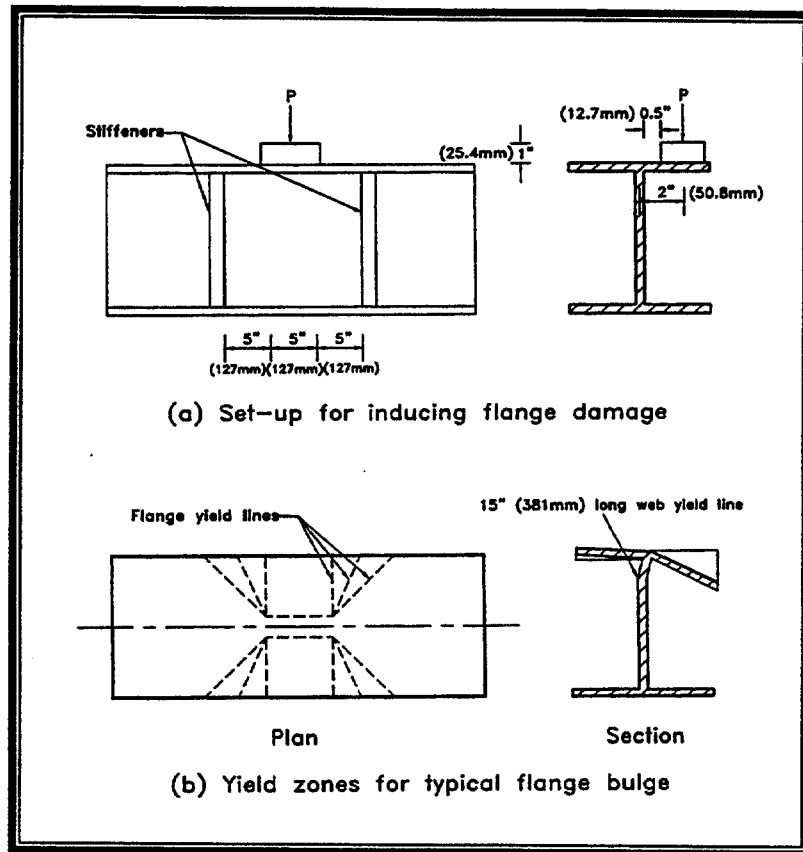


Figure 9.5. Inducement of damage to produce a flange bulge in the flange of a W 8x13.

Table 9.1. Configuration of Flange Damage for Category L/U Repairs in W8x13 Beams (25.4 mm = 1 in).

Beam	Maximum Damage Inducement Load (kN/Kips)	Maximum Deflection, (in)		Near side		Span/deflection ratio L_v/Δ_n	Elongation at Flange Edge			
		Δ_n	Δ_r	a (in)	b (in)		Side N		Side F	
							Length (in)	Multiple of ϵ_y	Length (in)	Multiple of ϵ_y
1	142/32	0.78	0.66	5	5	19.2	0.121	6.5	0.087	4.7
2	129/29	1.07	0.73	5	5	14.0	0.226	12.2	0.106	5.7
3	120/27	0.96	0.73	5	5	15.6	0.183	9.8	0.106	5.7
4	142/32	0.85	0.65	5	5	17.6	0.143	7.7	0.084	4.5

After some preliminary experimentation, it was found that four variables may play a significant role in heat straightening local damage. The first is the external restraining force. Consideration was given as to the magnitude of the restraining force and whether jacking on just the near side of the flange or both sides is most effective.

The second variable was vee heats on the flange. Three cases were considered: (1) no vee heats, (2) vee heats on the near side only, and (3) vee heats on both the near and far sides. The effect of vee angle was also investigated with both 20° and 45° vees evaluated.

The third variable was flange line heats. Again three cases were considered: (1) no line heats, (2) line heats on the near side, and (3) line heats on both sides.

The fourth variable was also a line heat. However, it was considered separately since it was applied to the web. The web yield line resulting from typical damage is usually distinct and is located near the web fillet.

These parameters were varied during the course of straightening the damage in the four W8 X 13 beams described in table 9.1. Plots of the near and far flange deflections after each heating cycle are shown in figs. 9.6-9.9 with specific parameters used for each cycle at the top of the figures. It is clear that certain combinations are highly effective while others are relatively ineffective. The pattern rankings are summarized in fig. 9.10. Of these, the three most effective have the following in common:

1. A restraining force is applied to both the near and far sides of the flange.
2. Flange line heats are applied to both the near and far sides of the flange on the convex surface.
3. A line heat is applied to the web on the convex surface.

The most surprising result was the response of the beam to the flange vee heats. The near side movements were inversely proportional to the size of the vees with the most effective pattern being the one with line heats and no vee heats. The use of two 20° vees in combination with the line heats on both sides of the flange was 20 percent less effective. Forty-five degree vees with line heats were 50 percent less effective. The far side flange movements followed a similar pattern although the 45° vees produced slightly more movement than the 20° vees. This behavior illustrates an important heat straightening principal: too much heating can reduce effectiveness. The heat-straightening process depends on heating small areas which are surrounded by cool areas. By superimposing vee heats and a number of line heats, the internal restraining effect is reduced. The most effective patterns are thus those dispersed over the damaged zone of the flange.

The specific heating pattern depends on the details of the damage geometry. The typical damaged cross section is shown in fig. 9.11a. There are three components of rotation: (1) the web/flange juncture, which remains at right angles, and has a rotation θ_w resulting from rotation about the web yield line; (2) the near side flange, N, which has a

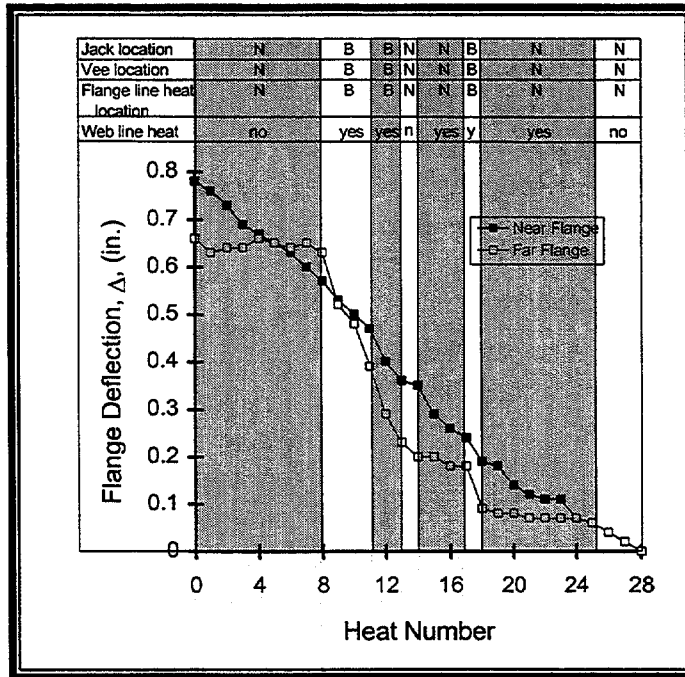


Figure 9.6. Flange movements for various heating patterns for Beam No. 1 with Category L/U damage (N and B refer to near and both sides of the flange, respectively and 25.4 mm = 1 in).

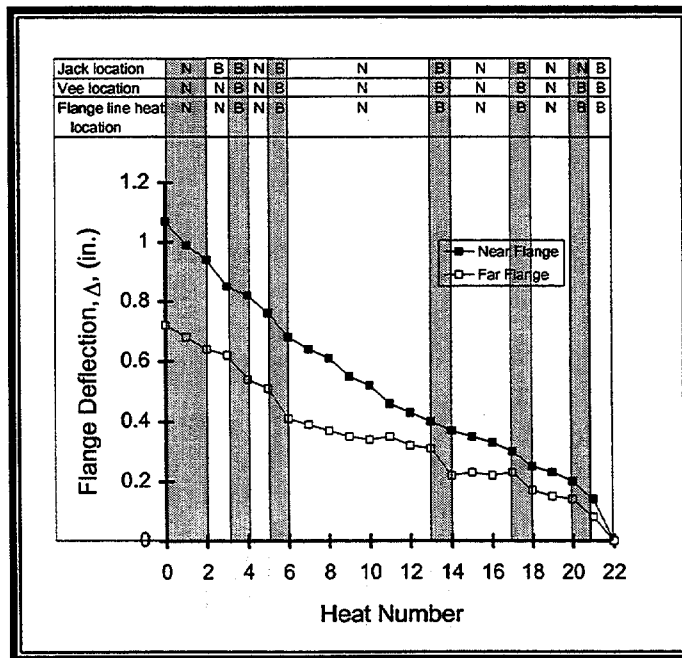


Figure 9.7. Flange movements for various heating patterns for Beam No. 2 with Category L/U damage (N and B refer to near and both sides of the flange, respectively and 25.4 mm = 1 in).

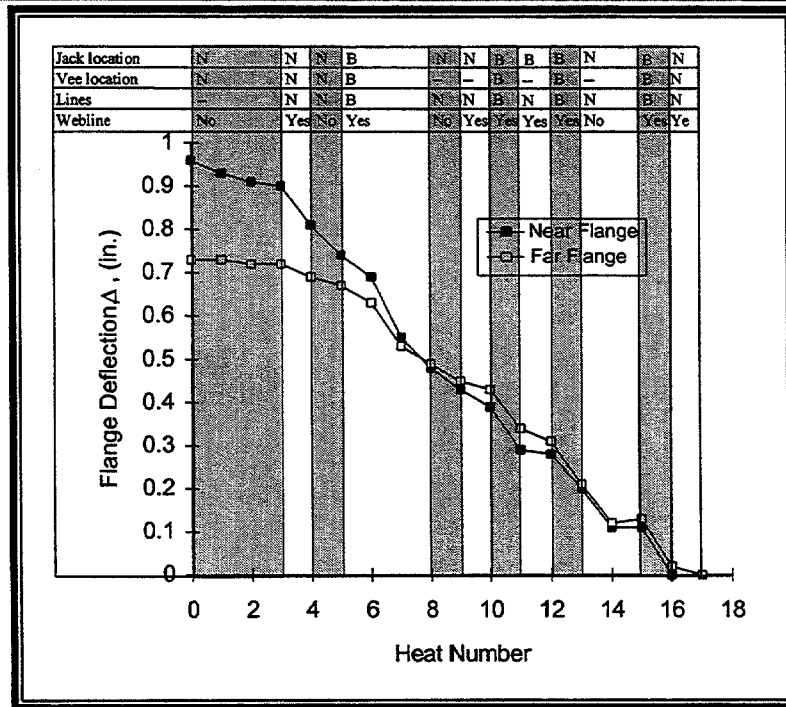


Figure 9.8. Flange movements for various heating patterns on Beam No. 3 with Category L/U damage (N and B refer to near and both sides of the flange, respectively and 25.4 mm = 1 in).

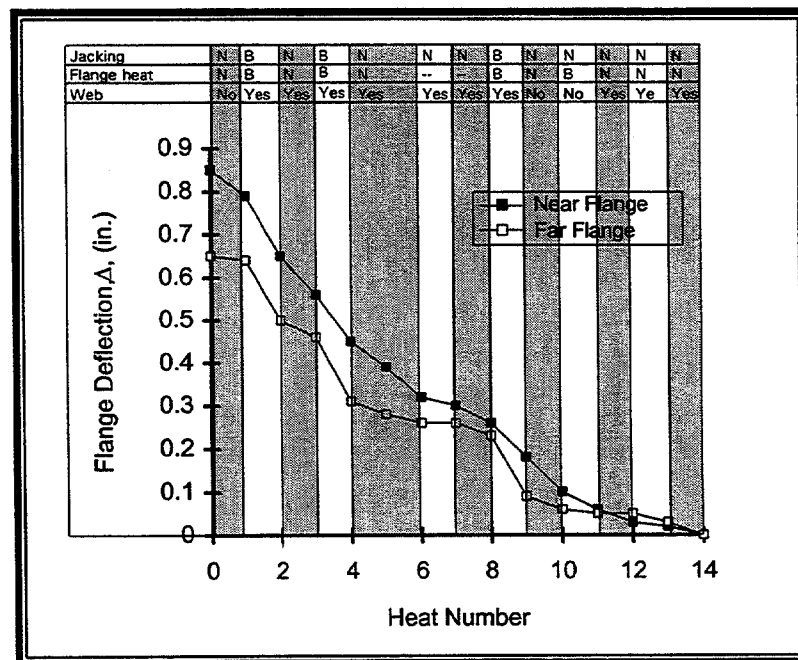


Figure 9.9. Flange movements for various heating patterns for Beam No. 4 with Category L/U damage (N and B refer to near and both sides of the flange, respectively and 25.4 mm = 1 in).

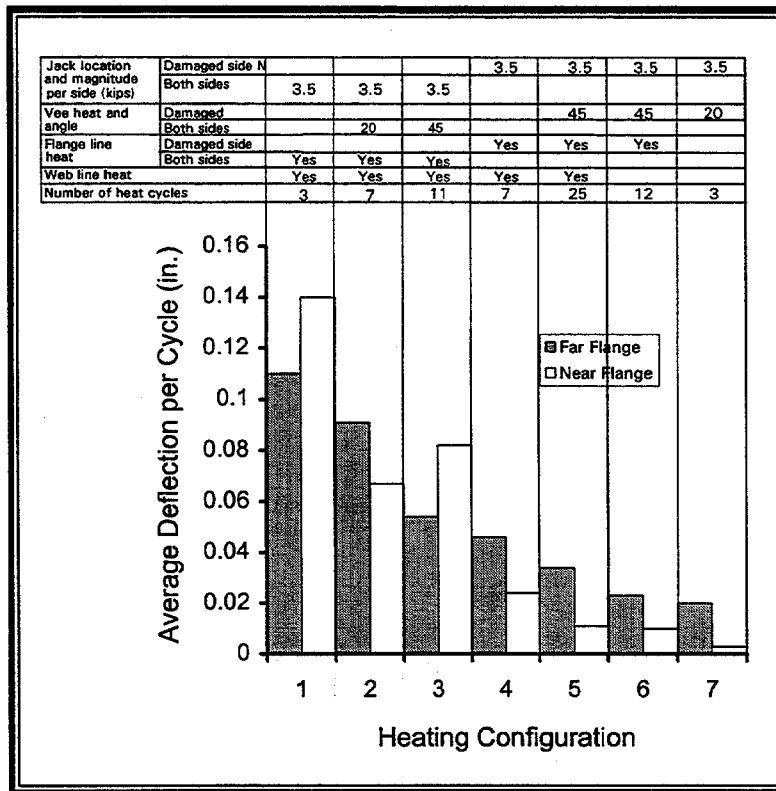


Figure 9.10. Average flange deflection per heating cycle for the most effective patterns (3 cycles minimum) for Category L/U damage (25.4 mm = 1 in).

rotation θ_n , resulting from additional rotation about the flange yield line; and (3) the far side flange, which has a reduced rotation, $\theta_w - \theta_p$, resulting from the resistance of flange F to rotation caused by forces applied to flange N. The heating/jacking pattern to straighten this damage will depend on how the geometry changes as heat straightening progresses. The following steps outline the process.

Phase I. -Initial heating and jacking patterns.- This phase is most effective with jacking forces on both the near and far sides of the flange. However, it can be conducted with jacking only on the near (impacted) side. The specific steps are:

1. Restraining forces

Place jacking forces on both the near and far sides of the damaged flange in the direction tending to restore the flange to its original condition. As shown in fig. 9.11a, a convenient arrangement on the near side is to place a jack, P_n , between the top and bottom flange. The far side jack, P_p , requires a clamping type force which is often more difficult to arrange in field applications. If the clamping force cannot be anchored from the opposite flange, a spreader beam arrangement can be used, as shown in fig. 9.11d, to anchor the reaction to the straight portions of the far side flange. An alternative is to only jack from the near side.

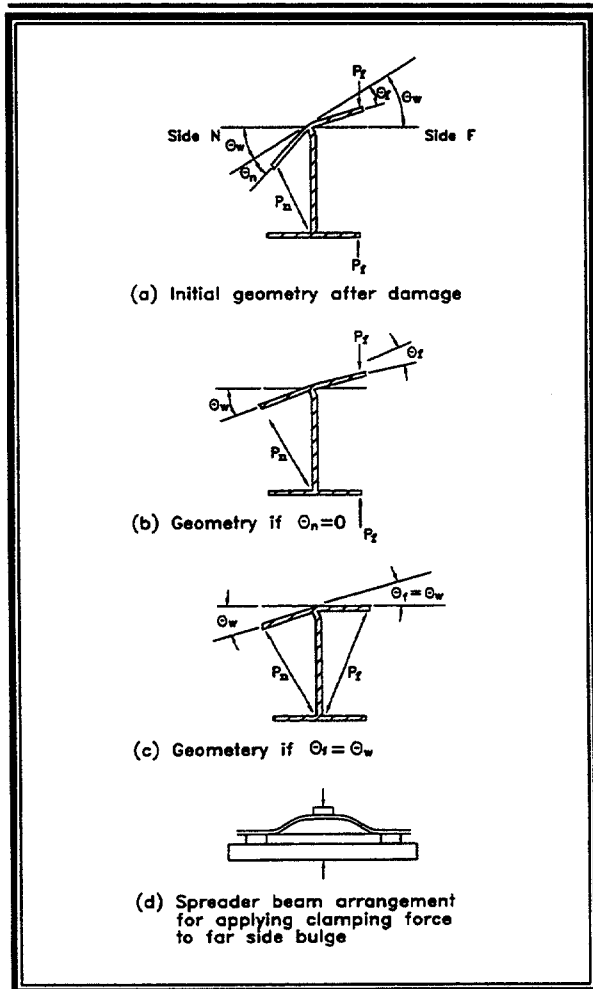


Figure 9.11. Arrangement of restraining forces during various stages of repair.

However, the average movement per cycle tends to be lower than similar cases jacked on both sides. This approach was used for configurations No. 4-7 shown in fig. 9.10. Care should be taken to limit the magnitude of jacking forces used. A discussion of methods to determine jacking forces is given in a later section.

2. Vee heats

Although vee heats may not be necessary, a limited number may be used to assist in the flange shortening effort. The vees should be approximately half depth and applied to both the near and

far sides of the flange to eliminate global curving of the member. The vee should be narrow with an angle of 20° or less and the open end of the vees should be at the flange tips. It is best to place the vee heats in regions where no line heats are required. No more than two vees should be used (preferably only one) in one heating cycle. The location should be shifted with each heating cycle so the same location is not re-heated for at least three cycles. A typical arrangement is shown in fig. 9.12b.

3. Line heats

All flange yield lines except line 11 should be heated (on the convex surface) after any vee heats used. A typical pattern is shown in fig. 9.12a. In yield surfaces of continuous plastic strain such as often occurs in regions such as ABC in fig. 9.12a, line heats should be spaced over the section at a spacing of approximately $b_f/4$ where b_f is the flange width. Similarly, line heats may also be used instead of vee heats on section BCDE. The order of heating the yield lines tends to have a minor impact although it is good practice to heat the ones at the largest damage locations first. It is also recommended to heat the near side lines prior to the far side.

4. Web line heat

The web yield line should be heated last. It is typically located at the fillet as shown in fig. 9.12c.

These four steps complete the cycle. The cycle should be repeated until the flange is straight.

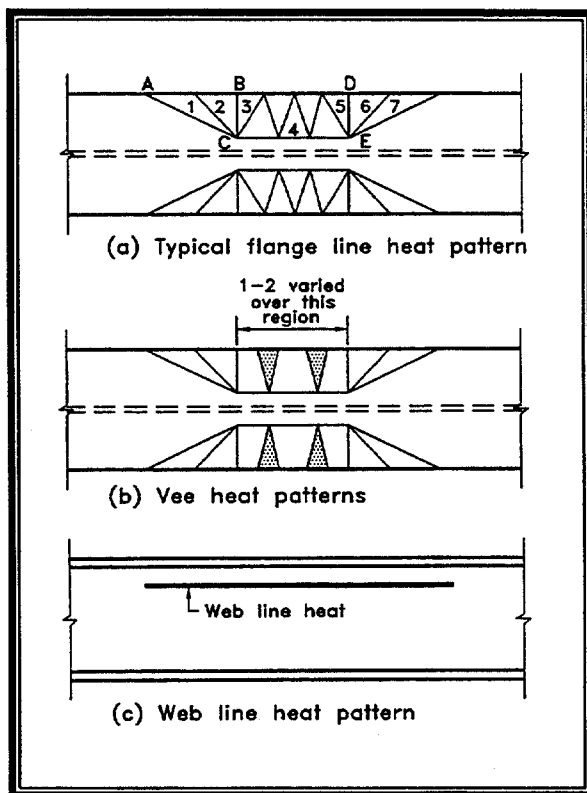


Figure 9.12. Arrangement of vee and line heats.

Phase II. Heating/Jacking Pattern if $\theta_n = 0$. Quite often phase I can be used to nearly straighten the section. However, the progress of the movement should be observed to insure that over-straightening does not take place. If the near flange movement progresses too quickly, then θ_n may become zero prior to θ_w . This situation is shown in fig.9. 11b. Should this behavior occur, a modification in the phase I pattern should be made in Step 3 for line heats. Rather than heating all seven lines on the near side (fig. 9.12a), line 4 should not be heated. Likewise, line 11 should not be heated.

Phase III. Heating Pattern if $\theta_f = \theta_w$. If straightening progresses to the point that $\theta_f = \theta_w$, then the far flange may over-straighten with the continuation of Phase I

heating. The pattern should be changed. The situation is depicted in fig. 9.11c. The modification is to reverse the direction of the far side jacking force while continuing the phase I patterns including lines 4 and 11. The force P_f will prevent over-straightening while allowing the near flange and web to continue corrective movement.

Flange Damage in Opposite Direction.-If the damage is reversed, i.e., side N is pushed away from the opposite flange instead of toward it, then the direction of the restraining forces should be reversed. The heating patterns are similar to those previously described and are shown in fig. 9.13.

It should be recognized that localized damage to unstiffened elements can have a wide variety of geometries. The cases shown here establish both the pattern and principals upon which heat straightening can be based. Judgement is needed to apply this methodology for specific cases.

Computation of Restraining Forces.-When a flange is damaged by a concentrated force, the flange initially behaves as a flexural plate and deforms into a series of yield lines. As the deformations increase into the large deflection range, the flange acts as a membrane with large tensile stresses. When the jacking force is applied, the reverse occurs. Initially, relatively large axial compression stresses will occur. As the plate straightens, the flexural stresses tend to become more dominant. Thus, the jacking force serves two purposes: to create compressive axial stresses which accelerate the flange shortening at both the line and vee heats; and to create bending stresses at yield lines which again accelerates straightening.

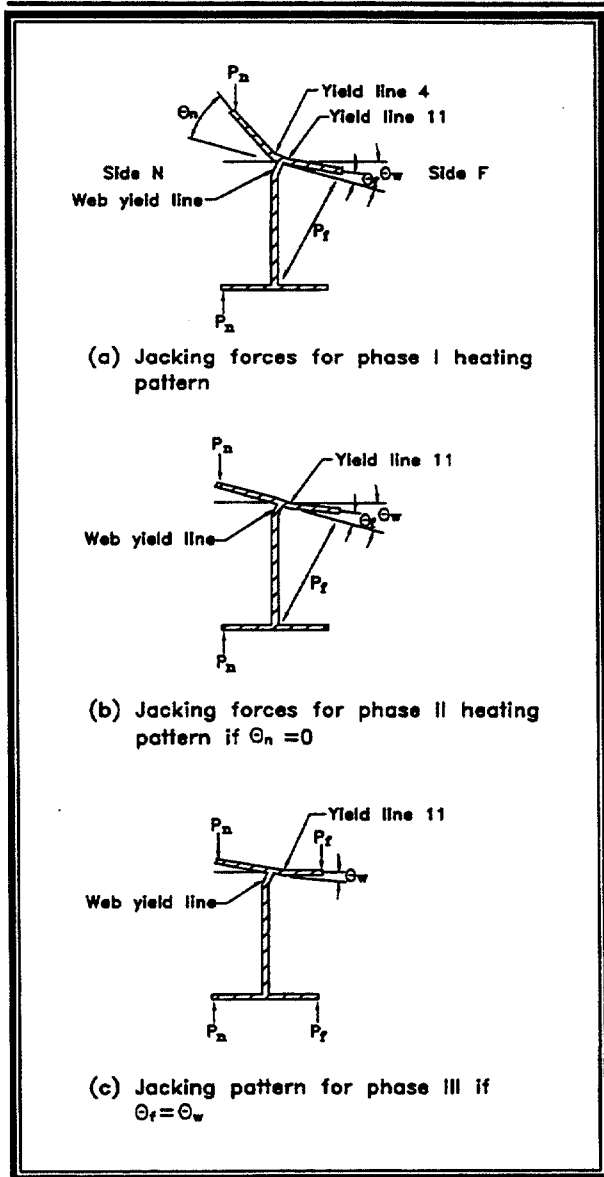


Figure 9.13. Jacking sequence if damage is reversed from that shown in Figure 9.11.

A conservative approach is to limit the jacking force to a percentage of the force required to produce a yield line collapse load which is defined as the formation of a mechanism in which deformations will continue under a constant load. This load can be computed by a yield line analysis. A generic layout to model typical flange bulge geometry is shown in fig. 9.14 where the

applied load, W_u , is assumed to be uniformly distributed over one-half of the center region shown in fig. 9.14.

The simplifying assumptions used for calculating restraining forces are: (1) The strength of the plate is governed by flexure alone and axial effects are ignored; (2) The plate is assumed to be a thin plate, i.e., the width of the plate is much greater than its thickness; (3) The steel is perfectly plastic and fully yielded at the yield-lines; (4) The plate deforms plastically at failure but is separated into elastic segments by the yield-lines; (5) Bending and twisting moments are uniformly distributed along the yield-lines; and (6) Elastic deformations are negligible compared to the plastic deformations, i.e., the plate segments rotate as plane segments when a mechanism forms.

Because of the arched folded plate, bending stresses induced by the load should be lower than those that would be induced in a flat plate. As long as the axial component of the load does not exceed the bending component, the yield-line load will give a conservative value of the allowable load. In most actual cases of flange bulge damage, the aspect ratio for the bulge is relatively low and the yield-line analysis is a good approximation. Referring to fig. 9.14, δ_u is the virtual deflection along line BC. The plate is isotropic so the moment yield line bending capacity is identical in all directions. The external load, W_u (force/area) is the load producing a mechanism and the moment capacity along a yield line, M_p , is given by

$$M_p = \frac{F_y t^2}{4} \quad (\text{Eq. 9.3})$$

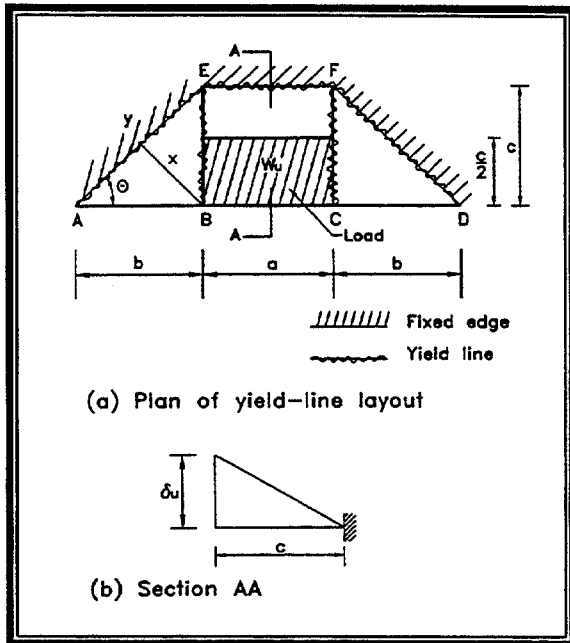


Figure 9.14. Yield-line analysis for idealized flange bulge geometry.

The work done, W_e , by external loads, W_u , is

$$W_e = (W_u \frac{ac}{2})(0.75\delta_u) \quad (\text{Eq. 9.4})$$

The internal work done, W_i , is computed from the moments along yield-lines AE, EF, FD, EB, and FC.

$$W_i = M_p \left\{ \frac{a\delta_u}{c} + \frac{2c\delta_u}{b} + \frac{2c\delta_u}{b} + \frac{2b\delta_u}{c} \right\} \quad (\text{Eq. 9.5})$$

Equating external and internal work done,

$$W_u = \frac{8 M_p}{3 ac} \left(\frac{a}{c} + \frac{4c}{b} + \frac{2b}{c} \right) \quad (\text{Eq. 9.6})$$

If a load ratio of 50 percent is used, then the jacking force on the bulge is

$$P_j = W_u \frac{ac}{4} \quad (\text{Eq. 9.7})$$

If $c = b/2$

$$P_j = \frac{W_u ab_f}{8} \quad (\text{Eq. 9.8})$$

The yield-line formula is applicable for obtaining an approximate estimate of the jacking force for flange bulges. Applying these formulas to the test beams assuming A36 steel where $a = b = 127 \text{ mm}$ (5 in), $c = b/2 = 51 \text{ mm}$ (2 in), and $M_p = 2.60 \text{ m-kN/kN}$ (0.585 in-k/in):

$$W_u = 9.79 \text{ MPa (1.42 ksi)}$$

$$P_j = 15.8 \text{ kN (3.55 kips)}$$

Thus, the jacking force used for the four experimental beams was approximately 50 percent of the yield line load.

Experimental Results of Active Heat Straightening.-A fifth W 8 X 13 beam (No. 5) was repaired after being damaged in a similar manner to those previously described. The repair procedure was that of configuration No. 1 in fig. 9.10 and consisted of line heats on both near and far sides of the flange as well as the web, but no vee heats. A jacking force of 15.6 kN (3.5 kips) was used on both the near and far side. However, this force was maintained throughout the heating/cooling cycle by continuously adjusting the jacks as the

flange straightened. This procedure is referred to as active heat straightening. The method proved effective. Four heats produced average flange deflections of $\Delta_n = 4$ mm (0.16 in) and $\Delta_f = 3$ mm (0.12 in) which was slightly more than configuration No. 1 in fig. 9.10. This procedure is not generally recommended in heat straightening. However, for shallow bulges, the jacks may loosen and fall out as movement occurs unless some jacking is done. Caution is advised when using this procedure to insure that over-jacking does not occur.

Mechanical Properties of test specimens.-Test specimens were taken from an undamaged beam, Beam No. 3 in the heated zone, and from the heated region of the beam No. 5. The results are shown in table 9.2. Both yield and ultimate strengths were similar. The percent elongation for heated specimens was somewhat smaller as typically found in heat straightening. Since the steel yield stress was significantly higher than assumed in the yield line analysis, the jacking ratio was actually 30 percent and not the assumed value of 50 percent.

Category L/S Damage for Stiffened Elements

Stiffened elements of a beam are defined as those supported on both sides by perpendicular elements. The web of a wide flange beam is a typical example in that the two flanges provide the support or stiffening effect. When stiffened elements are damaged, the pattern formed is usually a dish shaped bulge. This damage frequently approximates a shallow spherical shell. To evaluate methods of straightening Category L/S damage, bulges were induced in the web of several beams. For plastic deformations induced in Beam No. 7 of about 13 mm (1/2

in), the bulge had a base diameter of 127 mm (5 in) and a fairly smooth curvature as shown in fig. 9.15b. For Beam No. 6, the loading was continued longer to produce a base circumference of 343 mm (13.5 in) and a maximum deflection 42 mm (1.66 in). The curved surface again was relatively smooth as shown in fig. 9.15.a. In order to evaluate behavior during repair, deflection measurements were taken at the center and at the approximate point of contraflexure. These measurements were made on both the longitudinal and transverse axes of the beam. Since response was generally symmetrical, only the center point and one contraflexure point will be shown on plots as indicated by δ_i and δ_c in fig. 9.15.

The restraining force was applied by a jack at the center of the bulge using a spreader plate. The magnitude of the jacking force is a function of the bulge geometry. If the bulge is approximated as a shallow spherical shell, the constant radius of curvature, R , can be expressed as

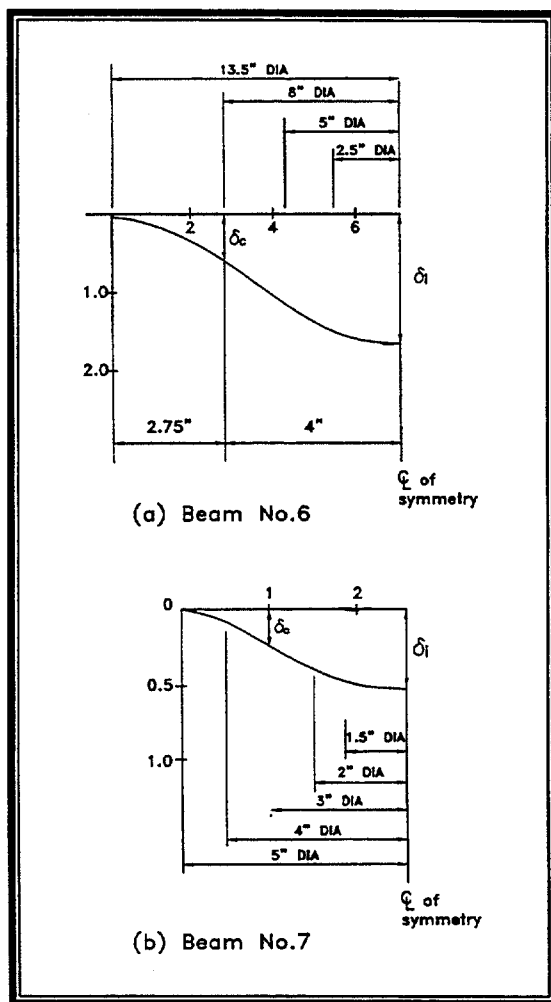
$$R = \left(\frac{\delta_i^2 + r_b^2}{2\delta_i} \right) \quad (\text{Eq. 9.9})$$

where r_b is the radius of the sphere at its base. The characteristic length, ℓ_c , is given by

$$\ell_c = \frac{\sqrt{(Rt)}}{[12(1-\nu^2)]^{.25}} \quad (\text{Eq. 9.10})$$

Table 9.2. Results of tensile tests on dent specimens.

Sample	Ultimate Strength		Yield Strength		Modulus of Elasticity (MPa ksi/)	Percent Elongation %
	(Mpa/ksi)	% dif	(Mpa/ksi)	% dif		
Undamaged	525/76.1	—	414/60.0	—	221,000/32,000	33
Beam No. 3	541/78.4	+3.0	419/60.8	+1.5	186,000/27,000	22
Beam No. 5	553/80.2	+5.4	430/62.4	+4.0	241,000/35,000	23



where t is the plate thickness and ν is Poisson's ratio. For shallow spherical shells with a concentrated load at the center, the critical stress results from bending about a circumferential line if $r/l_c \leq 1.6$ (Timoshenko, 1959) where r is the distance from the center to the line in question. The smaller r/l_c , the higher the stress. A practical limit for r could be taken as the radius of the jack utilized since a concentrated load produces a discontinuity at the actual center.

Here, a jack radius of $r = 0.84$ was used for both Beams 6 and 7. From Timoshenko (1959), the relationship between r/l_c and the factor $\beta = t^2\sigma/P_j$ is given in table 9.3 where σ is the maximum shell stress and P_j is the applied load at the center of the bulge.

By setting σ equal to the desired percentage of the yield stress, the appropriate jacking force, P_j can be computed for a given r/l_c ratio. This procedure provides an approximate method of determining the jacking force. As the bulge flattens, δ_i decreases and the jacking force should be reduced to maintain the same stress level.

Figure 9.15. Bulge cross section geometry (25.4 mm = 1 in).

Table 9.3. Relationship between r/ℓ_c and Shell Stress Factor.

Factor	Shell stress factor, β					
	0.4	0.6	0.8	1.0	1.2	1.4
r/ℓ_c	0.4	0.6	0.8	1.0	1.2	1.4
$t^2\sigma/P_j$	0.80	0.57	0.43	0.33	0.25	0.18

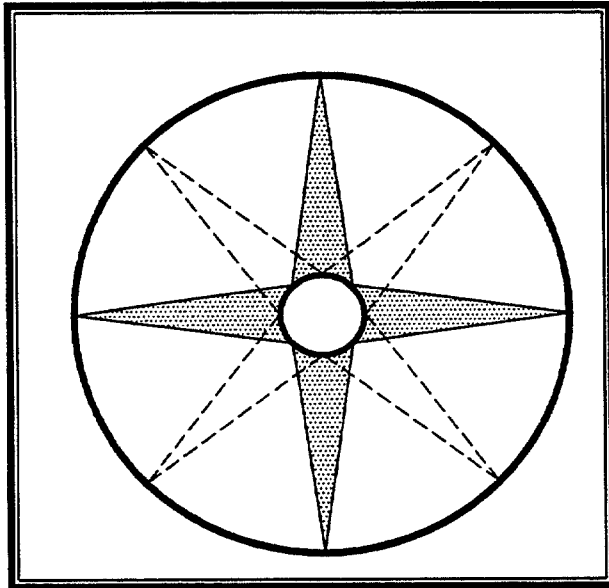


Figure 9.16. Star vee heat pattern.

Experimental Results.—Based on preliminary studies, Beam Nos. 6 and 7 were straightened using several different heating patterns. The patterns consisted of one or more of the following components:

1. Ring line heats

These heats are circumferential line heats in concentric circles around the center of the bulge. They should be located at regions of largest curvature and applied on the convex surface. Each ring is identified by its diameter.

2. Radial line heats

These heats are equally spaced and emi-

nate from the bulge center. The arrangement used here had eight radial lines spaced at 45°.

3. Star vee heats

The star vee heat pattern consists of a series of vees arranged symmetrically around the bulge center with the open end of the vees at the center. This arrangement gives the appearance of a star, hence the name. The pattern used here consists of four vees spaced at 90°. On alternate heats the four point pattern is shifted 45°. The vee angle was limited to 20°. The layout is shown in fig. 9.16. The size of the vees are here specified as the diameter of a circle through the tip of the vees.

Beam No. 6 was heated with 4 point star vees and ring line heats only. The heating patterns and movements are shown in fig. 9.17. Most of the star vee heats were located near the center portion, being inscribed in a 127 mm (5 in) diameter circle. A few 343 mm (13.5 in) diameter star patterns were used at the beginning and end of the repair. Several ring line heats were used ranging in diameter from 64 mm (2.5 in) to 445 mm (17.5 in). During the first 10 heats, the load ratio was kept in the 50-60 percent range. For the remaining heats it was reduced to the 25 - 30 percent range.

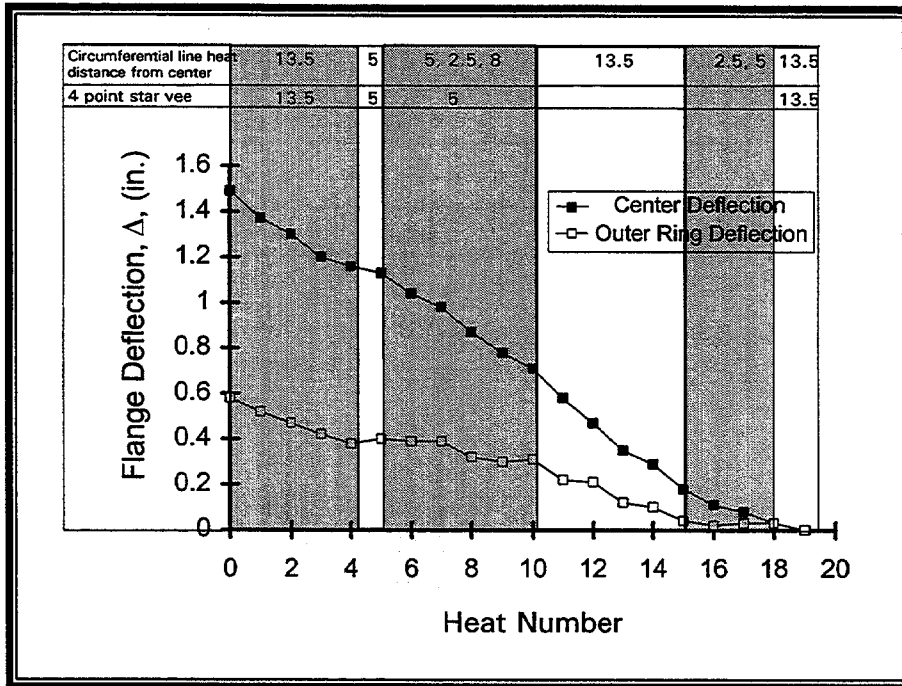


Figure 9.17. Decrease in deflections of stiffened web for Beam 6 (W 16x26) with Category L/S damage (25.4 mm = 1 in).

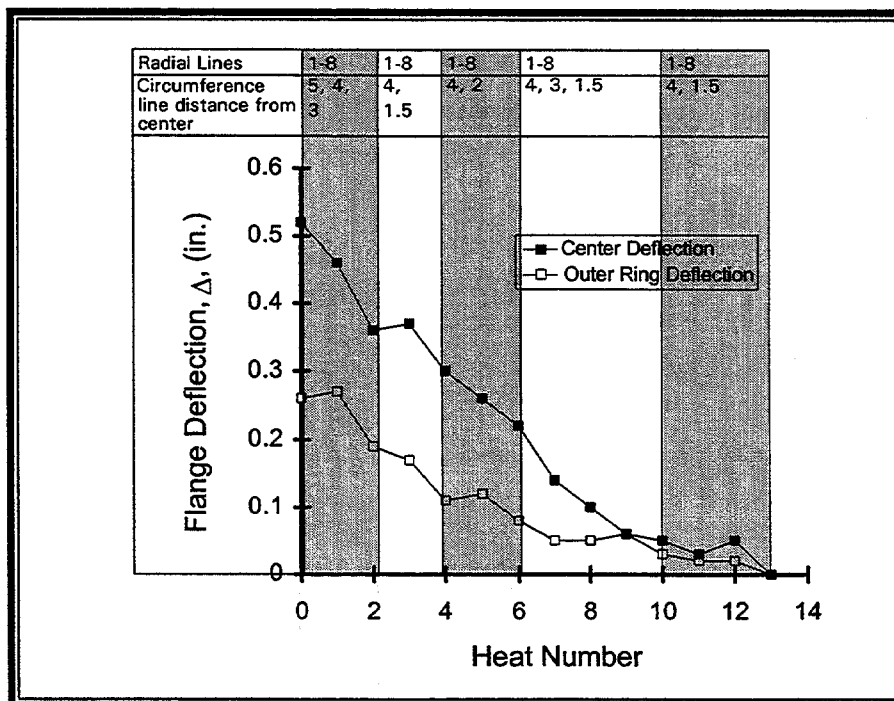


Figure 9.18. Decrease in deflection of stiffened web for Beam 7 (W 16x26) with Category L/S damage (25.4 mm = 1 in).

The center point deflection, δ_i , reduced steadily for all heating patterns with an average value per heat of 2 mm (0.08 in). The outer deflection, δ_o , followed a similar pattern except when both line and vees were concentrated in the central portion of the bulge.

For beam No. 7, only radial and ring lines heats were used. The deflections decreased in a regular manner until the last several heats as shown in fig. 9.18. The average deflection, δ_i , per heat was 1mm (0.04 in). The jacking ratio was initially 41 percent and was reduced incrementally to 14 percent by the final heat. Although the average central movement was less for Beam 7, this damage required a few less heats to complete. In terms of bulge span/maximum deflection ratios, d_b/δ_i , the two beams are quite similar. Beam No. 6 had a ratio approximately 10 percent smaller (8.1 versus 9.6). Thus, it is not surprising that Beam No. 6 required more heats.

The reciprocal of span/deflection ratio offers a good way to compare the rate of straightening for different size bulges. For example, Beam No. 6 heating patterns reduced the δ_i/d_b ratio by an average of 0.0065 per heat while the rate for Beam No. 7 was 0.0077 per heat. Using this criteria the combination of ring and radial line heats are more effective. This conclusion agrees with the results for unstiffened elements in which the line heats were somewhat more efficient than the line/vee combination.

Recommended Methodology.-

Judgement is required when selecting the heating patterns for damaged stiffened elements. Heating the regions of sharpest curvature with combinations of lines and/or narrow vees is the most effective approach.

Always follow the practice of heating only in the vicinity of regions with plastic curvature. As straightening progresses, this region may become smaller. The following methodology is recommended for bulges in stiffened elements.

1. Selection of Jacking force

The jacking force is typically applied at the crown of the bulge using a spreader plate. The jacking force may be selected by considering the bulge to be a shallow shell. First calculate the radius of curvature, α , from eq. 9.9. Then calculate the characteristic length, ℓ , from eq. 9.10. A value for the stress factor, β , can be interpolated from table 9.3 where

$$\beta = \frac{t^2 \sigma}{P_j} \quad (\text{Eq. 9.11})$$

For a load ratio of 0.5, $\sigma = F_y/2$. Thus, the jacking force for this load ratio is

$$P_j = \frac{t^2 F_y}{2\beta} \quad (\text{Eq. 9.12})$$

where F_y equals the nominal yield stress. As the bulge straightens, the jacking force should be reduced. One approach would be to use the above procedures to compute a new jacking force as δ_i decreases. However, by estimating the number of heats required to straighten the bulge, the jacking force can be reduced proportionally after each heat until it is one-half of its original value at the last heat.

2. Estimation of the Number of Heats Required and Modification of Jacking Force

While data is limited, a reasonable estimate of the reduction in the reciprocal span/deflection ratio per heat is 0.007 which is the average of the two cases presented here. The estimated number of heats, n , is

$$n = 140 \left(\frac{\delta_i}{d_b} \right) \quad (\text{Eq. 9.13})$$

Based on this estimate, the jacking force should be incrementally decreased. The jacking force for the i^{th} heat, P_i , is

$$P_i = \left(1 - \frac{i}{2n} \right) P_j \quad (\text{Eq. 9.14})$$

As the straightening progresses, if the estimate is found to be in error, adjust the jacking force up or down to compensate.

3. Initial Heating Pattern

The typical bulge will have reverse curvature bending as shown in fig. 9.19. The crown region should be heated first with the torch on the convex side. As movement progresses, the heating patterns can be expanded into the reverse curvature region again with the torch on the convex side. The initial heating patterns should consist of radial and ring line heats as illustrated in fig. 9.19. The exact number of ring heats will depend

on the size of this region. It is recommended that the diameter of the smallest ring be no less 51 mm (2 in) and that spacing between rings be at least 51 mm (2 in). For large bulges the ring spacing should be larger than 51 mm (2 in). For cases where the curvature is relatively uniform, equally spaced rings may be used. However, a ring heat should be placed at locations where sharp changes in curvature are indicated. Heat the outer ring on the concave side first and work inward. After the rings are heated, the radial lines should be heated. Again, work from the outside in but do not run the radial lines inside the last ring. Continue this pattern cyclically until the crown region begins to flatten. Allow the steel to completely cool between heating cycles.

4. Final Heating Pattern

As the crown section flattens, the heating pattern should be expanded into the reverse curvature regions. One alternative is to expand the number of ring heats and extend the radial heats as described in Step 3 and shown by dashed lines in fig. 9.19b. The second alternative is to use four-point star vee heats along with ring heats instead of radials. The star vee pattern is shown in fig. 9.16. The vees are heated first, working from tip to center. However, the central portion past where adjacent vees intersect should not be heated. Vees should be narrow with an angle of 20° or less. After star vee heating, the rings should be heated, starting with the outermost ring. A maximum of three ring heats should be used at one time with the star vees.

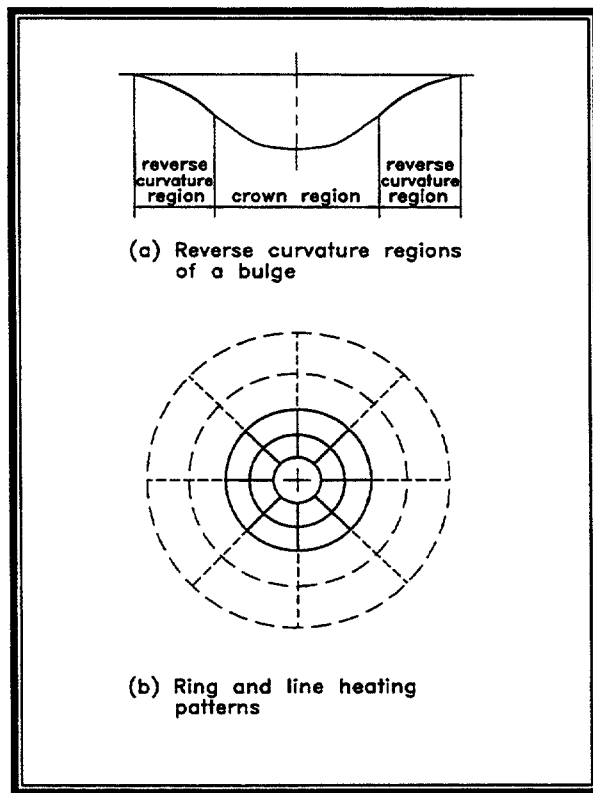


Figure 9.19. Curvature and line heating patterns for category L/S damage

Rotate the star vee pattern 30° after each cycle so that the same vees are not repetitively heated. Rings may be repetitively heated or shifted, depending on the degree of plastic curvature. The steel should completely cool before the next heating cycle begins.

Summary

A methodology has been presented to heat straighten localized damage (Category L). This category is subdivided into two sections: Category L/U referring to unstiffened elements, and Category L/S referring to stiffened elements. The basic

principles used for category L damage follows that for other types of heat straighten-

ing. Experimental data was presented to illustrate the effectiveness of the various heating patterns.

It should be emphasized that localized damage may have highly irregular patterns. Repairs may require a variety of heating patterns depending on the damage configuration. The principles discussed in this chapter provide a guide but judgement is needed for individual applications.

A second area of judgement relates to degree of damage. For plate elements bent about their weak axis, the strain ratio (ϵ/ϵ_y) may well exceed 100. Caution is urged in the repair of damaged elements with strain ratios in excess of 100. However, local damage often occurs at points on the cross section where live and dead load stresses are not large. As such the repair of large strain cases might be undertaken for Category L damage which would not be considered for Categories S, W, or T. In all cases engineering judgement is required.

Key Points to Remember

- Local damage to unstiffened elements (Category L/U) and stiffened elements (Category L/S) can be heat straightened.
- Local damage is most effectively straightened by using a relatively small number of line heats rather than a large number of vee heats.
- Jacking forces are usually required for straightening local damage.
- Straightening local damage is usually done in stages in which both jacking forces and heating patterns are varied in response to the progression of movements.

-
- As a general rule, apply the heat to the convex side of the surface.
 - For shallow surface configurations the jacking force may be greatly relieved during the cooling cycle. To insure effective movement, the jacking force may be maintained at the original level during cooling but, in no case, increased above the original value.
 - Heat straightening requires a number of cycles to complete the repair. Over-jacking to straighten in one or two cycles (hot mechanical straightening) is not heat straightening. Hot mechanical straightening is not recommended as it may be detrimental to the material.

Chapter 10. Heat-Straightening of Steel: Fact and Fable

Introduction

Although examples of heat-straightening techniques for the repair of damaged steel structures have been reported for over 50 years, relatively little research had been conducted prior to 1985. Much of that work was either published in relatively obscure and diverse publications or not published at all. As such, there was a lack of synthesis of available information. In addition, there were major gaps in the available research data leading to speculation and contradictory statements about various effects associated with the heat-straightening process. The recent research described in this manual has addressed many of these issues. However, it is important to specifically address the misconceptions that have evolved. It is also important to provide a review of the previously available literature on heat straightening. The purpose of this chapter is to summarize the earlier available information on the heat-straightening method and to address some of the more common misconceptions by providing the documented facts related to each one. This chapter thus serves as a literature review of heat straightening prior to the material developed in this manual.

One of the most basic fables relates to the concept itself:

Fable

Heat straightening of steel is a myth. The only way to straighten damaged steel is by cold or hot mechanical straightening.

Fact

Heat-straightening of steel can be traced in the literature to 1938 when Joseph

Holt wrote what appears to be the first paper (unpublished) describing heat-straightening procedures. A number of papers have followed that primarily describe basic techniques and successful field applications ("How" 1959; "Flame" 1959; Holt 1955, 1965, 1971; "Kinks" 1981; Newman 1959; "Oxyacetylene" 1959; Shanafelt and Horn 1984). The concept is based on using carefully controlled and applied heat without the use of an active force although passive restraining forces are often used.

The basic element of steel construction is the flat plate. Rolled or built-up members may be considered as plate elements assembled to obtain an advantageous shape. Expertise in heat-straightening, therefore, requires a thorough understanding of the behavior of plates during the heating and cooling process. There are two basic types of distortion generally associated with plates: bends about the strong axis, which are usually straightened with vee heats; and bends or bulges about the weak axes, which are usually straightened with line or spot heats. The concept of upsetting and controlled contraction have been described earlier in Chapter 2. This concept forms the basis for the use of vee, line, strip, and spot heats to straighten members as described in chapters 3-9.

Fable

Heat-straightening should never be used without temporary shoring, since the heating effect may weaken the steel and produce a collapse.

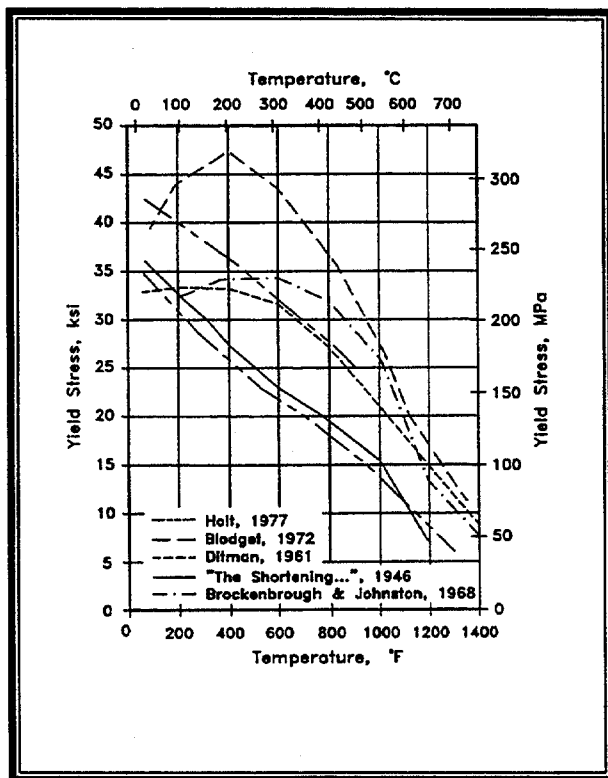


Figure 10.1. Variation of steel yield stress with temperature.

Fact

High heat reduces the yield stress of steel to very low values as shown in the plot of the yield stress versus temperature in fig. 10.1. It can be seen that the yield stress may be on the order of one-half or less of its original value when the temperature reaches 650 to 760°C (1200 to 1400°F). Yield stresses are rarely plotted for temperatures above 760°C (1400°F) because the values become so low. For example, at temperatures in the range of 870 to 980°C (1600 to 1800°F), the yield stress is between 5 and 15 percent of its value at room temperature (Ditman 1961). This behavior is one important reason why the metal temperature during heat-straightening should not exceed

650 to 760°C (1200 to 1400°F). When temperatures are limited to this range, the yield stress will be on the order of 30-50 percent of its original value. Consequently, if the maximum anticipated live load induced stress in the damaged region is equal to 30-50 percent of the total design stress, and if this total design stress is 50 to 60 percent of yield, then heat-straightening may usually be performed without shoring by removing (or controlling) the live loads. In addition, most heat-straightening procedures require that only a part of the cross section be heated. At any given time the average yield stress though an element of the section will therefore be even greater than 50 percent of its original value. As a result, many applications of heat-straightening can be safely completed without shoring. However, an engineer familiar with the live- and dead-load stress distributions should evaluate whether to use shoring.

Fable

Heat-straightening permanently weakens a steel structure.

Fact

Two criteria are often used as a measure of steel strength: yield stress and maximum tensile stress. A number of other researchers have measured the yield stress after the heating/cooling cycle of heat-straightening to determine the modified characteristics. A summary of these test results is shown in table 10.1. The tests on various types of steel represent over 50 specimens from nine investigations. It is apparent from this collection of data that in the long term, the heat-straightening process has a small but positive effect on the yield stress when heating temperatures are controlled. A similar conclusion can be drawn

from an evaluation of the maximum tensile stress corresponding to those for yield stress.

Again, these changes are small. In most of the test results reported, the yield and tensile stresses were measured on samples from the same piece before and after heating and the initial yields were used as the nominal values unless they were unavailable. In general, these initial values were larger than the rated stress for the grade in question. Since changes are small, the assumption of an unchanged yield and maximum tensile stress after heat-straightening indeed appears to be a valid one for most grades of steel as long as the maximum temperature is limited.

One early study (Crooker and Harrison 1965) reported that flame cambering weakened I-beams. However, later discussions (Higgins 1966) indicated that the failure criteria were improperly applied, thus negating this conclusion.

Fable

Heat-straightening reduces steel ductility to unacceptable levels.

Fact

Ductility is an index of the ability of steel to deform in the inelastic range. It is usually expressed as a percentage by comparing the difference between an initial gage length and its length after tensile fracture to the initial gage length. Ductility is important because it allows redistribution of high local stresses. Shown in table 10.1 are comparisons of ductility before and after heat-straightening. In comparing the ratio of ductility of heated members to values prior to heating, this ratio tended to range between 0.7 and 0.9. While these changes in ductility characteristics are significant, the magnitude of the reduction is not large. All steel grades have demonstrated adequate ductility

in field applications of heat straightening. As such, the measured reductions in ductility after heat-straightening are small enough to be acceptable in normal construction applications.

Fable

Heat-straightening produces brittle "hot" spots and thus should be avoided.

Fact

One of the primary causes of brittle failures in steel is usually associated with geometrical discontinuities such as a sharp discontinuity or notch especially when accompanied by high residual tensile stresses. Such discontinuities may occur as a result of the damage creating a potential fracture problem if not straightened. Since heat-straightening itself produces no new discontinuities, geometry otherwise would not be a factor in evaluating brittle-resistance. However, two other factors that influence brittleness—large strain rates and cold working—often occur during the damage inducement state ("Steels" 1966). To evaluate its fracture sensitivity, various researchers have tested heat-straightened steel. The resistance to fracture in the presence of a notch is widely used as a guide to the performance of steels in structures susceptible to brittle fracture.

The Charpy V-notch test is most commonly used to determine fracture resistance. The data are taken at a range of temperatures and a plot of energy versus temperature (on the abscissa) is generated. The resulting curve is S-shaped with an upper limit asymptote of constant energy absorption as the temperatures increase above a certain upper critical temperature and a lower limit asymptote as the temperature goes below the lower critical temperature.

Table 10.1. Summary of Experimental Results on Base Properties of Heat-Straightened Steel by Other Researchers.

Steel		Heat Conditions				
Type (1)	Designation (2)	σ_y (ksi) (3)	Elevated temperature (°F) (4)	Time (min) (5)	Cooling (6)	Applied strains (7)
Carbon	A-7 ^d	33	1.100-1.200	After five	Air	Dead + residual
				After five and V-heat	Air	Dead + residual
				After five and V-heat	Air	Dead + residual
				After five and V-heat	Air	Dead + residual
				After five and V-heat	Air	Dead + residual
				After five and V-heat	Air	Dead + residual
				After five and V-heat	Air	Dead + residual
	A-36 ^c	36	1.10.-1.200	From V heat	Air	Residual
	A-36 ^c	36	1.000	After line heat	Air	Residual
1.000			After line heat	Air	Residual	
1.000			After line heat	Air	Residual	
1.000			After line heat	Air	Residual	
1.000			After line heat	Air	Residual	
1.000			After line heat	Air	Residual	
1.000			After line heat	Air	Residual	
	A36	36	1.200	—	Air	25% yield
	A36	36	1.200	—	Air	25% yield
	ABS-B	40	1.300	½	Air	—
1.300			5	Air	—	
1.300			5	Quench	—	
1.100			½	Air	—	
1.100			5	Quench	—	
800			½	Air	—	
800			5	Air	—	
1.300	10	Air	5% tensile			
1.300	10	Air	5% compression			

Table 10.1 Continued.

Tensile Coupon Results			Charpy Results			Reference (14)
Yield Stress (σ_y / nominal σ_y) (8)	Elongation in 2 in. (Δ_ℓ / nominal Δ_ℓ) (9)	Tensile stress (σ_{ut} / nominal σ_w) (10)	Temperature (11)	Impact en- ergy/ nomi- nal impact energy (12)	Original $T_{50} - T_{50}$ after heating (13)	
1.13	1.63	1.02	—	—	—	"Flame" (1959)
1.17	0.59	1.00	—	—	—	
1.22	0.75	1.00	—	—	—	
1.18	0.85	1.01	—	—	—	
1.32	0.73	1.00	—	—	—	
1.14	0.77	1.00	—	—	—	
1.42	0.63	1.04	—	—	—	
1.00	0.87	1.01	—	—	—	Horton (1973)
1.18	0.96	1.06	—	—	—	Brockenbrough And Johnson (1970)
1.08	0.94	1.07	—	—	—	
1.06	0.93	1.07	—	—	—	
0.90	0.96	1.06	—	—	—	
0.97	0.96	1.04	—	—	—	
1.05	0.96	1.04	—	—	—	
1.01	1.00	1.04	—	—	—	
0.97	1.00	1.04	—	—	—	
1.00	1.00	1.04	—	—	—	
1.03 ^c	0.75 ^c	1.05	—	—	—	
1.00 ^c	0.87 ^c	1.01	—	—	—	Horton (1973)
—	—	—	Upper shelf	1.09	-3	Rothman and Monroe (1973)
1.07	0.97	0.98	Upper shelf	1.14	16	
1.10	1.03	1.03	Upper shelf	1.29	30	
—	—	—	Upper shelf	1.02	20	
—	—	—	Upper shelf	1.00	-2	
—	—	—	Upper shelf	1.10	-2	
—	—	—	Upper shelf	1.14	-14	
1.13	1.04	1.02	Upper shelf	1.04	15	
1.14	0.92	1.03	Upper shelf	1.10	45	

Table 10.1. Continued.

(1)	(2)	(3)	(4)	(5)	(6)	(7)
			1.100	10	Air	5% tensile
			1.100	10	Air	5% compression
	ABS-B		1.300-1.400	—	Quench	—
High-strength low-alloy	ABS-C		1.300	½	Air	—
			1.300	5	Air	—
			1.300	5	Quench	—
			1.100	½	Air	—
			800	½	Air	—
			800	5	Air	—
	A441	50	1.300	½	Air	—
			1.300	5	Air	—
			1.300	5	Quench	—
			1.100	½	Air	—
			800	½	Air	—
			800	5	Air	—
	A441		1.100-1.200	—	Quench	—
			1.300-1.400	—	Quench	—
	Not specified	50	1.100-1.300	From V-heat	Air	Residual
			1.100-1.300		Air	Residual
Heat-treated high-strength carbon	A537-A	50	1.300	½	Air	—
			1.300	½	Air	—
			1.300	5	Quench	—
			1.100	5	Air	—
			800	½	Air	—
			800	5	Air	—
			1.300	10	Air	5% tensile
			1.300	10	Air	5% compression
			1.100	10	Air	5% tensile
			1.100	10	Air	5% compression
	A537-A		1.100-1.200	—	Quench	—
			1.300-1.400	—	Quench	—
	A537-B	60	1.300	½	Air	
			1.300	5	Air	
			1.300	5	Quench	
			1.100	½	Air	
			1.100	5	Quench	
			800	½	Air	
			800	5	Air	5% tensile
			1.300	10	Air	
			1.300	10	Air	5% compression
			1.100	10	Air	5% tensile
			1.100	10	Air	5% compression

Table 10.1. Continued.

(8)	(9)	(10)	(11)	(12)	(13)	(14)
—	—	—	Upper shelf	0.93	29	
—	—	—	Upper shelf	0.98	11	
—	—	—	—	—	18 ^f	Horton (1973)
—	—	—	Upper shelf	0.99	21	Rothman and Monroe (1973)
0.98	0.83	0.98	Upper shelf	0.99	36	
1.03	0.79	1.05	Upper shelf	0.96	47	
—	—	—	Upper shelf	0.93	26	
—	—	—	Upper shelf	0.97	23	
—	—	—	Upper shelf	0.95	27	
—	—	—	Upper shelf	0.99	-3	Rothman and Monroe (1973)
1.03	0.84	0.99	Upper shelf	1.02	13	
1.04	0.83	1.02	Upper shelf	0.94	30	
—	—	—	Upper shelf	0.92	10	
—	—	—	Upper shelf	0.97	10	
—	—	—	Upper shelf	0.92	36	
—	—	—			16 ^f	Pattee et al. (1970)
—	—	—			12 ^f	
1.03	0.83	1.01	0	1.33	—	Harrison (1950)
1.03	0.79	1.00	35	1.00	—	
			65	1.17	—	
—	—	—	Upper shelf	1.00	-60	Rothman and Monroe (1973)
1.06	0.91	9.94	Upper shelf	1.00	-51	
1.13	0.91	0.96	Upper shelf	1.00	-6	
			Upper shelf	0.94	-61	
			Upper shelf	0.98	-26	
			Upper shelf	0.98	-41	
1.12	0.87	0.95	Upper shelf	0.99	-19	
1.10	0.84	0.94	Upper shelf	0.99	3	
			Upper shelf	0.92	-6	
			Upper shelf	0.92	-13	
					25 ^f	Pattee et al. (1970)
					28 ^f	
1.02	0.81	0.99	Upper shelf	1.13	36	Rothman and Monroe (1973)
1.05	0.88	1.05	Upper shelf	1.11	18	
			Upper shelf	1.10	-29	
			Upper shelf	1.00	33	
			Upper shelf	1.00	8	
			Upper shelf	1.00	0	
			Upper shelf	1.09	5	
1.04	0.86	0.99	Upper shelf	1.13	2	
1.04	0.82	0.99	Upper shelf	1.20	29	
			Upper shelf	1.04	18	
			Upper shelf	1.07	26	

Table 10.1 Continued.

(1)	(2)	(3)	(4)	(5)	(6)	(7)
Heat-treated constructional alloy	NAXTRA-100	100	1.300	½	Air	5% tensile 5% compression 5% tensile 5% compression
			1.300	5	Air	
			1.300	5	Quench	
			1.100	½	Air	
			1.100	10	Air	
			900	½	Air	
			900	10	Air	
			800	½	Air	
			800	5	Air	
			1.300	10	Air	
			1.300	10	Air	
			1.100	10	Air	
	A514-F	100	1.300	5	Air	5% tensile 5% compression 5% tensile 5% compression 5% tensile 5% compression
1.300			5	Quench		
1.100			5	Air		
800			5	Air		
1.300			10	Air		
1.300			10	Air		
1.300			10	Air		
1.300			10	Air		
1.100			10	Air		
1.100	10	Air				
	Amco QTC	100	900	¼	Quench	—
			1.100	¼	Quench	—
			1.300	¼	Quench	—
			900-1.050	1/15	Quench	Residual
	A517-A	100	1,100-1,200	—	Quench	—
			1,100-1,200	—	Quench	—
			1,300-1,400	—	Quench	—
			1,300-1,400	—	Quench	—

^aNominal values are from tests of as-received steel.

^bTemperatures at which 50% of upper shelf energy was absorbed.

^cAverage of unspecified number of specimens.

^dNominals are for A-7: $\sigma_v = 33$, % elongation = 24. $\sigma_u = 60$

^eNominals are for A-36: $\sigma_v = 36$, elongation = 34. $\sigma_u = 67$

^fResults are from drop-weight tear test where T_{50} is transition temperature at which fracture contains 50% shear area.

Table 10.1 Continued.

(8)	(9)	(10)	(11)	(12)	(13)	(14)
0.90	0.84	0.93	Upper shelf	1.09	-4	Rothman and Monroe (1973)
0.93	0.82	0.96	Upper shelf	1.09	-4	
			Upper shelf	1.16	-21	
			Upper shelf	1.02	-17	
			Upper shelf	1.00	0	
			Upper shelf	1.00	10	
			Upper shelf	1.00	10	
			Upper shelf	1.00	0	
			Upper shelf	1.00	0	
0.83	0.79	0.90	Upper shelf	1.36	-54	
0.81	0.77	0.89	Upper shelf	1.40	-8	
			Upper shelf	1.24	-11	
			Upper shelf	1.18	-11	
1.01	0.90	1.00	Upper shelf	1.02	-12	Rothman and Monroe (1973)
1.01	0.94	1.00	Upper shelf	1.00	-12	
			Upper shelf	1.00	0	
			Upper shelf	1.00	0	
0.88	0.78	0.93	Upper shelf	1.11	-12	
0.84	0.76	0.92	Upper shelf	1.04	-12	
			Upper shelf	1.16	-12	
			Upper shelf	1.13	-12	
			Upper shelf	1.07	-12	
			Upper shelf	1.04	-12	
1.02	1.10	1.00	Upper shelf	0.98	-8	Rothman (1973)
1.01	1.08	1.00	Upper shelf	1.00	-14	
1.04	1.03	1.00	Upper shelf	1.03	-21	
0.98	0.88	1.06	Upper shelf	1.03	-17	
—	—	—	—	—	113 ^f	Pattee et al (1970)
—	—	—	—	—	75 ^f	
—	—	—	—	—	205 ^f	
—	—	—	—	—	108 ^f	

These limits are referred to as the upper and lower shelf. One measure of toughness, quantifying the resistance to brittle failure, is the upper shelf energy limit. Positive differences represent a decrease in notch toughness due to heat straightening while negative numbers represent an increase. Results shown in table 10.1 vary considerably within a given steel grade. However, the average values indicate that only the quenched and tempered steels have a significant positive shift.

A second measure of the notch toughness can also be obtained from the Charpy tests. As shown in table 10.1, the temperature at which 50 percent of the upper shelf energy was absorbed, T_{50} , is tabulated in terms of the difference between the original T_{50} and the T_{50} after heat straightening. Positive differences represent a decrease in notch toughness, while negative numbers represent an increase. There is considerable variation within a given steel grade. However, the average values indicate that only the high-strength, low-alloy steels have a significant positive shift (0°C or 32°F), and even this shift is relatively small.

Another measure of notch toughness is the fracture transition temperature. This temperature is the one in which the percentage of shear fracture is 50 percent of the cross section. Since plastic deformation is associated with shear fracture, a rating of the brittle-fracture resistance is obtained. Pattee et al. (1969) used this criterion in evaluating several grades of steel that had been heat-straightened. The drop weight tear test was used instead of the Charpy test, with the results also shown in table 10.1. The fracture transition temperature changes are modest for all cases except the A517-A steel. Here is a significant positive shift, indicating

larger fracture sensitivity. It is interesting to note that a similar situation did not occur with the heat-treated alloy steels given in table 10.1.

Rockwell hardness tests have also been used on heat-straightened steel specimens. Changes in surface hardness before and after heating would indicate changes in mechanical properties. Pattee et al. (1969) conducted Rockwell hardness tests on a range of steel from mild to heat-treated alloys. Harrison (1950) and Harrison and Mills (1951) conducted similar tests on mild steel specimens. Seven specimens compared by Pattee et al. had differences of less than 6 percent except for one specimen with a 15 percent difference. A comparison of the 18 readings by Harrison, taken within the heated vee portion of the two specimens, showed a 3 percent difference or less. Both researchers found that the hardness values did not change appreciably before and after heat straightening.

An overview of the research data offers no basis for concluding that properly applied heat straightening should be avoided because of brittle-fracture concerns. Rather, it can be concluded that such toughness reductions, when they exist, are acceptable.

Fable

Fracture-critical members cannot be heat-straightened.

Fact

Fracture-critical members are tension members, or tension components of members, whose failure would be expected to result in the collapse of the structure. Current research data such as those shown in table 10.1 provide no grounds for excluding fracture critical members from heat straight-

ening. There is strong and consistent evidence that properly executed heat straightening has no degrading effect on mild-carbon steels and only minor effects on heat-treated steels. Strength and brittleness aspects have already been discussed in terms of simple material tests. However, direct fatigue tests also provide a meaningful measure.

Only one series of fatigue tests on members similar to heat-straightened members was found in the literature ("The shortening" 1946). In this case, three eye bars of A-7 steel were heat-shortened and then fatigue cycled. When compared to similar specimens that had not been heated, the fatigue strength at both 500,000 and 1,000,000 cycles was similar. Although data are sparse, there is no indication that mild carbon steels will have a shortened fatigue life solely due to heat straightening.

Shanafelt and Horn (1984) have recommended that heat straightening be avoided on fracture-critical members without offering any justification other than conservatism. Since there is no hard evidence to justify the avoidance of heat straightening, the question is not whether fracture critical members can be heat-straightened, but whether they should be.

Until around 1984, one ingredient was missing in heat-straightening technology: engineering analysis tools. The more accurate the analysis, the less conservatism is required. Since heat straightening had been in the hands of the contractor, even with guidelines such as Shanafelt and Horn (1984), the engineer has practically nothing similar to the analytical tools usually associated with structural engineering. For example, criteria as to number, location, and an-

gle of vee heats; effects of internal restraints; control of external restraints such as jacking; and effect of residual stresses had not been developed into analytical tools. As a consequence, even though evidence indicated that heat straightening could be used for fracture-critical members, it was not recommended prior to 1985. Although more information is now available, it is still a matter of engineering judgement as to whether to heat straighten fracture critical members.

Fable

There is no ideal temperature for heat straightening.

Fact

The ideal temperature for heat straightening depends on the grade of steel and method of heating. For carbon and low-alloy steels, the theoretical limit is the phase transition temperature of approximately 721°C (1330°F). For quenched and tempered steel, the limiting value is the minimum tempering temperature of 590-620°C (1100-1150°F). However, heat-straightening experiments at levels up to 870°C (1600°F) for carbon steels (Roeder, 1985, 1986) and 700°C (1300°F) for heat-treated steels (Rothman, 1973; Rothman and Monroe, 1973) have been conducted without serious detrimental effects to the material properties (see table 10.1). In addition, some theories have suggested that heating above a specified value will not materially increase the amount of straightening (Shanafelt and Horn 1984). Although experiments have shown that these theoretical maximums (which are based on simplifying assumptions) may be too low (Roeder 1985), it is likely that practical limits do not greatly exceed the transition temperature.

The consensus of researchers has been that a temperature of about 650°C (1200°F) should be used for carbon and low-alloy steels, 590°C (1100°F) should be used for A709 (Grade 70W) quenched and tempered steels, and 620°C (1150°F) for A514 and A709 (Grades 100 and 100W) quenched and tempered steels. These values provide a small safety factor to account for normal variation in a manual process and also produce relatively large movements as a result of the heat-straightening process.

Fable

While heat straightening may work under controlled laboratory conditions or in uncontrolled field applications, there are no documented field studies in which parameters were carefully measured and controlled.

Fact

Moberg (1979) was the first investigator to conduct a controlled field study of heat-straightening repair for damaged members. Careful daily measurements were recorded on the Bothwell Bridge (in the state of Washington) which was hit by an over-height vehicle. The initial damage was measured and daily measurements were taken as heat straightening progressed. The restraining forces used were also carefully recorded. This work illustrated that heat-straightening repairs can be engineered. Avent and Brakke (1996) conducted a study of an Iowa bridge where a composite beam was impacted by an over-height vehicle. The jacking force was calibrated and measurements taken after every heating cycle. The entire repair process was documented in detail illustrating the effectiveness of the method. Avent and Fadous (1988) also conducted a series of simulated field tests illustrating the efficiency of the method.

Fable

Heat straightening only works for simple bends of single curvature.

Fact

Vee heats are used primarily for strong axis curvature correction in plate elements, while line heats and spot heats are used for weak axis corrections. A vee heat produces a sharp point of curvature of small magnitude at the vee since the plastic deformation is restricted primarily to the area of the vee as it closes slightly (Nicholls and Weerth 1972; Roeder 1985, 1986). To produce a visually smooth curve over the length of the plate, a series of vee heats spaced along the length can be used. In reality, this approach will give the appearance of a smooth curve. By alternating the direction of the vees and varying the spacing, practically any type of curvature (sharp, gradual, single, or multiple) can be removed. Since each heat produces small changes in curvature, a number of heating/cooling cycles are usually required to straighten a damaged member completely. In a similar manner, line and/or spot heats can be used to remove weak axis damage such as bulges or buckles.

Fable

While heat straightening may work for simple plate elements, bends in rolled shapes are too complex for a rational approach.

Fact

In addition to the results described in this manual, a wide variety of rolled shapes, including wide flanges, channels, angles, and assemblies have been straightened (or curved) in both laboratory (Blodget 1972; Burbank 1968; Graham 1975; Harrison 1950; Holt 1977; Horton 1973; Meyers

1976; Pattee, et al. 1969, 1970; Roeder 1985, 1986; Rothman 1973; Rothman and Monroe 1973) and field applications (Bernard and Schulze 1966; Ciesicki and Butler 1968; "How" 1959; "Flame" 1959; Harrison 1950, 1952; Holt 1955, 1971; "Kinks" 1981; Moberg 1979; Morris 1949; Meyers 1976: "Oxyacetylene" 1959; Pfeiffer 1963; Thatcher 1967; Tsalman 1959; Watanabe and Satoh 1951; Yoch 1957). Rolled shapes generally require vee heats in combination with line and rectangular heats. The rectangular heats are necessary because of the perpendicular planes of the plate elements forming the shape. By using the proper pattern of vee and rectangular heats, sweep, camber or twisting movements can be obtained, to repair a wide variety of damage conditions. While most researchers have been in general agreement on the vee pattern, there have been no published studies directed toward quantifying the optimum heating patterns for rectangular heats in combination with the vee.

Fable

Internal and external restraining forces are unimportant in heat straightening.

Fact

Of almost equal importance to temperature are the constraints and forces acting on the member during the heat-straightening process. Practitioners have recognized this fact and usually employ some type of jacking or constraining force. The basic principle is that an applied force in the direction of the desired movement will impede the undesired additional distortion in the same direction as the damage during the heating phase, increase the through-thickness plastic strain, and thus produce more contraction during the cooling phase. Experiments discussed in

this manual as well as that of others show that the application of external forces have a significant effect on the amount of plastic rotation that occurs in a plate. The force applied produces a bending moment about the major axis tending to close the angle of the vee. For comparison purposes, the moment is nondimensionlized by computing the jacking ratio, which is the ratio of the moment at the vee from the applied load to the plastic moment capacity of the section, M/M_p . Nicholls and Weerth (1972), Rothman (1973), Weerth (1971), and Roeder (1985, 1986) measured the behavior of vee heated plates for various load ratios. Data from Roeder's tests were shown in fig. 5.11. The data points represent the average of 2 or 3 heats and reflect that the plastic rotation is proportional to the jacking ratio.

It can be seen from these results and the material in this manual that there is a distinct advantage to using an external force during the heat-straightening process. However, the constraining force should be used as a passive force rather than an active force once the heating has begun. The standard procedure is to apply the constraining force first and then proceed with the vee heats. The constraining force should not generally be externally increased at any time during the heating and cooling process.

Fable

Calibrated jacks to measure restraining forces are unnecessary because the appropriate value can be determined by "feel."

Fact

Over-jacking can result in buckling or fracture during the heat-straightening process as discussed in Chapter 7. In addition,

it may result in mechanical straightening which could be detrimental to the material. For these reasons, it is important to control the magnitude of the restraining force. The best method is to calibrate the jacks and compute the maximum safe force prior to jacking.

While some practitioners suggest that the jacking force can be controlled by "feel", the number of variables make this idea very unlikely. Consider the following variables associated with inducing stress by jacking a composite girder: diaphragm spacing, number of diaphragms, beam length, section modulus of beam, depth-to-web thickness ratio, and section modulus of lower flange. For a given stress level, the interaction of so many variables means that the jacking force could vary over a wide range. By using the "feel" method, it is erroneously assumed that the jacking force varies little from one bridge to the next.

Fable

Heat straightening is unlikely to be developed as an "engineered" process because sometimes a properly heated member does not straighten.

Fact

In addition to external restraints, a second type of force must also be considered in many structures, that is, internal constraints. These constraints are a result of structures that: (1) are carrying some load (e.g., dead load) during heating; (2) are statically indeterminate; or (3) have high residual stresses due to damage, initial fabrication or configuration. Since many structures are partially loaded during the heat-straightening process, a structural evaluation is required to determine whether the loading

will be beneficial or harmful. Other types of internal constraints are subtler in their effects, particularly those associated with statically indeterminate structures. Engineering methods were developed in Chapters 5-9 to quantify this aspect of the heat-straightening process.

Fable

Heat straightening is an art and the actual magnitude of movements cannot be predicted.

Fact

Several analytical methods have been developed for applications to plates. One approach (Holt 1965, 1971; Moberg 1979), generally referred to as the Holt formula, is a formula based on the assumptions of perfect single axis confinement, linear strain variation across the width of the plate, and a uniformly distributed temperature of 650°C (1200°F). This formula was modified by Moberg (1979) to include partial depth vees, eq. 5.2. This equation is quite approximate in nature, since typical vee heat behavior is not a perfect single axis confinement case and since the effect of restraining forces is neglected. However, these two effects sometimes cancel each other, occasionally resulting in fairly good agreement with actual measurements (Moberg 1979). The principle weakness of this formula is its neglect of the effect of constraining forces. No simple formulations were given that account for this effect prior to the developments in this manual.

The alternative approaches offered in the literature (Burbank 1968; For Chin 1962; Gipson and Ortiz 1986; Horton 1973; Roeder 1985, 1986, 1987; Weerth 1971) all basically combine a thermal analysis with an

inelastic finite element or finite strip stress analysis. These methods require excessive computational effort and have only been applied to a few simple flat plate cases. To address the deficiencies of these procedures, a set of formulas for predicting movement after heat straightening are developed in this manual.

Fable

The angle of a vee heat is unimportant.

Fact

A number of authors (Holt 1971; Moberg 1979; Nicholls and Weerth 1972; Roeder 1985, 1986; Weerth 1971) have concluded that amount of plastic rotation resulting from a vee heat is directly proportional to the angle of the vee. Various researchers (Harrison and Mills 1951; Holt 1971; Moberg 1979) have developed simplified analytical models that account for this effect, while others have developed finite element models (Brockenbrough 1970a; Roeder 1985, 1986). However, large angle vee heats may produce out-of-plane distortions (Roeder 1985, 1986) or buckling (Shanafelt and Horn 1984) due to compressive residual stresses. Caution should be used to minimize such effects. Holt (1971) and Shanafelt and Horn (1984) recommended that the maximum width of the base of the vee be limited to 250 mm (10 in). However, selecting the limit requires judgement based on plate width and thickness.

Fable

Residual stresses are not a serious concern in heat straightening.

Fact

In early research, the magnitude and effects of residual stresses in the heat-straightening process were not well understood (Kihara et al. 1961; Maeda and Yada 1961, 1963; Masubuchi 1960). Although Roeder (1985, 1986) measured residual strains, these measurements cannot be extrapolated into stresses because of the plastic flow that occurs during heat straightening. Brockenbrough and Ives (1970) measured residual stresses by the sectioning method for a heat-curved girder in which line heats were used. Brockenbrough later developed criteria for heat-curving (cambering) based on this work (Brockenbrough 1970b). Yield-point tensile stresses along the heated flange and smaller tensile stresses in the opposite flange characterized the residual stresses. Compressive stresses dominated the web. In a companion paper, Brockenbrough (1970a) developed a theoretical approach for computing the same residual stresses, as did Roeder (1985, 1986) and Nicholls and Weerth (1972) and Weerth (1971) for the vee-heated plate. These researchers concluded that as in welding, the residual stresses caused by heat straightening might be high. The most comprehensive study of residual stresses for both plates and rolled shapes is described in Chapter 5. Residual stresses were found to be as high as those in welded built-up members. Since residual stresses primarily cause strength reductions in compressive members, these stresses should not be ignored. Rather, a heat-straightened column should be treated as a welded, built-up member having residual stresses which may be equal to the yield stress. It was also suspected that residual stresses might influence the degree of movement during heat straightening by act-

ing as either a positive or negative constraining force. Harrison and Mills (1951) found that light hammering (peening) on the heated surface of a plate produced plastic elongation. By applying peening during the cooling cycle of the heat-straightening process, residual stresses might be reduced and the degree of contraction increased. Although recommended by some researchers (Shanafelt and Horn 1984), there had been no research data on peening related specifically to heat straightening. It is therefore premature to make a recommendation on its effectiveness.

Fable

No matter how light or severe the damage, heat straightening can be used if no fractures have occurred.

Fact

Surprisingly little information is available on the effect of damage level (strain history). It is known that cold bending into the yield range reduces the ductility of steel in general (Brockenbrough and Johnston 1968). However, the application of heat tends to restore the original material characteristics. Shanafelt and Horn (1984) recommended that the maximum allowable strain be limited to 15 times the yield strain and/or 5 percent nominal strain for repair of tension members. The limit approximately defines the delineation between the plastic region and the strain-hardening region. However, these recommendations were not backed by specific research data. No limits were suggested for compression members. The specific limits given for tension members in two categories were as follows. For primary members, straighten if strain is less than 5 percent which means: (1) For $F_y = 36$

ksi, the strain must be less than $40.3 \times \epsilon_y$; (2) For $F_y = 50$ ksi, the strain must be less than $29 \times \epsilon_y$; (3) For $F_y = 100$ ksi, the strain must be less than $14.5 \times \epsilon_y$. For primary members with severe fatigue sensitive details, straighten if strain is less than $15 \times \epsilon_y$.

The more recent research reported in this manual shows that material with strains up to $100 \epsilon_y$ can be repaired by heat straightening. Even larger strains can probably be repaired, but research has not been conducted past strains of $100 \epsilon_y$.

Shanafelt and Horn (1984) also suggested limits on the maximum radius of curvature for which heat straightening should be applied. The logic is that if the radius of curvature exceeds that which produces material yielding, heat straightening will be ineffective. Elastic curvature due to damage in the non-yielded portions will be elastic and will be eliminated when the plastic zones are straightened. The radius of curvature at yield (assuming plane sections perpendicular to the longitudinal axis before bending remained plane and perpendicular after bending), is given by:

$$R_y = \frac{WE}{2F_y} \quad (\text{Eq. 10.1})$$

where W = plate width; E = modulus; and F_y = yield stress. Heat straightening should not be applied for regions with larger radii of curvature than this limiting value, or in general, to portions of the member that have not plastically deformed.

Summary and Conclusions

Contained in this chapter is a summary of the previous literature on heat-straightening repair. Because of considerable misinformation on the topic, a number

of popular "fables" have arisen. The references cited, form a comprehensive bibliography on the subject of heat straightening and complement the material presented in this manual.

PART III. SPECIFICATIONS, GUIDES AND REFERENCES

Chapter 11. Engineering Guide

SECTION 1. GENERAL

1.1 Purpose

The purpose of this guide is to provide a summary of the methodology for an engineering assessment of the heat-straightening repair of damaged steel structures. Included will be damage assessment, analytical considerations, design of the repair, and field supervision of the repair.

1.2 Scope

This guide addresses engineering issues related to the analysis and design of heat-straightening repairs for damaged structural steel. Details associated with contractor implementation of heat-straightening repairs are included only to the extent necessary for engineering considerations. The intention is to provide the structural engineer with analysis and design procedures for heat-straightening repairs in a similar form to procedures associated with traditional structural design in new construction. For design of heat-straightening repairs, the required concepts are listed below.

1.2.1 Material Selection. Additional materials are not usually required except for occasional reinforcement or replacement of bracing or secondary elements.

1.2.2 Configuration. Rather than determining such parameters as framing type, member spacings or connectivity patterns typical of new designs, the term here includes the selection of heating patterns, number of specific heats and constraining force patterns.

1.2.3 Structural Analysis. The determination of internal stresses forms an integral part of designing repair schemes as related to the introduction of constraining forces during repair and the final stress configuration after repair.

1.2.4 Sizing. Since elements are not usually added in heat-straightening repairs, sizing here refers to number, dimensions, location, and magnitude of parameters such as temperature, heat zones and constraining forces along with the prediction of behavioral response within acceptable limits.

1.2.5 Iteration Process to Finalize Design. Through the analytical prediction of response, various alternatives are evaluated and the most efficient are selected for the final design of the repair.

1.3. Nomenclature and Glossary

A Glossary is given in Chapter 14 and Nomenclature in Chapter 15.

SECTION 2. DAMAGE ASSESMENT

2.1 Effect of Damage Type on Design of Repair

2.1.1 Causes of Damage. Knowledge of the specific cause of damage may influence the final decision on repair. Typical damage causes are:

1. Overheight or overwide vehicle impact.
2. Overweight vehicles or overloads.
3. Out-of-control vehicles or moving systems.
4. Mishandling.

-
5. Fire.
 6. Blast.
 7. Earthquakes.
 8. Wind.
 9. Movements of supports and/or substructure.

2.1.2 Design Considerations Associated with Damage Type. There are five engineering considerations which may be associated with the damage type.

- (1) **High heat.**-As long as the temperature does not exceed the phase transition temperature approximately of 720°C (1330°F) for carbon steel, no permanent degradation would be expected to occur in the steel. Similarly, for quenched and tempered steels, the temperature should not exceed the tempering temperature. However, if the damaged steel was exposed to higher temperatures, metallurgical tests should be performed to ensure material integrity before heat straightening is applied.
- (2) **Large strains.**-Heat-straightening repairs have been conducted on steel with strains up to $100\varepsilon_y$, where ε_y is the strain at initial yield. Repairs may be successful at even greater strains. However, engineering judgement should be used beyond this limit.

- (3) **Residual stresses.**-Plastic deformations during damage inducement may produce residual stresses in the structural system. It may be necessary to determine the type and magnitude of these stresses as an integral part of the repair design.

- (4) **Hairline fractures.**-On occasion, a hairline fracture will occur during an intermediate cycle of heat-straightening repair. The causes are believed to be: (1) Excessive restraining forces being applied during the heating process, and (2) Repetitive damaging and repairing an element. As the former is the primary cause, restraining forces should always be specified at safe limits and should be monitored during actual repair.

- (5) **Material age and load history.**-Fatigue and fracture considerations may be influenced by these factors.

2.2 Evaluation of Damage Geometry

2.2.1 Measurements of Damage. Measurements should be taken at all regions of primary damage. Measurements should be taken at intervals which allow for all primary damage to be clearly defined. The measurements should be in sufficient detail to define all yield zones associated with primary damage. Measuring procedures include the following:

-
- (1) Offset method-Offsets are measured from a taut line between two reaction constraints.
 - (2) Optical measurements- Optical equipment is used to define the deformed geometry of the system.
 - (3) Image processing- Photographic images are analyzed to define the deformed geometry of the system.

2.2.2 Characteristic Patterns of Damage. Damage can be classified into characteristic modes. Elements of the cross section will be distinguished as: (1) primary elements which are bent about the strong axis of their local axis, and (2) stiffening elements which are either bent about the weak axis of their local axis, or remain undeformed.

- (1) Category W-This damage pattern is usually associated with weak axis bending of the rolled shape, fig. 2.8b.
- (2) Category S-This damage pattern is associated with strong axis bending of the shape, fig. 2.8a.
- (3) Category T-This damage pattern is one of twisting about the longitudinal axis, fig. 2.8c.

- (4) Category L damage, refers to localized problems affecting cross section elements as opposed to damage through the entire cross section and is typified by bulges, crimps, dents, bellies, and dishes, fig. 2.8d.

2.2.3 Structural Analysis.

2.2.3.1 Strength of Damaged Structure. The capacity of the damaged structure can be based on the following assumptions:

- (1) Base the structural analysis on undeformed geometry except when deformed geometry of the frame or truss system produces changes in stresses of more than 20 percent when compared to the original geometry. Use a nonlinear analysis for these cases.
- (2) Compute member stresses based on section properties of deformed geometry of primary members. Such members can be idealized by linearizing the cross section based on element edge deformations and neglecting secondary damage.
- (3) Use allowable stresses based on the original properties of the material.

2.2.3.2 Redistribution of Internal Forces Due to Inflicted Damage. It may be necessary to determine the residual forces existing in the system after damage. Residual forces will not exist in determinate

structures (although residual stresses may). For indeterminate structures with full cross section yielding, residual forces may be introduced which tend to prevent movement during heat straightening.

The procedure to determine the residual forces is as follows for frames:

- (1) Conduct a plastic analysis of the original structural configuration using a concentrated load at point of impact. Then compute the ultimate load, P_u , and the moment diagram associated with the failure mechanism.
- (2) Conduct an elastic analysis of the original structural configuration with an applied loading of $-P_u$. Then compute the moment diagram.
- (3) Superimpose the moment diagrams of (1) and (2) to get the residual moment diagram.

For trusses, a similar analysis can be conducted by treating the truss as a rigid frame. However, for axially loaded members, an additional component is the $P-\delta$ effect associated with the axial forces. The truss is treated as an idealized pin connected system and the residual moment in a damaged member is computed by multiplying the axial force in the member by the lateral deflection of the damaged member (or members). The axial force is computed by a standard elastic truss analysis with a loading equal to the dead and live loads on the structure at the time the repair is conducted.

2.2.3.3 Residual Forces for Composite Girders with Impact at Lower Flange. The residual forces in a composite girder is complicated by the composite connection. Part of the residual moment (as well as any jacking force applied) is transferred through the web to the slab. The approach recommended is to compute the distribution factor, $\bar{\gamma}$, of the member for lateral loads applied to the bottom flange. This factor can be obtained from eqs. 7.15 and 7.16 and the equivalent stiffness, K_j , can be found from eq. 7.12. The composite girder can then be treated as described in section 2.2.5.2. Diaphragms can be considered as rigid lateral supports for analysis purposes.

SECTION 3. MATERIAL

ASSESSMENT

3.1 Material Assessments

The type of steel should be determined in one of the following ways:

- (1) Review of design plans.
- (2) Assumptions based on age of structure.
- (3) Metallurgical analysis.

3.1.2 Hairline Fracture. The yield zones should be examined closely for hairline fractures. Non-destructive testing (NDT) should be employed. Recommended methods are dye penetrant, magnetic particle, or ultrasonics. Heat straightening should not be attempted unless hairline fractures are repaired as part of the process.

3.2 Yield Lines

In general damaged steel should be heated in the vicinity of zones of plastic deformation. One type of characteristic yield zone is the yield line. Yield lines are typical of weak axis bending of plate elements. All yield line locations should be identified.

3.3 Plastic Hinges

Plastic hinges are characteristic of strong axis bending of plate elements. They may be single hinges at sharp bends or a string of hinges forming a zone.

3.3.1 Radius of Curvature at Yield Point Strain. Plastic hinge regions can be approximated as those with a radius of curvature less than R_y , where R_y is the radius of curvature producing yield at the extreme fiber, eq. 3.6.

3.3.2 Calculation of Damage Curvature. Since damage measurements are taken at discrete locations, the radius of curvature can be approximated as shown by eq. 3.2 or 3.3.

3.4 Local Buckling or Bulges

Localized bulges, buckling or crimps can be identified by both measurements (eq. 3.3) and visual inspection. The magnitude is usually designated by the ratio of maximum deflection to length of damage.

3.5 Evaluation of Residual Forces Affecting Heat Straightening

Residual forces induced by the damage effects can either expedite or restrain repair by heat straightening. At all regions of primary plastic deformation, the residual moments should be taken into account. Positive moments are defined as those which tend to act in a direction to straighten that portion of the member.

3.6 Effect of Residual Stresses after Heat-Straightening

Residual stresses generated during heat straightening may have maximum values at or near the material yield stress. However, distributions will vary depending on the heating pattern.

3.7 Degree of Damage Evaluation

Degree of damage is a valuable indicator as to time and effort required to repair a member. Based on measurements taken as described in section 2.2.1 (see fig. 3.2), degree of damage can be calculated from eq. 3.1.

3.8 Decision to Repair

A number of factors must be considered prior to deciding on a heat-straightening repair. Since overall engineering judgement should always be the deciding factor, it is recommended that heat straightening not be undertaken without competent engineering analysis. Relatively few quantitative limits have been established through research data. Most previously published limits result from the idea that if data does not exist, set extremely conservative limits. While not disagreeing completely with this philosophy, each case should be analyzed on its own merits before accepting such conservative limits. The following issues should be analyzed in the process of deciding whether to repair by heat straightening.

3.8.1 Member Type Limitations. There are no specific limitations to heat-straightening repair based on member type. Tension, compression, flexural or various combinations have been successfully repaired in the laboratory and field. In addition, rolled or built-up members can be repaired. As long as the heat can be applied at the proper locations and restraining forces can be placed as needed, repairs can be affected.

The primary question raised in the past is whether fracture critical members can be repaired. Complete data doesn't cur-

rently exist to answer this question. Therefore, the engineer should examine the service conditions associated with location, indeterminacy, stress level and cyclic load characteristics before deciding.

3.8.2 Strain Limitations. Since strains are related to radius of curvature, it is recommended that radius of curvature be used for evaluation purposes. Research data has established that damage strains are not a significant factor if

$$\varepsilon < 100 \varepsilon_y \quad (\text{Eq. 11.1})$$

$$R > \frac{R_y}{100} \quad (\text{Eq. 11.2})$$

Since research data does not extend past this level, the engineer must use his own judgment once this range is exceeded.

3.8.3 Steel Grade Limitations. Carbon steels can be safely heat straightened as long as the heating temperature does not exceed the phase transition temperature (approximately 700°C or 1300°F). Quenched and tempered steels require a lower heating temperature (less than 565-590°C or 1050°F-1100°F is recommended). Specific heating temperature limits are given in Section 4.3.

SECTION 4. DESIGN OF REPAIR SEQUENCE

4.1 Development of Constraint Plan

Constraints are passive forces, usually applied by hydraulic jacks prior to heat straightening.

4.1.1 Location of Jacks. Jacks to produce constraining forces should be located to pro-

duce a maximum moment effect at the plastic zones. Jacks should be placed so that stresses are controlled at safe levels throughout the structure.

4.1.2 Computation of Residual Moments. Residual moments may be calculated as outlined in section 2.2.5.2. For indeterminate structures in which all plastic hinges cannot be heated simultaneously, the distribution of residual moments will change after each heating cycle. Thus, jacking forces should be adjusted to account for these changes as the heat straightening progresses.

4.1.3 Magnitude of Jacking Force. Jacking forces should be measured at the time of application and limited to produce moments as follows:

- (1) For cases where the residual moments, M_r , at the heating zone are negligible:

$$M_j \leq \frac{M_y}{2} \quad (\text{Eq. 11.3})$$

where M_j = moment produced by jacking force at the heated zone.

- (2) For cases where residual forces exist

$$M_j \leq \frac{1}{2}(M_y \pm M_r) \quad (\text{Eq. 11.4})$$

where the sign of M_r is taken as positive when acting to straighten the member and negative when acting to resist straightening.

4.1.4 Direction of Jacking Forces.

Jacking forces should be directed to produce positive moments (moments tending to reduce damage curvature).

4.2 Development of Heating Patterns

4.2.1 Heating Zones. All plastically deformed zones should be heated. In general, elastic zones should not be heated except in the vicinity of the yield zones.

4.2.2 Heating Patterns for Specific Cross Section Shapes. For plates with strong axis bends, use vee heats as shown in fig. 2.2. Vee heats for any shape should follow the serpentine pattern shown in fig. 2.2.

- (1) For plates with strong axis bends, use vee heats as shown in fig. 2.2. Vee heats for any shape should follow the serpentine pattern shown in fig. 2.2.
- (2) For angles, use the vee and/or rectangular heat combinations shown in fig. 2.15.
- (3) For Category S damage, use the vee and rectangular heat combination shown in fig. 2.11.
- (4) For Category W damage, use the vee and rectangular heat combination shown in Fig 2.12.
- (5) For Category T damage, use the vee and strip heat combinations shown in fig. 2.13.
- (6) For Category L damage, use the heating patterns shown in fig. 2.14.

4.2.3 Plastic Rotation Computations for Plates and Rolled Shapes. The amount of plastic rotation removed per vee (or vee/rectangular) heat can be generalized for various structural shapes. Multiple vee heats increase the plastic rotation in direct proportion as long as spacing between vees is greater than W . For a steel heating temperature of 650°C (1200°F) and A36 steel

$$\phi_p = F_t F_s F_a \phi_b \quad (\text{Eq. 11.3})$$

where

$$\phi_b = 0.0147 \sin \frac{\theta}{3} \quad (\text{Eq. 11.4})$$

$$F_t = 0.6 + 2 \frac{M_j}{M_p} \quad (\text{Eq. 11.5})$$

$$F_s = 1 + \frac{1}{2} \left(\frac{b_s d_s}{d^2} \right) \quad (\text{Eq. 11.6})$$

$$F_a = 1 - 2 \left\{ 1 - \frac{2}{3} \left(\frac{Z}{S} \right) \right\} \frac{M_j}{M_p} \quad (\text{Eq. 11.7})$$

where

M_j = the moment at the heated zone due to the jacking force;

M_p = the ultimate plastic moment capacity about the axis of damage;

Z/S = The ratio of plastic-to-elastic section modulus about the axis of damage (except for angles in which the ratio is multiplied by F_s);

b_s = width of stiffening element;

d_s = distance from apex of vee heat on primary member to intersection of stiffening element; and

d = depth of the vee heated elements (assuming a vee depth of at least three-quarters of this depth).

4.2.4 Composite Deck-Girder Systems

- (1) Use the heating pattern shown in fig. 7.3
- (2) The amount of plastic rotation removed from the bottom flange per vee heat can be calculated by eq. 11.3 where $F_s = 1$, ϕ_b is given by eq. 11.4, and

$$F_\ell = 0.6 + 2\gamma \frac{M_j}{M_p} \quad (\text{Eq. 11.8})$$

$$F_a = \left(\frac{d/t_w}{46}\right)^2 \quad (\text{Eq. 11.9})$$

$$\gamma = \frac{d/t_w}{10000} (15 + 2.75d/t_w) \quad (\text{Eq. 11.10})$$

4.2.5 Axially Loaded Wide Flange Beams

- (1) Use vee heat patterns similar to those of wide flange sections without axial loads.
- (2) The amount of plastic rotation can be estimated by eq. 11.3 where ϕ_b is given by eq.

11.4, F_s by eq. 11.6, F_ℓ by eq. 11.5 and

$$F_a = \left\{ 1 - 2 \left[1 - \frac{2}{3} \left(\frac{Z}{S} \right) \frac{M_j}{M_p} \right] \left(1 - \frac{f_a}{\bar{F}_a} \right) \right\} \quad (\text{Eq. 11.11})$$

where \bar{F}_a is the allowable axial stress.

4.3 Temperature Limitations

- (1) Temperature shall be limited to 650°C (1200°F) for carbon steel.
- (2) For quenched and tempered steel, the temperatures shall be limited to 590°C (1100°F) for A514 and A709 (grades 100 and 100W) and 565°C (1050°F) for A709 (grade 70W).
- (3) After heating, the steel shall be allowed to cool to below 121°C (250°F) before re-heating.
- (4) A guide for torch tip size and type with respect to plate thickness is given in table 2.1.

4.4 Selection of Vee Depth

In general the depth of the vee should be equal to the width of the plate element being heated. Shortening of the member will not be reduced by using shallower vee depths (between ½ and full depth)

4.5 Selection of Vee Angle

The angle of the vee to be used should be as large as practical for heating

with a point source torch. A good procedure is to limit the open end vee width to approximately 10 in for a one in thick plate. The vee angle will thus depend on the depth of the vee. If the vee depth, d_v , equals the plate element width, W , then the vee angle can be computed as

$$\theta = 2 \tan^{-1} \frac{V}{2W} \quad (\text{Eq. 11.12})$$

where V = the width at the open end of the vee.

4.6 Selection of Number of Simultaneous Vees to Heat

- (1) Simultaneous vee heats may be performed in a single plastic hinge zone provided they are spaced at least a plate element width, W .
- (2) Simultaneous vee heats should be performed if the damage mechanism of a structural unit has produced multiple plastic hinges. Each hinge should be heated simultaneously.

4.7 Estimation of Number of Vee Heats Required to Straighten an Element

The number of heats required may be estimated by taking the plastic rotation, ϕ_d ; that is,

$$n = \frac{\phi_d}{\phi_p} \quad (\text{Eq. 11.13})$$

4.8 Location of Vee Heats within Plastic Hinge Zones

Vee heat locations within a hinge zone should be varied with each heat by at least the width of the plate element. The same exact location should be re-heated only after at least three heats at other locations.

4.9 Selection of Constraining Forces

The largest constraining force practical within the limits of section 4.1.3 should be used. When necessary, a structural analysis should be used to insure that adjacent members are not over-stressed as a jack reaction. The techniques of sections 2.2.5.2 and 4.1.3 should be employed to determine the optimum jacking force required.

4.10 Repair of Previously Heat-Straightened Members

Repair of previously heat-straightened members may be conducted once but further repetitions are not recommended without an engineering evaluation.

SECTION 5. FIELD SUPERVISION OF REPAIR

5.1 Control of Constraint Forces

Jacking forces should be monitored and controlled by the use of calibrated gauges. Maximum allowable jacking forces should be specified in the plans and specifications.

5.2 Review of Heating Patterns

The engineer may review all heating patterns. Modifications may be approved depending on the progression of movement.

5.3 Monitoring Temperature

Heating temperature should be monitored by one of the following:

-
- (1) Use of temperature sensing crayons
 - (2) Use of contact pyrometer or infrared devices
 - (3) Observations of steel color (satiny silver at torch tip to produce a temperature of 1200°F or 650°C).

5.4 Tolerances

- (1) Tolerances may conform to those specified for fabrication and erection of new construction. However, such tol-

erances may be over-restrictive because:

- (a) Damage may not be in most highly stressed region.
- (b) Tighter tolerances increase time and cost of repair.
- (c) Local indentations may preclude tight tolerances.

- (2) Recommended Tolerances are given in table 12.1.

Chapter 12. Specifications for the Selection of contractors and the Conduct of Heat-Straightening Repairs

This chapter contains some suggested specifications for contractor selection and the conduct of heat-straightening repairs. The criteria presented here are guidelines only. The Engineer should use judgment in selecting the criteria appropriate for his organization and the complexity of the project.

Selection of Contractor (or the Contractor's field supervisor)

The selection of a contractor can be based on one or more of the following criteria: experience, training, certification, and educational background. Since there is neither a certification or established training program currently available, experience and educational background are the primary criteria for selecting a heat-straightening contractor. Typical experience criteria are:

The contractor (or the contractor's field supervisor) shall have at least _____ years of experience in conducting heat-straightening repairs for damaged steel structures. During the preceding three year period, he shall have conducted an average of at least _____ heat-straightening projects per year. Experience documentation shall include: date of project, location, bridge owner, number and type of members straightened, and duration of project.

The years of experience and number of projects conducted can be varied at the discretion of the bridge engineer. Factors which may influence this decision include: complexity of damage, degree of damage,

accessibility, climatic conditions, and scale of the project.

As an alternative educational background with specific training can be used to qualify a contractor in the field of heat straightening. Licensing as a professional engineer is often related to this training in such fields as metallurgical, structural, mechanical, or welding engineering. Typical educational background criteria are:

The contractor (or the contractor's field supervisor) shall have a baccalaureate degree from an accredited program in one of the following engineering disciplines and be a licensed professional engineer qualified to practice in one of the following disciplines: structural, metallurgical, mechanical, or welding engineering.

The bridge engineer may wish to specify the qualifications of the technicians involved in the conduct of the heat applications. These qualifications may be less than the contractor or his field supervisor, such as:

Technicians involved in the conduct of heat applications during heat straightening shall have at least _____ years of experience on a minimum of _____ projects.

For additional quality control, the bridge engineer may wish to specify a series of technical specifications on the conduct of the project. Suggested specifications are outlined in the following sections.

Tolerances

One approach to specifying the tolerance for heat straightening repair is to use a standard specification for manufacture or fabrication. One commonly referenced standard is the ANSI/AASHTO/AWS Bridge Welding Code D1.5, American Welding Society (1996 or latest edition). Member dimensional tolerances are given in Section 3.5 and flat plate tolerances are given in Section 9.19. The use of this or similar construction standards for heat straightening tolerances may be too limiting for the following reasons.

- (1) The tighter the tolerances, the longer the repair will take. Costs and traffic delays will thus increase.
- (2) In many cases, the area of damage is small and not necessarily located at the most highly stressed region. Less restrictive tolerances can safely be used in such instances since the engineer can assess the specific structural configuration.
- (3) The steel in the vicinity of impact may have material distortions, such as changes in thickness, which may preclude highly restrictive tolerances.

As a consequence, engineering judgement for the specific situation is recommended as the most effective approach in setting tolerances.

In order to provide some general guidelines, a set of recommended tolerances are given in table 12.1. These tolerance levels are less restrictive than specified in the Bridge Welding Code.

Technical Specifications for the Conduct of Heat-Straightening Repairs

The following technical specifications are suggested for incorporation into repair contracts. The Engineer should use judgement in selecting the criteria that best fits the specific damage situation.

1. Equipment

1.1 Fuel for heating shall be an oxygen-fuel combination. The choice of the fuel may be propane, acetylene or other similar fuel as selected by the contractor.

1.2 Heat application shall be by single or multiple orifice tips only. The size of the tip shall be proportional to the thickness of the heated material. As a guide, the tip sizes shown in table 12.2 are recommended.

1.3 Jacks, come-alongs or other force application devices may be either hydraulic or mechanical but shall be gauged so that the force exerted by the device may be measured. No force shall be applied to the structure unless it can be measured.

2. Damage Assessment

2.1 Suspected areas of cracking shall be called to the attention of the Engineer and shall be inspected by one or more of the following methods as applicable.

2.1.1 Visual Inspection

2.1.2 Liquid penetrant examination as described in ASTM E165 (1994 or latest edition).

2.1.3 Magnetic-Particle testing as described in ASTM E709 (1994 or latest edition).

Table 12.1. Recommended Tolerances for Heat Straightening Repair.

Member Type	Recommended Minimum Tolerance ^{1,2}	
	English (in)	SI (mm)
Beams, Truss members, or Columns		
overall	½ in over 20 ft	13 mm over 6 meters
at impact point	¾ in over 20 ft	19 mm over 6 meters
Local Web Deviations	d/100 but not less than ¼ in	d/100 but not less than 6 mm
Local Flange Deviations	b/100 but not less than ¼ in	b/100 but not less than 6 mm

¹Units of member depth, d, and flange width, b, are inches and millimeters, respectively, for English and SI units

²Tolerances for curved or cambered members should account for the original shape of the member

Table 12.2. Recommended torch tips for various material thicknesses.

Steel Thickness (in)	Orifice Type	Size
< ¼	Single	3
3/8	Single	4
½	Single	5
5/8	Single	7
¾	Single	8
1	Single Rosebud	8 3
2	Single Rosebud	8 4
3	Rosebud	5
> 4	Rosebud	5

2.1.4 Ultrasonic examination as described in section 6, part C of the ANSI/AASHTO/AWS Bridge Welding Code D1.5, American Welding Society (1996 or latest edition).

2.1.5 Radiographic examination as described in section 6, part B of the ANSI/AASHTO/AWS Bridge Welding Code D1.5, American Welding Society (1996 or latest edition).

2.2 The cost of the inspections under 2.1 shall be additional to other testing required and costs shall be negotiated between the Engineer and contractor.

2.3 Contractor shall identify all yield zones and yield lines prior to initiation of heat straightening by either visual inspection or measurements.

2.4 Steel with strains up to 100 times the yield strain may be repaired by heat straightening. For strains greater than this limit, the decision to heat straighten should be based on the judgement of the Engineer.

2.5 Cracks and/or strains exceeding 100 times the yield strain, or other serious defects may require changes in the scope of the contract which shall be negotiated between the Engineer and the contractor.

3. Heat Application

3.1 The temperature of the steel during heat straightening shall not exceed the following:

3.1.1 650°C (1,200°F) for Carbon Steels.

3.1.2 620°C (1,100°F) for A514 and A709 (grades 100 and 100W) steels.

3.1.3 565°C (1,050°F) for A709 grade 70W steel.

3.2 The Contractor shall use one or more of the following methods for verifying temperatures during heat straightening:

3.2.1 Temperature sensitive crayons

3.2.2 Pyrometer

3.2.3 Infrared non-contact thermometer

3.3 Material should be heated in a single pass following the specified pattern and allowed to cool to below 121°C (250°F) prior to re-heating.

3.4 Heating patterns and sequences shall be selected to match the type of damage and cross section shape.

3.5 Vee heats shall be shifted over the yield zone on successive heats

3.6 Simultaneous vee heats may be used provided that the clear spacing between vees is greater than the width of the plate element

3.7 Repair of previously heat-straightened members in the same region of damage may be conducted once. Further repairs are not recommended unless approved by the Engineer.

4. Application of Jacking forces

4.1 Jacks shall be placed so that forces are relieved as straightening occurs during cooling.

4.2 Magnitude of Jacking Forces

4.2.1 Jacking shall be limited so that the maximum bending moment in the heated zone shall be less than 50 percent of the plastic moment capacity of the member.

4.2.2 If residual moments are present, the jacking force shall be further reduced so that the sum of jacking moments and residual moments shall be less than 50 percent of the plastic moment capacity of the member. As an alternative to computing residual moments, the moment due to jacking forces can be limited to 25 percent of the plastic moment capacity of the member during the first two heating cycles. For additional heating cycles, the limit of 50 percent may again be used.

4.3 Control of jacking forces by deflection limitations

Subject to approval by the engineer, the maximum jacking force may be controlled by measuring the deflection resulting from the jacking force. The deflection limitation can be computed by one of the following methods.

4.3.1 Computation of deflection based on a structural analysis of the system.

4.3.2 For a span with the jacking force located near the center, the deflection limit associated with a 50 percent jacking ratio can be approximated by one of the following procedures

4.3.2.1 Assuming simple end supports, the deflection should be limited to

$$\delta_{\max} = \frac{1}{y_{\max}} \left(\frac{\ell}{140} \right)^2 \quad \text{for 36 ksi steel}$$

$$\delta_{\max} = \frac{1}{y_{\max}} \left(\frac{\ell}{120} \right)^2 \quad \text{for 50 ksi steel}$$

where y_{\max} is the distance from the centroid to the extreme fiber about the axis of bending.

4.3.2.2 For partially restrained end conditions, the maximum deflection can be estimated by interpolating between the deflection for the simple support and fixed support cases. For the fixed support case

$$\delta_{\max} = \frac{1}{y_{\max}} \left(\frac{\ell}{200} \right)^2 \quad \text{for 36 ksi steel}$$

$$\delta_{\max} = \frac{1}{y_{\max}} \left(\frac{\ell}{170} \right)^2 \quad \text{for 50 ksi steel}$$

4.4 The calibration of jacks should be certified within a two year period.

5. Field Supervision of Repair

5.1 Jacking forces shall be monitored to insure that limits are not exceeded.

5.2 Heating patterns shall be approved by the bridge engineer.

5.3 Heating temperatures shall be monitored to insure compliance with specified limits.

6. Tolerances

6.1 The dimensions of heat-straightened structural members shall conform to the tolerances specified in table 12.1 except as noted below.

6.2 Tolerance limits may be relaxed at the discretion of the Engineer based on one or more of the following considerations:

- (a) Type and location of damage in the member.
- (b) Time considerations resulting from the nature of traffic congestion during the repair operation.

-
- (c) *Cost of repair.*
 - (d) *Degree of restoration required to restore structural integrity.*

Chapter 13. Glossary

Austenite: A uniform solid solution that steel assumes upon being heated above the upper phase transition temperature.

Brittle Hot spots: Small areas in the heated zone having a molecular change which reduces ductility and produces a zone subject to a sudden fracture at high stress.

Bulge: Localized spherically shaped damage typically found in the web of damaged members.

Category L: A damage classification characterized by localized damage to plate elements of a cross section such as bulges, crimps, buckles, and kinks.

Category L/U: Local damage in unstiffened cross section elements.

Category L/S: Local damage in stiffened cross section elements.

Category S: A damage classification characterized by bending about the major (or strong) axis of the member.

Category T: A damage classification characterized by twisting of a member about the longitudinal axis.

Category W: A damage classification characterized by bending about the minor (or weak) axis of the member.

Cementite: Iron-carbon molecules, Fe_3C .

Charpy V-notch Tests: An ASTM standard test of steel coupons which measures the fracture toughness of the material at a specified temperature.

Coefficient of Thermal Expansion: A parameter expressing the ratio of change in temperature and the produce of the original length times the change in length.

Cold Mechanical Straightening: A method in which steel is straightened through the use of jacks or other mechanical means without the use of heat.

Contact Pyrometer: A temperature measuring device consisting of a contact thermocouple and digital readout which requires physical contact of the devise to the surface to measure temperature.

Degree of Damage: A measure of flexural Category S and W damage which is computed by the measuring the change in angle of tangents to the member on either side of the damaged area.

Depth ratio: The ratio of vee depth to width of the plate element upon which the vee heat is applied.

Drop Weight Tear Test: A test to measure the fracture toughness of steel coupons.

Ductility: The ability of a material to withstand extensive deformations without failure under high tensile stresses.

Edge Heats: A line heat placed at the flange tip of a rolled shape.

Elastic Strain: The strain that occurs prior to yielding.

External Restraints (Jacking or restraining forces): The external forces applied to the damaged member (by jacks) such as to produce stresses tending to straighten the member. These forces are passive and generally should not be increased during a heat straightening cycle. The stresses produced should be limited to approximately one-half the yield stress at ambient temperature.

Fatigue Life: The number of cycles of alternating stress reversals at a specified level required to initiate a fracture in the material.

Ferrite: Iron particles with no carbon attached.

Flame Cambering: The use of heat typically applied as line heats at flange tips to produce a camber in the member.

Fracture Critical Members: A Primary member of a bridge superstructure whose fracture would produce an unstable structure and result in a collapse.

Fracture Toughness: The ability of a material to withstand an impact blow.

Hairline fracture: A fracture in the steel which is so small as to be difficult to visually observe without nondestructive testing techniques.

Heating Pattern: The combination of vee, line, strip, and spot heats utilized to heat straighten a specific type of damage.

Heat sink: A portion of a steel cross section tending to absorb additional heat during heat straightening, such as the flange-web juncture of a rolled shape.

Heat Straightening: A method of straightening damaged steel which relies on heating steel below the lower phase transition temperature or tempering temperature. The method relies on plastic flow during heating and contraction during cooling.

Hot Mechanical Straightening: A straightening technique which relies on large jacking forces to straighten steel which has been heated above the lower phase transition temperature.

Internal restraints: Forces produced during damage of indeterminate systems tending to either impede or enhance movement during heat straightening.

Jacking force: Applied forces to expedite heat straightening (see External Restraints).

Jacking Ratios: The ratio of moment generated by the jacking force to the plastic moment capacity of the section specified.

Line Heat: A heating pattern made by moving a torch in a straight line across the plate element.

Lower critical (or lower phase transition) Temperature: The lowest temperature at which molecular change occurs in the steel in which the body centered cubic molecular structure begin to assume a face centered cubic form.

Martensite: A strong, hard brittle phase resulting from rapid cooling of steel below the lower phase transition temperature that precludes the complete in molecular change which occurs during slow cooling.

Maximum Tensile Strength: The peak tensile stress for a steel coupon which occurs in the strain-hardening range.

Modulus of Elasticity: A parameter expressing the ratio of uniaxial tensile stress to uniaxial tensile strain for steel in the linear elastic range.

Notch Toughness: A measure of the ability of a notched coupon to absorb impact energy.

P- Δ effects: The moment in a deformed axial compression member due to the axial load, P, acting through the lateral deflection, Δ .

Pearlite: A mixture of cementite (12 percent) and ferrite (88 percent).

Plastic deformations: Permanent deformations resulting from strains exceeding the yield strain of the steel.

Plate elements: Individual flat plates forming the cross section of rolled or built-up steel shapes.

Plastic flow: The redistribution of material as a result of yielding during heating when expansion is restrained in one or more directions.

Plastic Moment: The moment capacity of a section based on full yielding of the cross section.

Plastic Rotation: The angular change produced by tangents to a member on either side of a vee heated area after a heating/cooling cycle is complete.

Plastic strain: The strain that occurs after yielding during which no significant change in stress occurs (usually in the range of 10-15 times the yield strain).

Primary member: A load-bearing member designed on the basis of a structural analysis.

Residual force: The restraining forces produced after yield level damage due to the redundancy of the structural system preventing full elastic rebound.

Residual Stresses: Stresses that remain in structural members after rolling, fabrication or heat straightening.

Ring line heat: A heat made in a single torch pass in a circular pattern typically used in heat straightening local bulge damage.

Rockwell Hardness Test: A non-destructive standard ASTM test to measure the hardness of the steel.

Rosebud torch tip: A multiple orifice torch tip supplying fuel to the flame.

Secondary Member: A bracing or minor support member not designed as load-carrying but rather as brace against buckling or non-structural applications.

Shoring: Refers to temporary supports used during heat straightening. Such supports are not usually required, however, the decision should be based on engineering analysis.

Single Orifice torch tip: A brazing tip with a single opening for supplying fuel to the flame.

Spot Heats: A heat applied to a single spot location having a diameter of approximately 25 mm (one inch).

Star Vee heat: A series of vee heats forming a star pattern used to heat straighten bulges.

Strain Aging: The effect of increased yield and tensile strength with decreased ductility when steel has been strained into the strain hardening range, unloaded, and reloaded after several days of aging.

Strain Hardening: The range of strain after the plastic range in which additional stress is required to produce additional strain.

Strain Ratio: The ratio of the actual strain in an element to the yield strain.

Strip Heat: A rectangular heating pattern on a plate element in which the torch is moved in a serpentine pattern across a rectangle.

Strong (or major) axis: The axis of bending for a section associated with the largest moment of inertia and, consequently, the highest flexural stiffness.

Stiffness Factor: The ratio of the nominal jacking force moment to the actual moment in the bottom flange of a composite beam.

Temperature Sensing Crayons: Crayons with a specified melting temperatures used to bracket surface temperature by striking several crayons on the steel and observing which melt.

Upper Critical (or upper phase transition) Temperature: The temperature at which the steel molecular change is complete and the steel assumes a form of uniform solid solution called austenite.

Upsetting: Plastic flow occurring through the thickness of the material as a result of heat straightening.

Vee angle: The angle at the apex of a vee heat.

Vee heat: A heating pattern on a steel plate section in the shape of a vee in which the heat is applied by torch, starting at the apex and moving across the vee in a serpentine pattern until the entire vee is heated.

Vee depth: The dimension of a vee heat as measured from the apex to the open end of the vee.

Weak (or Minor) axis: The axis of bending for a section associated with the smallest moment of inertia and, consequently, the smallest flexural stiffness.

Web buckling: Bulges in webs of damaged rolled or built-up shapes.

Web Crippling: Buckling in webs of damaged rolled or built-up shapes due to excessive bearing stresses at reactions or load points.

Yield strain: The strain that is produced at the yield stress.

Yield stress: The largest stress which the material can withstand without being permanently deformed.

Yield zone: A region which includes all fibers that have equaled or exceeded the yield strain.

Chapter 14. Nomenclature

a, b, c	= Dimensional constants	I_f	= Moment of inertia of bottom flange of composite girder about strong axis of flange
b_f	= Flange width	I_j	= Equivalent moment of inertia for composite beam with lateral load applied to bottom flange
b_s	= Width of stiffening element	K_f	= Flange stiffness, $4EI_f / \ell$
C	= Temperature in degrees Celsius	K_j	= Stiffness of composite girder with lateral load applied to bottom flange (eq. 7.2)
c_d	= Chord length across the yield zone of a curved beam	ℓ	= Span length of flexural member
d	= Depth of wide flange beam or primary plate element	ℓ_c	= Characteristic length for flange bulge
d_b	= Diameter of local bulge	L, L_r	= Lengths between offsets
d_s	= Distance between the vee apex edge of the primary plate element and the stiffening element	L_d	= Length of free edge of flange after localized damage
d_v	= Depth of vee in flat plate	L_u	= Length of free edge of flange before localized damage
E	= Modulus of elasticity	M_j	= Moment produced by jacking forces
E_o	= Modulus of elasticity at ambient temperature	M_f	= Actual moment in bottom flange of composite girder due to an applied jacking force generating an apparent moment, M_j .
f_a	= Axial stress in a compression member due to live and dead loads	M_p	= Plastic moment capacity of a member
F_a	= Stress factor for calculating plastic rotation in rolled shapes	M_r	= Residual moment
\bar{F}_a	= Allowable design stress for a compression member	M_y	= Moment at initial yield
$F_\ell(M)$	= Jacking load factor	n	= Number of single vee heats required to remove a specified amount of damage
$F_\ell(T)$	= Temperature function		
F_s	= Shape factor for calculating plastic rotation in rolled shapes		
F_y	= Yield stress		
F_{y_o}	= Yield stress at ambient temperature		

P	= Axial load in compression member	W_I	= Internal work done during local damage flange movement
P_a	= Total jacking force for an axially loaded member	W_u	= Externally applied load on locally damaged flange
P_{ec}	= Additional jacking force required to cancel eccentric moments due to axial loads	y_o	= Initial out-of-straightness of compression member
P_{euler}	= Euler buckling load for axially loaded member	y_r	= Measured offsets at point r
P_f	= Portion of jacking force transferred to lower flange of composite girder	y_{max}	= Distance from centroid to extreme fiber
P_j	= Jacking force	Z	= Plastic section modulus
P_n, P_f	= Jacking force on near and far side of locally damaged flange	Z_x, Z_y	= Plastic section modulus about x and y axis, respectively
P_u	= Ultimate load computed from a plastic analysis	Z'/S'	= Ratio of plastic to elastic section modulus about the axis of bending for an angle
r	= Radius of arbitrary circle on flange bulge	α	= Coefficient of thermal expansion
R	= Actual radius of curvature	β	= Shell stress factor for bulge
R_l	= Jacking ratio M_j / M_p	δ	= Closure of open end of vee after heat straightening
R_y	= Radius of curvature at initial yield	δ_c	= Bulge deflection at point of counterflexure
S	= Shortening of member after heat straightening or section modulus	δ_b, δ_n	= Deflection of locally damaged flange on far and near side, respectively
S_p	= Plastic strain for single axis perfect confinement at temperature T	δ_i	= Initial deflection of flange bulge
S_x, S_y	= Section modulus about strong and weak axis, respectively	δ_{max}	= Maximum deflection of laterally loaded beam
T	= Heating temperature	Δ	= Lateral deflection of loaded member
t_w	= Web thickness	Δ_b, Δ_n	= Average deflection of flange edge after localized damage for far and near side, respectively
V	= Width at open end of vee	ϵ	= Actual strain
W	= Primary plate element width	ϵ_e	= Elastic strain at open end of vee
W_e	= External work done during local damage flange movement		

ε_{\max}	= Actual strain at extreme fiber of member	ϕ_p	= Plastic rotation resulting from a single vee heat on a plate or rolled shape
$\varepsilon_p(T)$	= Strain under conditions of perfect confinement at temperature T	θ	= Vee angle
ε'_p	= Plastic strain at open end of vee after heat straightening	θ_f	= Slope of flange on side away from impact for locally damaged member
ε_t	= Unconfined thermal strain at open end of the vee	θ_n	= Slope of flange on impact side of locally damaged flange
ε_y	= Strain at initial yield of material	θ_w	= Slope of web for beam with local flange damage
$\bar{\gamma}$	= Distribution factor for unheated composite beam	σ	= Bulge axial stress due to jacking force
γ	= Distribution factor for heated composite beam	σ_r	= Residual stress
μ	= Ratio of maximum strain to yield strain, $\varepsilon_{\max}/\varepsilon_y$	ν	= Poisson's ratio
ϕ_b	= Basic plate rotation factor		
ϕ_c	= Plastic rotation of composite girder		
ϕ_d	= Degree of damage		

Chapter 15. Bibliography

- American Institute of Steel Construction, (1989). *Manual of Steel Construction*, 9th Ed., AISC, Chicago, IL.
- American Railway Engineering Association, *Flame Shortening Eyebars to Equalize Stresses*, Bulletin No. 460.
- American Welding Society, (1996). *Bridge Welding Code*, ANSI/AASHTO/AWS D1. 5-96, Miami, FL.
- Avent, R.R. (1987). "Use of Heat Straightening Techniques for Repair of Damaged Steel Structural Elements in Bridges." *Final Report*, Louisiana Transportation Research Center, Louisiana State Univ., Baton Rouge, La.
- Avent, R.R. (1988). "Heat Straightening of Steel: From Art to Science." *Proceedings, National Steel Construction Conference*. Miami Beach, June, pp. 6-21.
- Avent, R.R. (1989). "Heat-Straightening of Steel: Fact and Fable." *Journal Structural Engineering*, ASCE, 115(11), 2773-2793.
- Avent, R.R. (1992). "Designing Heat-Straightening Repairs." *Proceedings, National Steel Construction Conference*, AISC, Las Vegas, Nev., June, pp. 21-23.
- Avent, R.R. and Brakke, B.C. (1996). "Anatomy of Steel Bridge Heat-Straightening Project" *Transportation Research Record*, No. 1561, TRB, National Research Council, Washington, D.C. pp. 26-36.
- Avent, R.R. and Fadous, G.M. (1988). "Heat-Straightening Prototype Damaged Bridge Girders", *Journal of Structural Engineering*, ASCE, Vol. 15, No. 7, July pp.1631-1649.
- Avent, R.R. and Fadous, G.M. (1989). "Heat-straightening Techniques for Repair of Damaged Structural Steel in Bridges," LTRC 223, Louisiana Transportation Research Center, Baton Rouge, LA.
- Avent, R.R. and Fadous, G.M., and Boudreaux, R.J. (1991). "Heat-Straightening of Damaged Structural Steel in Bridges," *Transportation Research Board*, No. 1319 TRB, National Research Council, Washington, DC. pp. 86-93.
- Avent, R.R., Robinson, P.F., Madan, A., and Shenoy, S. (1993) "Development of Engineering Design Procedures for Heat-Straightening Repair of Damaged Structural Steel in Bridges," LTRC 251, Louisiana Transportation Research Center, Baton Rouge, LA.
- Avent, R.R., A. Madan, and Shenoy, S. (1993) "Design and Implementation of Heat-Straightening Repair for Composite Deck-Girder Bridges." *Transportation Research Record 1392*, TRB, National Research Council, Washington, D.C., pp. 90-98.
- Avent, R.R. (1995) "Engineered Heat Straightening Comes of Age." *Modern Steel Construction*, Vol. 35, No.2, Feb., pp. 32-39.

- Avent, R.R. and Wells, S. (1982). "Experimental Study of Thin-Web Welded H Columns," *Journal of the Structural Division, ASCE*, Vol. 108, No. ST7, July.
- Anderson, R.B. Math-CAD (Student Edition, vers. 2.0) Addison-Wesley and Benjamin Cummings, Reading, MA, 1991.
- Barsom, J.M. and Rolfe, S.T. (1987), *Fracture and Fatigue Control in Structures-Applications of Fracture Mechanics, 2nd Edition*, Prentice-Hall, Englewood Cliffs, New Jersey.
- Bernard, P., and Schulze, K. (1966). "Flame Straightening in Ship-Building." *Mittlung der BEFA (Beratungsstelle für Autogen Technik)*, Köln, West Germany, 17(11), 2-6 (in German).
- Blodgett, O. W. (1972). "Distortion . . . How Metal Properties Affect It." *Welding Engr.*, 57(2), 40-46.
- Boudreaux, R.J. (1987). "Heat Straightening of Steel: Identifying the Important Parameters and Predicting Member Response," thesis presented to Louisiana State University at Baton Rouge, LA., in partial fulfillment of the requirements for the degree of Master of Science.
- Brockenbrough, R. L. (1970-a). "Theoretical Stresses and Strains From Heat Curving." *Journal of the Structural Division, ASCE*, 96(7), 1421-1444.
- Brockenbrough, R. L., (1970-b). "Criteria for Heat Curving Steel Beams and Girders." *Journal of the Structural Division, ASCE*, 96(10), 2209-2226.
- Brockenbrough, R. L., and Ives, K. D. (1970). "Experimental Stress and Strains from Heat Curving." *Journal of the Structural Division, ASCE*, 96(7), 1305-1331.
- Brockenbrough, R. L., and Johnston, B. G. (1968). *USS Steel Design Manual*. U. S. Steel Corp., Pittsburgh, Pa.
- Burbank, B. B. (1968). "Straightening Distorted Weldments." *Report SR-185*, Report to the Ship Structure Committee, U. S. Coast Guard, Washington D. C., July.
- Ciesicki, H., and Butler, S. (1968). "Flame and Camber Your Own Beams." *Industry and Welding*, 31(4), 76-79.
- Clough, R.W., and Penzien, J. (1975c). *Dynamics of Structures, Part IV: Random Vibrations*. McGraw-Hill, New York, N.Y.
- Cooley, J.W., Lewis, P.A., and Welch, P.D. "The Fast Fourier Transform and its Applications. *Transactions on Education, IEEE*, 1969, 12(1), 27-34.
- Cooley, J.W., Lewis, P.A., and Welch, P.D. The Finite Fourier Transform. *Transactions on Audio and Electroacoustics, IEEE*, 1969, AU-17(2), 77-85.
- Crandall, S.H., and Mark, W.D. (1963). *Random Vibrations in Mechanical Systems*. Academic Press, New York, N.Y.
- Crooker, T. W. , and Harrison, H. L. (1965). "The Effects of Flame Cambering on the Bending Strengths of I-Beams." *Welding Journal*, 44(12), Res. Supplement, 545s-548s.

- de Béjar, L.A., Robinson, P.F., and Avent, R.R. (1992). "Risk Consistent Estimate of Heat-Straightening Applications. I: Plates." *Journal of Structural Engineering*, ASCE, 118(12), 3394-3409.
- de Béjar, L.A., Robinson, P.F., and Avent, R.R. (1992). "Risk Consistent Estimate of Heat-Straightening Applications. II: Beams." *Journal of Structural Engineering*, ASCE, 118(12), 3440-3426.
- Ditman, O. (1961). "Determination of Thermal Shrinkage in Structural Steel," thesis presented to the University of Washington, at Seattle, Wash., in partial fulfillment of requirements for Master of Science degree.
- Engineering-News Record, (1959). "How Fire Destroyed and Fire Repaired Air Force Hangers," June 18, pp. 42-43.
- "Flame Buckled This Steel . . . and Flame Straightened It, part 1." (1959) *Welding Engineer*, 44(2), 43.
- For Chin, W. (1962). "Linear Shrinkage of Steel," thesis presented to the University of Washington, at Seattle, Wash., in partial fulfillment of the requirements for the Master of Science degree.
- Gipson, G. S., and Ortiz, J. C. (1986). "Toward an Analytical Description of the Heat-Straightening Phenomenon-The Thermal Problem." *SECTAM XIII Proc.*, 772-778.
- Graham, R. (1975). "Investigation of Flame Straightening Methods for Steel Structures." *Manufacturing Development Report MDR 2-32075*, Boeing Co., Oct. 30.
- Hasofer, A.M., and Lind, N.C. (1974). "Exact and Invariant Second-Moment Code Format." *Journal of Engineering Mechanics Division*, ASCE, 100(1), 111-121.
- Harrison, H. L. (1950). "A Study of the Holt Method of Heat (Contraction) Straightening," thesis presented to the University of Washington, at Seattle, Wash., in partial fulfillment of the requirements for Master of Science degree.
- Harrison, H. L. (1952). "Straightening Structural Members in Place." *Welding Journal*, 31(5), Res. Supplement, 257s-262s.
- Harrison, H. L., and Mills, B. D., Jr. (1951). "Effects of light peening on the yielding of steel." *Welding Journal*, 30(5), Res. Supplement, 251s-253s.
- Hicks, C.R. (1982) *Fundamental Concepts in the Design of Experiments*, 3rd Ed., Holt, Rhinehart and Winston, New York.
- Higgins, T. R. (1966). "Discussion on the Effects of Flame Cambering on the Bending Strength of I-beams." *Welding Journal*, 45(6), Res. Supplement, 284s-288s.
- Holt, J. E. (1955). "Flame Straightening: A Friend in Need." *Welding Engineering*, 40(10), 44-46, (12), 30-31.
- Holt, R. E. (1965). "Flame Straightening Basics." *Welding Engineer*, 50(9), 49-53.

- Holt, R. E. (1971). "Primary Concepts in Flame Bending." *Welding Engineer*, 56(6), 416-424.
- Holt, R. E. (1977). "How to Control and Correct Warping." *Welding Design and Fabrication*, 49(6), 98-102.
- Horton, D. L. (1973). "Heat Curved Mild Steel Wide Flange Sections: An Experimental and Theoretical Analysis," thesis presented to the University of Washington, at Seattle, Wash., in partial fulfillment of the requirements for the Master of Science degree.
- "How Fire Destroyed and Fire Repaired Air Force hangars." (1959). *Engineering News Record*, 162(24), 50-53.
- Kihara, H., Nisida, M., and Fujita, Y. (1961). "On the Residual Stresses due to spot heating." *Document No. X-267-61*, Int. Inst. of Welding, Commission X, Tokoyo, Japan.
- "Kinks Go Up in Flames." (1981) *Engineering News Record*, 206(15), 17.
- Maeda, T., and Yada, T. (1961). "Investigation of Shrinkage Due to Multiple Spot Heating." *Document No. X-268-61*, Int. Inst. Of Welding, Commission X, Tokoyo, Japan.
- Maeda, T., and Yada, T., (1963). "Fundamental Nature of Shrinkage Distortion Due to Spot Heating on a Rectangular plate." *Document No. X-327-63*, International Institute of Welding, Commission X, Tokoyo, Japan.
- Masubuchi, K. (1960). "Calculation and Measurement of Residual Stresses Due to spot heating." *Document No. X-259-60*, Int. Inst. of Welding, Commission X, Tokoyo, Japan.
- Melchers, R.E. (1987). *Structural Reliability: Analysis and Prediction*. John Wiley and Sons, New York, N.Y.
- Meyers, P. S. (1976). "Fundamentals of Heat Flow in Welding." *Welding Research Council Bulletin*, 123 (July).
- Mishler, H.W., *Evaluation of Repair Techniques for Damaged Steel Bridge Members*, To be published by the Transportation Research Board, Project 12-17, FY77.
- Moberg, K. L. (1979). "Damage Assessment and Contraction Straightening of Steel Structures," thesis presented to the University of Washington, at Seattle, Wash., in partial fulfillment of the requirements for Master of Science Degree.
- Morris, J. J. (1949). "Controlled Distortion—An aid to metal working." *Welding Journal*, 28(11), 1080-1082.
- Newland, D.E. (1984). *An Introduction to Random Vibrations and Spectral Analysis*. Longman House, Inc., New York, N.Y.
- Newman, E. M. (1959). "Repair of Fire Damaged Structural Steel." *Military Engineering*, 9(4), 488-450.
- Nicholls, J. I., and Weerth, D. E. (1972). "Investigation of Triangular Heats Applied to Mild Steel Plates." *Engineering Journal*, Oct., 137-141.
- "Oxyacetylene Torches Straighten Fire-Warped Steel." (1959). *Welding Engineering*, Mar., 44(3), 31-34.

- Pattee, H. E., Evans, R. M., and Monroe, R. E. (1969). "Flame Straightening and its Effect on Base Metal Properties." *Summary Report to Ship Structure Committee concerning first phase of Project SR-185, Straightening Distorted Weldments*, Battelle Memorial Inst., Columbus, Ohio, Aug.
- Pattee, H. E., Evans, R. M., and Monroe, R. E. (1970). "Effect of Flame and Mechanical Straightening on Material Properties of Weldments." *Summary Report on Ship Structure Committee on Project SR-185, Straightening Distorted Weldments*, Battelle Memorial Inst., Columbus, Ohio.
- Pfeiffer, R. (1963). "The Flame Straightening of Sheeting and Sheet Metal Structures." *Mitteilungen der BEFA*, Köln, West Germany, 14(9), 1-7 (in German).
- Putherickal, J. (1992). "Effects of Heat Straightening Structural Steel", *Final Report for MLR-91-3*, Iowa Dept. of Transportation, Ames, Iowa.
- Robinson, P.F. (1991). "Behavioral Characteristics of Damaged Steel Repaired by Heat Straightening," PhD thesis, Louisiana State Univ., Baton Rouge, LA.
- Roeder, C. W. (1985). "Use of Thermal Stress for Seismic Damage Repair." *Final Report on NSF Grant CEE-82-05260*, Univ. of Washington, Seattle, Wash., Oct.
- Roeder, C. W. (1986). "Experimental Study of Heat Induced Deformation." *Journal of Structural Engineering*, ASCE, 112(10), 2247-2262.
- Roeder, C. W. (1987). "Predictions of Deformations Due to Heat Curving." *Bridges and Transmission Line Structural*, ASCE, New York, N. Y., 101-110.
- Rothman, R. L. (1973). "Flame Straightening Quenched and Tempered Steels in Ship Construction." *Report No. 247*, Ship Structs. Committee, U. S. Coast Guard, Washington D. C.
- Rothman, R. L., and Monroe, R. E. (1973). "Effect of Temperature and Strain Upon Ship Steels." *Report No. 235*, Ship Structs. Committee, U. S. Coast Guard, Washington D. C.
- Shanafelt, G. O., and Horn, W. G. (1984). "Guidelines for Evaluation and Repair of Damaged Steel Bridge Members." *NCHRP Report No. 271*, Transportation Research Board, National Research Council, Washington, D. C., June.
- "Steels for Elevated Temperature Service." (1966). *ADUSS 43-1089*, U. S. Steel Corp., Pittsburgh, Pa.
- Structural Stability Research Council (SSRC) (1976), *Guide to Stability Design Criteria for Metal Structures*, Third Edition, John Wiley and Sons, New York.
- Thatcher, W. M. (1967). "Horizontally Curved Steel Girders-Fabrication and Design Considerations." *Engineering Journal*, 4(3), 107-112.
- "The shortening of eyebars to equalize the stress." (1946). *Bulletin No. 460*, American Railway Engineering Association, Chicago, Ill., April.

Tsalman, L. B. (1959). "Straightening Welded Structures by Heating with an Oxyacetylene Flame." *Welding Production*, Cambridge, U. K., 1(5), 29-31 (in Russian).

Watanabe, M., and Satoh, K. (1951). "On the Correction of Distortion in Welded Thin Plate Structures." *Journal of Japan Welding Society*, Tokyo, Japan, 20, 194-202 (in Japanese).

Weerth, D. E. (1971). "Theoretical and Experimental Analysis of Heat Curved Mild Steel," thesis presented to the University of Washington, at Seattle, Wash., in partial fulfillment of the requirements for the degree of Master of Science.

Yang, C.Y. (1986). *Random Vibration of Structures*. Wiley-Interscience, New York, N.Y.

Yoch, A. E. (1957). "Flame Cambering Beams for Bridges." *Welding Engineering*, 42(2), 71.

0
1
2
3
4
5
6
7
8
9
10
11
12
13
14
15
16
17
18
19
20
21
22
23
24
25
26
27
28
29
30
31
32
33
34
35
36
37
38
39
40
41
42
43
44
45
46
47
48
49
50
51
52
53
54
55
56
57
58
59
60
61
62
63
64
65
66
67
68
69
70
71
72
73
74
75
76
77
78
79
80
81
82
83
84
85
86
87
88
89
90
91
92
93
94
95
96
97
98
99

